

Sensor and Simulation Notes

Note 181

August 1973

PL IPA 16 DEC 96

ELECTROMAGNETIC FIELDS NEAR THE CENTER OF TORUS
PART 1: FIELDS ON THE PLANE OF TORUS

H. Chang
The Dikewood Corporation
Albuquerque, New Mexico 87106

Abstract

A mode theory is introduced to derive the solutions for the electric and magnetic fields near the center of TORUS. The main interest of this note is the fields on the plane of TORUS up to one-fourth of the radius from the center. This analysis decomposes the fields into various Fourier modes which depend only on the coordinate system being chosen. Even if the antenna properties are unknown, one may still calculate the Fourier modes which are independent of source distribution and independent of the frequency dependent loading impedance. As the loading impedance and source function are determined, one can compute the excitation factor of each mode, which is related to the current distribution on the antenna. Loaded with a uniform resistance, the frequency response with a delta-function source and the transient behavior of the fields with a step-function excitation are shown for various cases. The possibility of extending the mode method to other symmetric types of antenna is also discussed.

PL 96-0981

Acknowledgments

I would like to thank Dr. C. Baum, Dr. P. Castillo, Mr. A. Griffin, and Capt. R. Blackburn for their comments; and Pat McCormick of Dikewood for typing the manuscript. The numerical calculations were carried out by Mr. J. Martinez of Dikewood.

TABLE OF CONTENTS

<u>Chapter</u>	<u>Page</u>
ABSTRACT	1
ACKNOWLEDGMENTS	2
I. INTRODUCTION	8
II. CURRENT ON THE TOROIDAL SURFACE	15
III. FOURIER EXPANSIONS FOR THE GREEN'S FUNCTION	19
IV. FOURIER MODES FOR THE E-FIELD	22
V. E-FIELD AS A FUNCTION OF ψ AND ϕ IN THE FREQUENCY DOMAIN	33
VI. FOURIER MODES FOR THE H-FIELD	42
VII. H-FIELD AS A FUNCTION OF ψ AND ϕ AT LOW FREQUENCIES	44
VIII. E AND H FIELDS AT HIGH FREQUENCIES	51
IX. PARAMETER STUDIES FOR FIELDS NEAR THE CENTER IN FREQUENCY AND TIME DOMAINS	57
X. SUMMARY	106
XI. REFERENCES	108

LIST OF FIGURES

<u>Figure</u>		<u>Page</u>
1-1	TORUS in a Full Toroid Configuration	9
1-2	Geometry of TORUS Simulator for Use With System on the Earth Surface	10
1-3	Relation of a Vertically Oriented TORUS on a Perfectly Conducting Ground Plane to a Full Circular TORUS With Three Coordinate Systems	11
2-1	Absolute Value of i_n for $Z/Z_0 = \ln(8a/b) - 2$	16
2-2	$i(\phi)$ for $Z/Z_0 = \ln(8a/b) - 2$ and $ka = 9$	18
3-1	$G_n(\psi)$ for $\psi = 0.1$	23
3-2	$G_n(\psi)$ for $\psi = 0.25$	24
4-1	$N_{\phi_n}(\psi, 0)$ for $\psi = 0.1$	29
4-2	$N_{\psi_n}(\psi, 0)$ for $\psi = 0.1$	30
4-3	$N_{\phi_n}(\psi, 0)$ for $\psi = 0.25$	31
4-4	$N_{\psi_n}(\psi, 0)$ for $\psi = 0.25$	32
5-1	Electric Field Very Close to the Center	35
5-2	Relative Field Strength for the Electric Mode $i_n N_{\phi_n}$ at Various Distances from the Center	36
5-3	Relative Field Strength for the Electric Mode $i_n N_{\psi_n}$ at Various Distances from the Center	37
5-4	E_{ϕ} for $b/a = 0.02$, $\psi = 0.25$ and $\phi = 0$ With the Numbers of Modes Taken into Account Ranging from Four to Twenty-five	39
6-1	$M_{z_n}(\psi, 0)$ for $\psi = 0.1$	45
6-2	$M_{z_n}(\psi, 0)$ for $\psi = 0.25$	46
7-1	Magnetic Field Very Close to the Center	48

LIST OF FIGURES (Cont'd.)

<u>Figure</u>		<u>Page</u>
7-2	Relative Field Strength for the Magnetic Mode $i_n M_{zn}$ at Various Distances from the Center.	49
8-1	E_ϕ and Asymptotic Forms for $\psi = .25$ and $\phi = 0$	53
8-2	Electric Field in Terms of Mode Expansions and Asymptotic Forms for $\psi = 0.25$, $\phi = 45^\circ$ and $b/a = 0.02$	55
8-3	H_z in Terms of Mode Expansions and Asymptotic Forms for $\psi = 0.25$, $\phi = 45^\circ$ and $b/a = 0.02$	56
9-1	E -field for $b/a = 0.1$ and $\psi = 0.1$ with ϕ as a Parameter . .	58
9-2	Step-function Response for the E -field for $b/a = 0.1$ and $\psi = 0.1$ with ϕ as a Parameter	60
9-3	H -field for $b/a = 0.1$ and $\psi = 0.1$ with ϕ as a Parameter . .	61
9-4	Step-function Response for the H -field for $b/a = 0.1$ and $\psi = 0.1$ with ϕ as a Parameter	63
9-5	E -field for $b/a = 0.1$ and $\psi = 0.25$ with ϕ as a Parameter .	64
9-6	Step-function Response for the E -field for $b/a = 0.1$ and $\psi = 0.25$ with ϕ as a Parameter	66
9-7	H -field for $b/a = 0.1$ and $\psi = 0.25$ with ϕ as a Parameter .	67
9-8	Step-function Response for the H -field for $b/a = 0.1$ and $\psi = 0.25$ with ϕ as a Parameter	69
9-9	E -field for $b/a = 0.05$ and $\psi = 0.1$ with ϕ as a Parameter .	70
9-10	Step-function Response for the E -field for $b/a = 0.05$ and $\psi = 0.1$ with ϕ as a Parameter	72
9-11	H -field for $b/a = 0.05$ and $\psi = 0.1$ with ϕ as a Parameter .	73
9-12	Step-function Response for the H -field for $b/a = 0.05$ and $\psi = 0.1$ with ϕ as a Parameter	75

LIST OF FIGURES (Cont'd.)

<u>Figure</u>		<u>Page</u>
9-13	E -field for $b/a = 0.05$ and $\psi = 0.25$ with ϕ as a Parameter	76
9-14	Step-function Response for the E -field for $b/a = 0.05$ and $\psi = 0.25$ with ϕ as a Parameter.	78
9-15	H -field for $b/a = 0.05$ and $\psi = 0.25$ with ϕ as a Parameter	79
9-16	Step-function Response for the H -field for $b/a = 0.05$ and $\psi = 0.25$ with ϕ as a Parameter.	81
9-17	E -field for $b/a = 0.01$ and $\psi = 0.1$ with ϕ as a Parameter	82
9-18	Step-function Response for the E -field for $b/a = 0.01$ and $\psi = 0.1$ with ϕ as a Parameter.	84
9-19	H -field for $b/a = 0.01$ and $\psi = 0.1$ with ϕ as a Parameter	85
9-20	Step-function Response for the H -field for $b/a = 0.01$ and $\psi = 0.1$ with ϕ as a Parameter	87
9-21	E -field for $b/a = 0.01$ and $\psi = 0.25$ with ϕ as a Parameter	88
9-22	Step-function Response for the E -field for $b/a = 0.01$ and $\psi = 0.25$ with ϕ as a Parameter.	90
9-23	H -field for $b/a = 0.01$ and $\psi = 0.25$ with ϕ as a Parameter	91
9-24	Step-function Response for the H -field for $b/a = 0.01$ and $\psi = 0.25$ with ϕ as a Parameter.	93
9-25	E -field for $b/a = 0.001$ and $\psi = 0.1$ with ϕ as a Parameter	94
9-26	Step-function Response for the E -field for $b/a = 0.001$ and $\psi = 0.1$ with ϕ as a Parameter	96

LIST OF FIGURES (Cont'd.)

<u>Figure</u>		<u>Page</u>
9-27	H -field for $b/a = 0.001$ and $\psi = 0.1$ with ϕ as a Parameter	97
9-28	Step-function Response for the H -field for $b/a = 0.001$ and $\psi = 0.1$ with ϕ as a Parameter	99
9-29	E -field for $b/a = 0.001$ and $\psi = 0.25$ with ϕ as a Parameter	100
9-30	Step-function Response for the E -field for $b/a = 0.001$ and $\psi = 0.25$ with ϕ as a Parameter.	102
9-31	H -field for $b/a = 0.001$ and $\psi = 0.25$ with ϕ as a Parameter	103
9-32	Step-function Response for the H -field for $b/a = 0.001$ and $\psi = 0.25$ with ϕ as a Parameter.	105

I. Introduction

In the previous note [1], the fields at the center of a full circular TORUS (Fig. 1-1) and a vertically oriented TORUS (Fig. 1-2 with $\xi_1 = 0$) on a perfectly conducting earth have been studied. There, a special toroidal coordinate system as shown in Fig. 1-3 was introduced and its relationship with the conventional rectangular, cylindrical and spherical coordinates has been discussed in detail. The general solutions for the electric field E and the magnetic field H in space have also been obtained. For the field components expressed in cylindrical coordinates (ψ, ϕ, z) , but with toroidal coordinates (λ', ξ', ϕ') for the surface current J components, the fields are

$$\begin{aligned} \frac{\gamma}{Z_0} E_\psi &= \frac{\partial}{\partial \psi} \iint_{S_1} G(\vec{r}, \vec{r}') \left\{ \frac{\partial}{\partial \xi'} \left[(a + b \cos(\xi')) J_{S_{\xi'}}(\xi', \phi') \right] + \left[b \frac{\partial}{\partial \phi'} J_{S_{\phi'}}(\xi', \phi') \right] \right\} d\xi' d\phi' \\ &- \gamma^2 b \iint_{S_1} G(\vec{r}, \vec{r}') \left[a + b \cos(\xi') \right] \left\{ -\sin(\xi') \cos(\phi - \phi') J_{S_{\xi'}}(\xi', \phi') \right. \\ &\left. + \sin(\phi - \phi') J_{S_{\phi'}}(\xi', \phi') \right\} d\xi' d\phi', \end{aligned} \quad (1.1)$$

$$\begin{aligned} \frac{\gamma}{Z_0} E_\phi &= \frac{1}{\psi} \frac{\partial}{\partial \phi} \iint_{S_1} G(\vec{r}, \vec{r}') \left\{ \frac{\partial}{\partial \xi'} \left[(a + b \cos(\xi')) J_{S_{\xi'}}(\xi', \phi') \right] + \left[b \frac{\partial}{\partial \phi'} J_{S_{\phi'}}(\xi', \phi') \right] \right\} d\xi' d\phi' \\ &- \gamma^2 b \iint_{S_1} G(\vec{r}, \vec{r}') \left[a + b \cos(\xi') \right] \left\{ \sin(\xi') \sin(\phi - \phi') J_{S_{\xi'}}(\xi', \phi') \right. \\ &\left. + \cos(\phi - \phi') J_{S_{\phi'}}(\xi', \phi') \right\} d\xi' d\phi', \end{aligned} \quad (1.2)$$

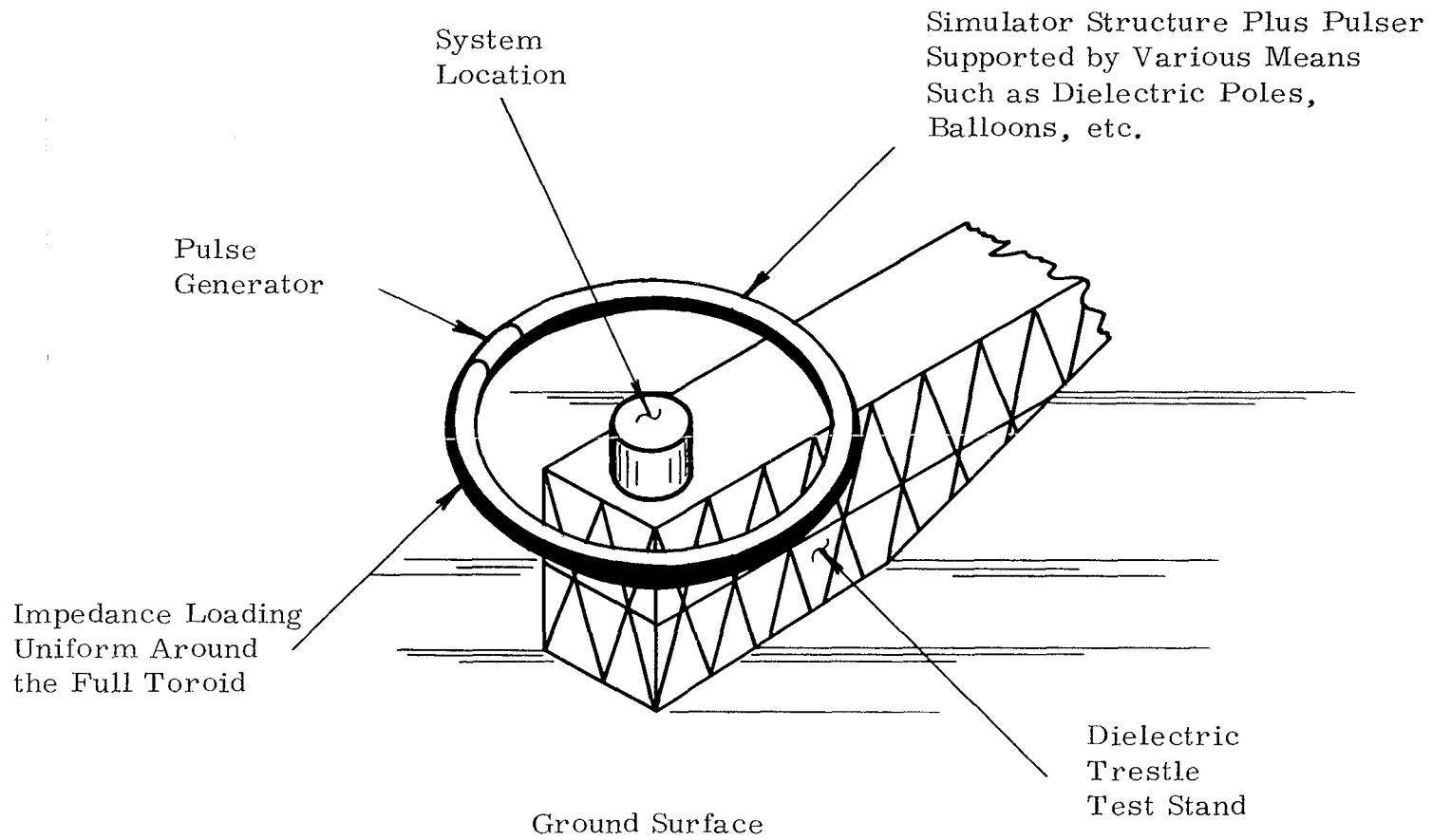


Figure 1-1. TORUS in a Full Toroid Configuration

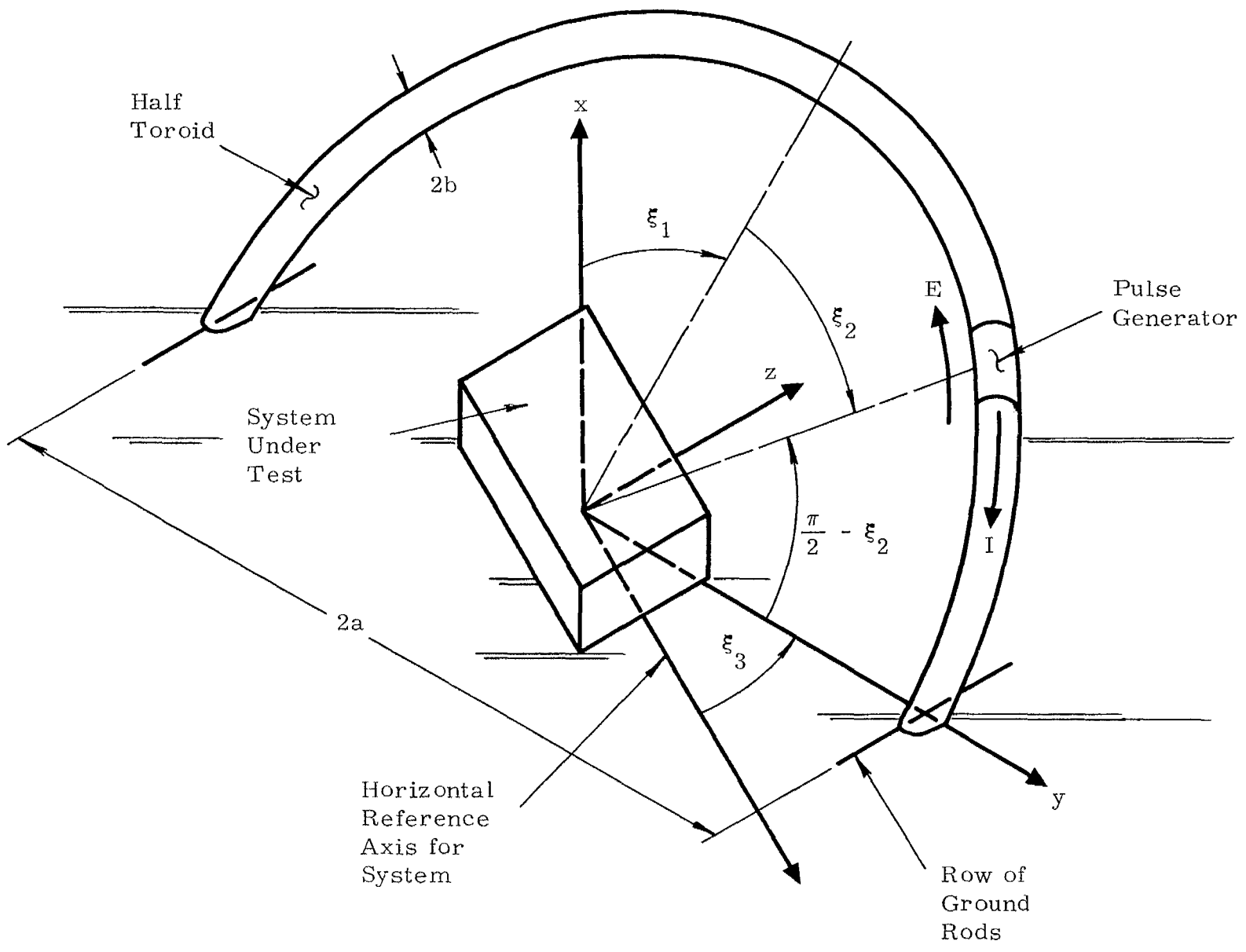


Figure 1-2. Geometry of TORUS Simulator for Use with System on the Earth Surface

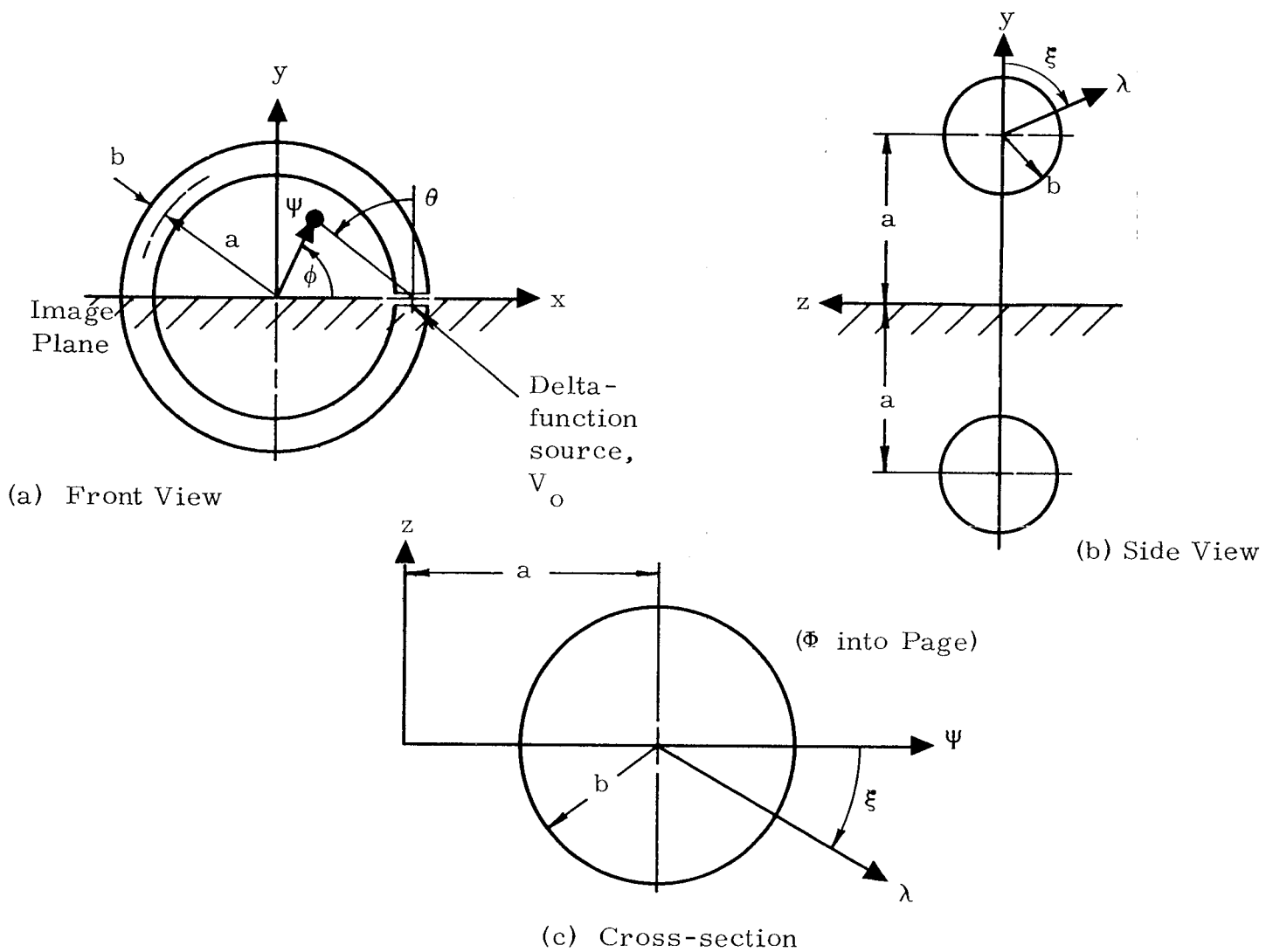


Figure 1-3. Relation of a Vertically Oriented TORUS on a Perfectly Conducting Ground Plane to a Full Circular TORUS with Three Coordinate Systems

$$\begin{aligned} \frac{\gamma}{Z_0} E_z &= \frac{\partial}{\partial z} \iint_{S'} G(\vec{r}, \vec{r}') \left\{ \frac{\partial}{\partial \xi'} \left[(a + b \cos(\xi')) J_{s_{\xi'}}(\xi', \phi') \right] + \left[b \frac{\partial}{\partial \phi'} J_{s_{\phi'}}(\xi', \phi') \right] \right\} d\xi' d\phi' \\ &- \gamma^2 b \iint_{S'} G(\vec{r}, \vec{r}') \left[a + b \cos(\xi') \right] \left[-\cos(\xi') J_{s_{\xi'}}(\xi', \phi') \right] d\xi' d\phi'; \quad (1.3) \end{aligned}$$

and

$$\begin{aligned} H_\psi &= \frac{b}{\psi} \frac{\partial}{\partial \phi} \iint_{S'} G(\vec{r}, \vec{r}') \left[a + b \cos(\xi') \right] \left\{ -\cos(\xi') J_{s_{\xi'}}(\xi', \phi') \right\} d\xi' d\phi' \\ &- b \frac{\partial}{\partial z} \iint_{S'} G(\vec{r}, \vec{r}') \left[a + b \cos(\xi') \right] \left\{ \sin(\xi') \sin(\phi - \phi') J_{s_{\xi'}}(\xi', \phi') \right. \\ &\left. + \cos(\phi - \phi') J_{s_{\phi'}}(\xi', \phi') \right\} d\xi' d\phi' \quad (1.4) \end{aligned}$$

$$\begin{aligned} H_\phi &= b \frac{\partial}{\partial z} \iint_{S'} G(\vec{r}, \vec{r}') \left[a + b \cos(\xi') \right] \left\{ -\sin(\xi') \cos(\phi - \phi') J_{s_{\xi'}}(\xi', \phi') \right. \\ &\left. + \sin(\phi - \phi') J_{s_{\phi'}}(\xi', \phi') \right\} d\xi' d\phi' - b \frac{\partial}{\partial \psi} \iint_{S'} G(\vec{r}, \vec{r}') \left[a + b \cos(\xi') \right] \\ &\left\{ -\cos(\xi') J_{s_{\xi'}}(\xi', \phi') \right\} d\xi' d\phi', \quad (1.5) \end{aligned}$$

$$\begin{aligned} H_z &= \frac{b}{\psi} \frac{\partial}{\partial \psi} \iint_{S'} G(\vec{r}, \vec{r}') \psi \left[a + b \cos(\xi') \right] \left\{ \sin(\xi') \sin(\phi - \phi') J_{s_{\xi'}}(\xi', \phi') \right. \\ &\left. + \cos(\phi - \phi') J_{s_{\phi'}}(\xi', \phi') \right\} d\xi' d\phi' - \frac{b}{\psi} \frac{\partial}{\partial \phi} \iint_{S'} G(\vec{r}, \vec{r}') \left[a + b \cos(\xi') \right] \\ &\left\{ -\sin(\xi') \cos(\phi - \phi') J_{s_{\xi'}}(\xi', \phi') + \sin(\phi - \phi') J_{s_{\phi'}}(\xi', \phi') \right\} d\xi' d\phi'. \quad (1.6) \end{aligned}$$

Here, "a" is the major radius and "b" is the minor radius of the toroid;
 Z_0 is the characteristic impedance of free space, about 377 ohms;
 $G(\vec{r}, \vec{r}')$ is the Green's function defined as

$$G(\vec{r}, \vec{r}') = \frac{e^{-\gamma |\vec{r} - \vec{r}'|}}{4\pi |\vec{r} - \vec{r}'|} ; \quad (1.7)$$

and

$$|\vec{r} - \vec{r}'|^2 = [\psi - a - b \cos(\xi')]^2 + [z + b \sin(\xi')]^2 + 4\psi \sin^2\left(\frac{\phi - \phi'}{2}\right) [a + b \cos(\xi')] \quad (1.8)$$

Since the field solutions are in integral form, some Fourier expansion techniques were suggested to simplify these equations. Under the assumption that $b^2 \ll a^2$ and $kb \ll 1$, J_{s_ξ} may be neglected and the total current may be written as

$$I(\phi) = 2\pi b J_{s_\phi}(\phi). \quad (1.9)$$

This current was Fourier expanded as

$$I(\phi) = \sum_{n=-\infty}^{\infty} I_n e^{-in\phi}. \quad (1.10)$$

For a delta-function voltage source V_0 and a total loading impedance Z uniformly distributed on the TORUS, it was found that

$$I_n = I_{-n} = V_0 \left\{ Z + \pi Z_0 a \left[\left(\frac{n^2 K_n}{ika} \right) + \frac{ika}{2} (K_{n-1} + K_{n+1}) \right] \right\}^{-1}, \quad (1.11)$$

where

$$K_o = \frac{1}{a\pi} \left\{ \ln \left(\frac{8a}{b} \right) - \pi S_o(ka) \right\}, \quad (1.12)$$

$$K_n = \frac{1}{a\pi} \left\{ K_o \left(\frac{nb}{a} \right) I_o \left(\frac{nb}{a} \right) + C_n - \pi S_{2n}(ka) \right\}, \quad (1.13)$$

and

$$C_n = \gamma_o - 2 \sum_{m=0}^{n-1} \frac{1}{2m+1} + \ln(4n). \quad (1.14)$$

Analytical approximations and numerical techniques for the integral of the Anger-Weber function S_m have been given in detail in Mathematics Note 25 [2] ; γ_o is Euler's constant, numerically about 0.5772157; I_o and K_o are the zero order of the modified bessel functions of the first and second kind respectively.

In order to produce a plane-wave-like field at the center of TORUS, it has been found that the suitable loading impedance on TORUS is a pure resistance

$$R_o = Z_o [\ln(8a/b) - 2] \quad (1.15)$$

This load will be used for Z in the following analysis. For convenient comparisons, the field will be normalized to the fields at the center at low frequencies as given below:

$$E_o = \frac{V_o Z_o}{2aR_o}, \quad (1.16)$$

$$H_o = \frac{V_o}{2aR_o}. \quad (1.17)$$

II. Current on the Toroidal Surface

Let's normalize the current in Eq. (1.10) by its D.C. values V_o/R_o . That is,

$$\dot{i}(\phi) = R_o I(\phi)/V_o = \dot{i}_o + 2 \sum_{n=1}^{\infty} \dot{i}_n \cos(n\phi), \quad (2.1)$$

where

$$\dot{i}_n = \dot{i}_{-n} = \left\{ \frac{Z}{R_o} + \pi \frac{Z_o}{R_o} a \left[\left(\frac{n^2 K_n}{ika} \right) + \frac{ika}{2} (K_{n-1} + K_{n+1}) \right] \right\}^{-1}. \quad (2.2)$$

The current mode \dot{i}_n is plotted in Fig. 2-1 with respect to ka for n from 0 to 10 for $Z = R_o$. Here, \dot{i}_n is a function of loading impedance and without load, the peak of \dot{i}_n will occur at $ka = n$. For a pure resistive load, the peak of \dot{i}_n appears near $ka = n$. For a given mode, the amplitude of \dot{i}_n increases as the b over a ratio is reduced. Although it has been shown by Wu [3] that \dot{i}_n is inversely proportional to n^2 for large n , the peak of \dot{i}_n actually decreases very slowly as n increases for small n . Therefore, it seems necessary to include a sufficient number of modes in order to get the total current distribution by Eq. (2.1). However, we will show in the following chapters that only a few modes are necessary for the fields near the center.

Figure 2-2 gives an example of $\dot{i}(\phi)$ for a given ka . Since a delta-gap source was used to approximate the actual drive terminals in the mathematical model, the result shall not apply to $\phi = 0$. Other than this point, the figure shows a very nice convergence after adding for more than 25 terms of Fourier components. The real part of current shows a faster convergence with the summation of as little as ten terms because a pure resistance R_o is used for the load. Here,

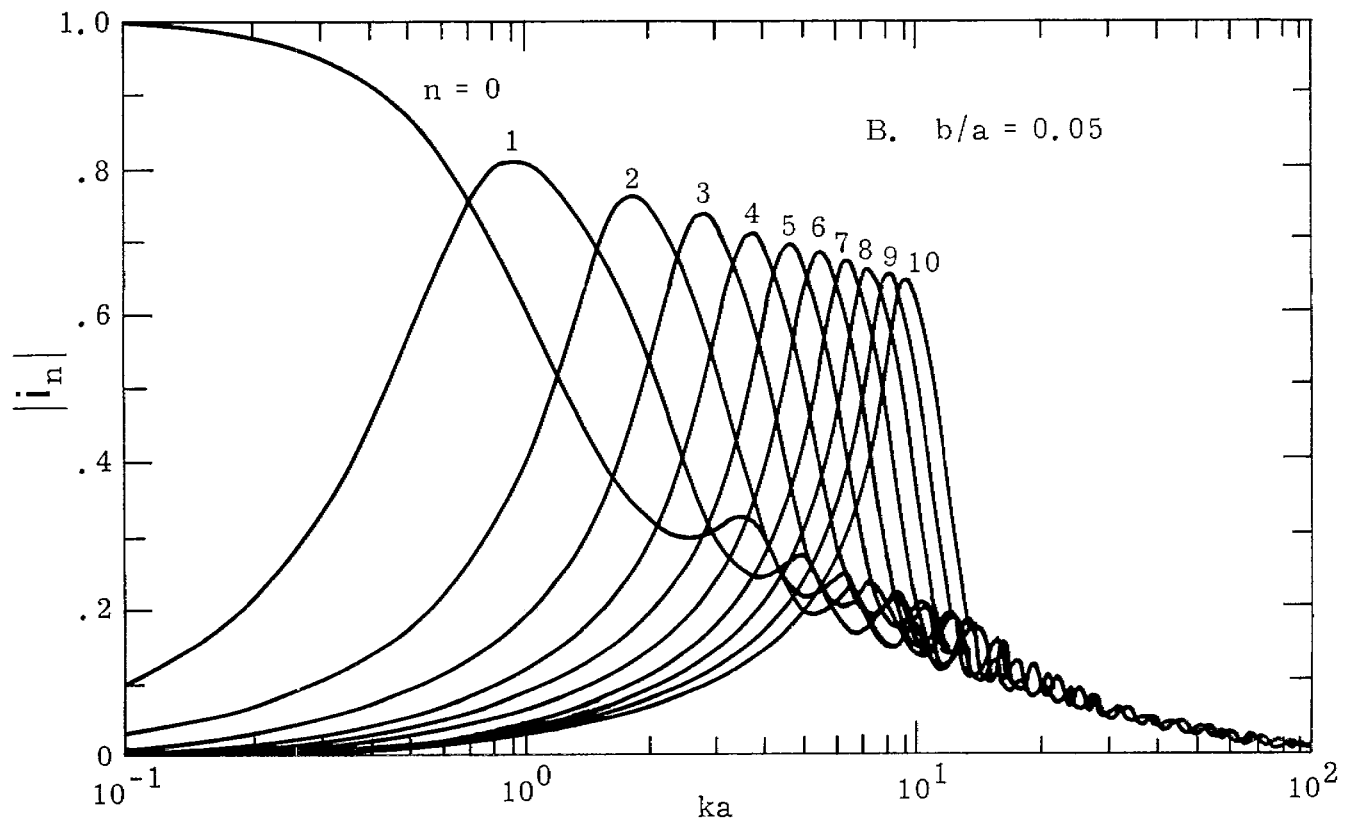
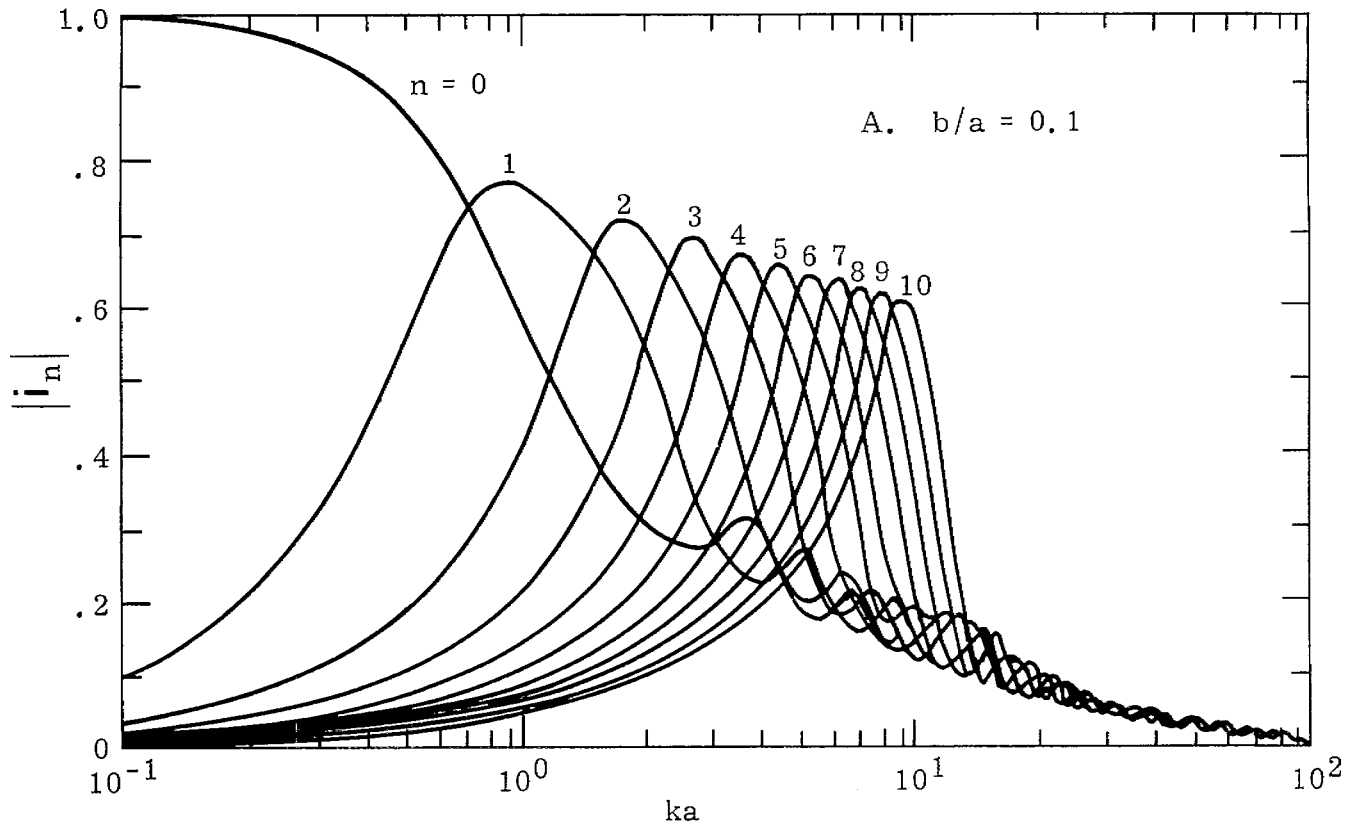


Figure 2-1. Absolute Value of i_n for $Z/Z_0 = \ln(8a/b) - 2$

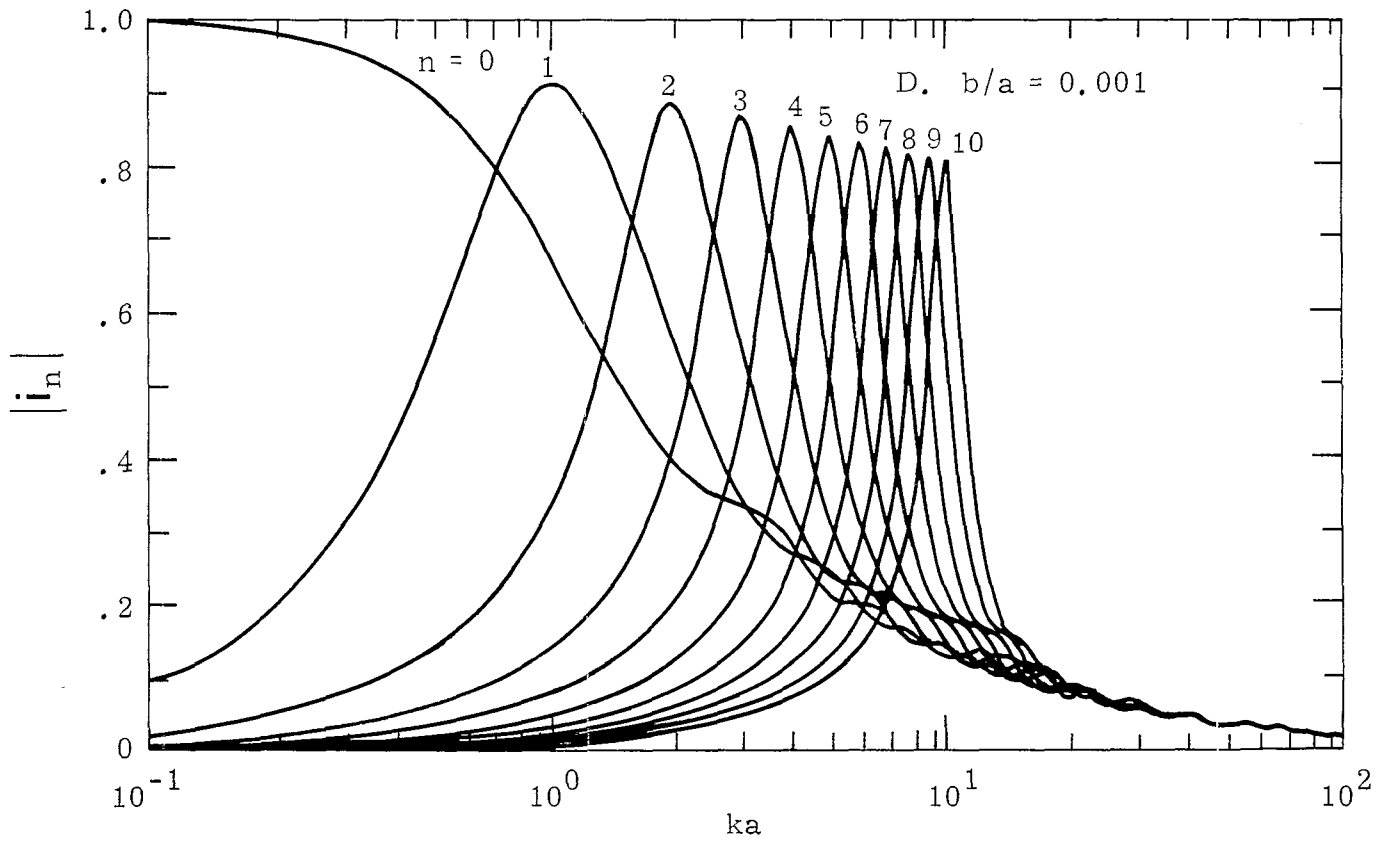
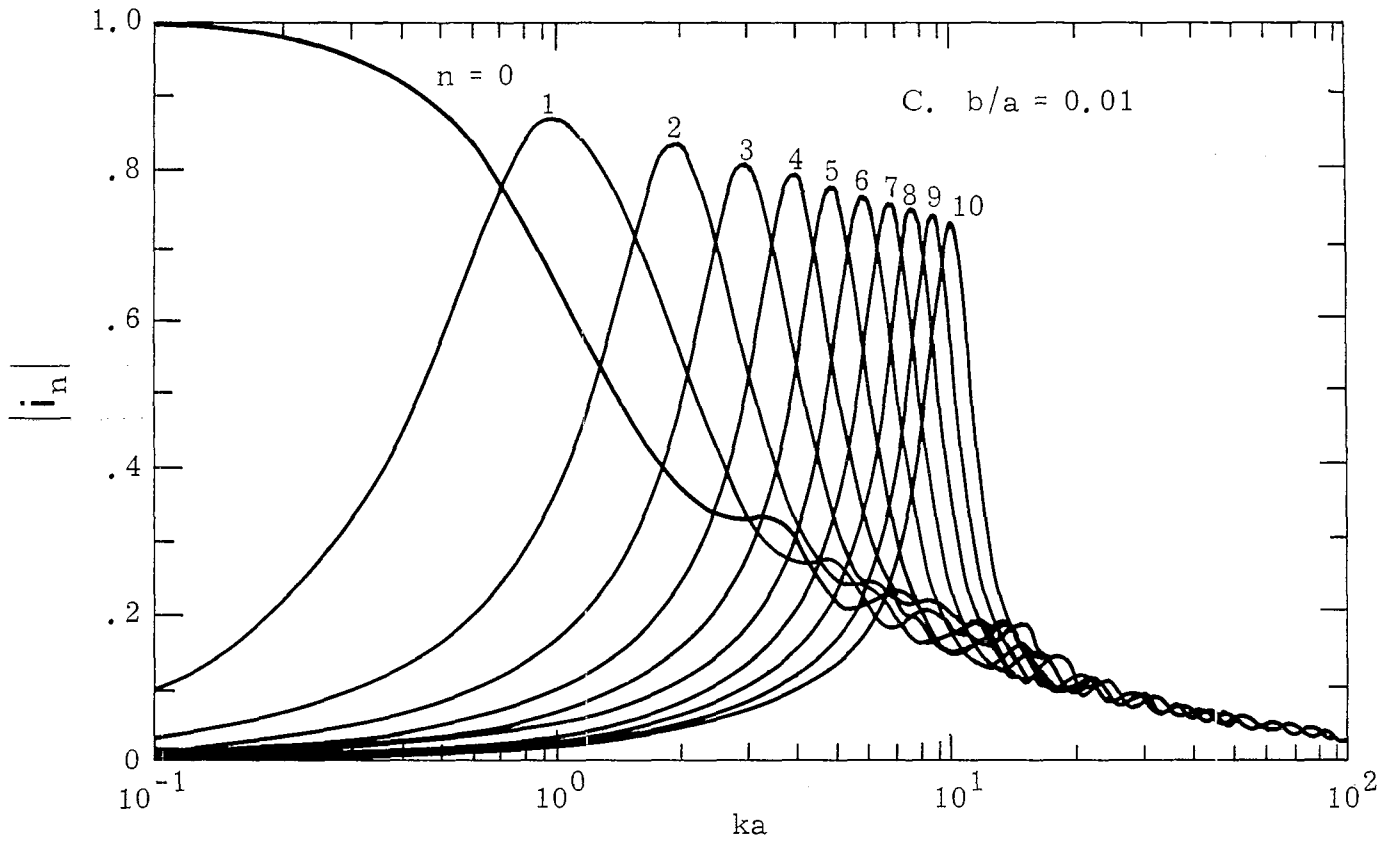


Figure 2-1. (continued)

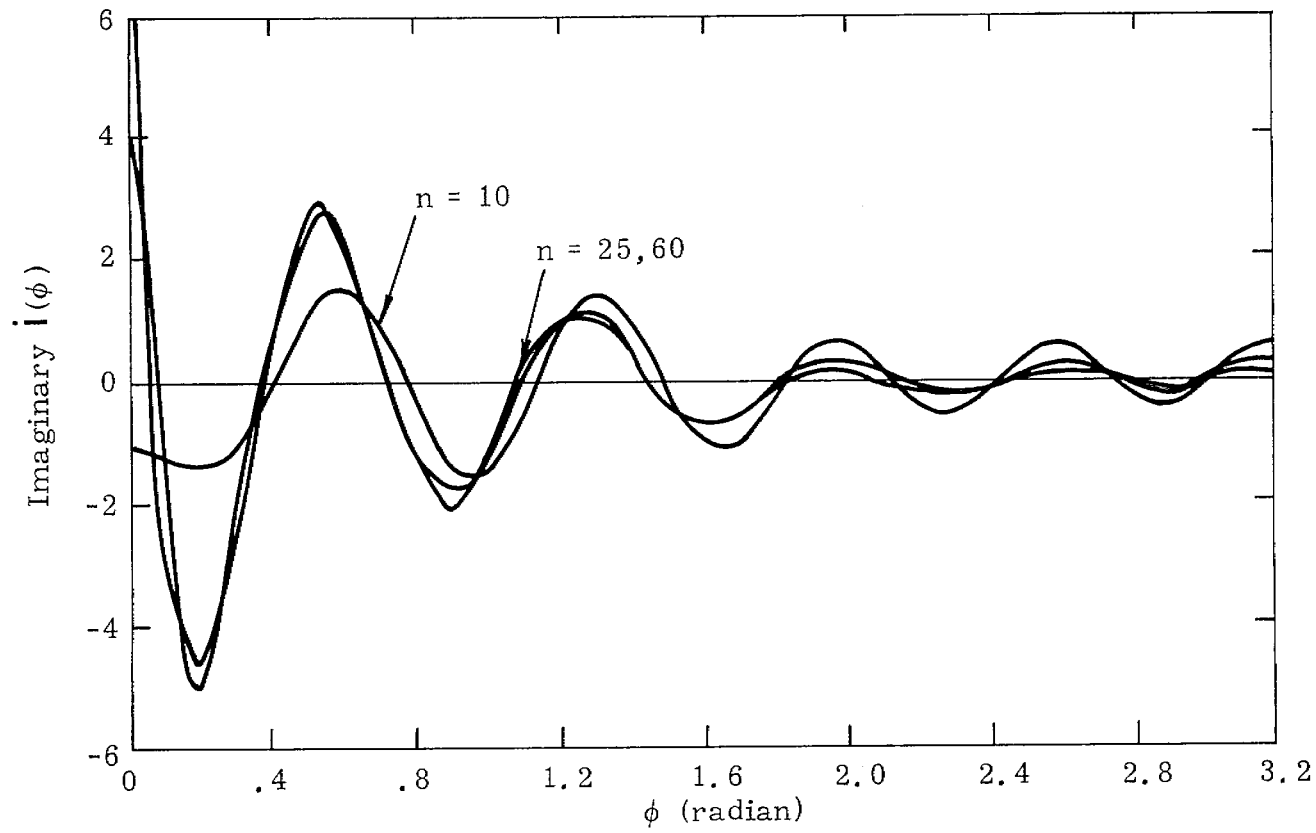
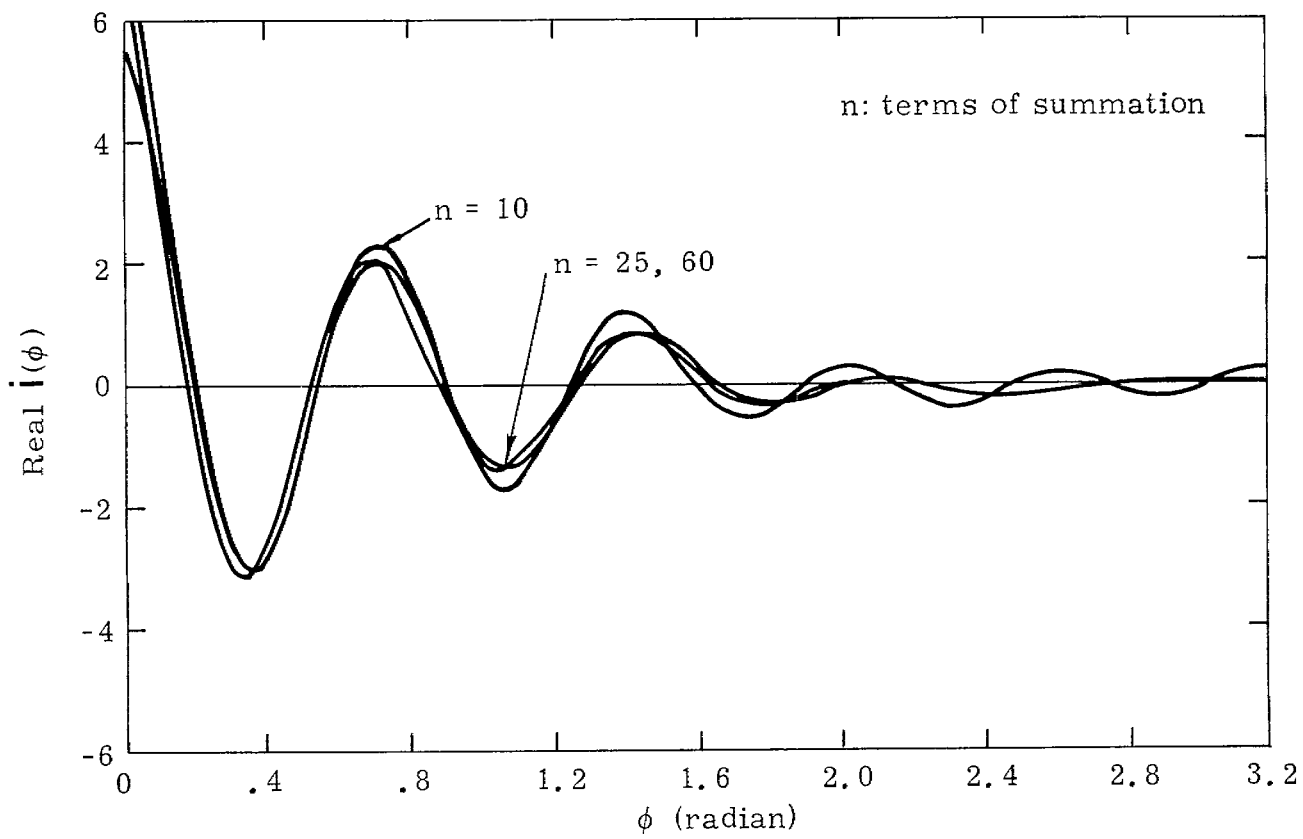


Figure 2-2. $\tilde{i}(\phi)$ for $Z/Z_0 = \ln(8a/b) - 2$ and $ka = 9$

$\ln(2\pi a/b) = 10$ (or $b/a = 0.042$) was used in order to compare with the calculation from direct integrations by Licking, et al. [4]. Both results appear similar except that in this note a somewhat lower amplitude is obtained due to a loading resistance. The computation here, of course, is much faster as compared to their numerical integration because analytical expressions were used for the integral of the Anger-Weber function [2].

III. Fourier Expansions for the Green's Function

The field near the center is the main interest of this study. Let $\psi = \psi a$, the field on the plane of TORUS, namely $z = 0$ and the range of ψ from 0 to 0.25 will be considered first in this note. Since $a^2 \gg b^2$ was assumed, Eq. (1.7) now becomes

$$G(\psi, \phi, 0) = \frac{e^{-ikaD}}{4\pi aD} \quad (3.1)$$

where

$$D = [(\psi - 1)^2 + 4\psi \sin^2(\frac{\phi}{2})]^{1/2} \quad (3.2)$$

This Green's function may be written in terms of Fourier coefficients

$$G(\psi, \phi, 0) = \sum_{n=-\infty}^{\infty} a^{-1} G_n(\psi) e^{-in\phi} \quad (3.3)$$

where

$$\begin{aligned}
 G_n(\psi) &= \frac{1}{2\pi} \int_0^{2\pi} \frac{e^{-ikaD}}{4\pi D} e^{in\phi} d\phi \\
 &= G_{-n}(\psi).
 \end{aligned}
 \tag{3.4}$$

It will be very time-consuming to calculate Eq. (3.4) by direct numerical integration. Since $\psi < 0.25$ is the range of interest, one may use some Taylor expansion technique to reduce Eq. (3.4) into an analytical form. Neglecting terms of the order of ψ^3 and higher,

$$D \approx 1 - \psi \cos(\phi) + \frac{\psi^2}{4} [1 - \cos(2\phi)]
 \tag{3.5}$$

and

$$D^{-1} \approx 1 + \psi \cos(\phi) + \frac{\psi^2}{4} [1 + 3 \cos(2\phi)]
 \tag{3.6}$$

Therefore, for $n \geq 0$, Eq. (3.4) becomes

$$\begin{aligned}
 G_n(\psi) &= \frac{1}{2\pi} \int_0^{2\pi} \frac{e^{-ika [1 - \psi \cos(\phi) + \frac{\psi^2}{4} (1 - \cos(2\phi))]} e^{in\phi}}{4\pi [1 - \psi \cos(\phi) + \frac{\psi^2}{4} (1 - \cos(2\phi))]} d\phi \\
 &\approx \frac{e^{-\frac{ika\psi^2}{4}}}{8\pi^2} \int_0^{2\pi} e^{-ika[1 - \psi \cos(\phi)]} e^{in\phi} [1 + \psi \cos(\phi) + \frac{\psi^2}{4} (1 + 3 \cos(2\phi))] \\
 &\quad \times [1 + \frac{ika\psi^2}{4} \cos(2\phi)] d\phi
 \end{aligned}$$

$$\approx \frac{e^{-ika\psi^2/4}}{8\pi^2} \int_0^{2\pi} e^{-ika[1-\psi \cos(\phi)]} e^{im\phi} \left[\left(1 + \frac{\psi^2}{4}\right) + \frac{\psi}{2} (e^{i\phi} + e^{-i\phi}) + \frac{\psi^2}{8} (3 + ika)(e^{i2\phi} + e^{-i2\phi}) \right] d\phi. \quad (3.7)$$

For a periodic function, [5]

$$\begin{aligned} P_m &= \frac{1}{2\pi} \int_0^{2\pi} e^{-ika[1-\psi \cos(\phi)]} e^{im\phi} d\phi = \frac{e^{-ika}}{2\pi} \int_{-\pi/2}^{3\pi/2} e^{ika\psi \cos(\phi)} e^{im\phi} d\phi \\ &= \frac{e^{-ika}}{2\pi} \int_{-\pi}^{\pi} e^{-ika\psi \sin(\phi)} e^{im\phi} e^{i\frac{m\pi}{2}} d\phi \\ &= \frac{e^{-i(ka - \frac{m\pi}{2})}}{2\pi} \left\{ \int_0^{\pi} e^{i[m\phi - ka\psi \sin(\phi)]} d\phi + \int_{-\pi}^0 e^{i[m\phi - ka\psi \sin(\phi)]} d\phi \right\} \\ &= e^{-i(ka - \frac{m\pi}{2})} \int_0^{\pi} \frac{\cos[m\phi - ka\psi \sin(\phi)]}{\pi} d\phi \\ &= e^{-i(ka - m\pi/2)} J_m(ka\psi) \end{aligned} \quad (3.8)$$

So, an analytical expression for Eq. (3.7) is now obtained,

$$\begin{aligned}
G_n(\psi) = & \frac{e^{-ika(1+\psi^2/4)+in\pi/2}}{4\pi} \left\{ \left(1 + \frac{\psi^2}{4}\right) J_n(ka\psi) \right. \\
& - \frac{\psi^2}{8} (3+ika) [J_{n+2}(ka\psi) + J_{n-2}(ka\psi)] \\
& \left. + \frac{\psi}{2} i [J_{n+1}(ka\psi) - J_{n-1}(ka\psi)] \right\} = G_{-n}(\psi) \quad (3.9)
\end{aligned}$$

This formula is very accurate for $n=0, 1, 2, 3$ and the accuracy decreases as n increases. Since $\psi \leq 0.25$ is the range of interest, the maximum n needed to consider is probably around 15. The error in Eq. (3.9) for $n \leq 15$ is less than 10%. Actually, the field depends on G_n in a very complex manner. An analytical expression for the G_n certainly is much desired. Moreover, the computation for Eq. (3.9) is hundreds of times faster than for direct integration. Figures 3-1 and 3-2 give examples for G_n for $\psi = 0.1$ and $\psi = 0.25$. The peak of G_n decreases as n increases; this is also a general tendency observed for the \dot{i}_n . This phenomenon becomes more apparent as we move toward the center. On the other hand, the number of oscillations for G_n increase with respect to the frequency as ψ increases.

IV. Fourier Modes for the E-Field

In the following analysis, we will consider that the TORUS is located in free space, i. e., $\gamma = ik = i\omega\sqrt{\mu_0\epsilon_0}$. Using Eq. (1.9) and neglecting J_ξ by assuming $b^2 \ll a^2$, Eqs. (1.1) and (1.2) will be reduced to

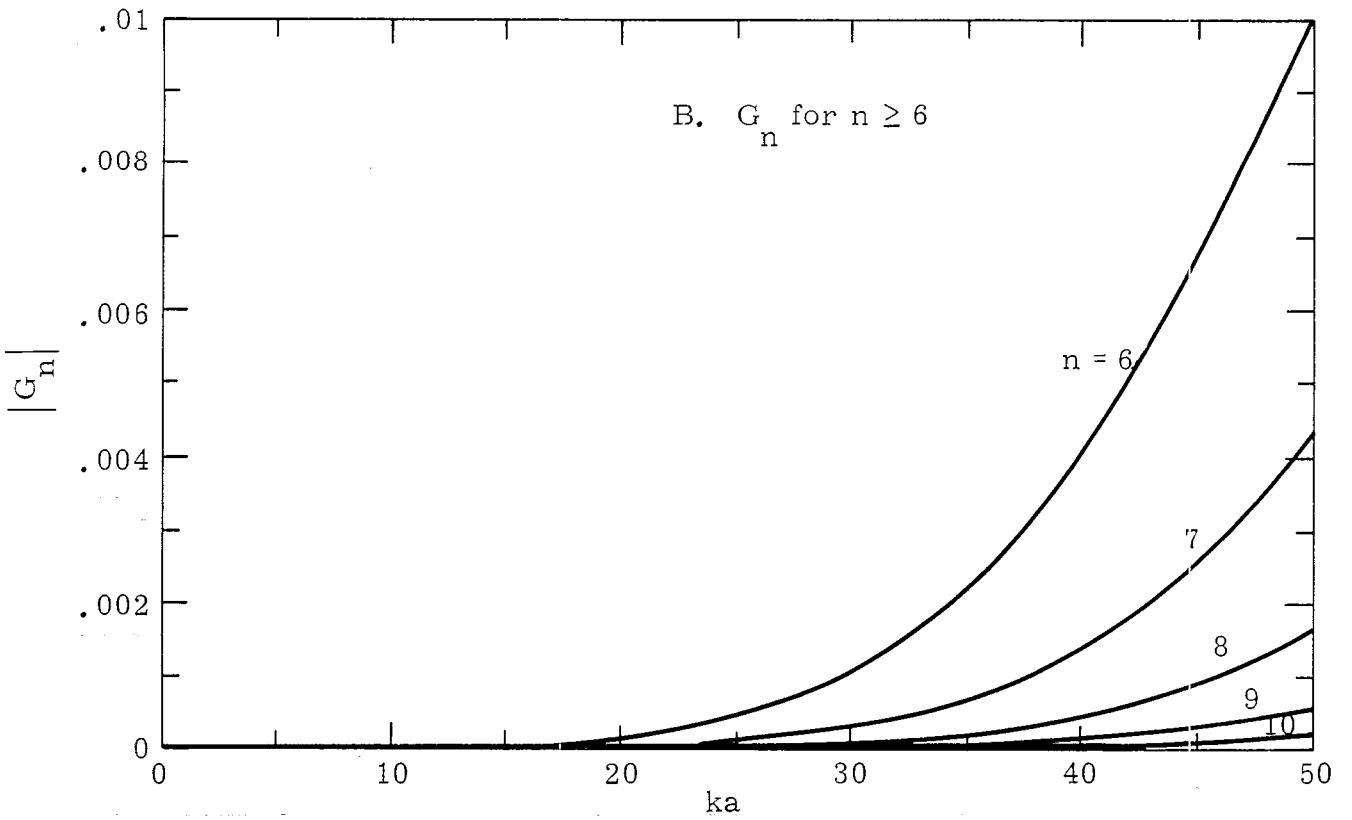
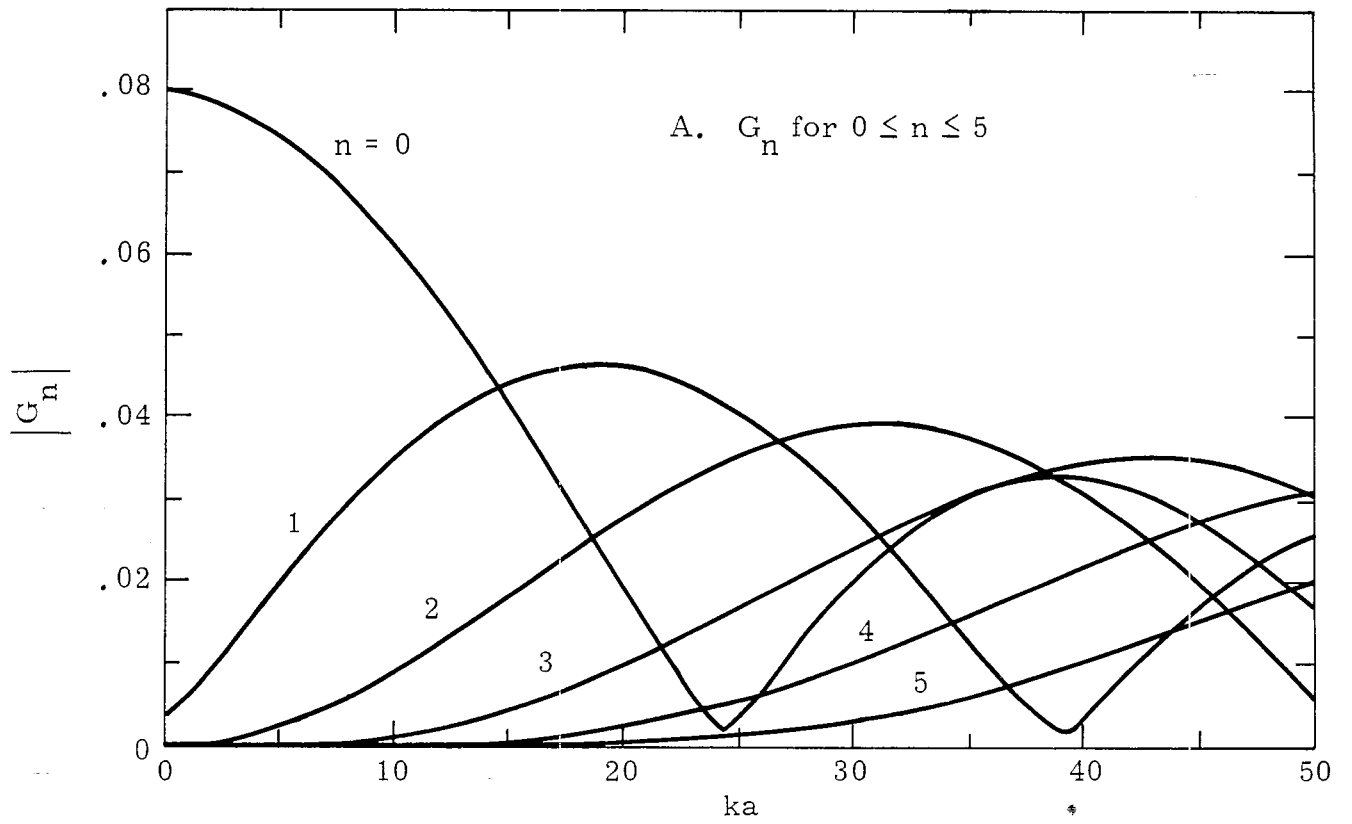


Figure 3-1. $G_n(\psi)$ for $\psi = 0.1$

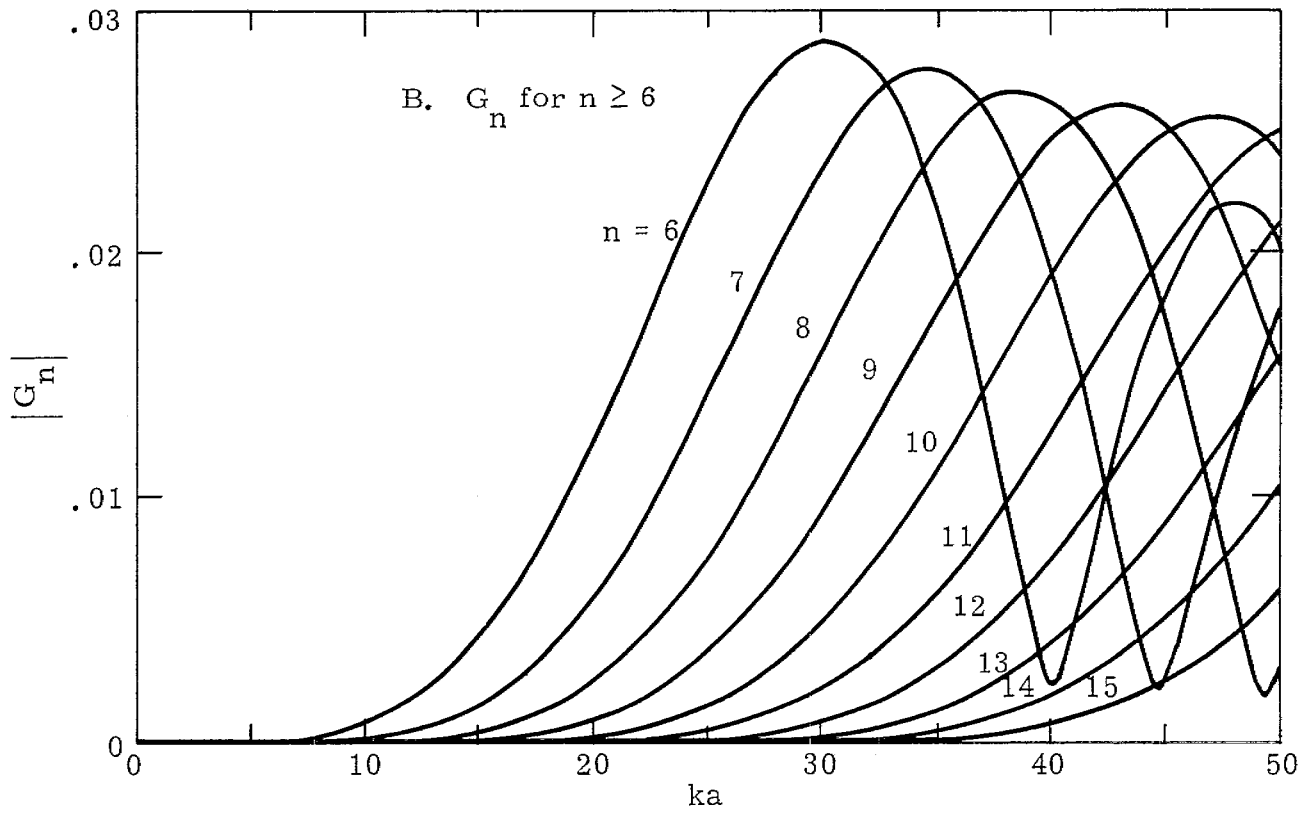
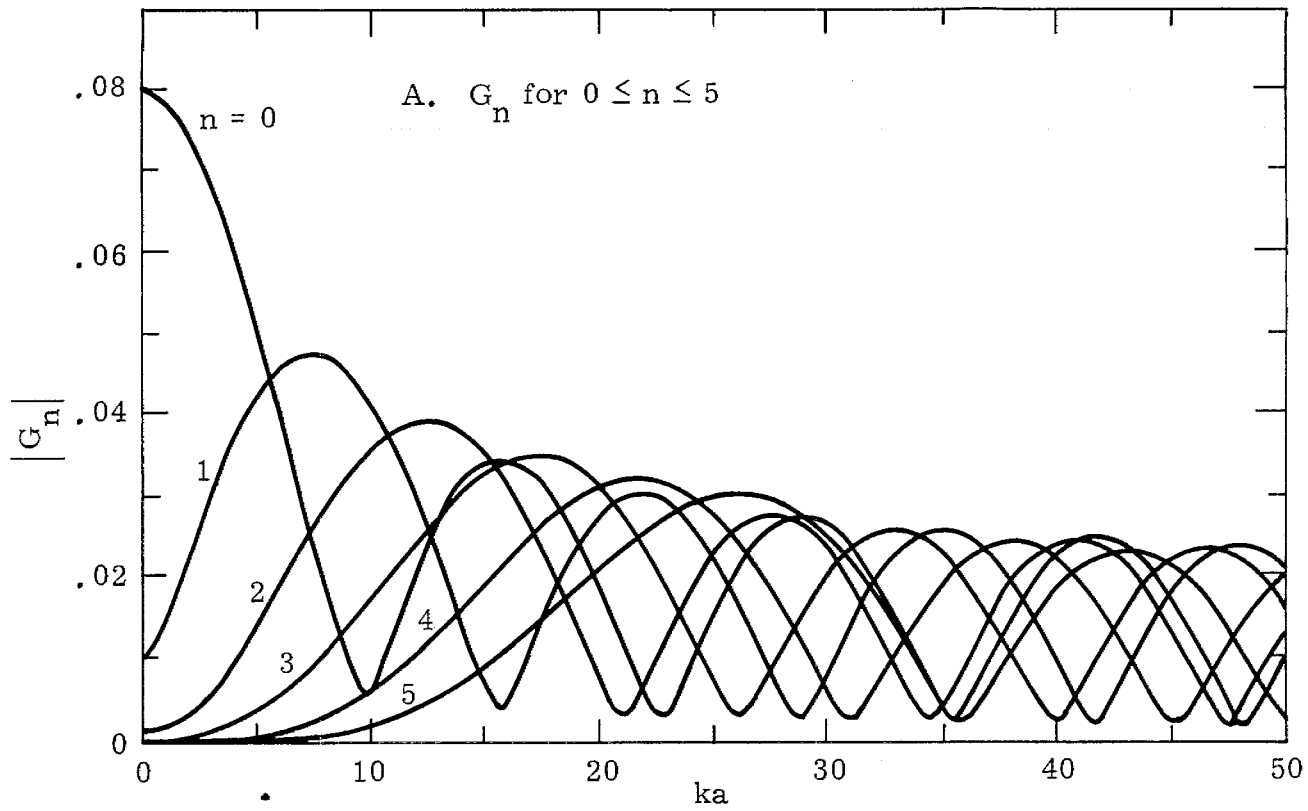


Figure 3-2. $G_n(\psi)$ for $\psi = 0.25$

$$\begin{aligned} \frac{ik}{Z_0} E_\psi &= \frac{\partial}{\partial \psi} \iint_{S'} \left\{ G(\vec{r}, \vec{r}') \frac{\partial}{\partial \phi'} \left[\frac{I(\phi')}{2\pi} \right] \right\} d\xi' d\phi' \\ &+ k^2 a \iint_{S'} \left\{ G(\vec{r}, \vec{r}') \sin(\phi - \phi') \left[\frac{I(\phi')}{2\pi} \right] \right\} d\xi' d\phi', \end{aligned} \quad (4.1)$$

$$\begin{aligned} \frac{ik}{Z_0} E_\phi &= \frac{1}{\psi} \frac{\partial}{\partial \phi} \iint_{S'} \left\{ G(\vec{r}, \vec{r}') \frac{\partial}{\partial \phi'} \left[\frac{I(\phi')}{2\pi} \right] \right\} d\xi' d\phi' \\ &+ k^2 a \iint_{S'} \left\{ G(\vec{r}, \vec{r}') \cos(\phi - \phi') \left[\frac{I(\phi')}{2\pi} \right] \right\} d\xi' d\phi' \end{aligned} \quad (4.2)$$

And $E_z(\psi, \phi, o)$ is identically zero by symmetry.

For locations near the center, the Green's function depends only on ψ and ϕ as given in Eq. (3.1). Therefore Eqs. (4.1) and (4.2) now become

$$\begin{aligned} \frac{ika}{Z_0} E_\psi(\psi, \phi, o) &= \frac{\partial}{\partial \psi} \int_0^{2\pi} \left\{ G(\psi, \phi - \phi', o) \frac{\partial I(\phi')}{\partial \phi'} \right\} d\phi' \\ &+ k^2 a^2 \int_0^{2\pi} G(\psi, \phi - \phi', o) \sin(\phi - \phi') I(\phi') d\phi', \end{aligned} \quad (4.3)$$

$$\begin{aligned} \frac{ika}{Z_0} E_\phi(\psi, \phi, o) &= \frac{1}{\psi} \frac{\partial}{\partial \phi} \int_0^{2\pi} \left\{ G(\psi, \phi - \phi', o) \frac{\partial I(\phi')}{\partial \phi'} \right\} d\phi' \\ &+ k^2 a^2 \int_0^{2\pi} \left\{ G(\psi, \phi - \phi', o) \cos(\phi - \phi') I(\phi') \right\} d\phi'. \end{aligned} \quad (4.4)$$

If this field is normalized to its D. C. value at the center given in Eq. (1.16), one obtains

$$\begin{aligned} E_{\psi}(\psi, \phi, 0) = \frac{\partial}{ika} \left\{ \frac{\partial}{\partial \psi} \int_0^{2\pi} \sum_{m=-\infty}^{\infty} G_m(\psi) e^{-im(\phi - \phi')} \sum_{n=-\infty}^{\infty} (-in i_n) e^{-in\phi'} d\phi' \right. \\ \left. - k^2 a^2 \int_0^{2\pi} \sum_{m=-\infty}^{\infty} G_m(\psi) e^{-im(\phi - \phi')} \sin(\phi - \phi') \sum_{n=-\infty}^{\infty} i_n e^{-in\phi'} d\phi' \right\}, \end{aligned} \quad (4.5)$$

$$\begin{aligned} E_{\phi}(\psi, \phi, 0) = \frac{\partial}{ika} \left\{ \frac{1}{\psi} \frac{\partial}{\partial \phi} \int_0^{2\pi} \sum_{m=-\infty}^{\infty} G_m(\psi) e^{-im(\phi - \phi')} \sum_{n=-\infty}^{\infty} (-in i_n) e^{-in\phi'} d\phi' \right. \\ \left. - k^2 a^2 \int_0^{2\pi} \sum_{m=-\infty}^{\infty} G_m(\psi) e^{-im(\phi - \phi')} \cos(\phi - \phi') \sum_{n=-\infty}^{\infty} i_n e^{-in\phi'} d\phi' \right\} \end{aligned} \quad (4.6)$$

They are finally reduced to

$$E_{\psi}(\psi, \phi, 0) = \sum_{n=-\infty}^{\infty} -2\pi i_n \left\{ \left(\frac{2n}{ka} \right) G_n'(\psi) + ka [G_{n+1}(\psi) - G_{n-1}(\psi)] \right\} e^{-in\phi} \quad (4.7)$$

$$E_{\phi}(\psi, \phi, 0) = \sum_{n=-\infty}^{\infty} -2\pi i_n \left\{ \left(\frac{2n^2}{\psi ika} \right) G_n(\psi) + ika [G_{n+1}(\psi) + G_{n-1}(\psi)] \right\} e^{-in\phi}. \quad (4.8)$$

Now, we may define the Fourier modes for the E-field as follows:

$$N_{\psi n}(\psi, \phi, 0) = -iN_{\psi n}(\psi, 0) e^{-in\phi} \quad (4.9)$$

$$N_{\psi_n}(\psi, \phi) = 2\pi \left\{ \left(\frac{2n}{ika} \right) G_n'(\psi) - ika \left[G_{n+1}(\psi) - G_{n-1}(\psi) \right] \right\}, \quad (4.10)$$

$$N_{\phi_n}(\psi, \phi, \phi) = N_{\phi_n}(\psi, \phi) e^{-in\phi} \quad (4.11)$$

$$N_{\phi_n}(\psi, \phi) = -2\pi \left\{ \left(\frac{2n^2}{\psi ika} \right) G_n(\psi) + ika \left[G_{n+1}(\psi) + G_{n-1}(\psi) \right] \right\} \quad (4.12)$$

It is not difficult to show that

$$N_{\psi_n}(\psi, \phi) = -N_{\psi_{(-n)}}(\psi, \phi), \quad (4.13)$$

$$N_{\psi_0}(\psi, \phi) = 0 \quad (4.14)$$

and

$$N_{\phi_n}(\psi, \phi) = N_{\phi_{(-n)}}(\psi, \phi). \quad (4.15)$$

Then the electric field can be written in terms of these Fourier modes:

$$E_{\psi}(\psi, \phi, \phi) = \sum_{n=-\infty}^{\infty} i_n N_{\psi_n}(\psi, \phi, \phi) = -2 \sum_{n=1}^{\infty} i_n N_{\psi_n}(\psi, \phi) \sin(n\phi) \quad (4.16)$$

and

$$E_{\phi}(\psi, \phi, \phi) = \sum_{n=-\infty}^{\infty} i_n N_{\phi_n}(\psi, \phi, \phi) = i_0 N_{\phi_0}(\psi, \phi) + 2 \sum_{n=1}^{\infty} i_n N_{\phi_n}(\psi, \phi) \cos(n\phi). \quad (4.17)$$

The above analysis concentrates on the plane of TORUS for the purpose of demonstration. Actually, the mode expansion technique is also valid at other locations. So, we may write the field in terms of the Fourier modes in the following general form:

$$\vec{E}(\psi, \phi, z) = \sum_{n=-\infty}^{\infty} i_n \vec{N}_n(\psi, \phi, z) \quad (4.18)$$

These Fourier modes \vec{N}_n are the general solutions for a circular loop and are completely independent of the loading impedances as well as the source functions of the antenna. They are equivalent to the mode structures in a waveguide and can be calculated in advance regardless of the current distribution on the loop. The factor i_n may be considered as the excitation factor of each mode. It depends on the antenna property such as the source functions and the loading impedances; and in this case, a over b ratio. Here, i_n may be calculated analytically such as that described in Chapter II or numerically such as that discussed in references [6, 7, 8]. Figures 4-1 to 4-4 give some example of the mode structures. Near the center (e.g., $\psi = 0.1$), the zero order mode dominates the ϕ component in the low frequencies up to $ka = 30$ and the first order mode dominates the ψ component for ka up to 15. Although some other modes might become important at higher frequencies, the amplitude for mode numbers greater than five decays very fast as n increases. Away from the center (e.g., $\psi = 0.25$), a few modes still dominate the field at very low frequencies. But then, one would require about 15 modes as ka approaches 50. Therefore, at low frequencies or at locations very close to the center (symmetry point), only a few modes are important. As the frequency increases or as one moves away from the center, then more and more modes have to be taken into account to get the field pattern. The highest frequency

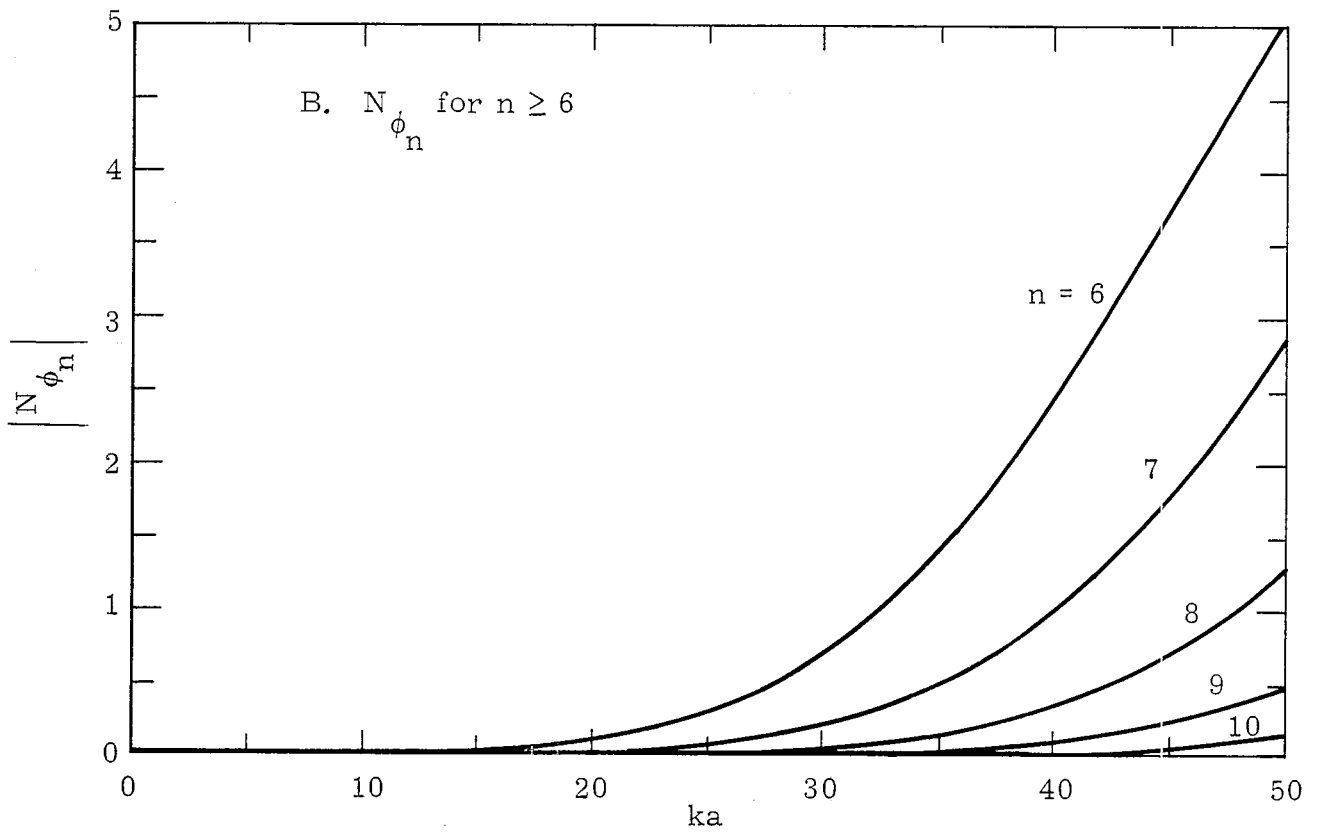
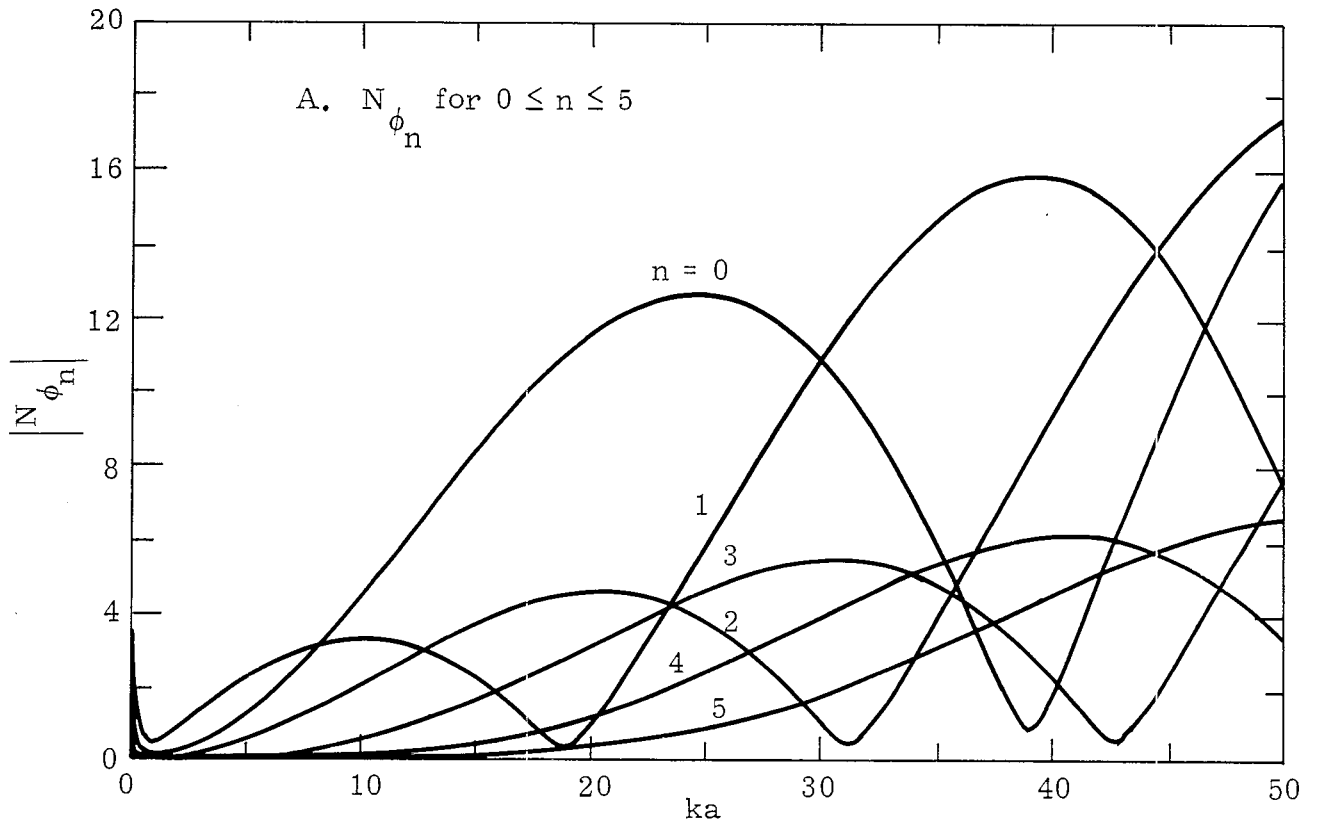


Figure 4-1. $N_{\phi_n}(\psi, 0)$ for $\psi = 0.1$

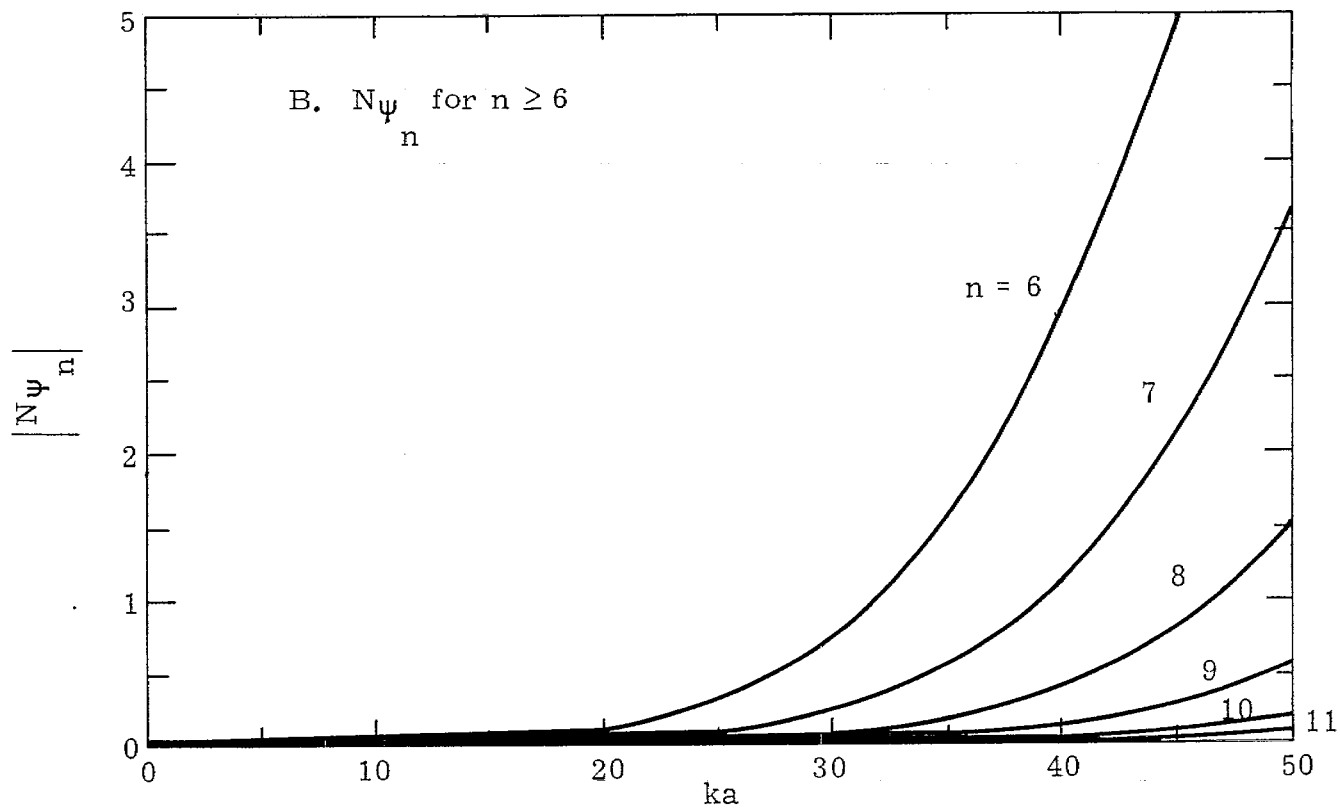
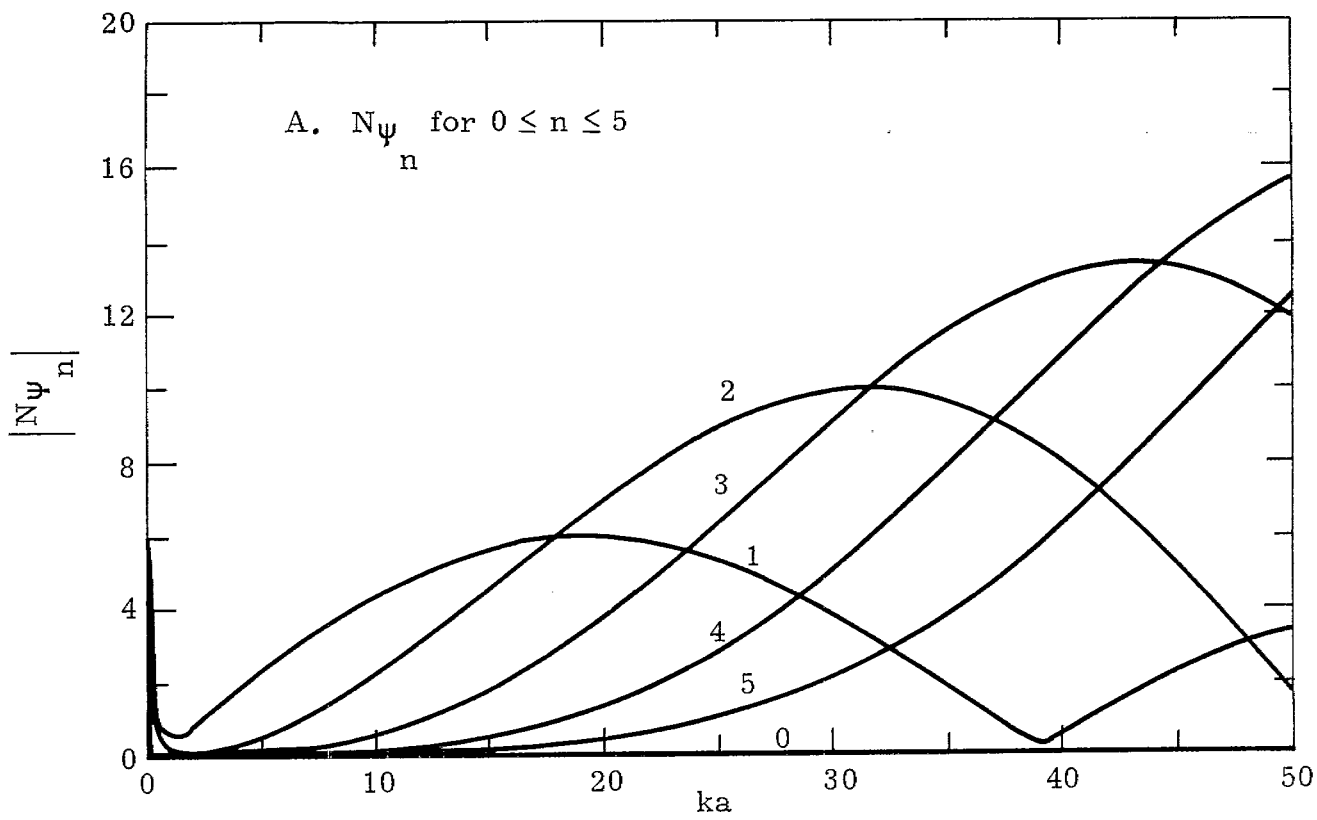


Figure 4-2. $N_{\psi_n}(\psi, 0)$ for $\psi = 0.1$

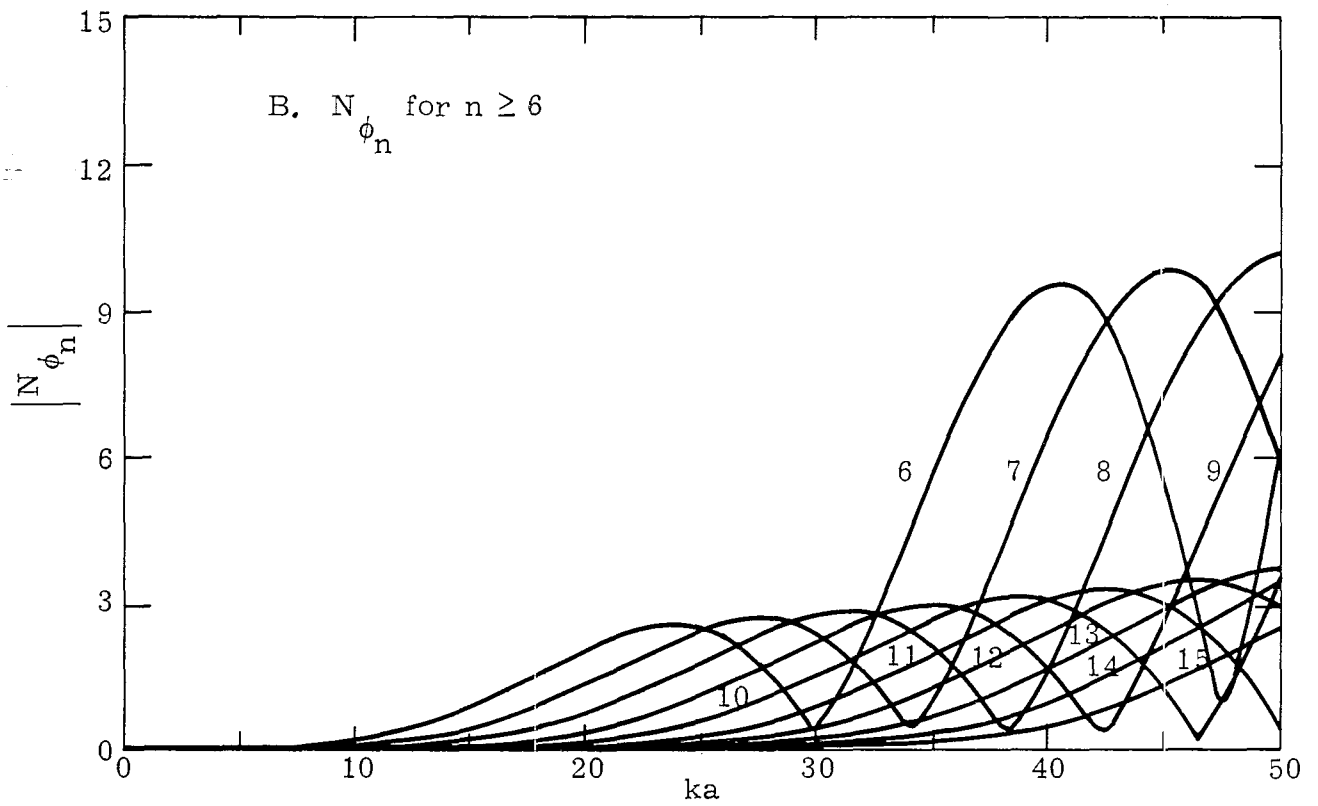
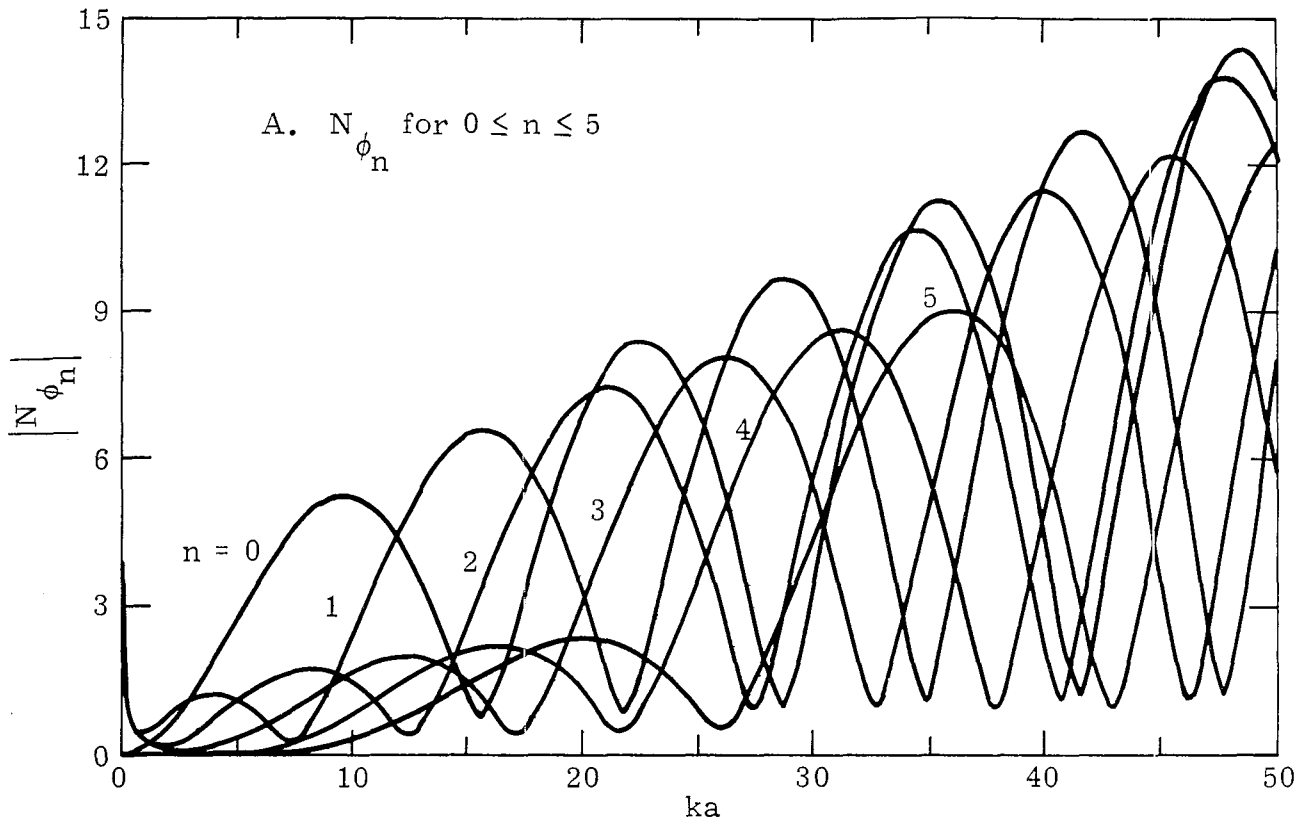


Figure 4-3. $N_{\phi_n}(\psi, 0)$ for $\psi = 0.25$

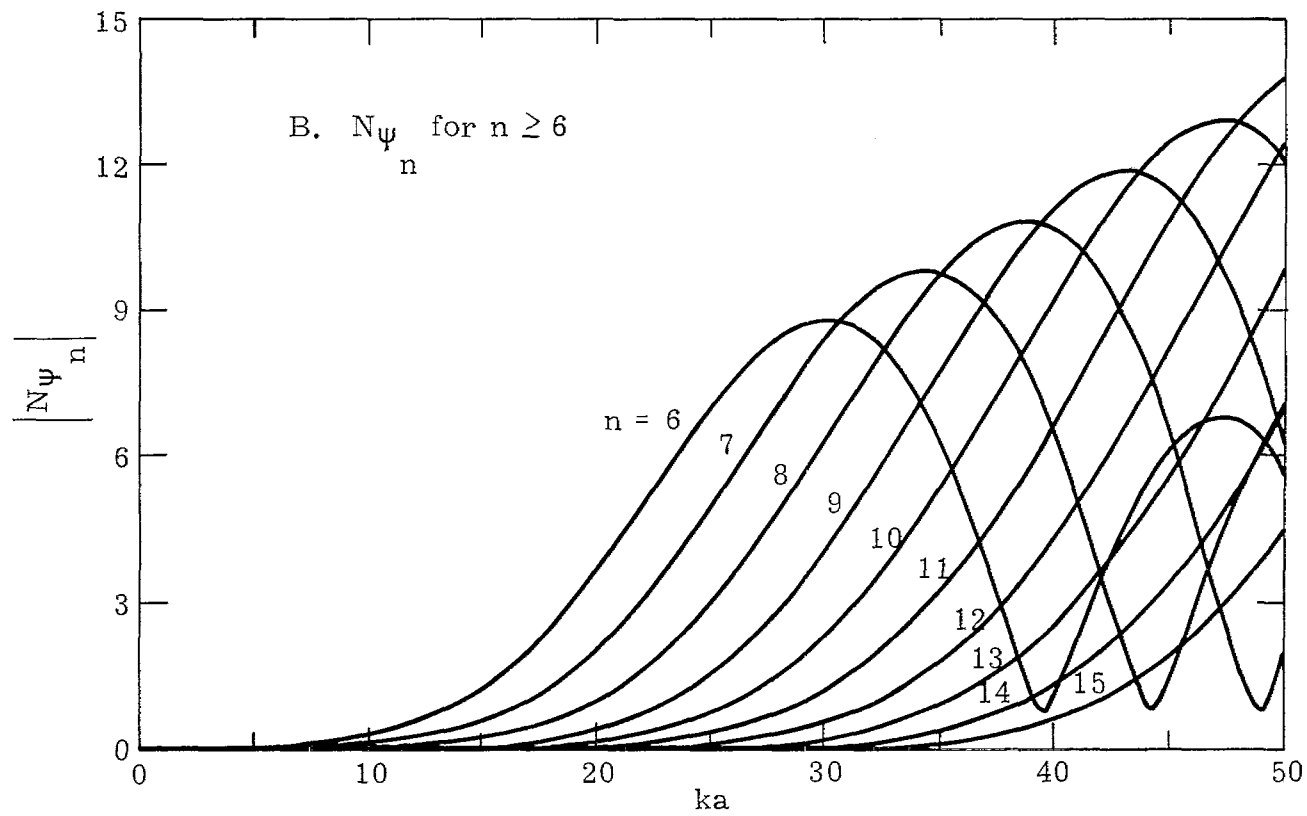
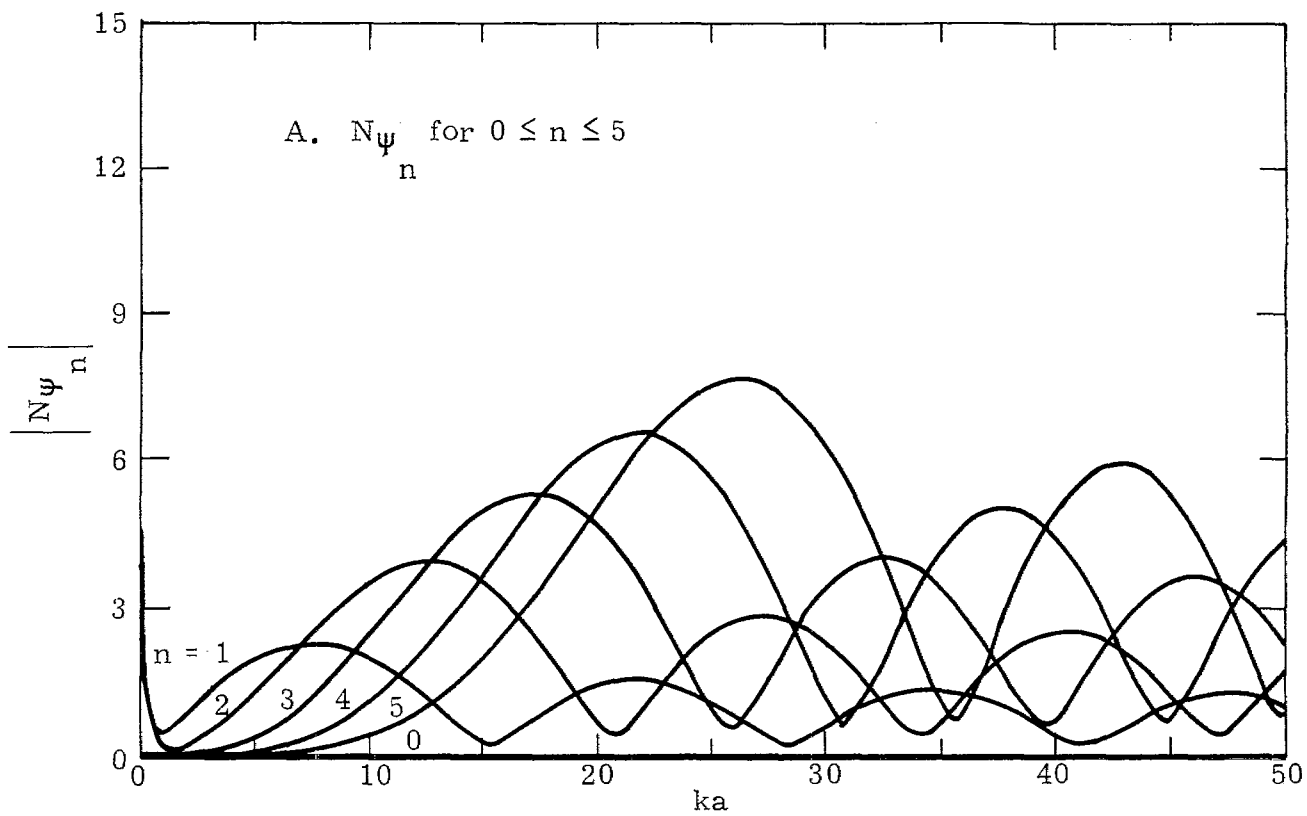


Figure 4-4. $N_{\psi_n}(\psi, 0)$ for $\psi = 0.25$

presented in this note by the mode theory is for $ka = 50$. This is because the analytical formula for the current given in Chapter II is only valid up to this region and one should not regard this as the frequency limit for the mode theory. Nevertheless, the mode theory is convenient for calculating the field at low frequencies since some simple asymptotic formulas can be used for high frequencies.

V. E-Field as a Function of ψ and ϕ in the Frequency Domain

Because of symmetry, only the first order mode will contribute to the electric field and the zero order mode to the magnetic field at the center. We will show here that Eq. (4.16) for $\phi = \pi/2$ and Eq. (4.17) for $\phi = 0$ as $\psi \rightarrow 0$ actually converges to that obtained in the previous note [1] by a different method.

The Fourier component of the Green's function $G_n(\psi)$ derived in Eq. (3.9) is related to the Bessel function which has the following property

$$J_n(x) \cong \frac{1}{\Gamma(n+1)} \left(\frac{x}{2}\right)^n \quad \text{for } x \ll 1 \quad (5.1)$$

where $\Gamma(n)$ is the Gamma function. Therefore, from Chapter IV,

$$\begin{aligned} E_{\phi}(\psi \rightarrow 0, 0, 0) &\cong 2i_1 \lim_{\psi \rightarrow 0} N_{\phi_1}(\psi) \\ &\cong -4\pi i_1 \lim_{\psi \rightarrow 0} \left\{ \left(\frac{2}{\psi ika} \right) G_1(\psi) + ika [G_2(\psi) + G_0(\psi)] \right\} \end{aligned}$$

$$\begin{aligned}
\Re &= i_1 e^{-ika} \lim_{\psi \rightarrow 0} \left\{ i \left(\frac{2}{\psi ika} \right) [\mathbf{J}_1(ka\psi) - \frac{\psi}{2} i \mathbf{J}_0(ka\psi)] + [ika \mathbf{J}_0(ka\psi)] \right\} \\
\Re &= i_1 e^{-ika} \left\{ \frac{2}{\psi ka} \left[\left(\frac{\psi ka}{2} \right) - \frac{\psi}{2} i \right] + ika \right\} \\
&= - i_1 \left(ika + 1 + \frac{1}{ika} \right) e^{-ika} \tag{5.2}
\end{aligned}$$

$$\begin{aligned}
\mathbf{E}_\psi(\psi \rightarrow 0, \pi/2, 0) &\cong - 2 i_1 \lim_{\psi \rightarrow 0} N_{\psi_1}(\psi) \\
&\cong - 4\pi i_1 \lim_{\psi \rightarrow 0} \left\{ \left(\frac{2}{ika} \right) G_1'(\psi) - ika [G_2(\psi) - G_0(\psi)] \right\} \\
&\cong - i_1 e^{-ika} \lim_{\psi \rightarrow 0} \left\{ \left(\frac{2}{ika} \right) \left[i \frac{\partial \mathbf{J}_1(ka\psi)}{\partial \psi} + \frac{1}{2} \mathbf{J}_0(ka\psi) \right] + ika \mathbf{J}_0(ka\psi) \right\} \\
&\cong - i_1 e^{-ika} \left\{ \left(\frac{2}{ika} \right) \left(\frac{ika}{2} + \frac{1}{2} \right) + ika \right\} \\
&= - i_1 \left(ika + 1 + \frac{1}{ika} \right) e^{-ika} \tag{5.3}
\end{aligned}$$

Equations (5.2) and (5.3) agree with our previous analysis using a different approach [1]. Figure 5-1 gives examples for the electric field very close to the center of TORUS calculated by the mode method and is identical to what has been obtained in SSN 160.

In the following plots, we will set the turn-on time for the source at

$$t = - \sqrt{(a-b)^2 - 2\psi a(b-a) \cos(\phi) + \psi^2 a^2} / c \tag{5.4}$$

In other words, the fields at various locations start to build up at $t = 0$. Using the results in Chapters II and IV, the relative field strength for the electric mode $i_n N_n$ in ϕ and ψ directions is shown in Figs. 5-2 and 5-3 at various distances from the center. The first order mode dominates

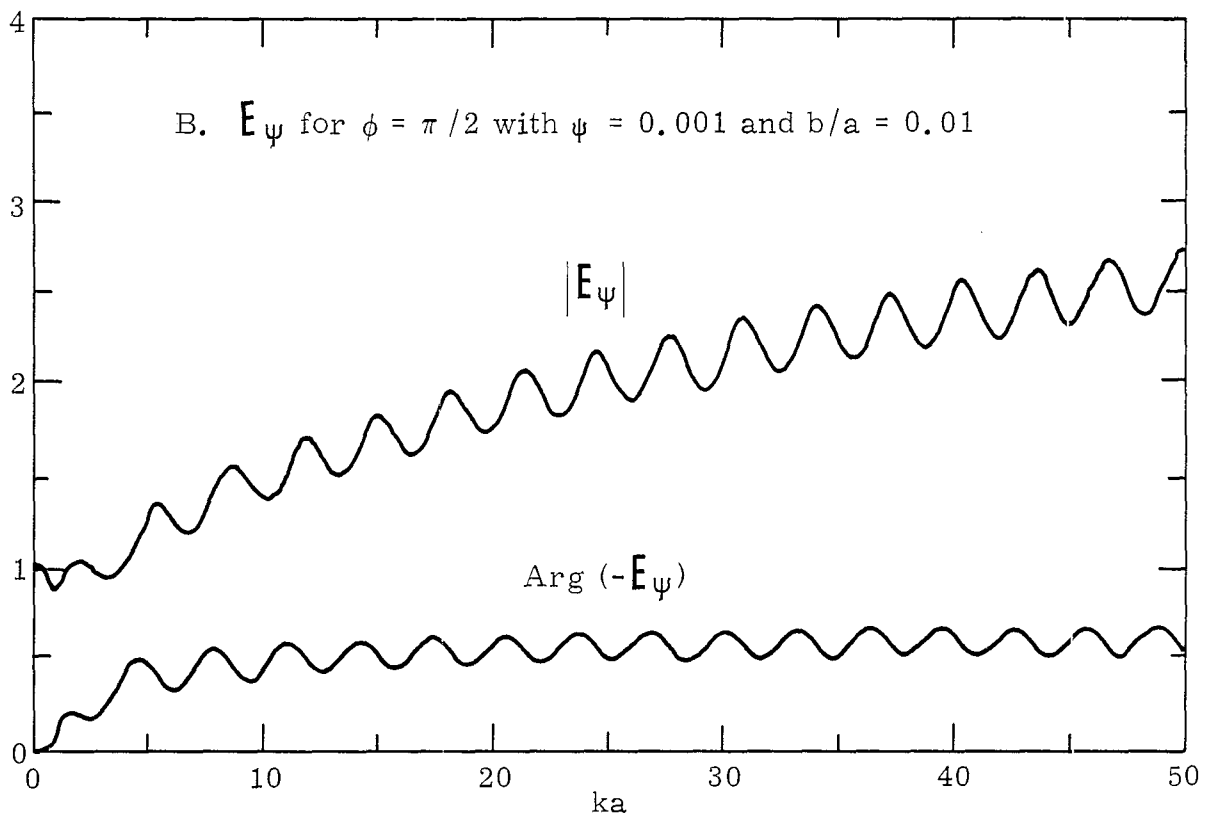
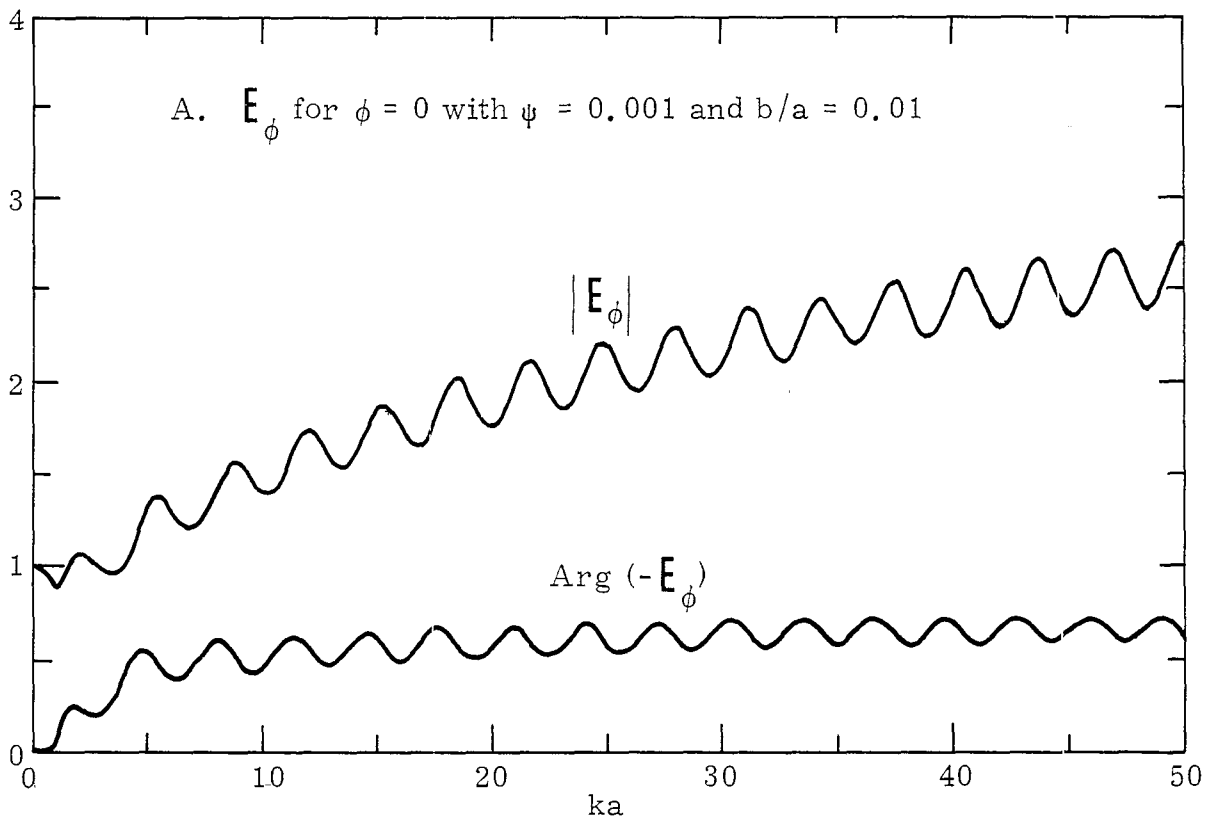


Figure 5-1. Electric Field Very Close to the Center

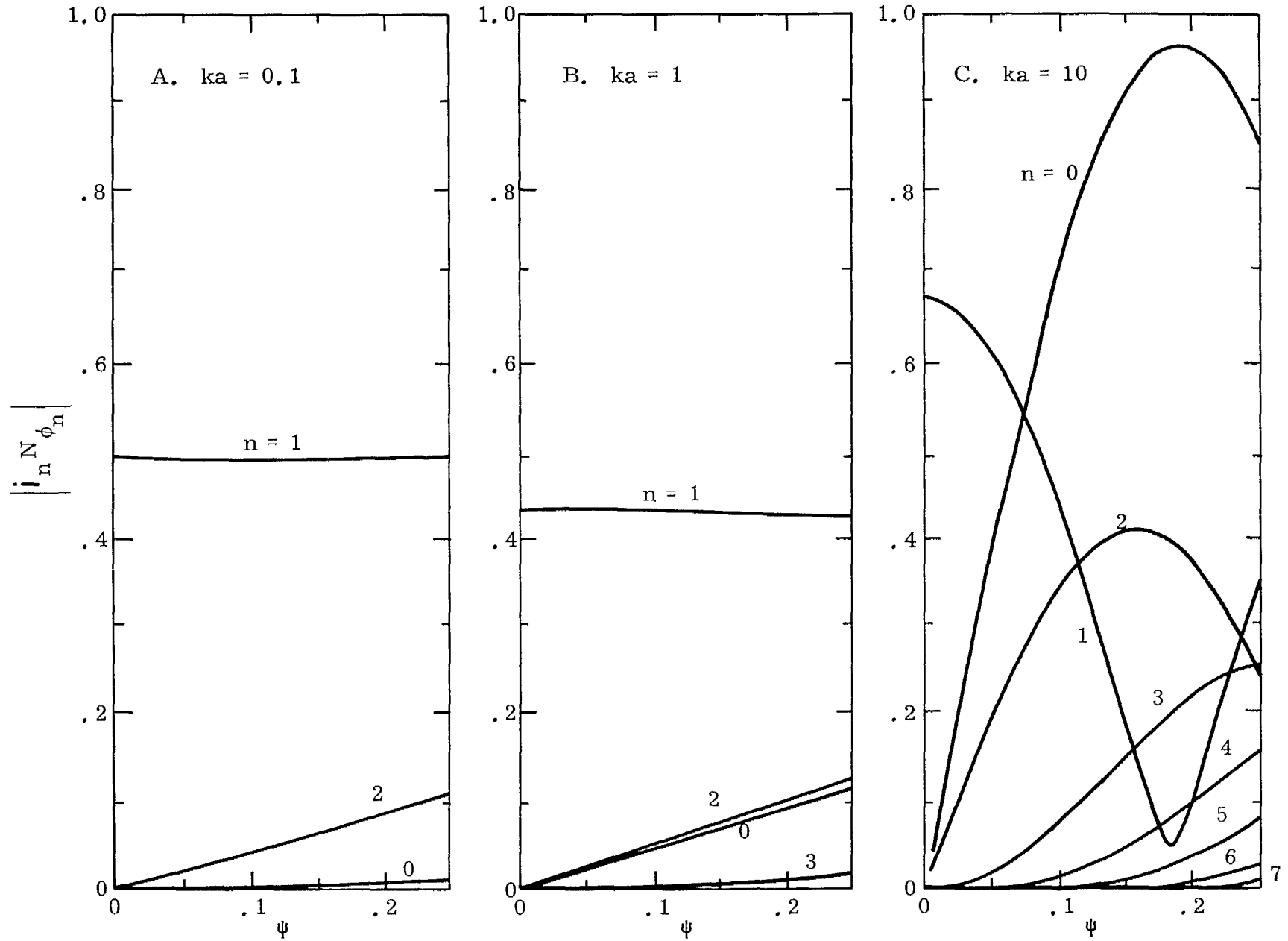


Figure 5-2. Relative Field Strength for the Electric Mode $i_n N_{\phi_n}$ at Various Distances from the Center

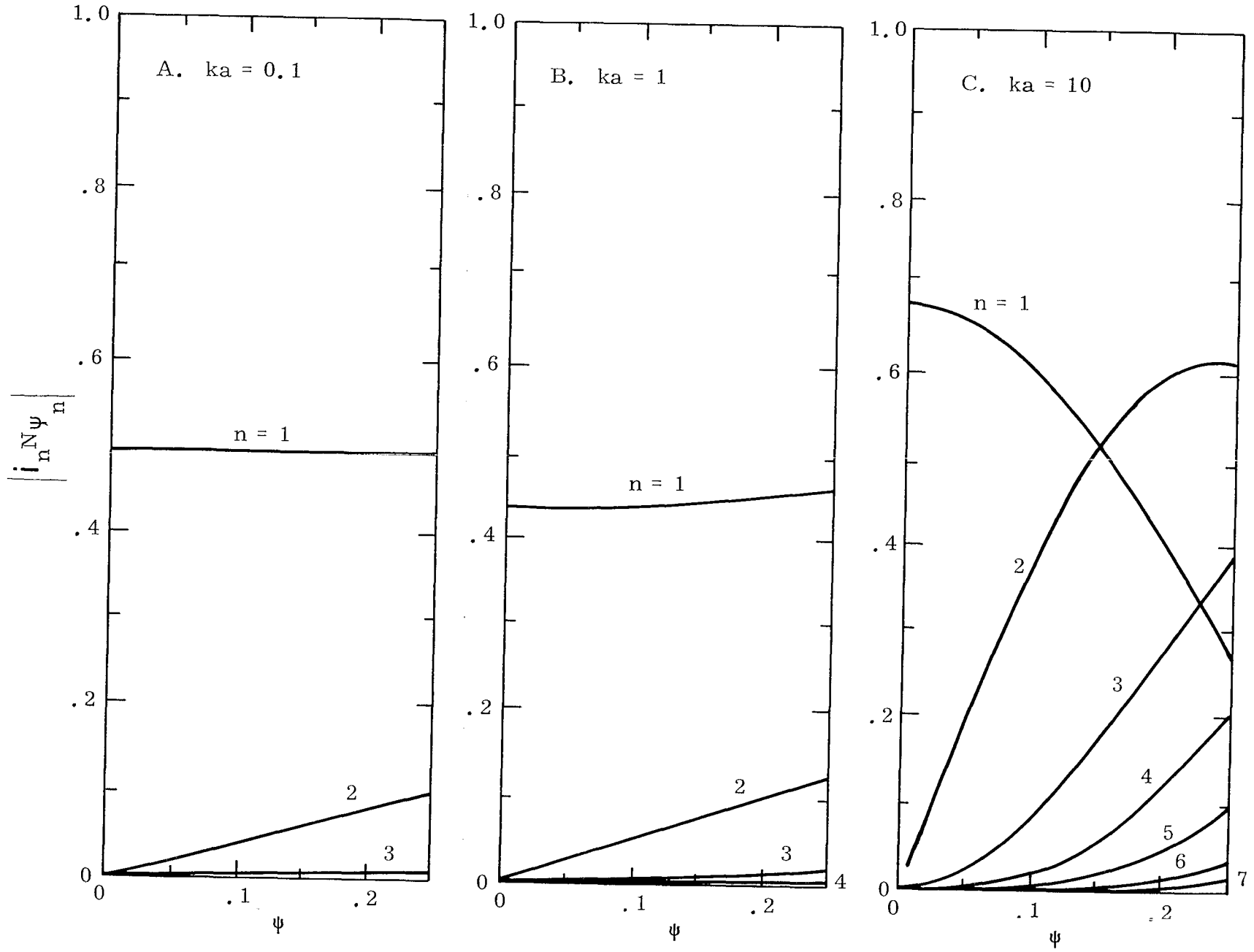


Figure 5-3. Relative Field Strength for the Electric Mode $i_n N \psi_n$ at Various Distances from the Center

the field very close to the center. The other modes gradually become important as we move away from the center. Actually, at very low frequencies, the first order mode can almost represent the total field in quite a wide distances from the center. At intermediate frequencies, however, many modes have significant field strength away from the center. But still, the higher the order of the mode, the smaller the field strength so that only a limited number of modes could give us a reasonably close value of the actual field. How much contributions from each mode to the total field also depends on the $\sin(n\phi)$ and $\cos(n\phi)$ factors in Eqs. (4.16) and (4.17). Taking $\phi = \pi/2$ for instance, all the even order modes do not contribute to the field E_ψ and all the odd order modes do not contribute to E_ϕ .

Figure 5-4 gives the field pattern for various number of modes used in the summation. Although $\psi = 0.25$ is a little far away from the symmetry point (the center), we actually only need four modes for frequencies below $ka = 10$. As the frequency goes higher, more and more modes have to be taken into account. With 25 modes used, the field shows a very nice convergence for frequencies up to $ka = 50$. However, at such a high frequency, one probably can use the asymptotic expansion for the radiation field from a circular cylindrical antenna, which will be discussed in detail in Chapter IX. The mode method is particularly useful at low frequencies where no analytical formula is available. In the frequency range of our interest, $ka < 50$, probably as low as 14 modes will give us a nice field pattern. So, in the latter calculations, we will take the round-off integer part of $\psi / 0.18$ as the number of modes to be used in the summation, in addition to the zero order mode. This is set for this note only and some other criteria should be used for different frequency and space ranges of interest as well as the accuracy requirements for the field pattern.

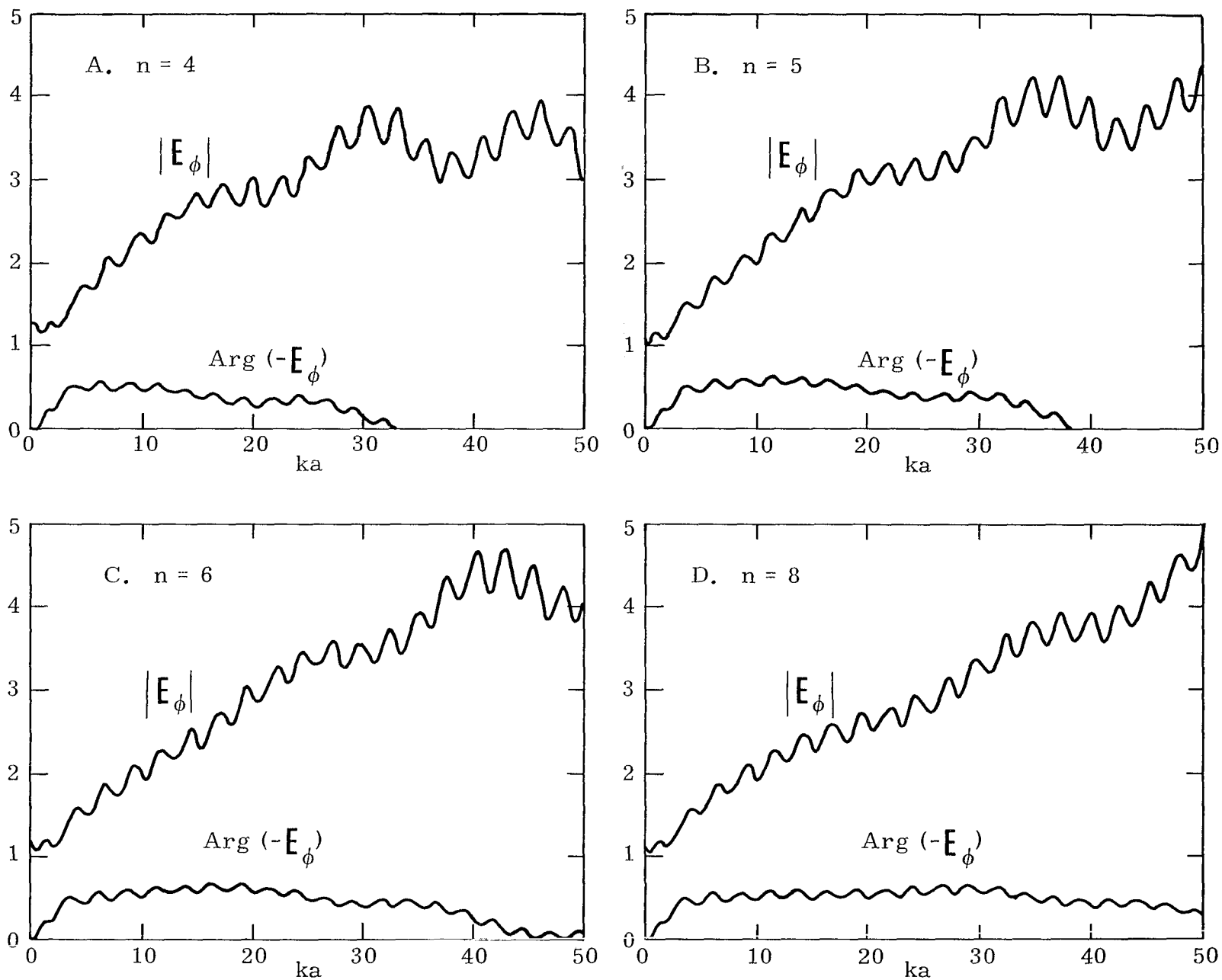


Figure 5-4.

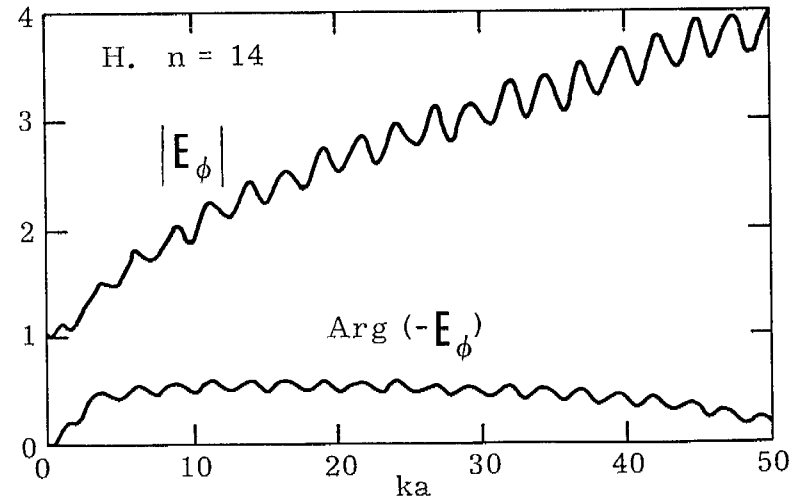
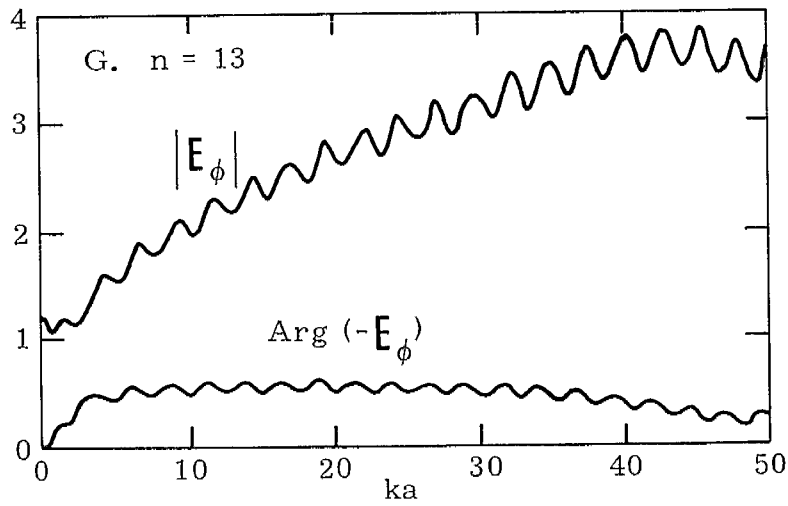
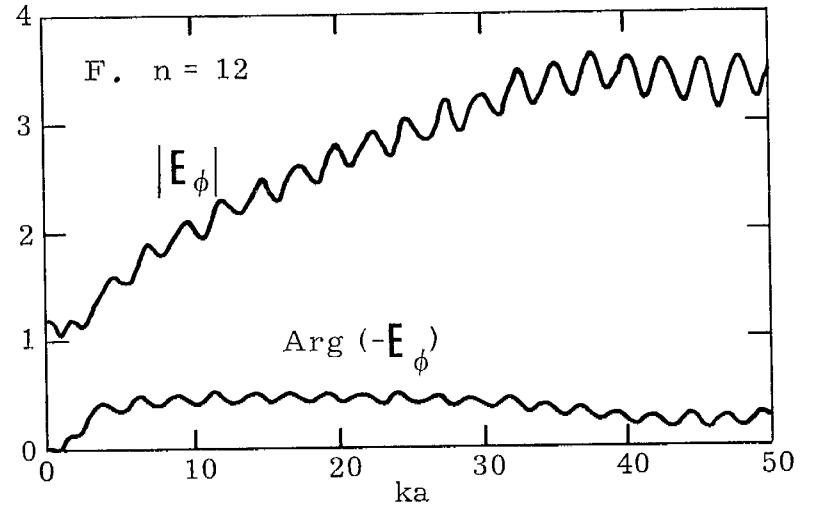
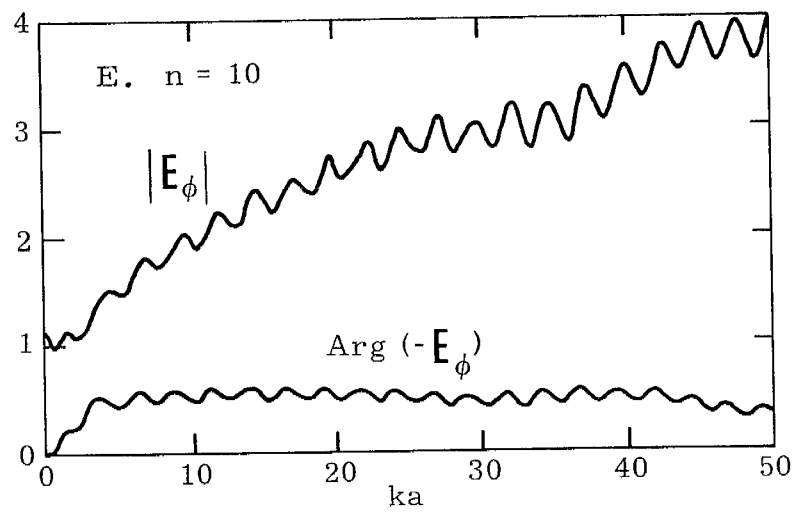


Figure 5-4.

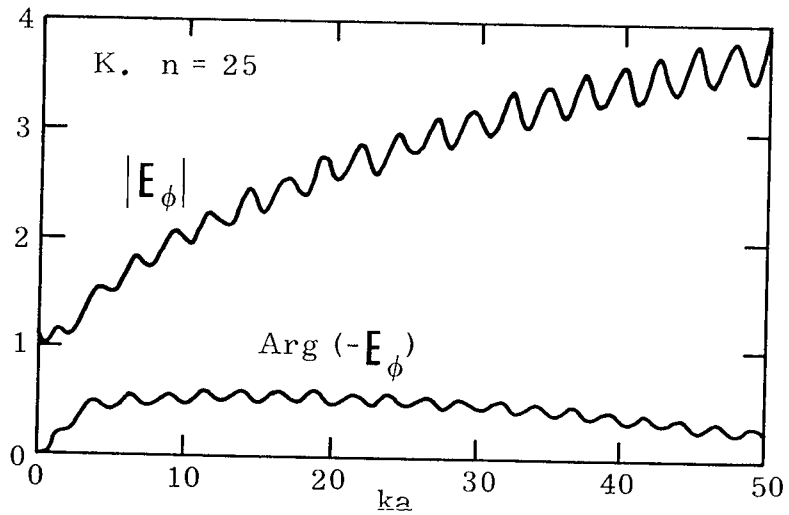
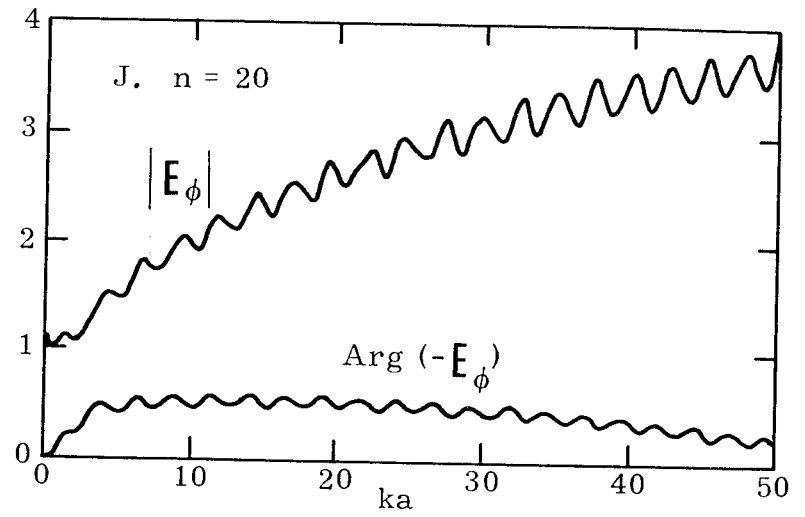
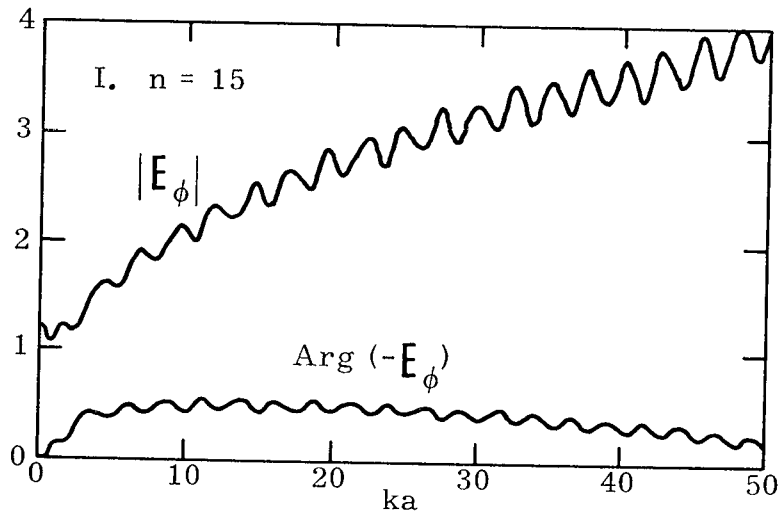


Figure 5-4. E_ϕ for $b/a = 0.02$, $\psi = 0.25$ and $\phi = 0$ with the Numbers of Modes Taken into Account Ranging from Four to Twenty-five

VI. Fourier Modes for the H-Field

From Eqs. (1.4) to (1.6) one can see that the dominant term for the H-field on the plane of TORUS near the center is

$$\begin{aligned} H_z &= \frac{1}{2\pi\psi} \frac{\partial}{\partial\psi} \iint_{S_1} \psi a G(\vec{r}, \vec{r}') \cos(\phi - \phi') I(\phi') d\xi' d\phi' \\ &\quad - \frac{1}{2\pi\psi} \frac{\partial}{\partial\phi} \iint_{S_1} a G(\vec{r}, \vec{r}') \sin(\phi - \phi') I(\phi') d\xi' d\phi'. \end{aligned} \quad (6.1)$$

The Green's function may be written in terms of ψ and ϕ such that

$$\begin{aligned} H_z(\psi, \phi, 0) &= \frac{\partial}{\psi \partial\psi} \int_0^{2\pi} \psi G(\psi, \phi - \phi') \cos(\phi - \phi') I(\phi') d\phi' \\ &\quad - \frac{1}{\psi} \frac{\partial}{\partial\phi} \int_0^{2\pi} G(\psi, \phi - \phi') \sin(\phi - \phi') I(\phi') d\phi'. \end{aligned} \quad (6.2)$$

Substituting the Fourier expansion formula for the Green's function as well as the current into the above equation and normalizing the H-field by its D.C. value at the center which is $H_0 = \frac{V_0}{2aR_0}$, one obtains

$$\begin{aligned} H_z(\psi, \phi, 0) &= \frac{2}{\psi} \left\{ \frac{\partial}{\partial\psi} \int_0^{2\pi} \psi \sum_{m=-\infty}^{\infty} G_m(\psi) e^{-im(\phi - \phi')} \cos(\phi - \phi') \sum_{n=-\infty}^{\infty} i_n e^{-in\phi'} d\phi' \right. \\ &\quad \left. - \frac{\partial}{\partial\phi} \int_0^{2\pi} \sum_{m=-\infty}^{\infty} G_m(\psi) e^{-im(\phi - \phi')} \sin(\phi - \phi') \sum_{n=-\infty}^{\infty} i_n e^{-in\phi'} d\phi' \right\}. \end{aligned} \quad (6.3)$$

After some manipulation, this equation finally reduces to

$$\begin{aligned} H_z(\psi, \phi, o) = \sum_{n=-\infty}^{\infty} 2\pi i_n \left\{ \left[G'_{n+1}(\psi) + G'_{n-1}(\psi) \right] + \frac{1}{\psi} \left[G_{n+1}(\psi) + G_{n-1}(\psi) \right] \right. \\ \left. + \frac{n}{\psi} \left[G_{n+1}(\psi) - G_{n-1}(\psi) \right] \right\}. \end{aligned} \quad (6.4)$$

And similar to Chapter IV, one may define the Fourier modes for the H field as follows:

$$\begin{aligned} M_{z_n}(\psi, o) = 2\pi \left\{ \left[G'_{n+1}(\psi) + G'_{n-1}(\psi) \right] + \frac{1}{\psi} \left[G_{n+1}(\psi) + G_{n-1}(\psi) \right] \right. \\ \left. + \frac{n}{\psi} \left[G_{n+1}(\psi) - G_{n-1}(\psi) \right] \right\} \end{aligned} \quad (6.5)$$

and

$$M_{z_n}(\psi, \phi, o) = M_{z_n}(\psi, o) e^{-in\phi}. \quad (6.6)$$

These modes are completely independent of the loading impedances of the antenna and in this case,

$$M_{z_n}(\psi, o) = M_{z_{(-n)}}(\psi, o) \quad (6.7)$$

Therefore, the magnetic field distribution can be written as

$$H_z(\psi, \phi, o) = \sum_{n=-\infty}^{\infty} i_n M_{z_n}(\psi, \phi, o) = i_o M_{z_o}(\psi, o) + 2 \sum_{n=1}^{\infty} i_n M_{z_n}(\psi, o) \cos(n\phi) \quad (6.8)$$

Examples of the Fourier modes M_{z_n} is shown in Figs. 6-1 and 6-2. There are the general solutions for the magnetic field for a circular loop antenna and are independent of the loading impedance and source. These modes have the similar characteristics as that of the electric field. At low frequencies, only a few modes are important and the field strength of the higher order modes decreases very fast as n increases. Again, the mode theory is applicable to other planes of interest so that one may write the magnetic field in terms of the Fourier modes in a general form as follows:

$$\vec{H}(\psi, \phi, z) = \sum_{n=-\infty}^{\infty} i_n \vec{M}_n(\psi, \phi, z) \quad (6.9)$$

Here, \vec{M}_n depends only on the space parameters so that it can be calculated in advance. When the loading impedance and the source function are given, then one can compute the excitation factor i_n and the field can be found readily. For locations near to the symmetry point, only a few modes are necessary.

VII. H-Field as a Function of ψ and ϕ at Low Frequencies

Using the mode equation (6.8), we can show that only the zero order mode contributes to the magnetic field at the center.

$$\begin{aligned} H_z(\psi \rightarrow 0, \phi, 0) &\cong i_0 \lim_{\psi \rightarrow 0} M_{z_0}(\psi, 0) \\ &\cong 4\pi i_0 \lim_{\psi \rightarrow 0} \left[G_1'(\psi) + \frac{1}{\psi} G_1(\psi) \right] \end{aligned}$$

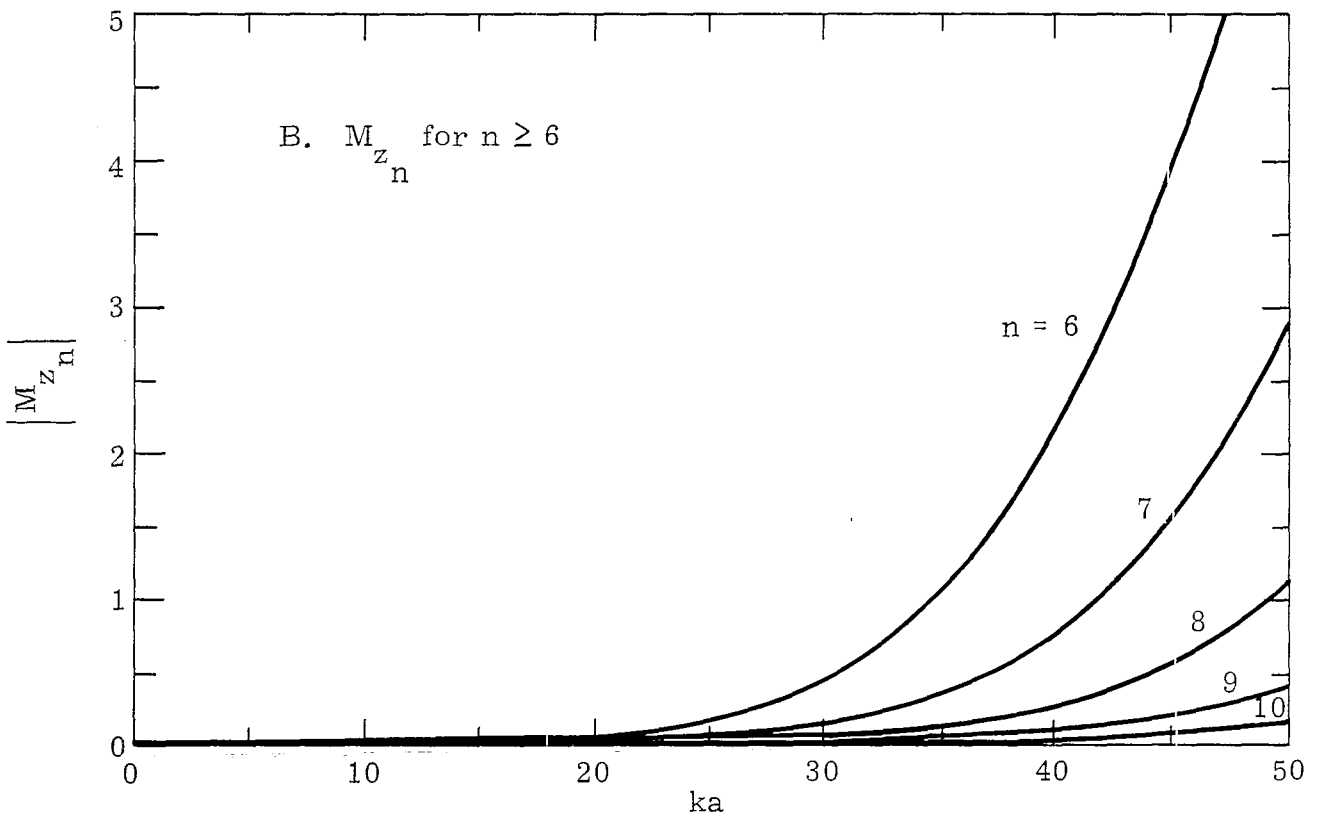
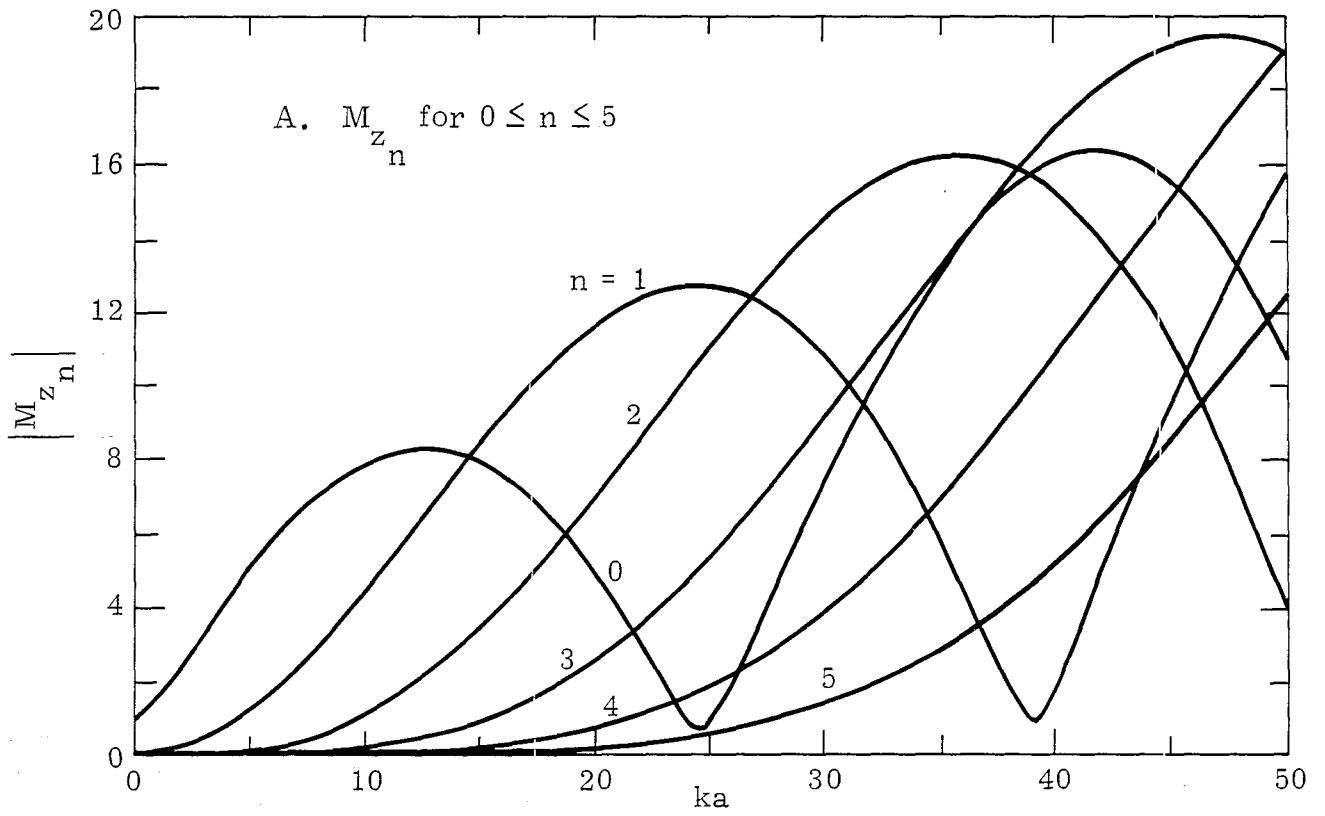


Figure 6-1. $M_{z_n}(\psi, 0)$ for $\psi = 0.1$

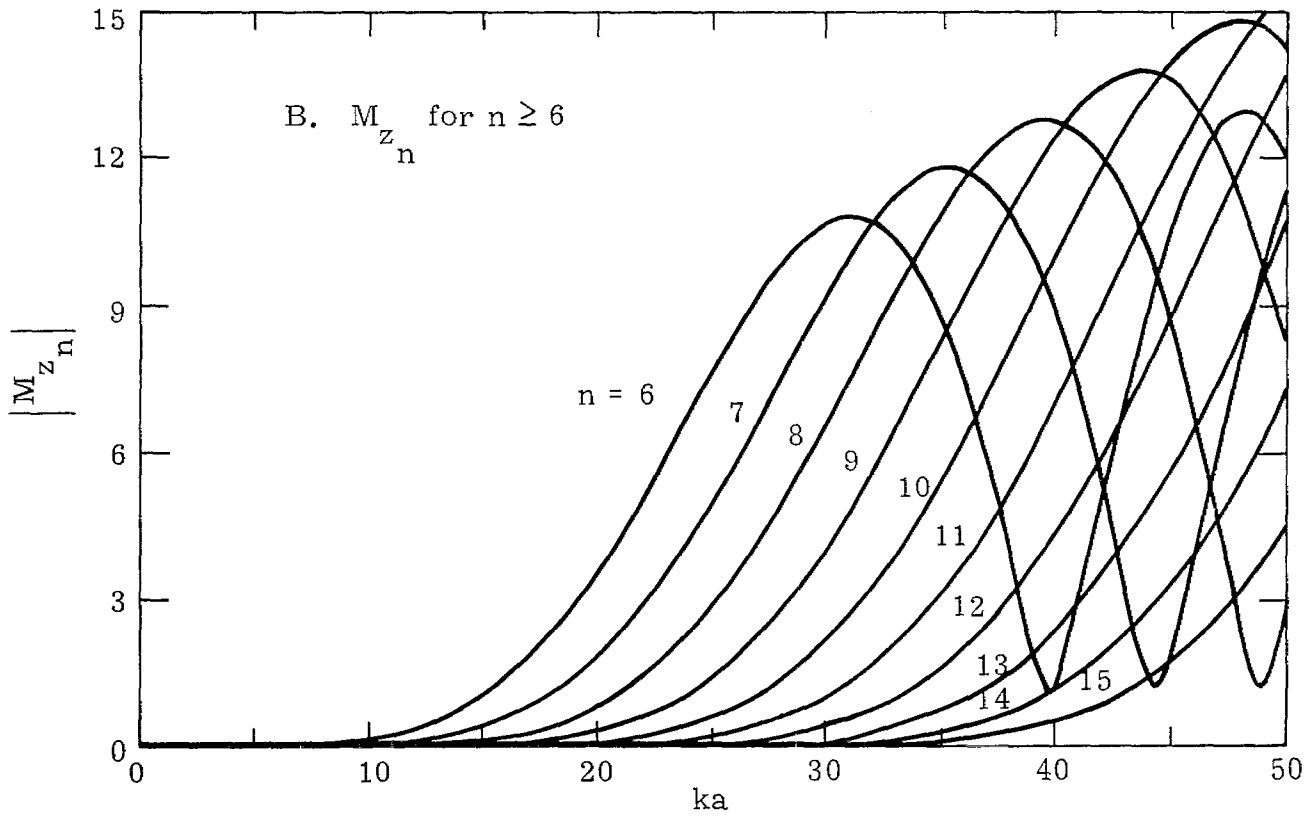
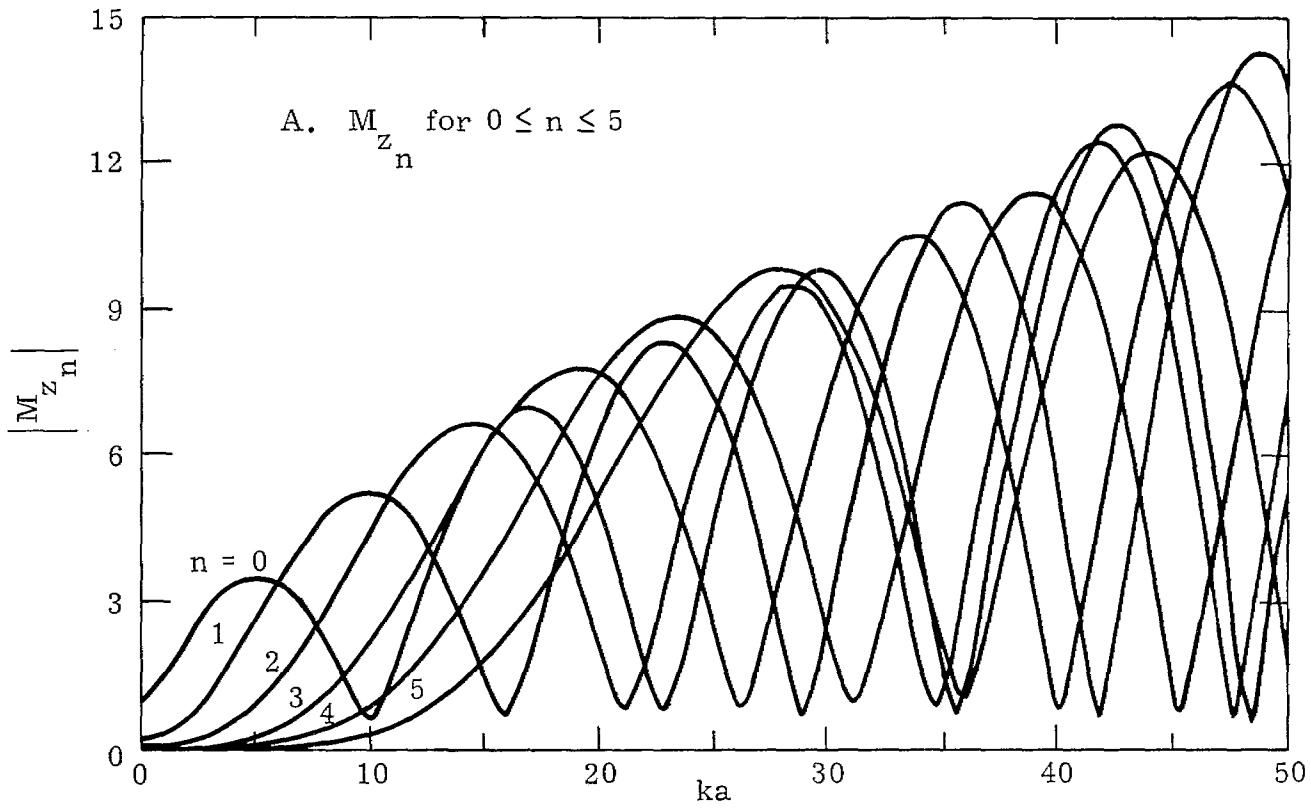


Figure 6-2. $M_{z_n}(\psi, 0)$ for $\psi = 0.25$

$$\begin{aligned}
&\approx i_0 e^{-ika} \lim_{\psi \rightarrow 0} \left\{ \left[i \frac{\partial \mathbf{J}_1(ka\psi)}{\partial \psi} + \frac{1}{2} \mathbf{J}_0(ka\psi) \right] \right. \\
&\quad \left. + \frac{1}{\psi} \left[i \mathbf{J}_1(ka\psi) + \frac{\psi}{2} \mathbf{J}_0(ka\psi) \right] \right\} \\
&\approx i_0 e^{-ika} \left[\frac{ika}{2} + \frac{1}{2} + \frac{ika}{2} + \frac{1}{2} \right] \\
&= i_0 (1 + ika) e^{-ika} \tag{7.1}
\end{aligned}$$

This is in agreement with our previous derivation [1]. As shown in Fig. 7-1, the field is identical to what has been obtained in SSN 160.

In a manner similar to Figs. (5-2) and (5-3), the relative field strengths are plotted for the magnetic modes $i_n M_z^n$ at various distances from the center. As shown in Fig. 7-2, the zero order mode is the most important at very low frequencies. It even dominates the field at intermediate frequencies as long as the observation point is very close to the center. From these figures, one can conclude that only a limited number of modes are necessary for frequencies up to $ka = 50$ and this is the main advantage of the mode theory.

For a sinusoidal field in free space, one may write the Maxwell's equations in terms of the propagation constant $k = \omega \sqrt{\mu_0 \epsilon_0}$ and the characteristic impedance $Z_0 = \sqrt{\mu_0 / \epsilon_0}$ as follows:

$$\begin{aligned}
\nabla \times \vec{E} &= -i\mu_0 \omega \vec{H} \\
&= -ikZ_0 \vec{H} ; \tag{7.2}
\end{aligned}$$

$$\begin{aligned}
\nabla \times \vec{H} &= i\omega \epsilon_0 \vec{E} \\
&= ik\vec{E}/Z_0 . \tag{7.3}
\end{aligned}$$

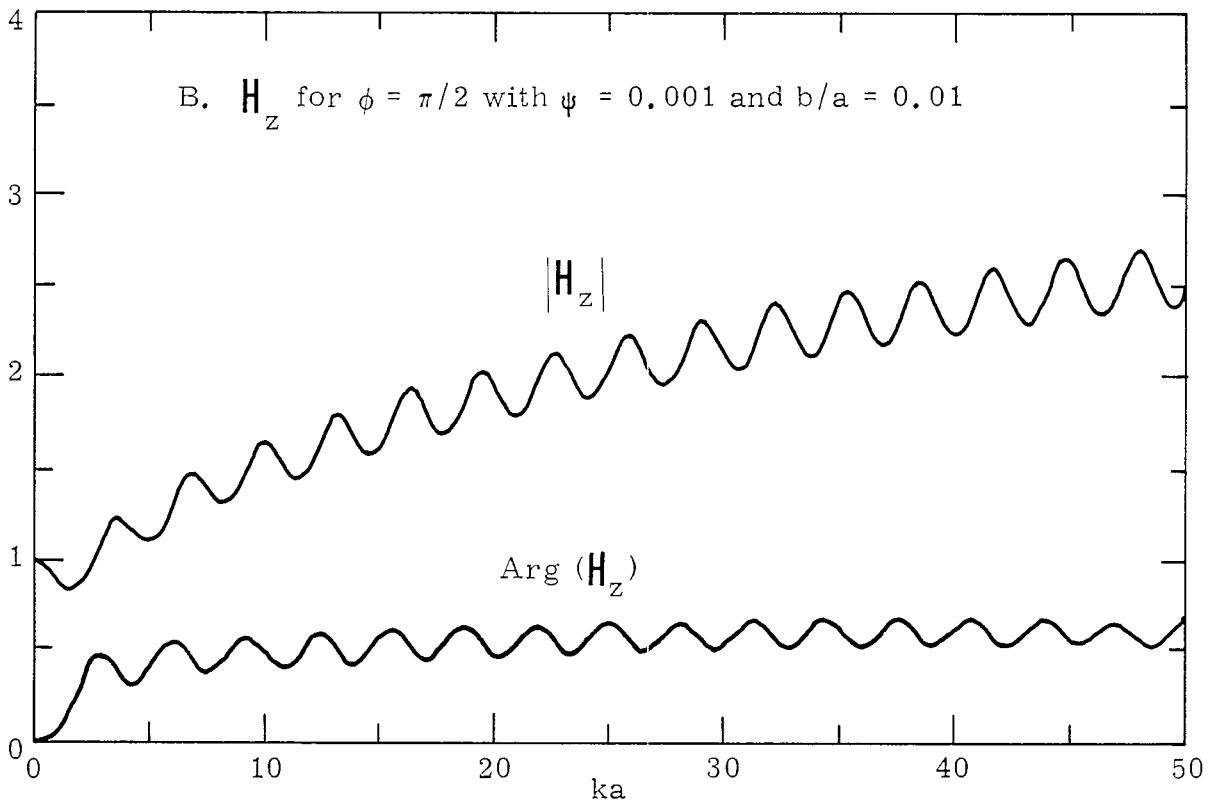
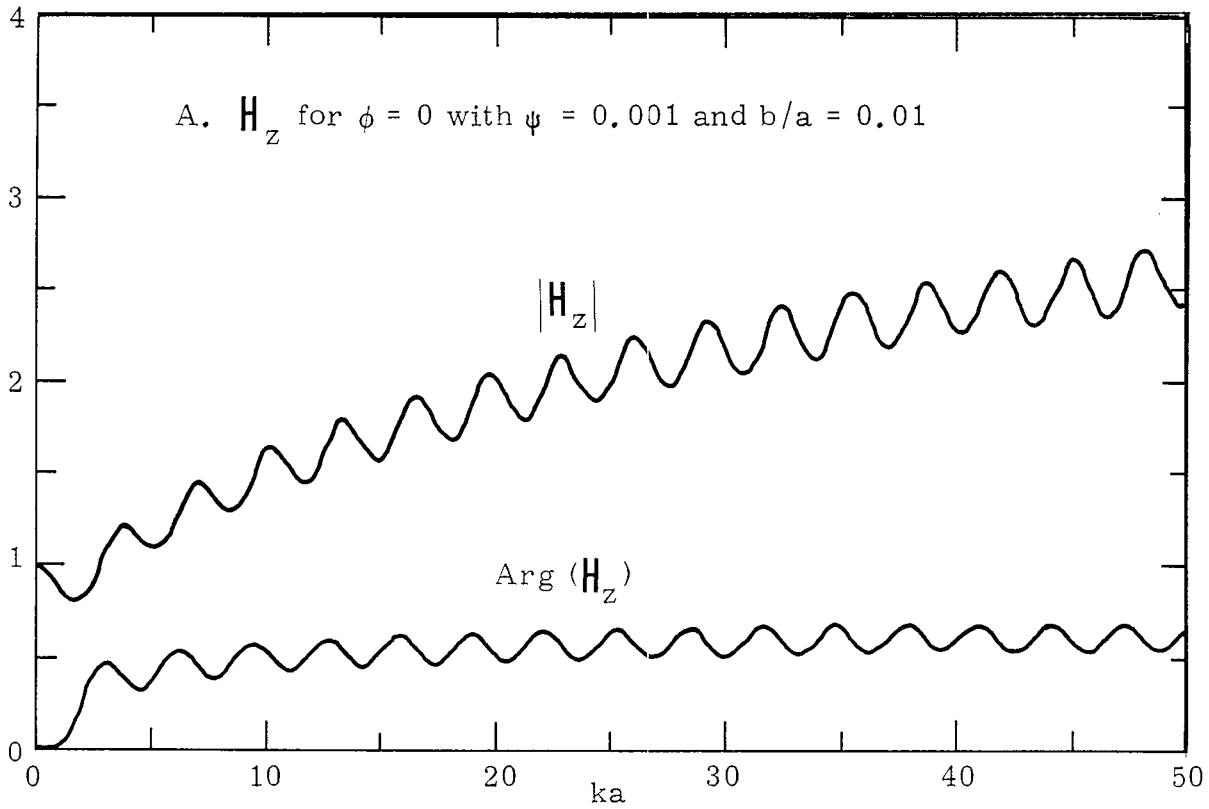


Figure 7-1. Magnetic Field Very Close to the Center

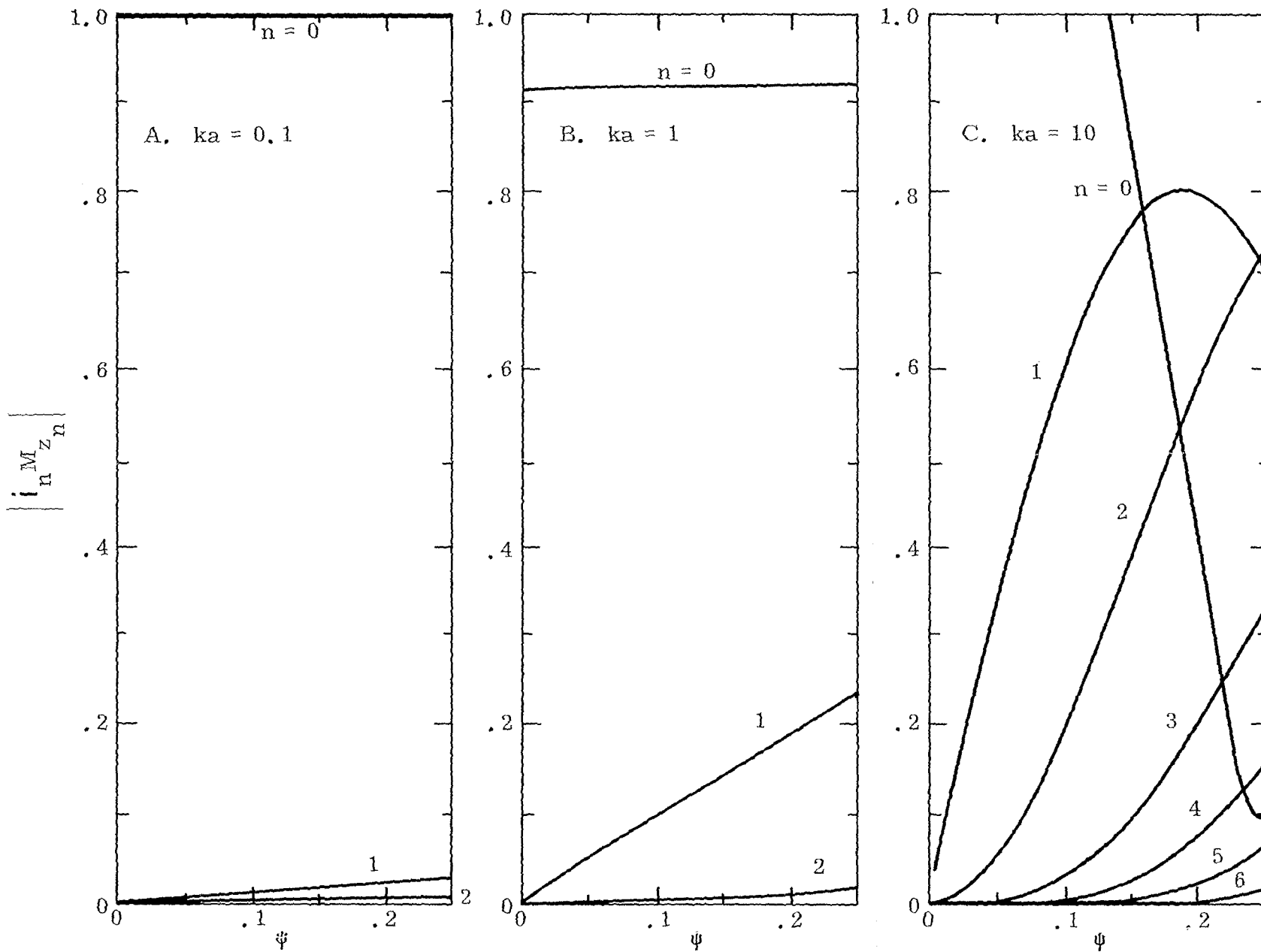


Figure 7-2. Relative Field Strength for the Magnetic Mode $i_n M_{z_n}$ at Various Distances from the Center

Normalizing \vec{E} and \vec{H} by Eqs. (1.16) and (1.17), we get

$$\nabla \times \vec{E} = -ik \vec{H} \quad (7.4)$$

and

$$\nabla \times \vec{H} = ik \vec{E} . \quad (7.5)$$

These fields, according to our analysis in this note, can be represented by the electric and magnetic modes defined in Eqs. (4.18) and (6.9).

That is,

$$\nabla \times \sum_{n=-\infty}^{\infty} i_n \vec{N}_n = ik \sum_{n=-\infty}^{\infty} i_n \vec{M}_n ; \quad (7.6)$$

$$\nabla \times \sum_{n=-\infty}^{\infty} i_n \vec{M}_n = ik \sum_{n=-\infty}^{\infty} i_n \vec{N}_n . \quad (7.7)$$

Although the excitation factor i_n depends on the loading impedance as well as the source distributions, it is not a function of space. So, the relationships between the electric and magnetic modes are easily obtained:

$$\vec{M}_n = \frac{1}{-ik} \nabla \times \vec{N}_n ; \quad (7.8)$$

$$\vec{N}_n = \frac{1}{ik} \nabla \times \vec{M}_n . \quad (7.9)$$

VIII. E and H Fields at High Frequencies

In the previous chapters, we have obtained the electric and magnetic field distributions at low and intermediate frequencies. For high frequencies, one may use the far field formula for an infinitely long cylindrical antenna since the currents are largest near the generator. The other part of the antenna, whether it is curved or straight, has very little effect on the field near the center where it is in the far zone. Referring to [9], [10] and Fig. 1-3, it is not difficult to show that

$$E_{\theta} = \frac{-2ie^{-ika\sqrt{1-2\psi\cos(\phi)+\psi^2}}}{\pi[1-\psi\cos(\phi)]}$$

$$\left(\frac{R_o}{Z_o}\right) \left\{ H_o^{(2)}[kb\sin(\theta)] - i\left(\frac{b}{a}\right) \left(\frac{Z}{Z_o}\right) \csc(\theta) H_1^{(2)}[kb\sin(\theta)] \right\}^{-1} \quad (8.1)$$

where

$$\theta = \tan^{-1} \frac{1-\psi\cos(\phi)}{\psi\sin(\phi)} \quad (8.2)$$

and $Z = R_o$ in Eq. (1.15) is the loading impedance used in this note.

The field components can now be obtained:

$$E_{\psi} = -E_{\theta} \cos(\theta - \phi) \quad (8.3)$$

$$E_{\phi} = -E_{\theta} \sin(\theta - \phi) \quad (8.4)$$

and

$$H_z = Z_o E_{\theta} \quad (8.5)$$

for the high frequencies

For an observation point near the center at $(\psi, \phi, 0)$, the closest point of the source is at $(1 - b/a, 0, 0)$. The distance between them is:

$$d = \sqrt{\left[a - b - \psi a \cos(\phi)\right]^2 + \left[\psi a \sin(\phi)\right]^2} = \sqrt{(a-b)^2 - 2\psi a(a-b) \cos(\phi) + \psi^2 a^2} \quad (8.6)$$

So, the fields on the observation point will be $t = d/c$ seconds later after the turn-on of the source, where c is the speed of light (3×10^8 m/sec).

In the following plots, we will set the turn-on time for the source at

$$t = - \sqrt{(a-b)^2 - 2\psi a(b-a) \cos(\phi) + \psi^2 a^2} / c. \quad (8.7)$$

In other words, the field equations in the frequency domain should be multiplied by a factor e^{ikd} . This includes Eqs. (8.1) for the high frequencies, and Eqs. (4.16), (4.17) and (6.8) for the low frequencies. Figure 8-1 shows E_ϕ in mode expansions as well as the asymptotic forms for $\psi = 0.25$ and $\phi = 0$ with various b/a ratio. The low and high frequency formulas agree very well at the intermediate frequencies. This fine agreement also appears in Figs. (8-2) and (8-3) for E_ψ and E_ϕ at $\phi = \pi/4$, and H_z at $\phi = 0$. This fact in addition to the comparisons in Chapters V and VII for fields at the center seem to indicate that the mode formulas we have derived are correct.

So, according to these figures, one may use the mode equations for fields at low frequencies and then switch to high frequency asymptotic formula at $ka = 20$ for b/a equal or less than 0.05. For $b/a = 0.1$, the switching point may be chosen at $ka = 6$.

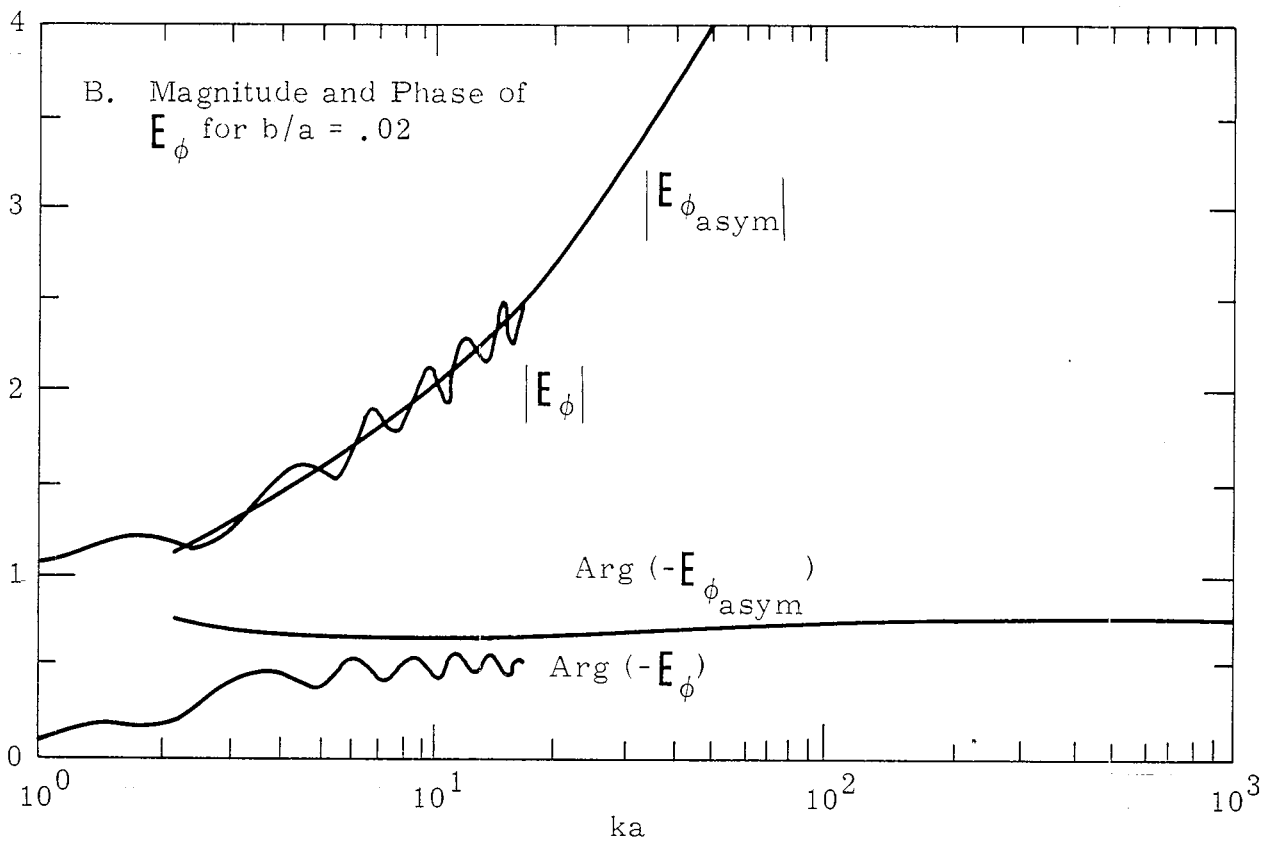
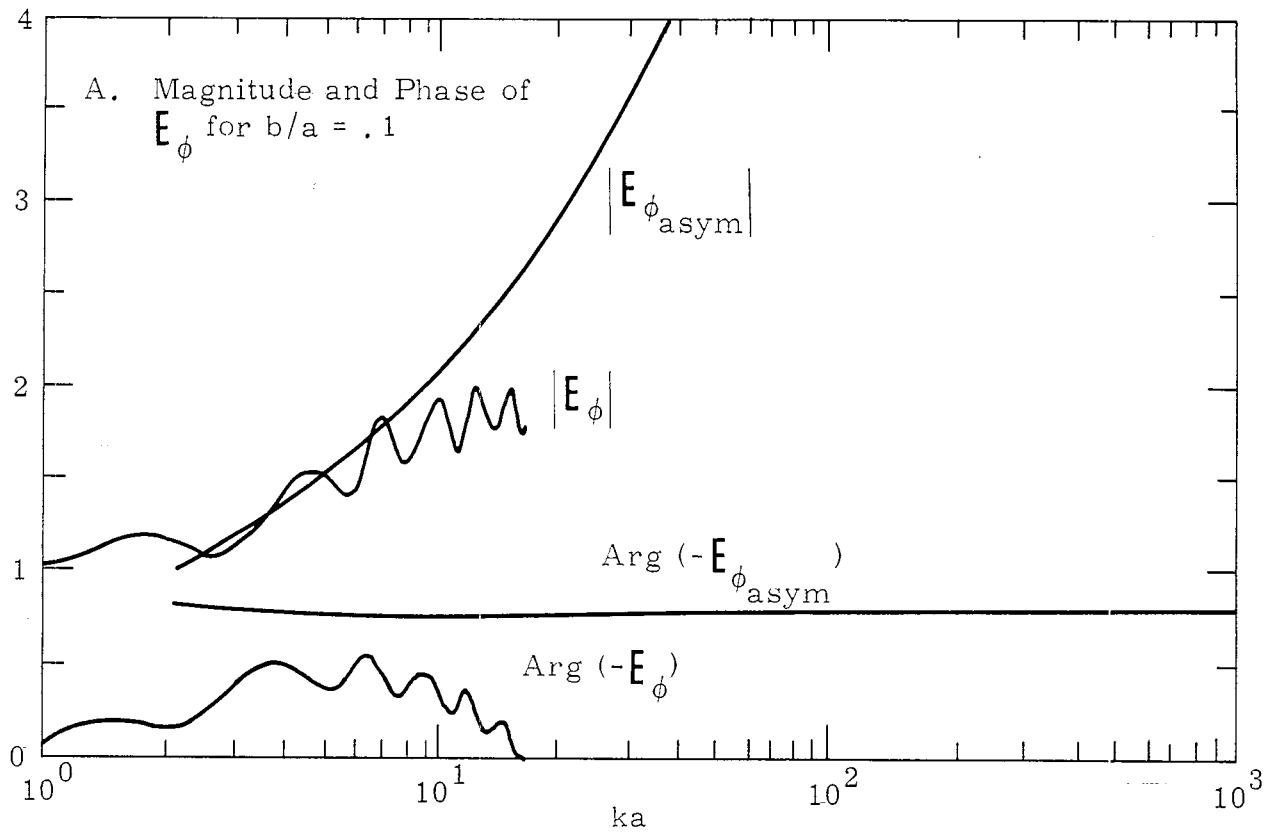


Figure 8-1. E_ϕ and Asymptotic Forms for $\psi = .25$ and $\phi = 0$

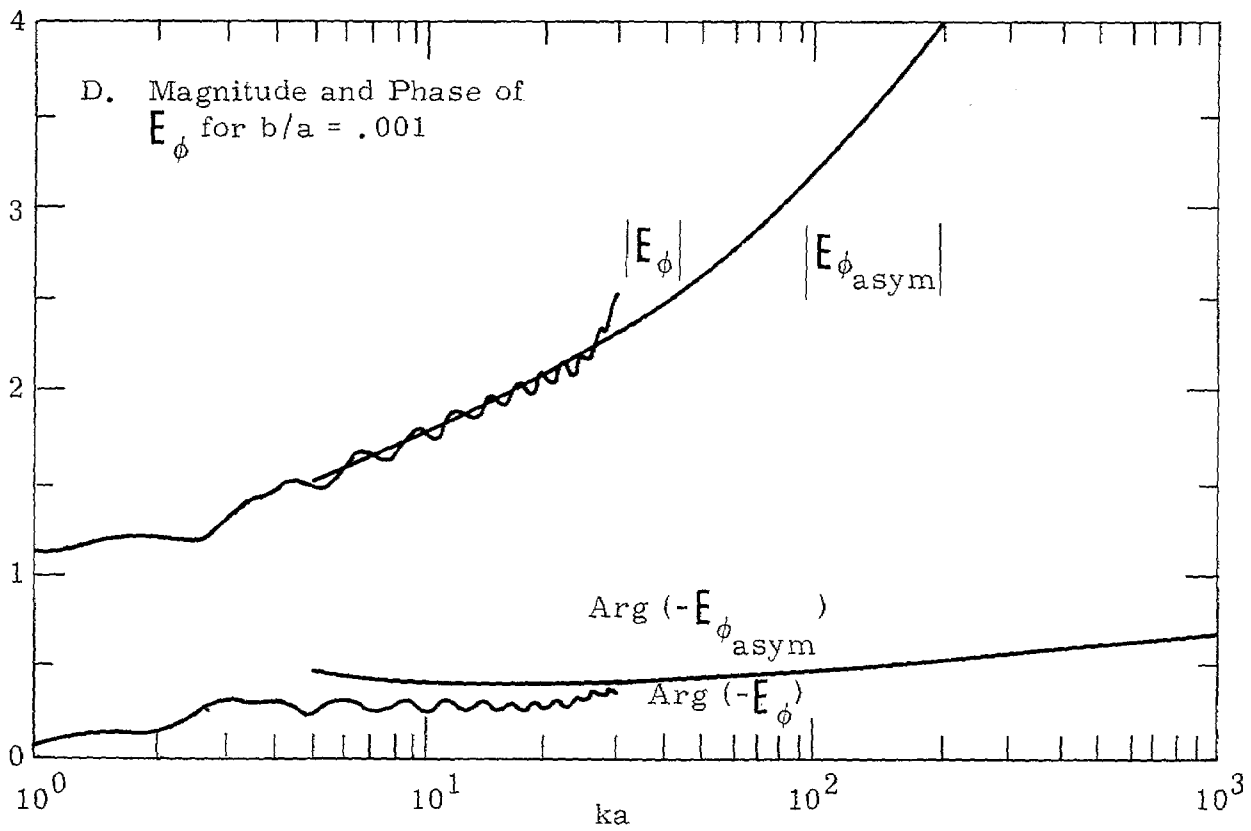
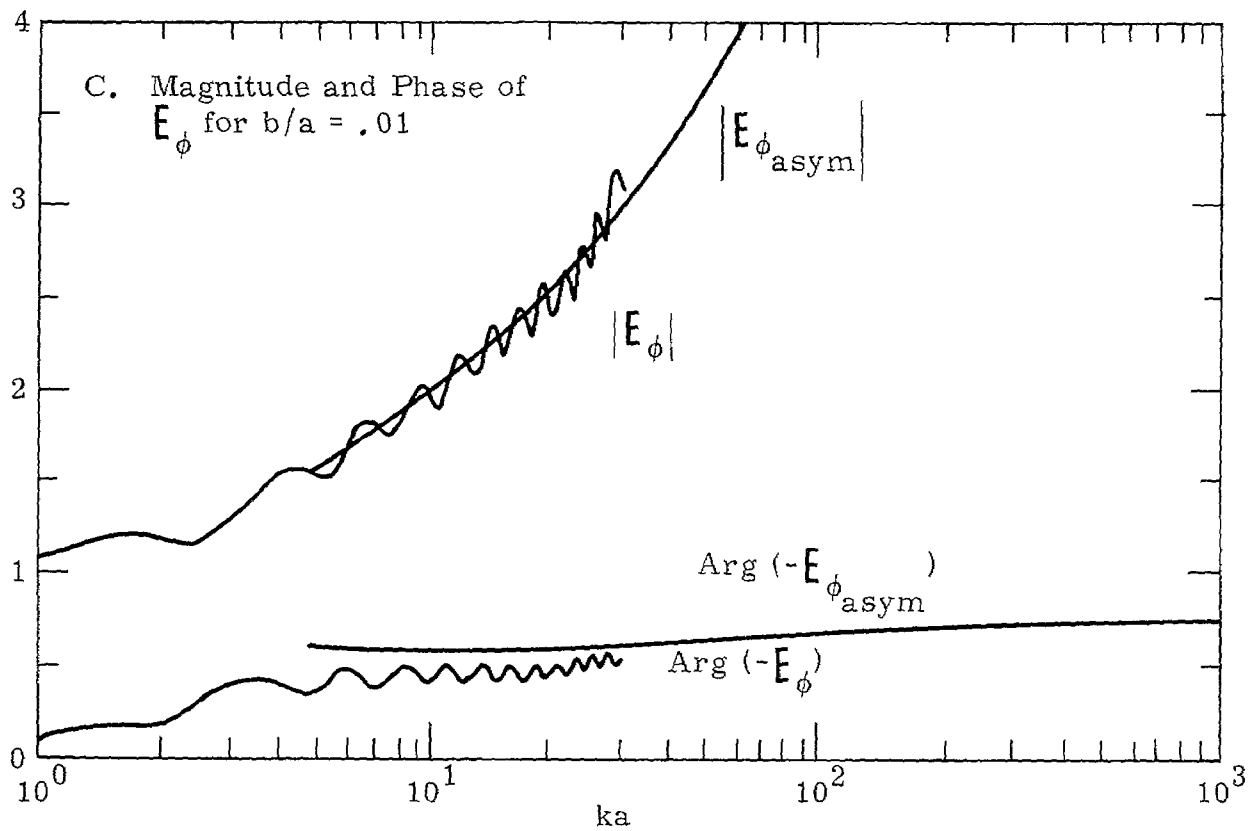


Figure 8-1. Continued

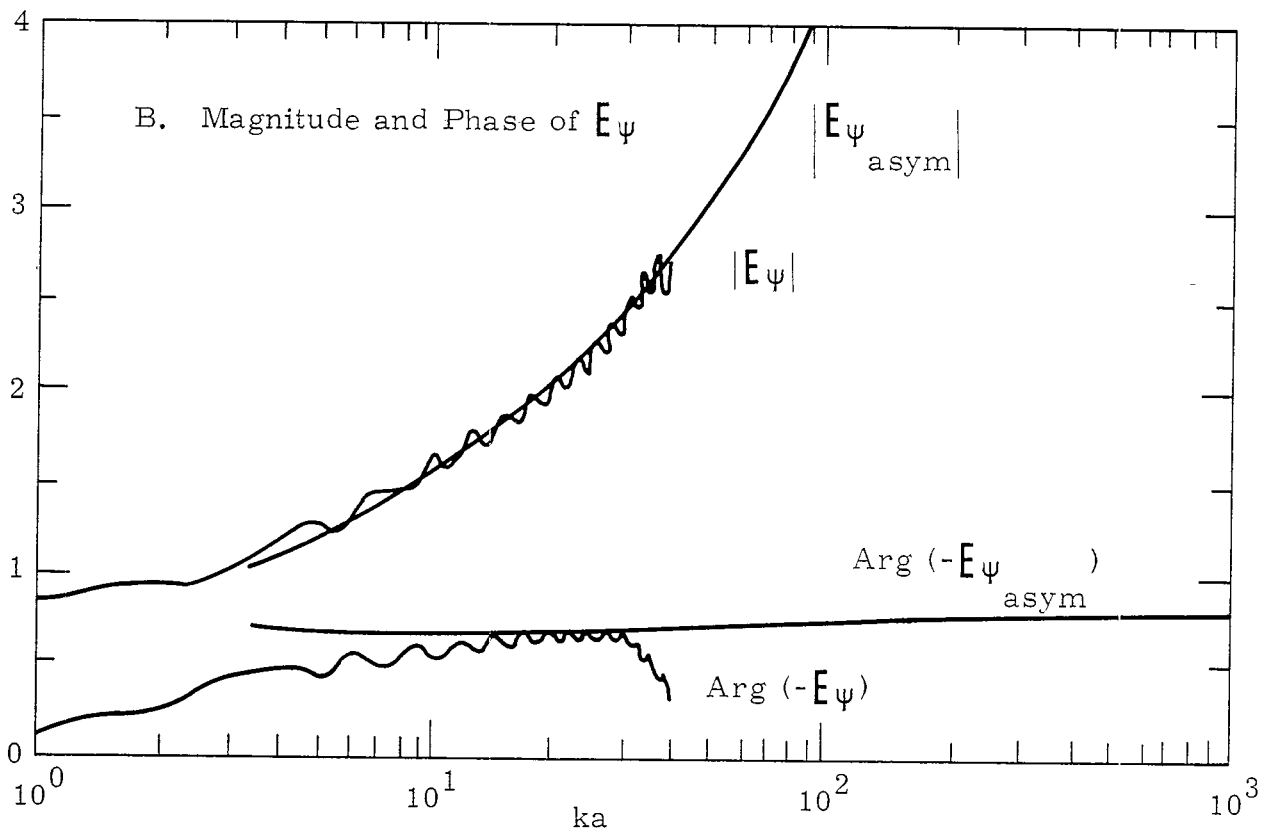
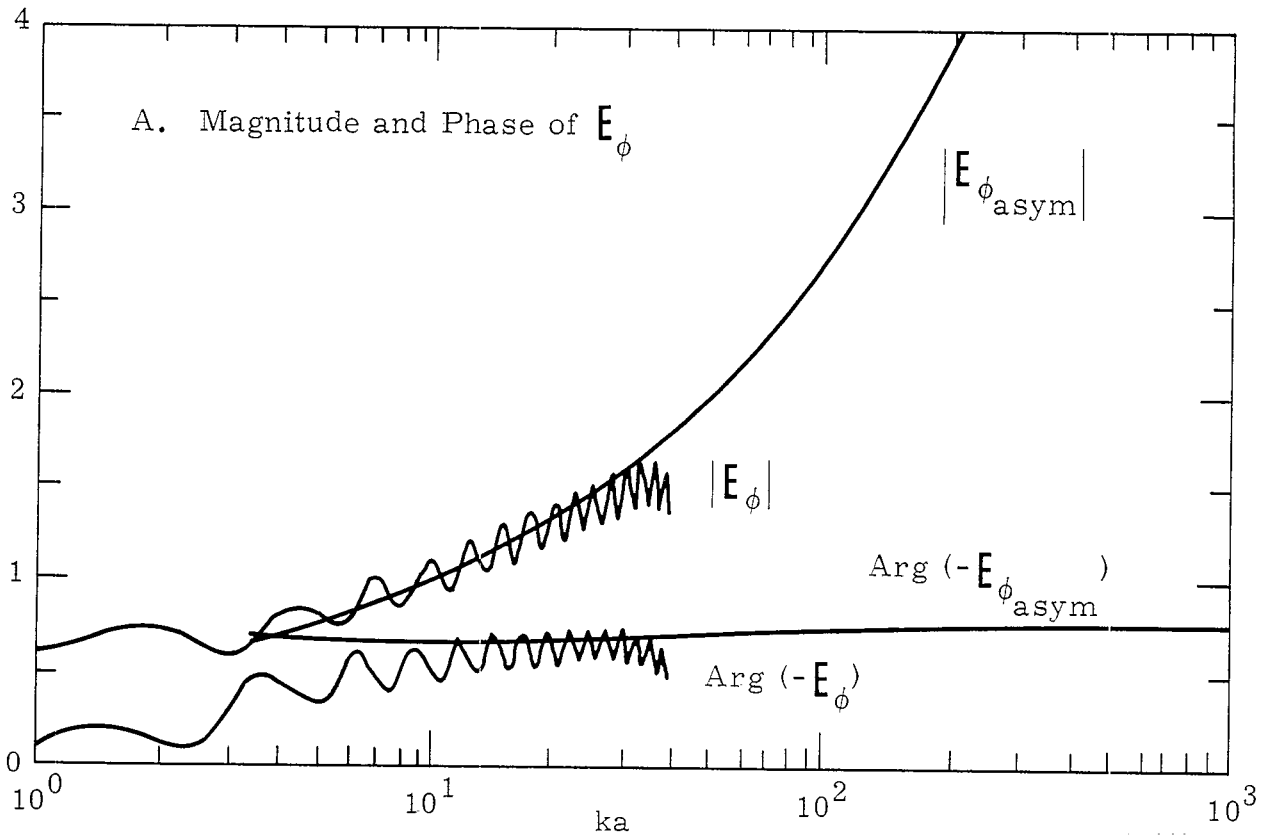


Figure 8-2. Electric Field in Terms of Mode Expansions and Asymptotic Forms for $\psi = 0.25$, $\phi = 45^\circ$ and $b/a = 0.02$

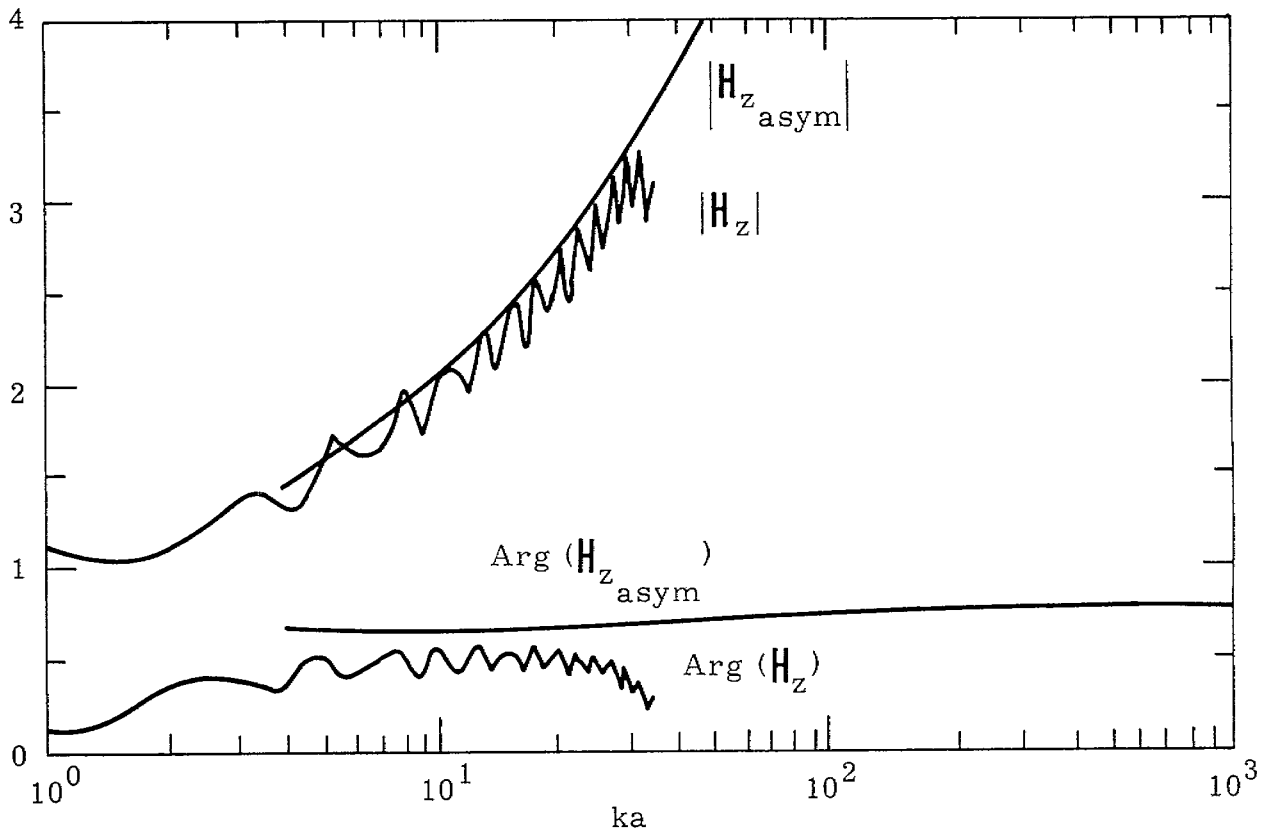
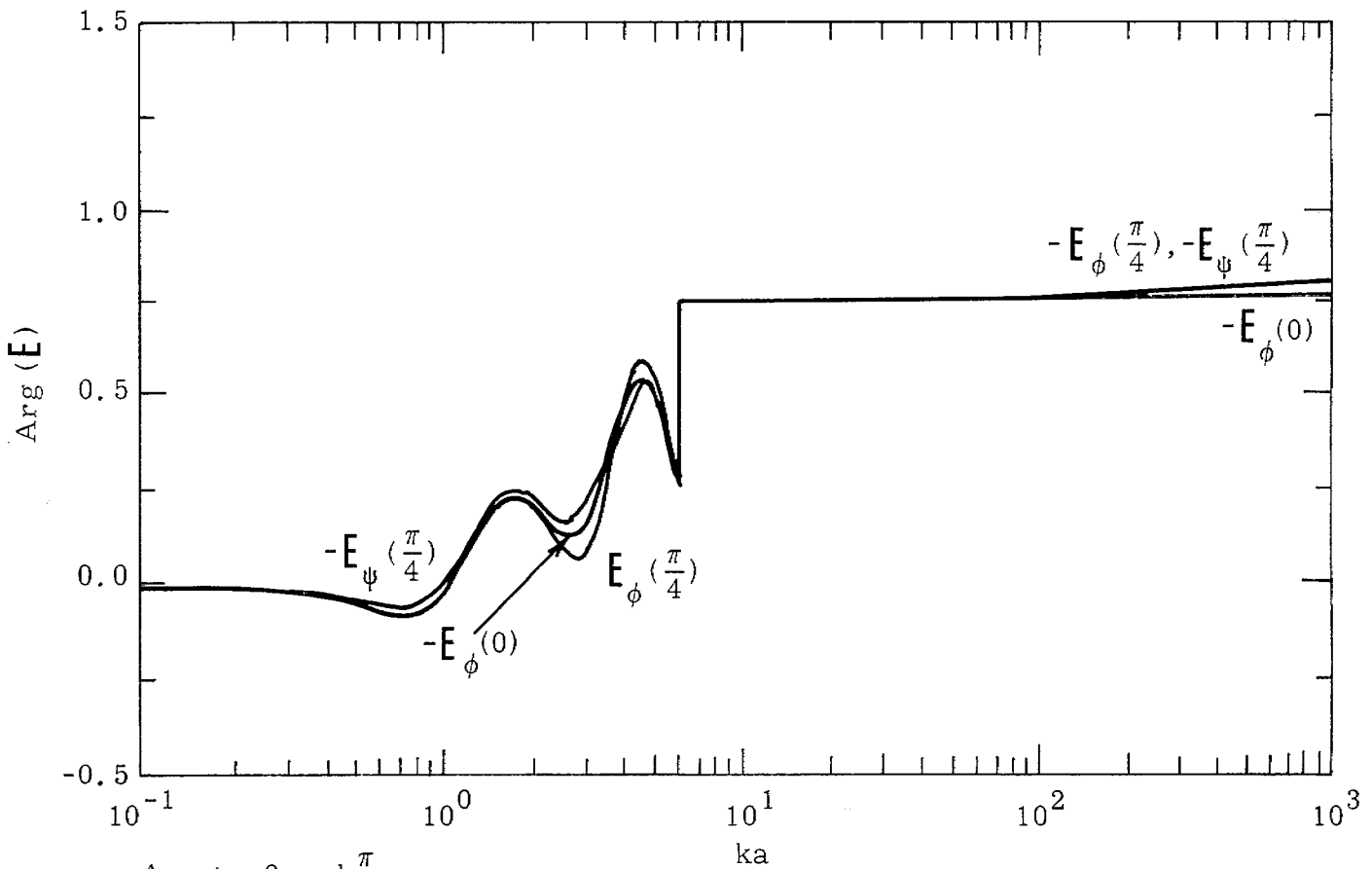
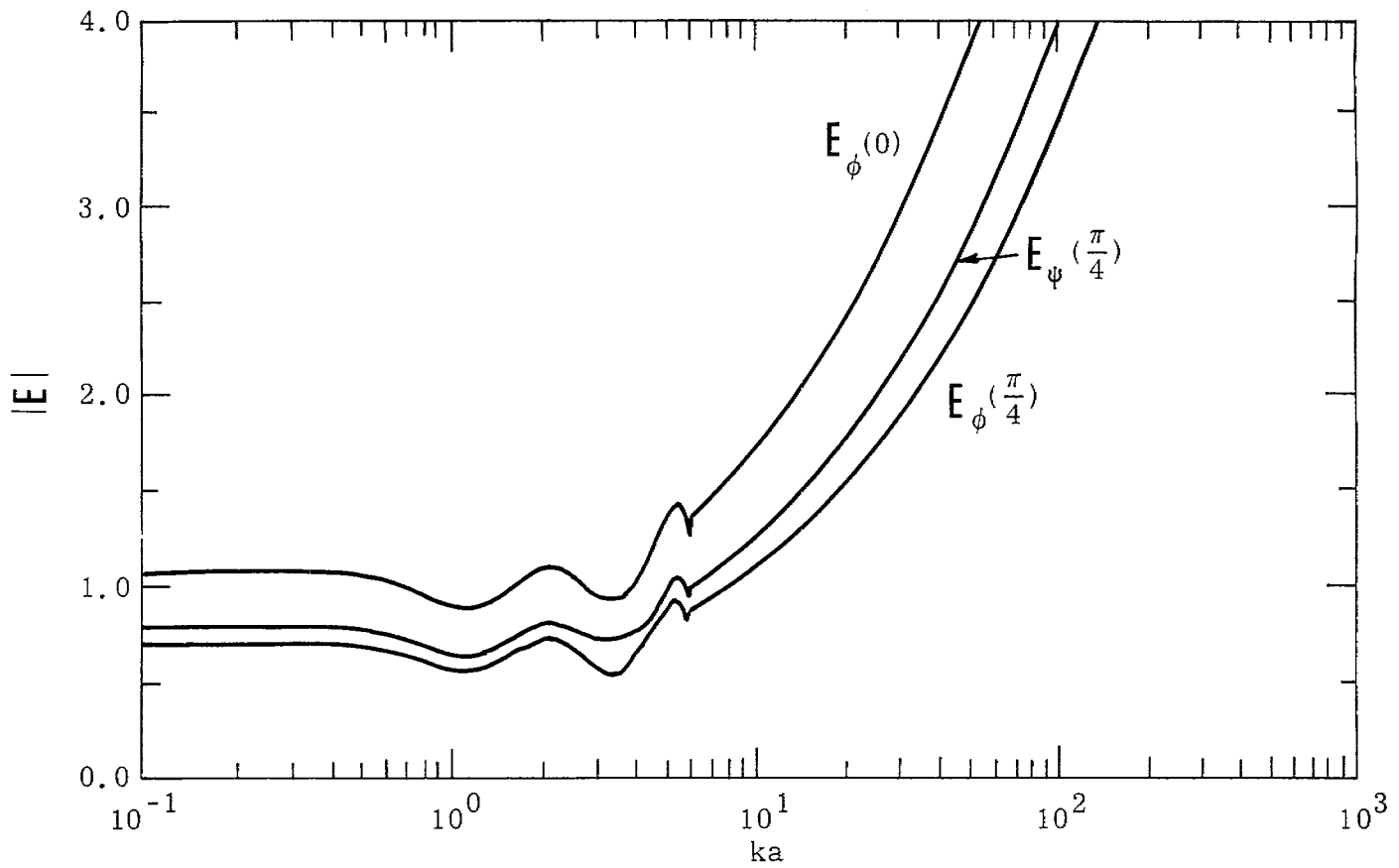


Figure 8-3. H_z in Terms of Mode Expansions and Asymptotic Forms for $\psi = 0.25$, $\phi = 45^\circ$ and $b/a = 0.02$

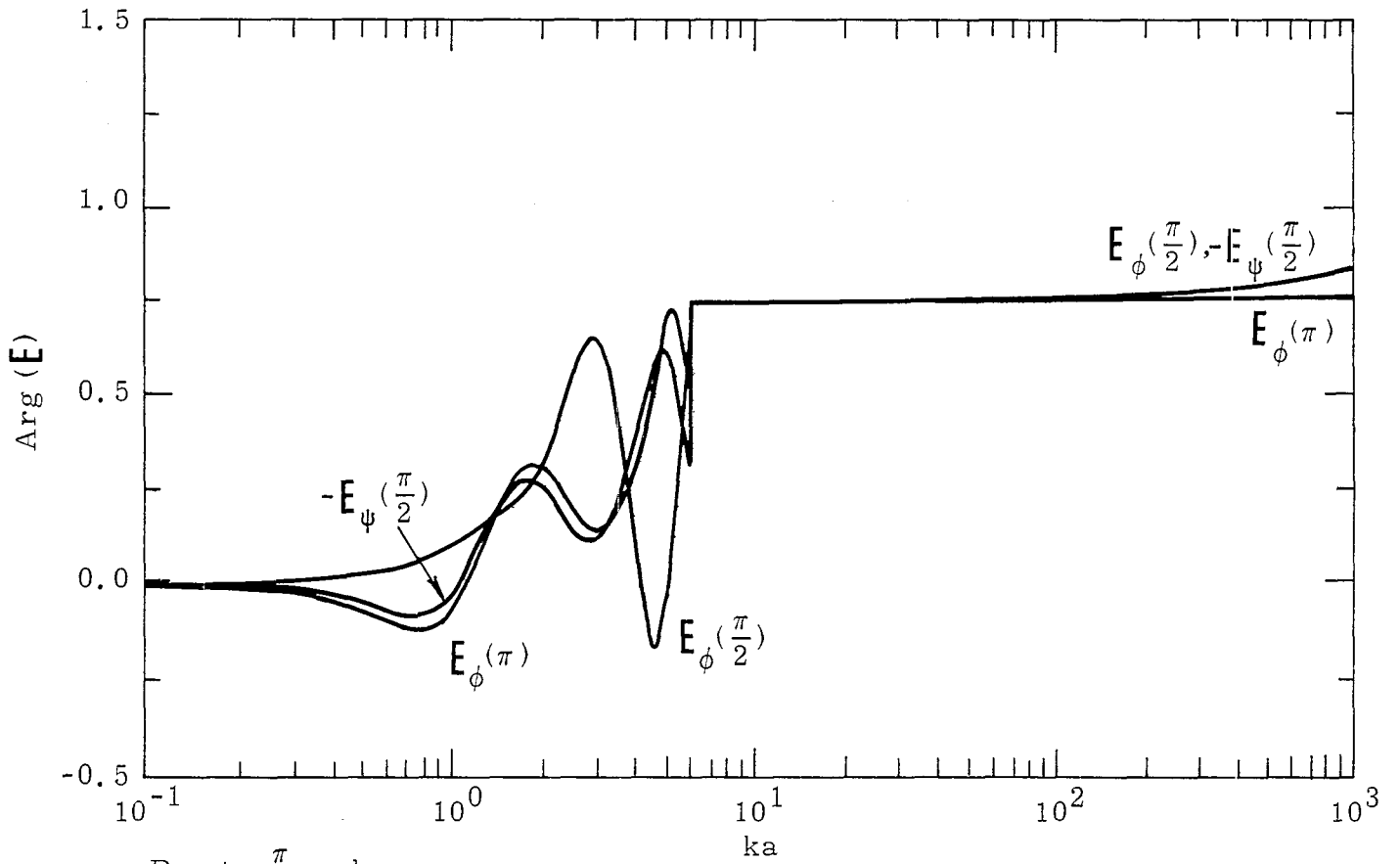
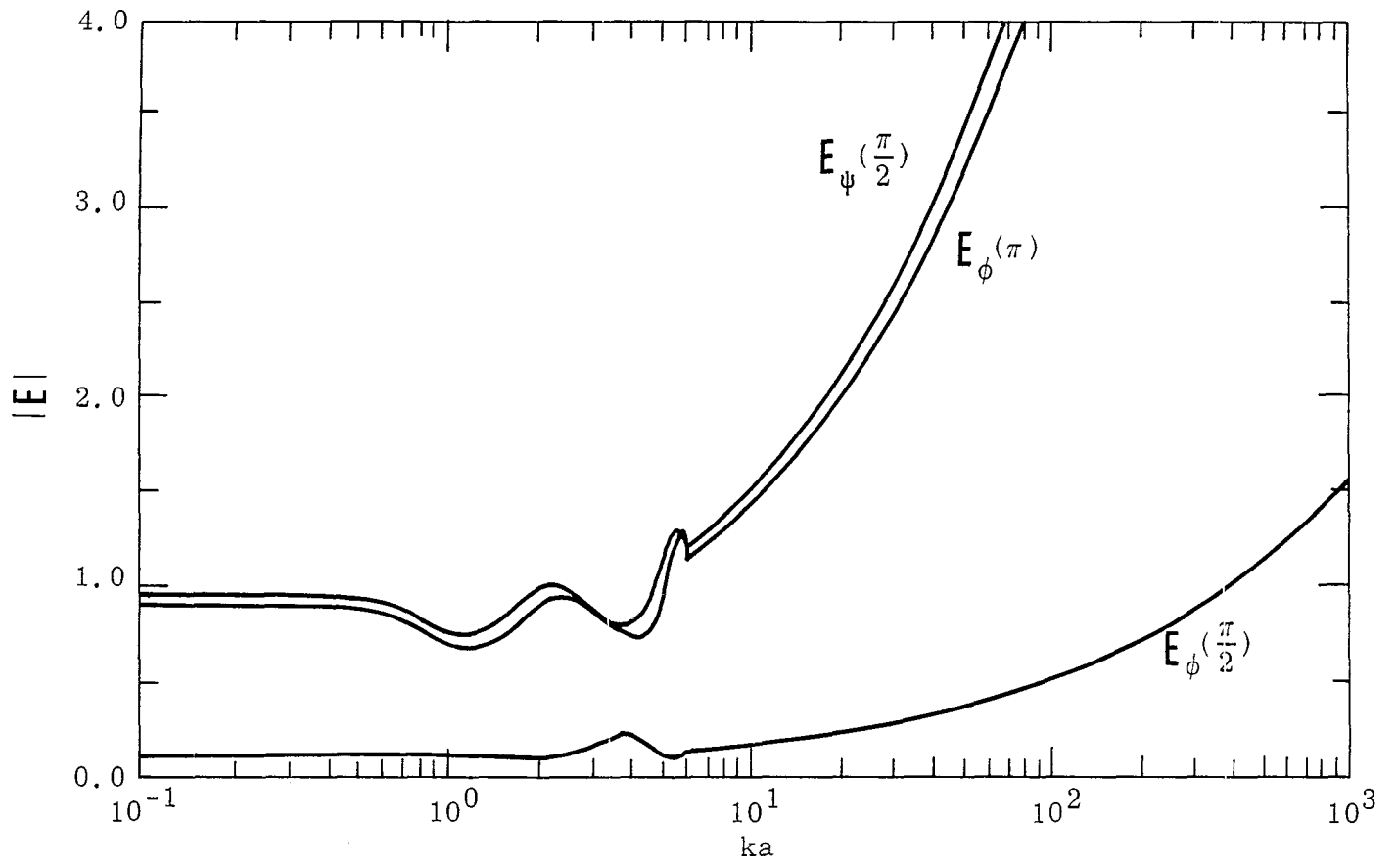
IX. Parameter Studies for Fields Near the Center in Frequency and Time Domains

Using the techniques of the past chapters, we plot in the following pages the fields near the center of the toroid in the frequency domain for a delta-function source and in the time domain for a unit-step function source. The load is a uniform resistance $Z = R_0$ and $\psi = 0.1$ as well as $\psi = 0.25$ are selected for these figures. The ratio b/a considered includes 0.1, 0.05, 0.01 and 0.001. The figures in the following pages are shown as examples only. Since the theory and the program are developed, one can readily generate the fields at any other locations of interest.



A. $\phi = 0$ and $\frac{\pi}{4}$.

Figure 9-1. E -field for $b/a = 0.1$ and $\psi = 0.1$ with ϕ as a Parameter



B. $\phi = \frac{\pi}{2}$ and π .

Figure 9-1. Continued

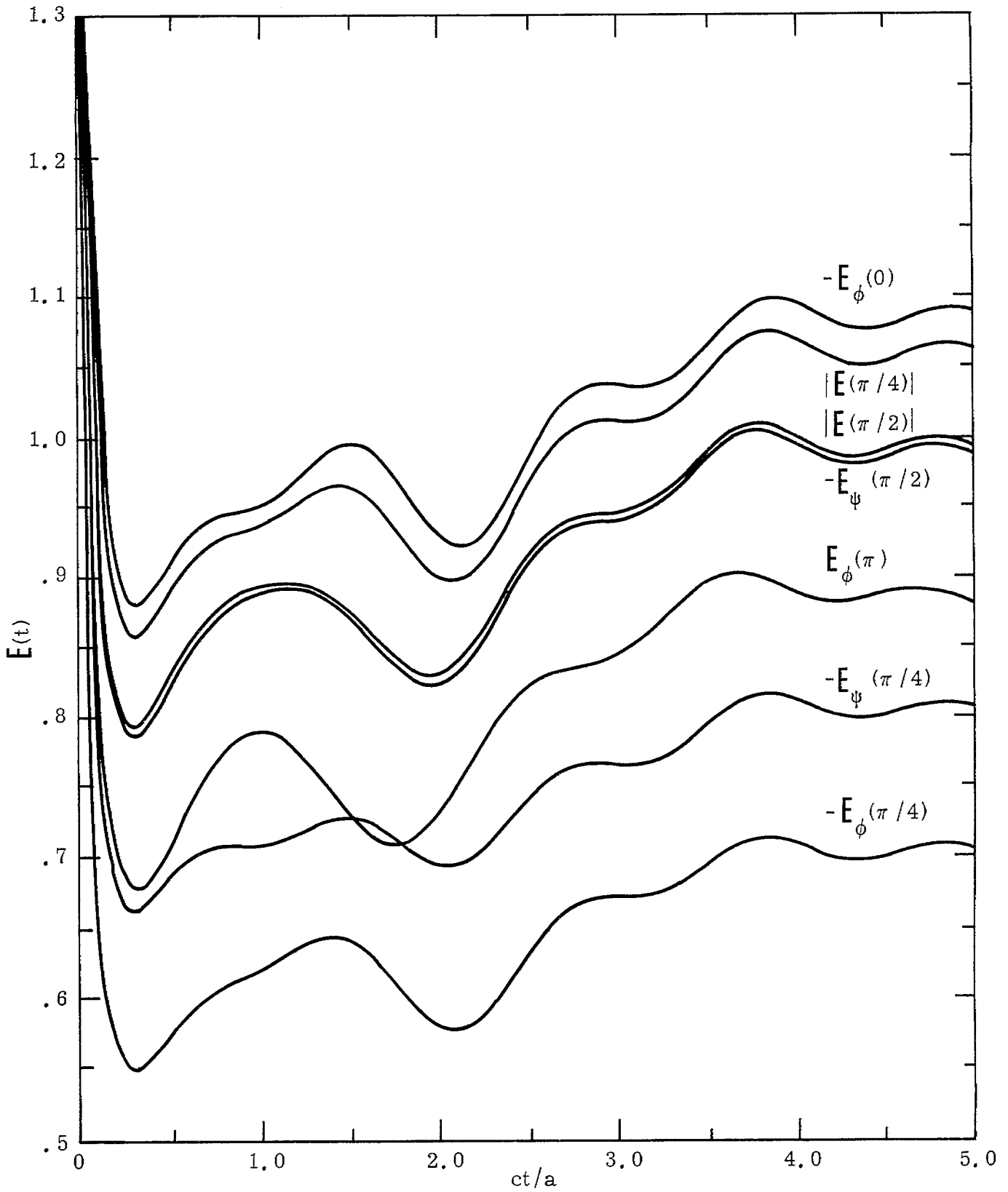
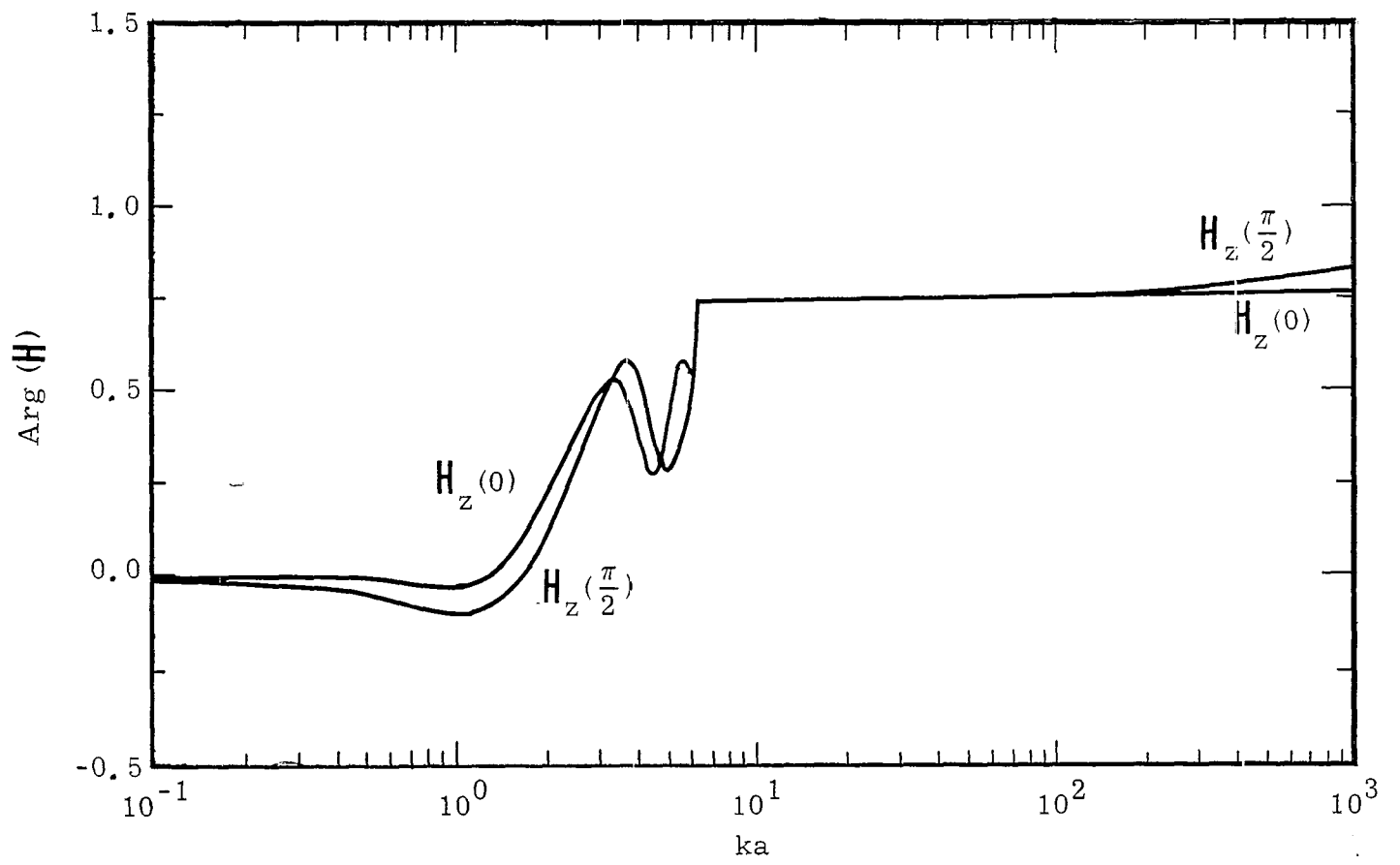
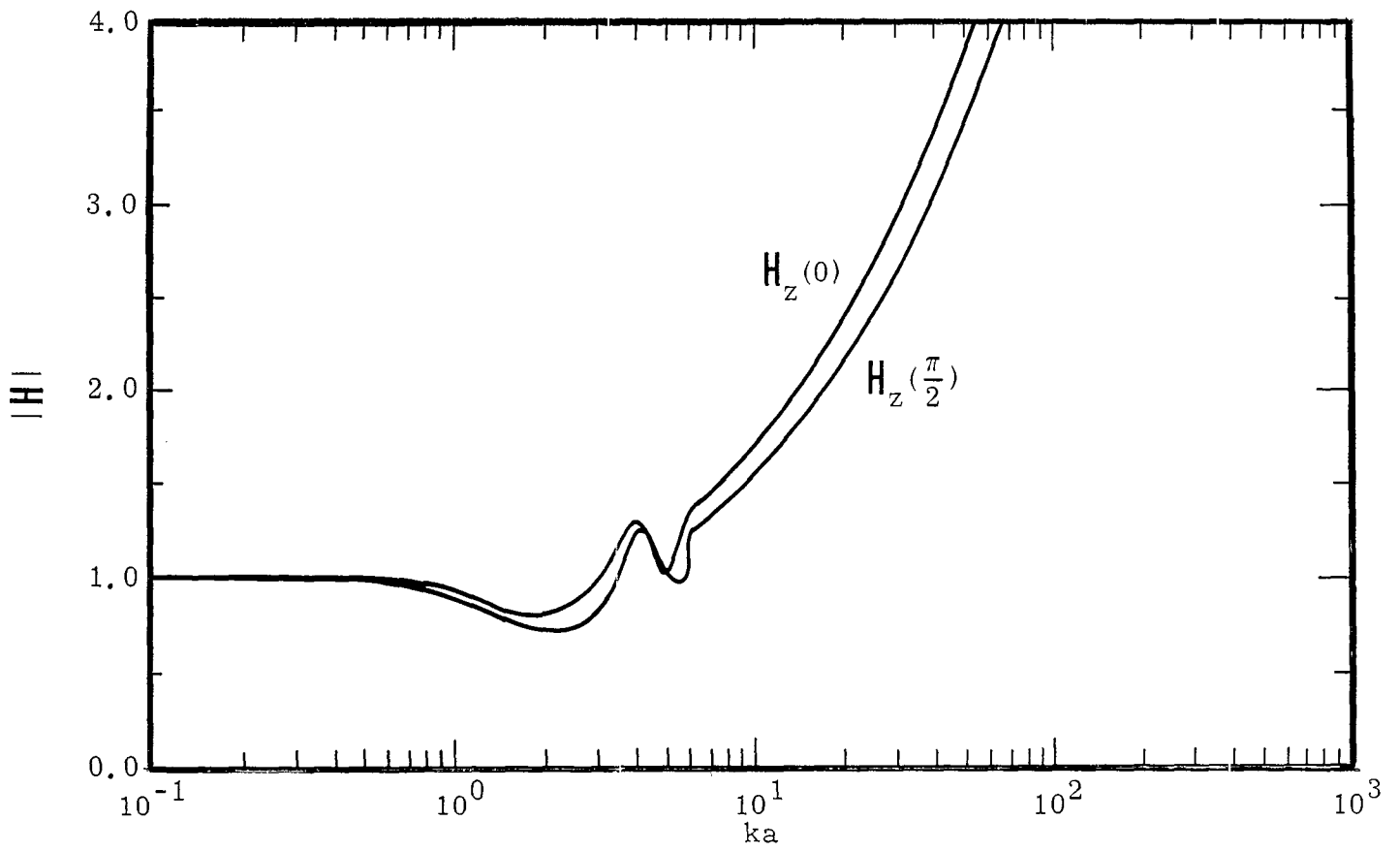
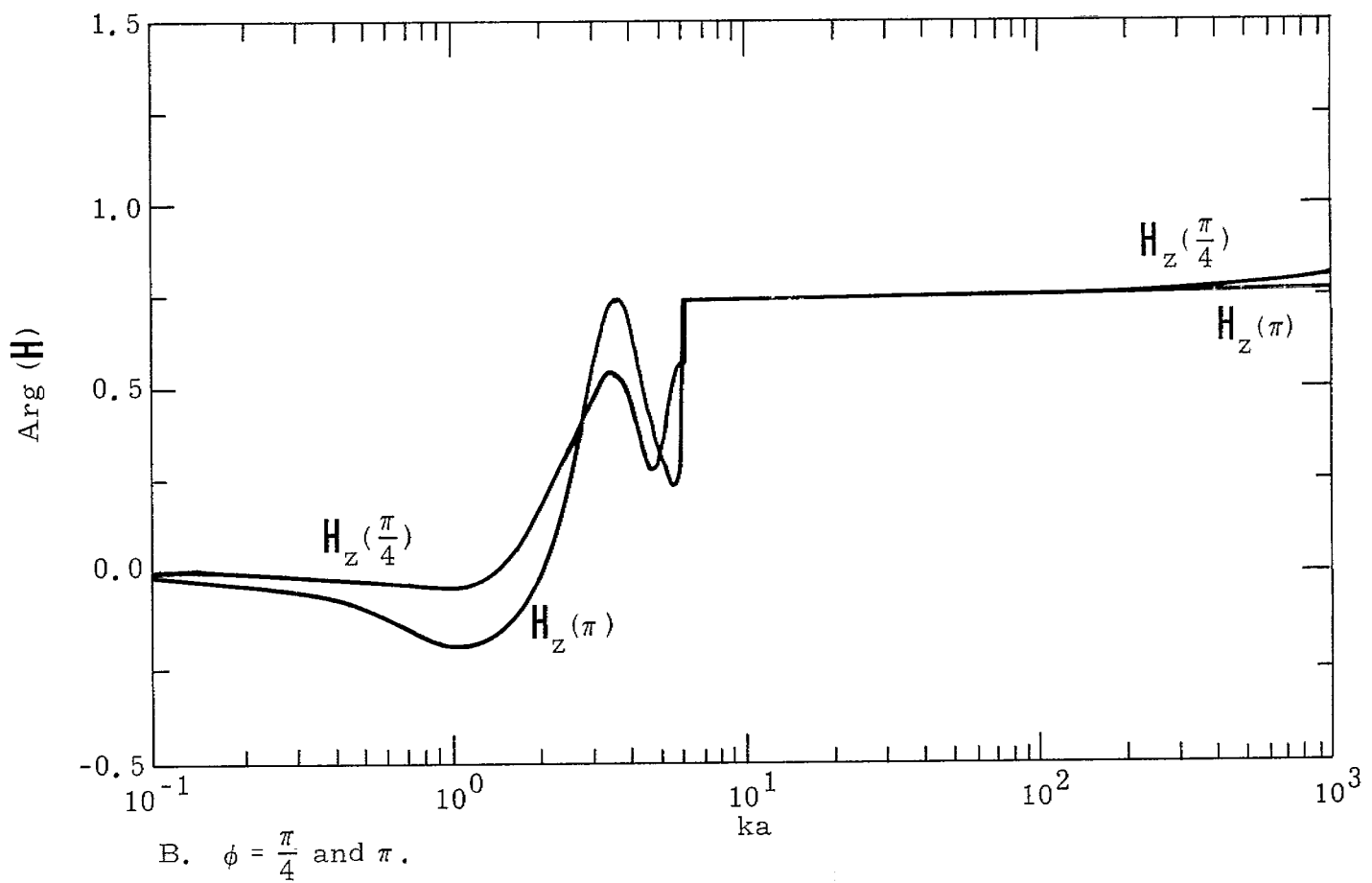
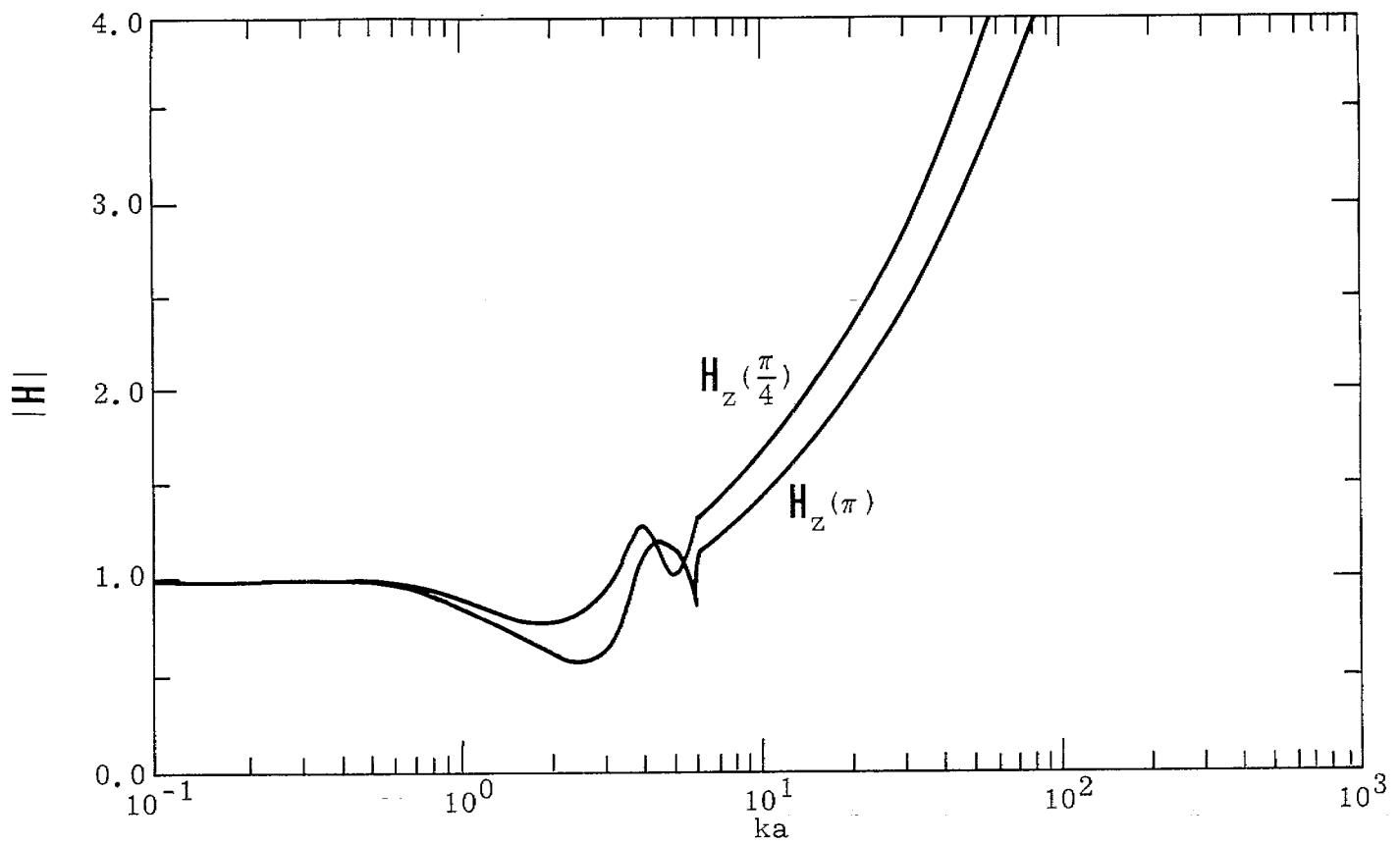


Figure 9-2. Step-function Response for the E -field for $b/a = 0.1$ and $\psi = 0.1$ with ϕ as a Parameter



A. $\phi = 0$ and $\frac{\pi}{2}$.

Figure 9-3. H -field for $b/a = 0.1$ and $\psi = 0.1$ with ϕ as a Parameter



B. $\phi = \frac{\pi}{4}$ and π .

Figure 9-3. Continued

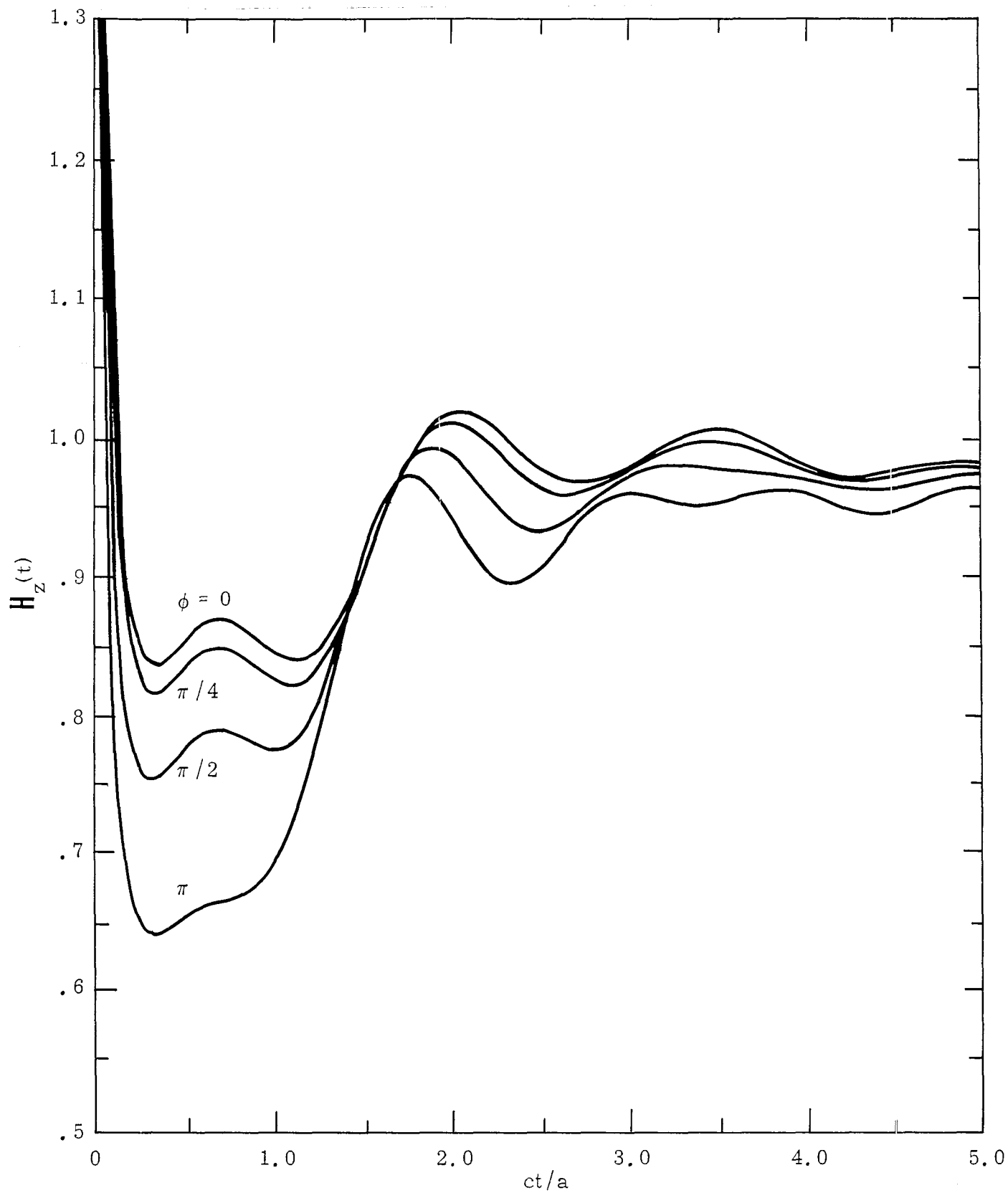
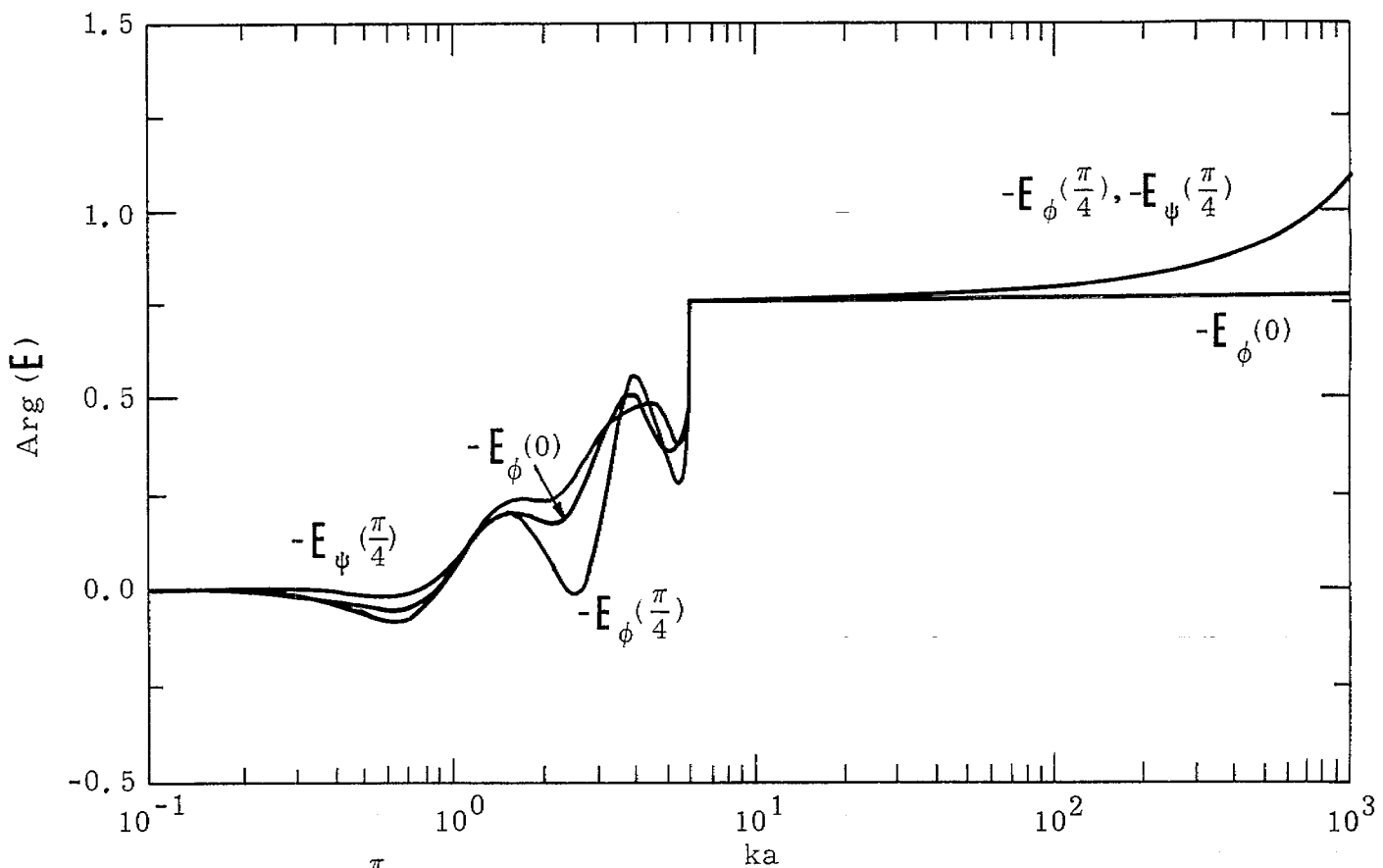
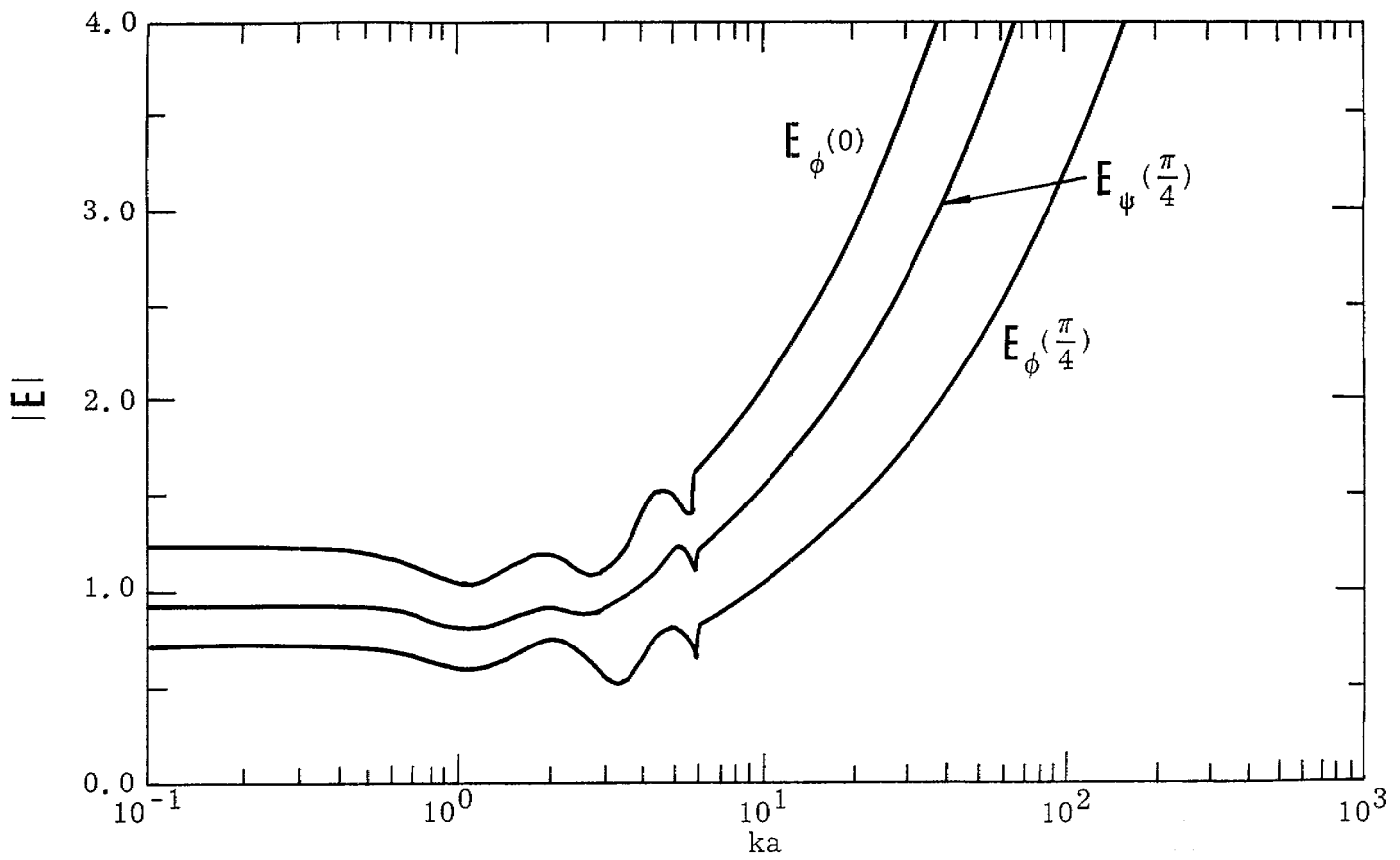
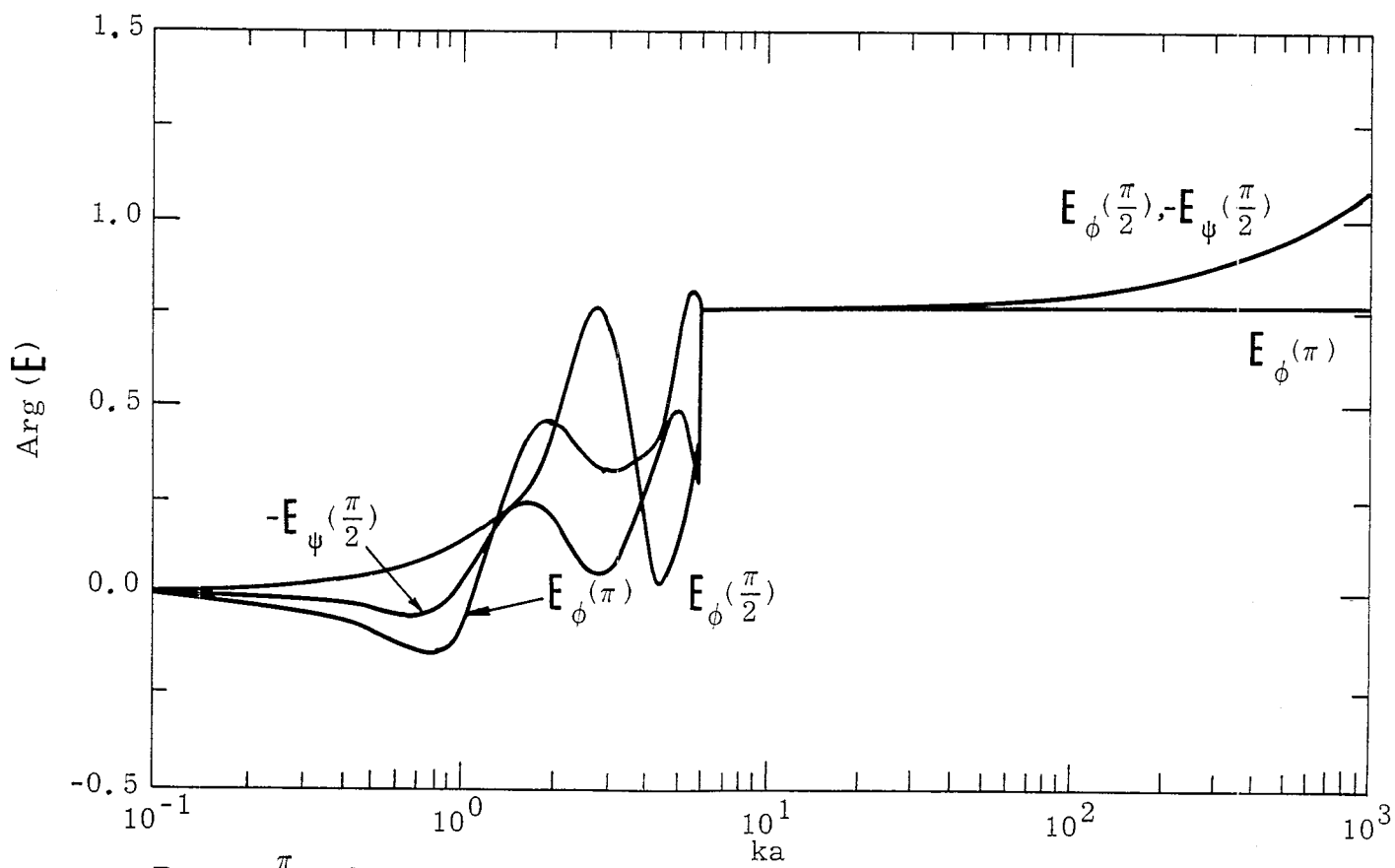
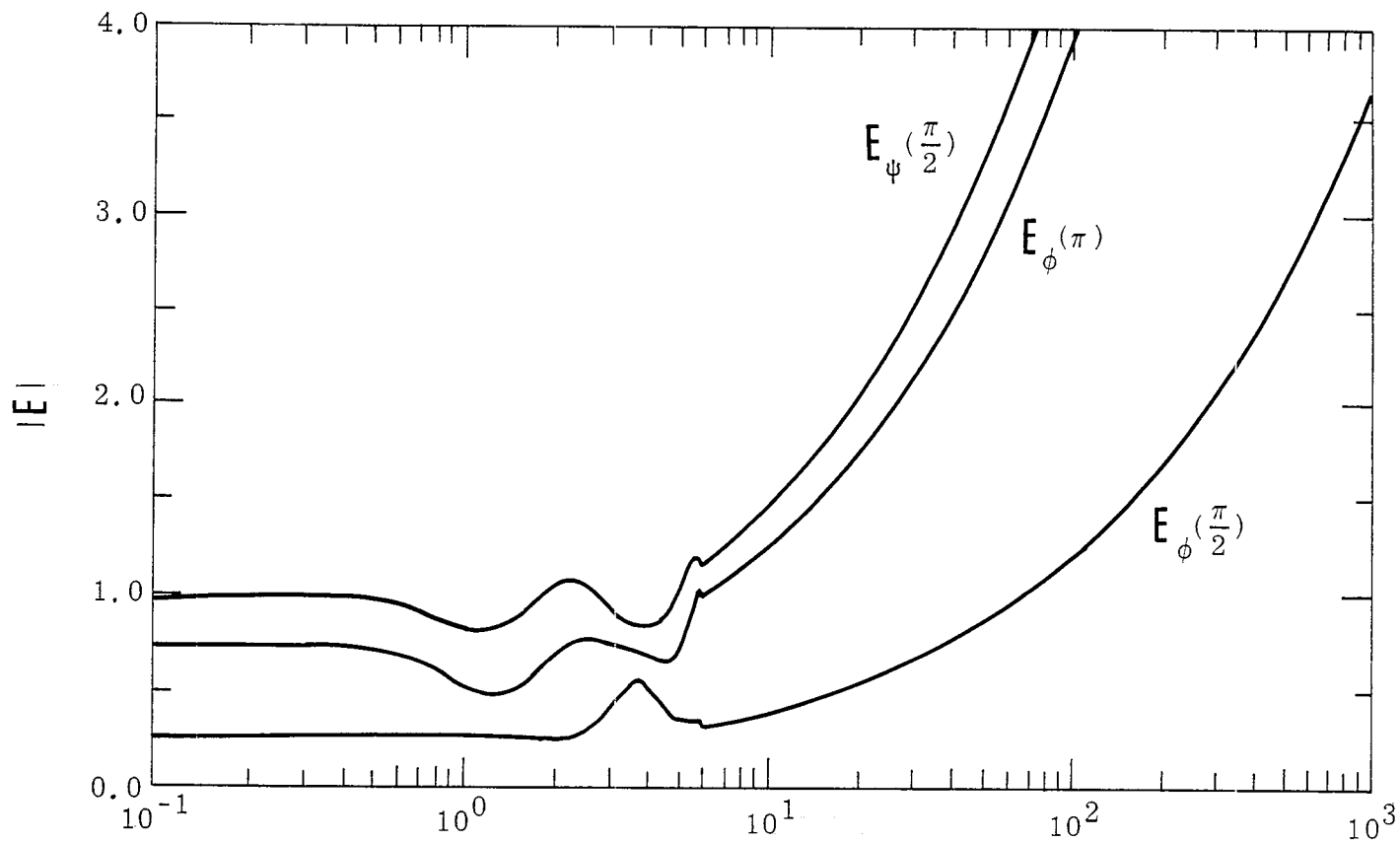


Figure 9-4. Step-function Response for the H -field for $b/a = 0.1$ and $\psi = 0.1$ with ϕ as a Parameter



A. $\phi = 0$ and $\frac{\pi}{4}$.

Figure 9-5. E -field for $b/a = 0.1$ and $\psi = 0.25$ with ϕ as a Parameter



B. $\phi = \frac{\pi}{2}$ and π .

Figure 9-5. Continued

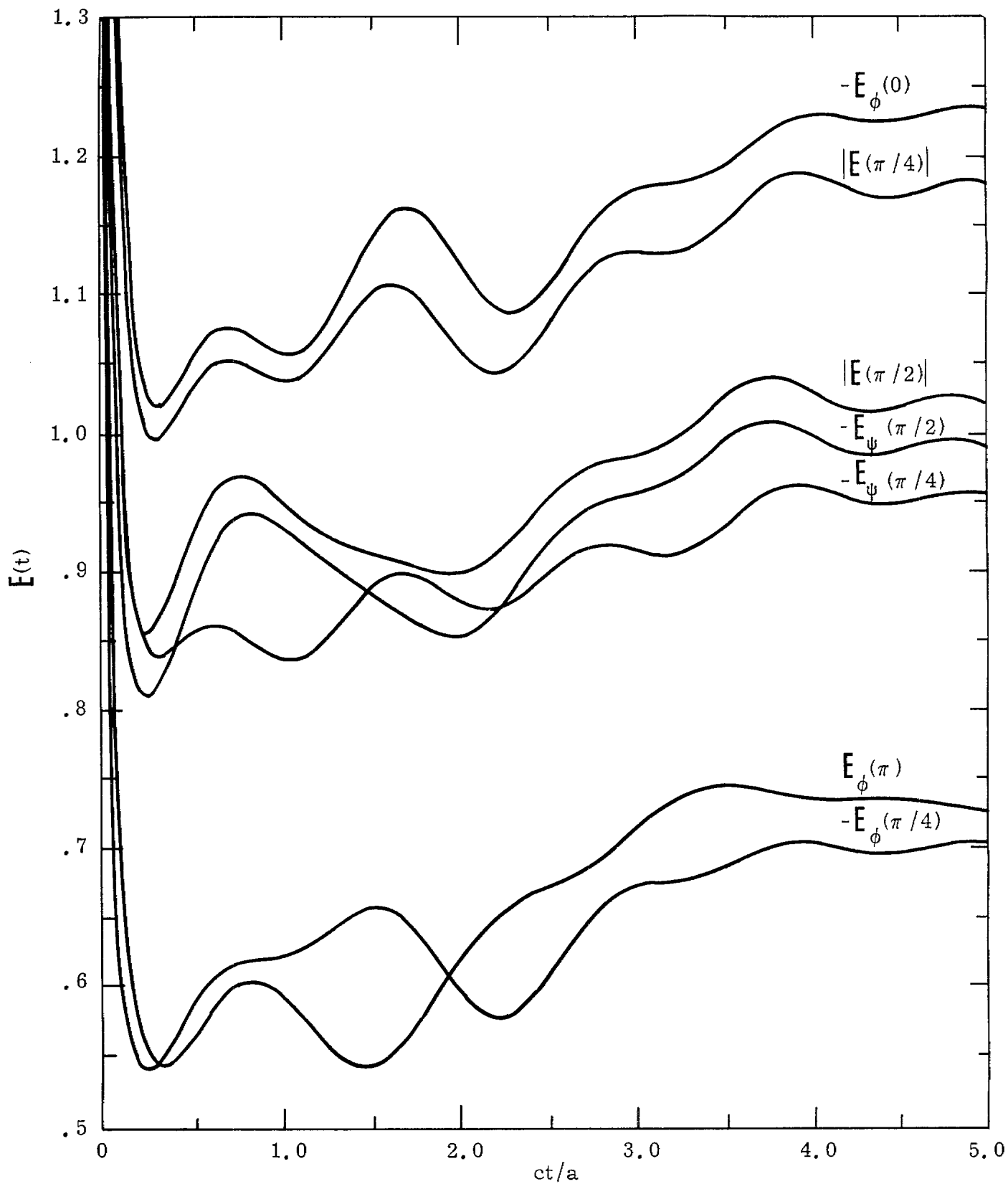
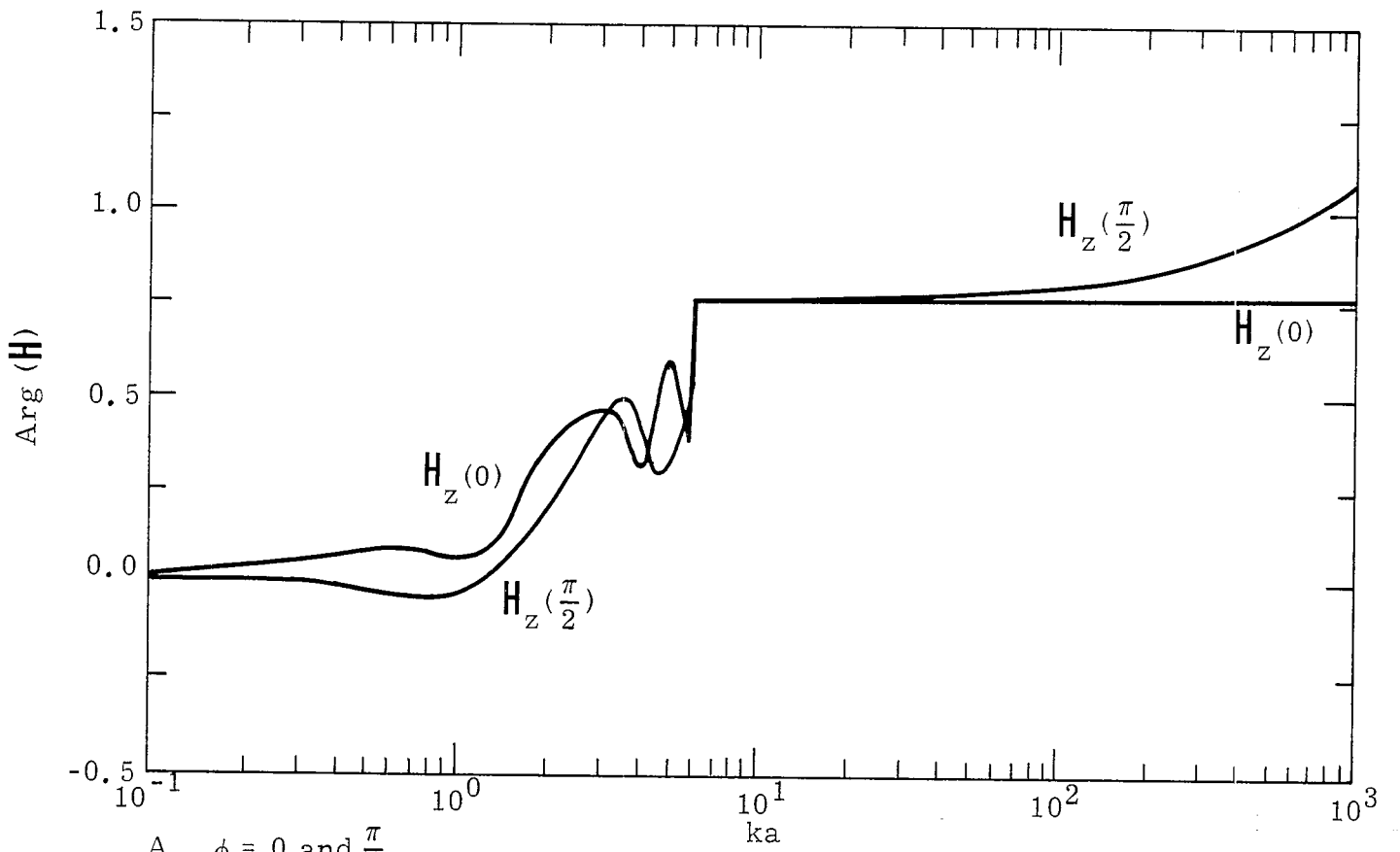
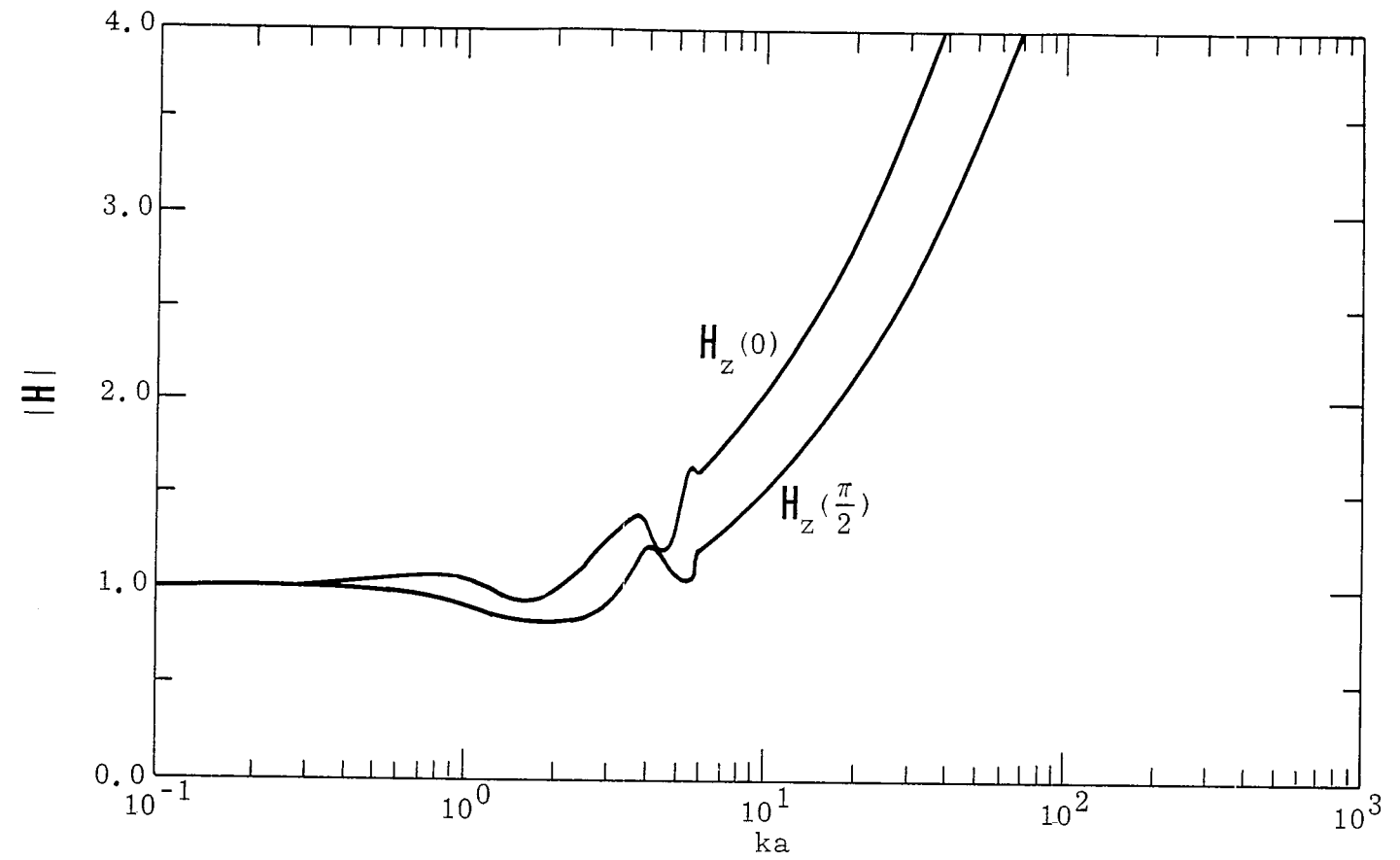
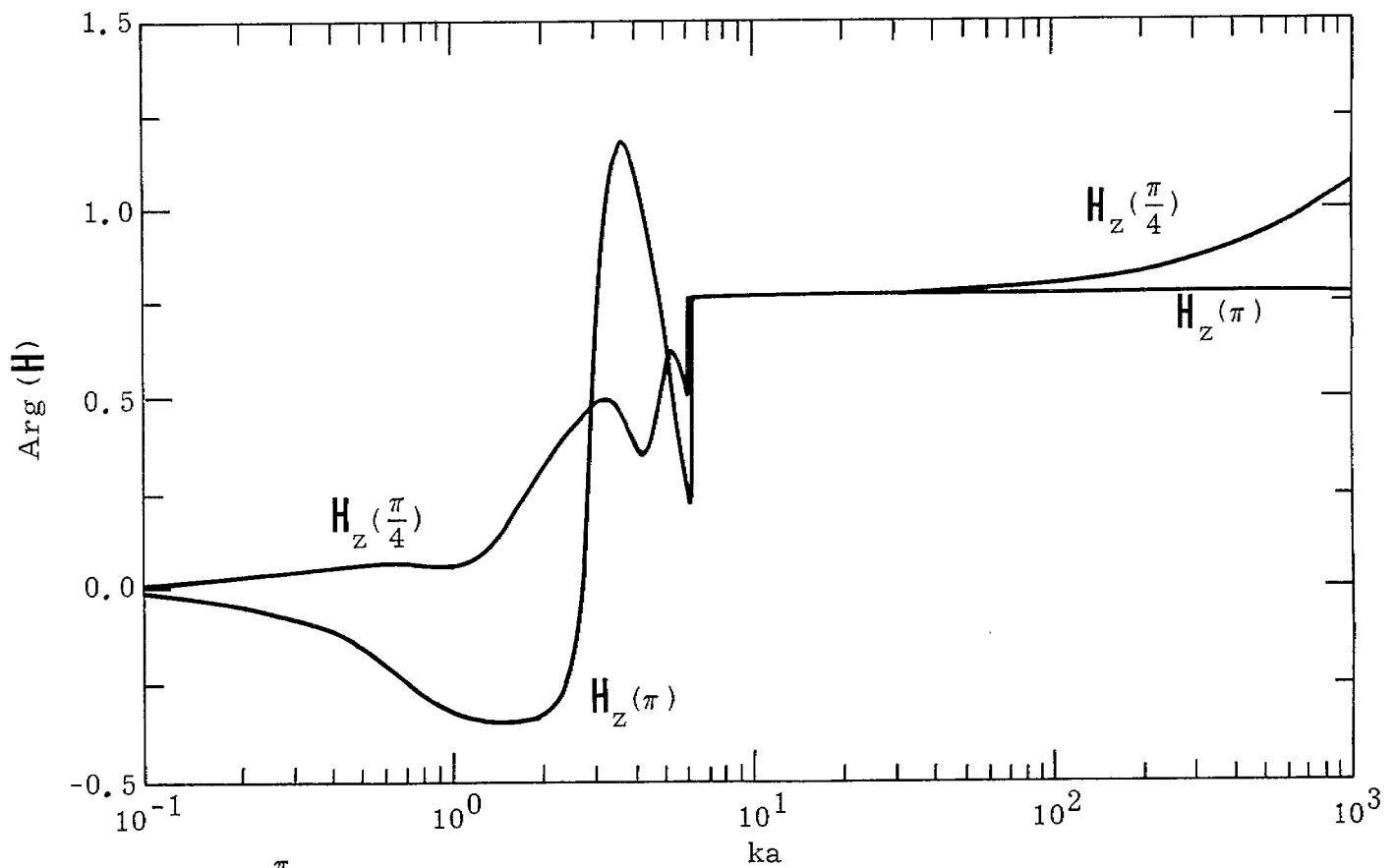
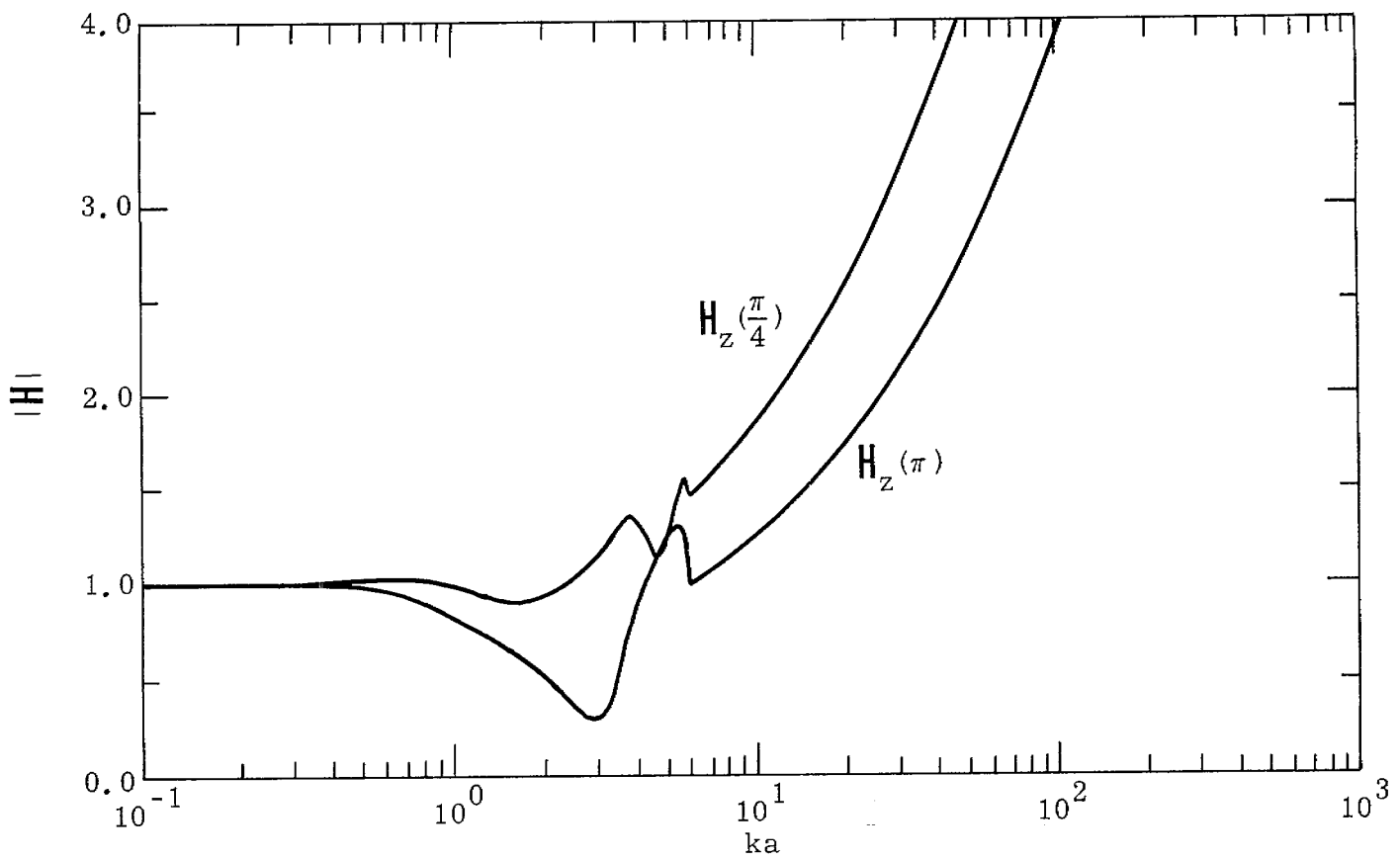


Figure 9-6. Step-function Response for the E -field for $b/a = 0.1$ and $\psi = 0.25$ with ϕ as a Parameter



A. $\phi = 0$ and $\frac{\pi}{2}$.

Figure 9-7. H -field for $b/a = 0.1$ and $\psi = 0.25$ with ϕ as a Parameter



B. $\phi = \frac{\pi}{4}$ and π .

Figure 9-7. Continued

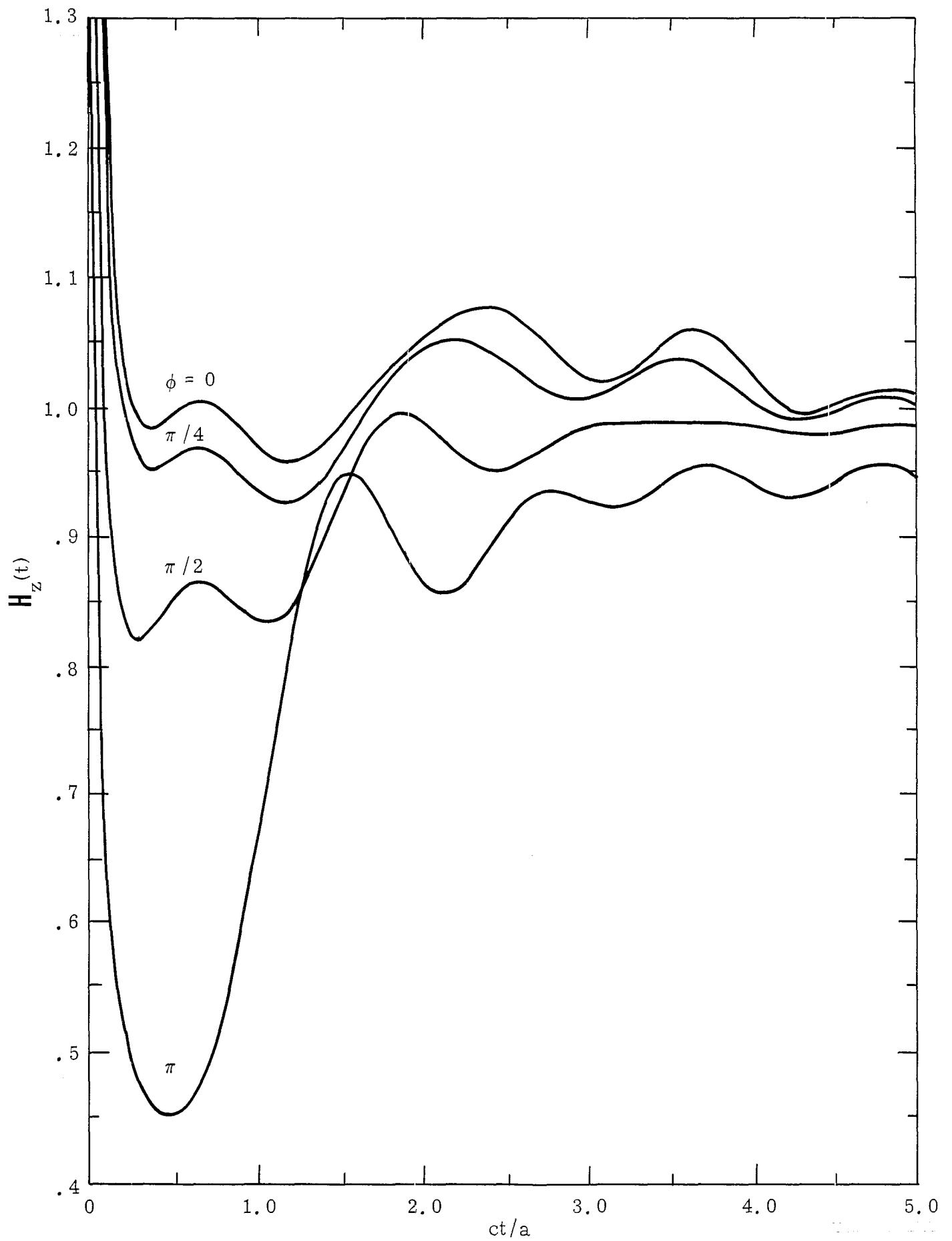
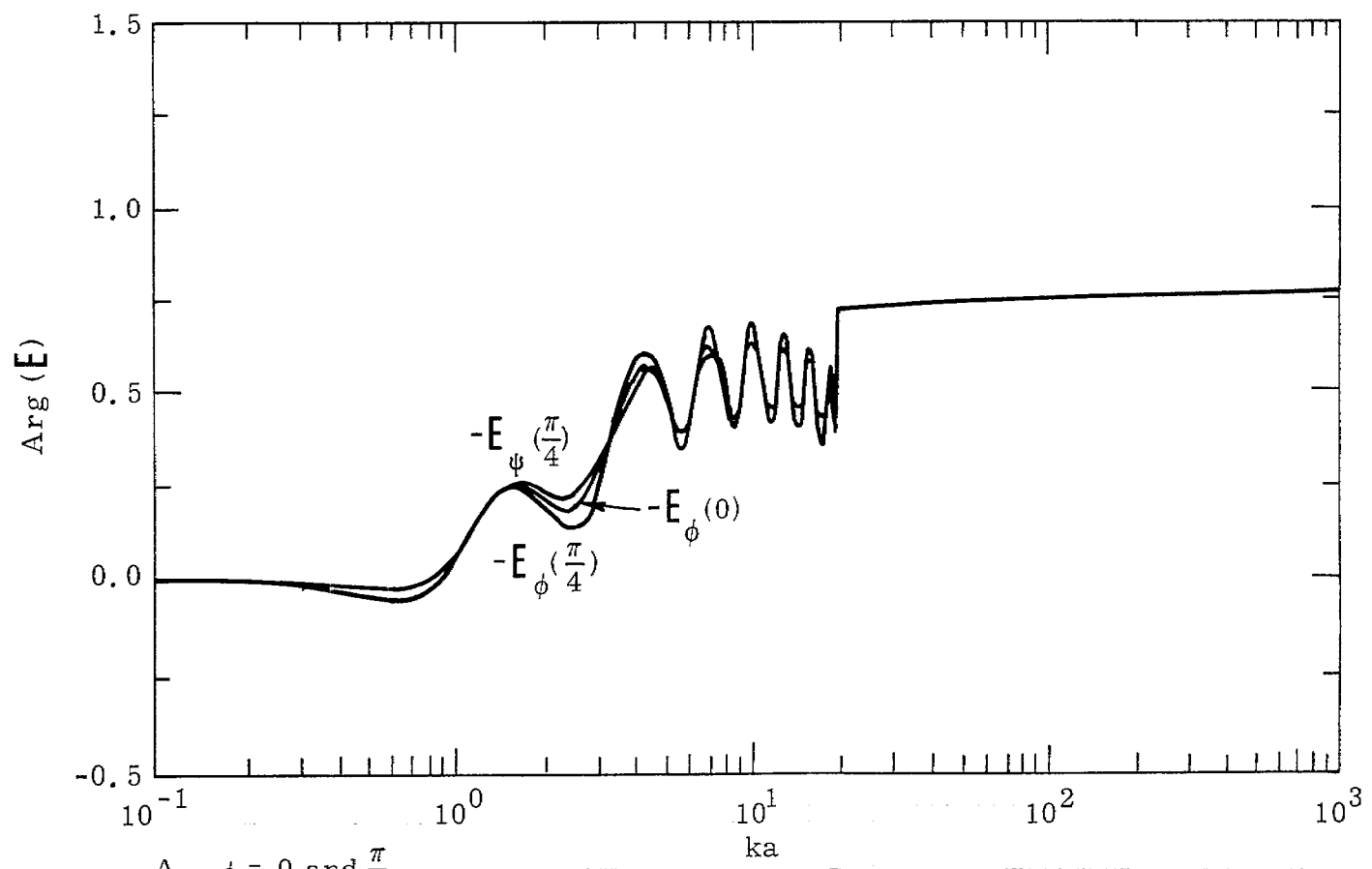
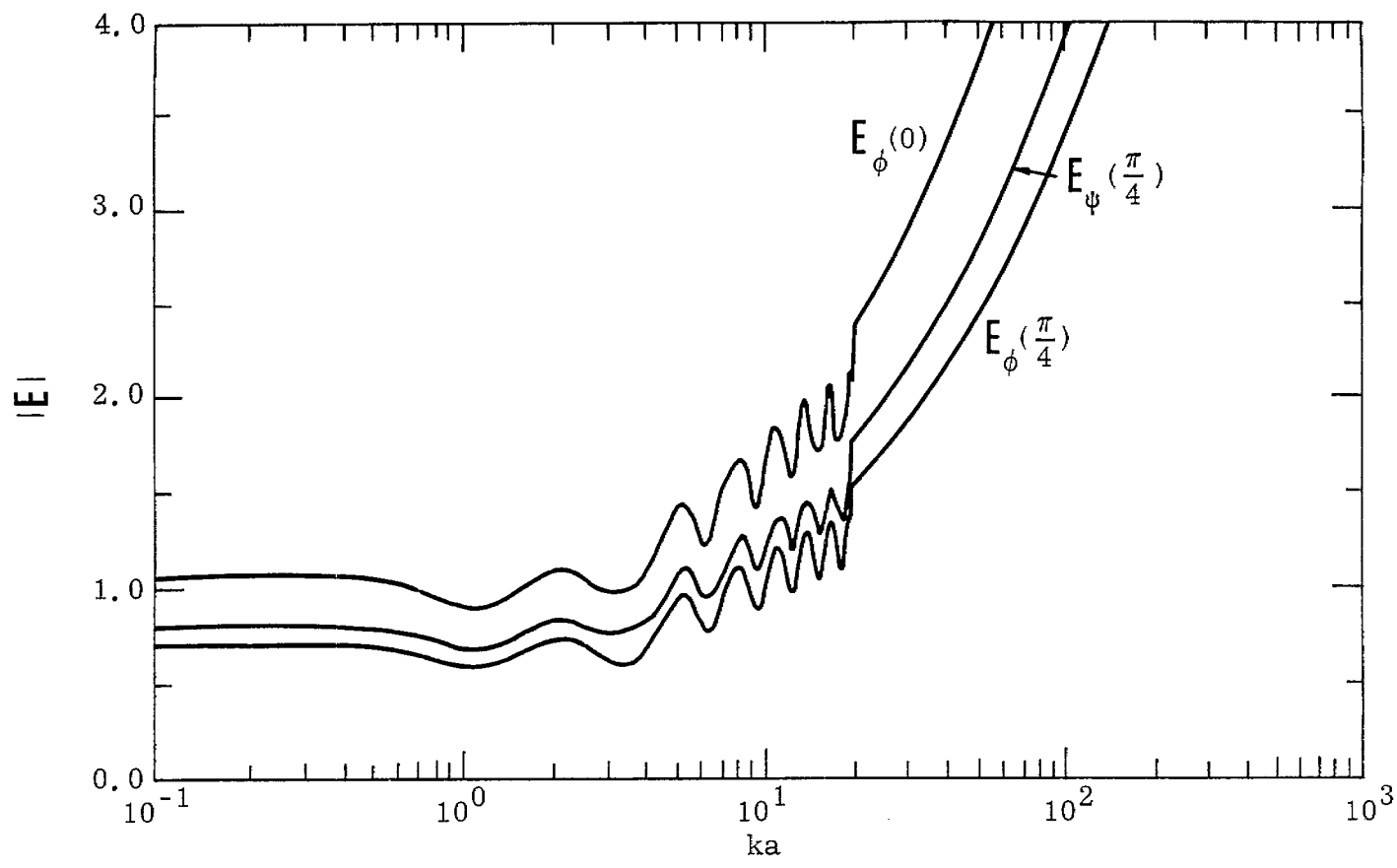


Figure 9-8. Step-function Response for the H -field for $b/a = 0.1$ and $\psi = 0.25$ with ϕ as a Parameter



A. $\phi = 0$ and $\frac{\pi}{4}$.

Figure 9-9. E -field for $b/a = 0.05$ and $\psi = 0.1$ with ϕ as a Parameter

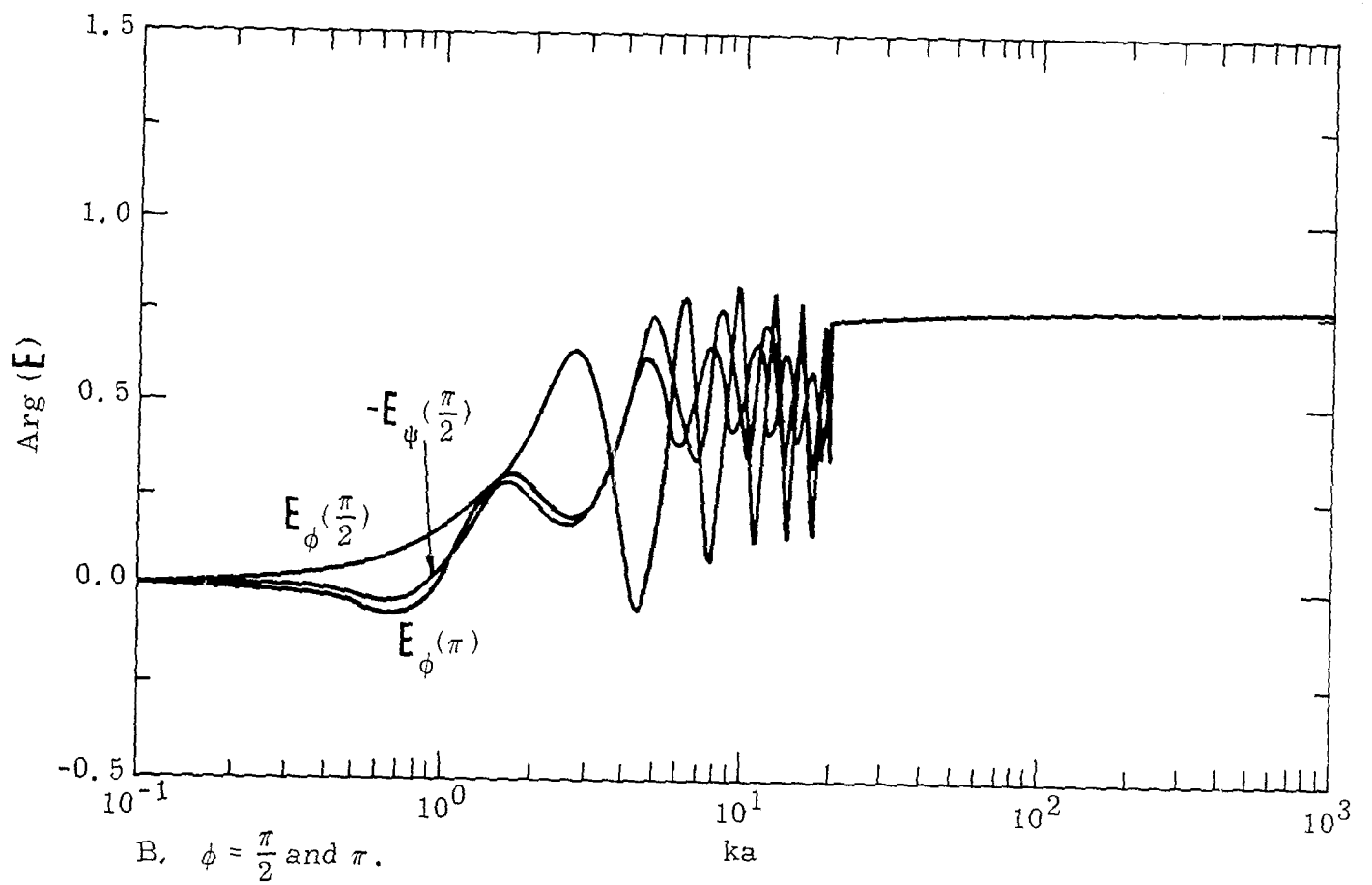
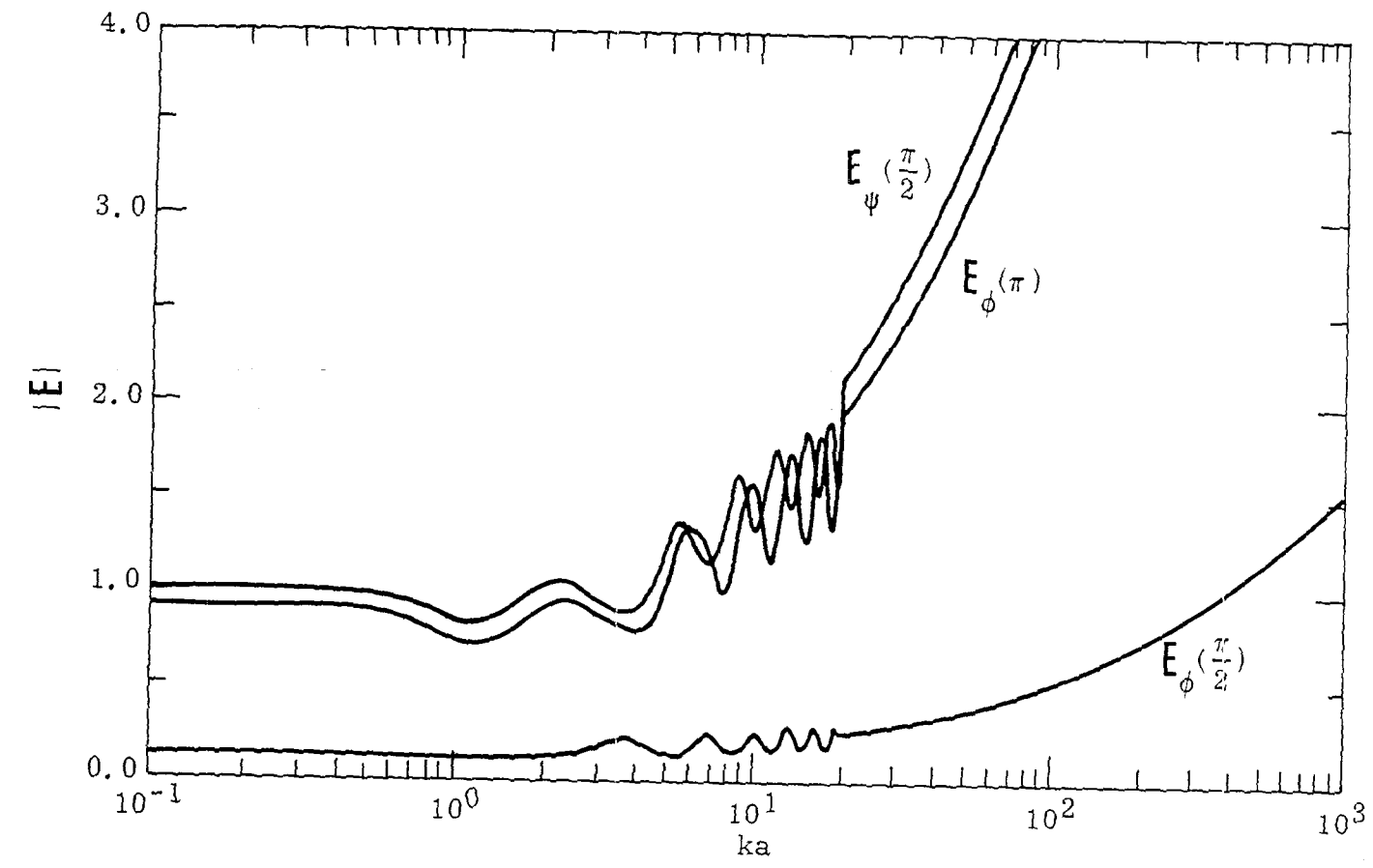


Figure 9-9. Continued

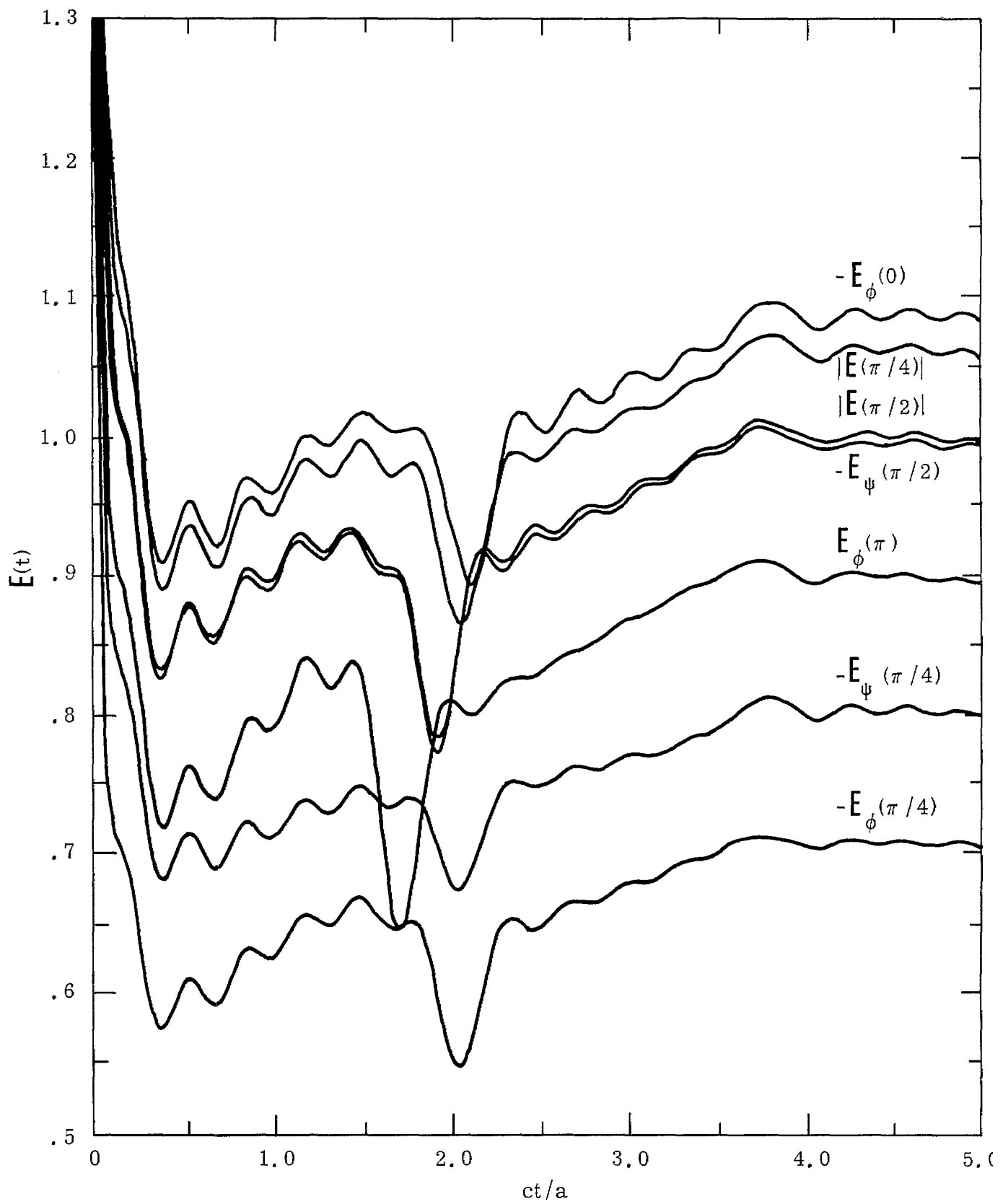
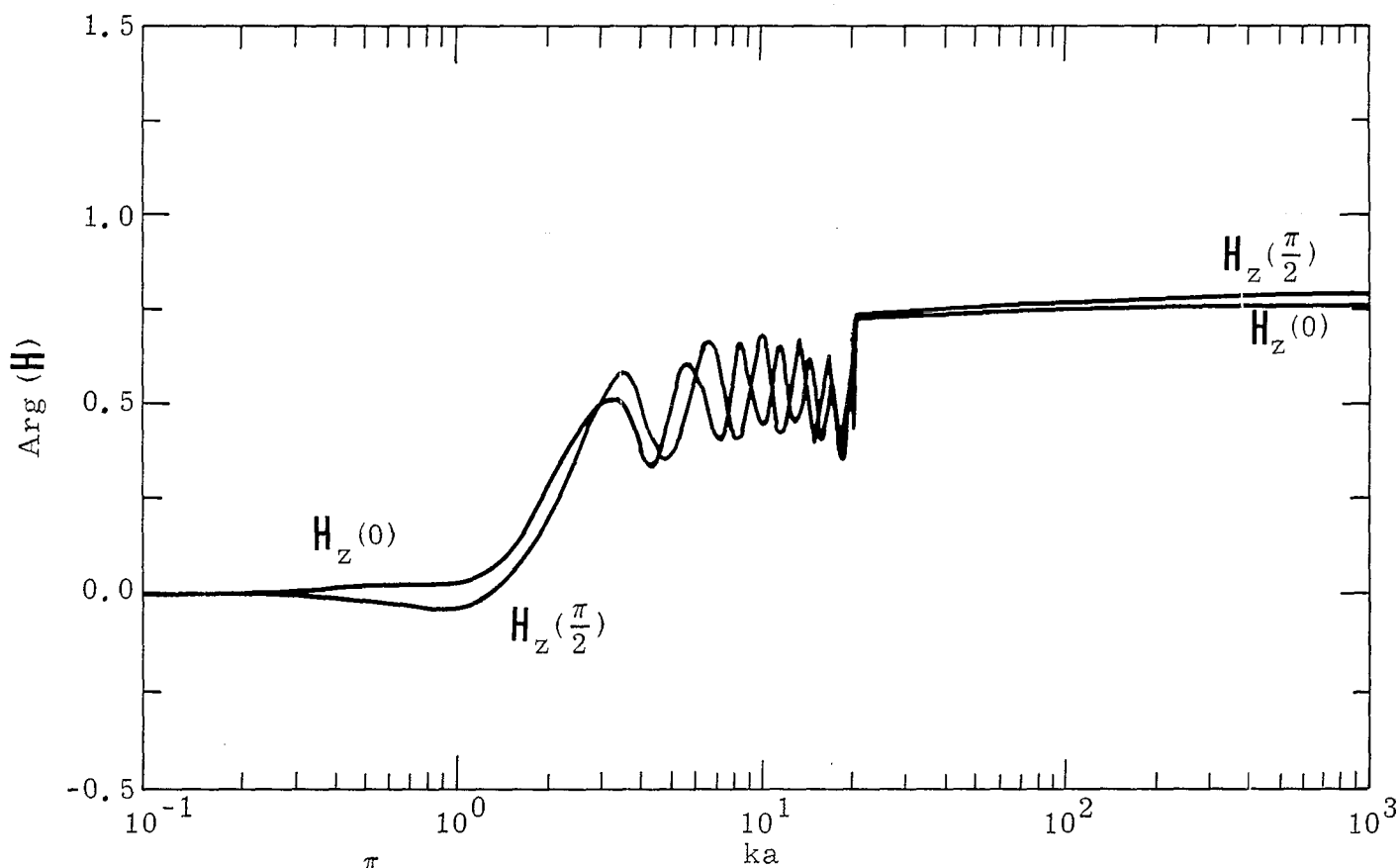
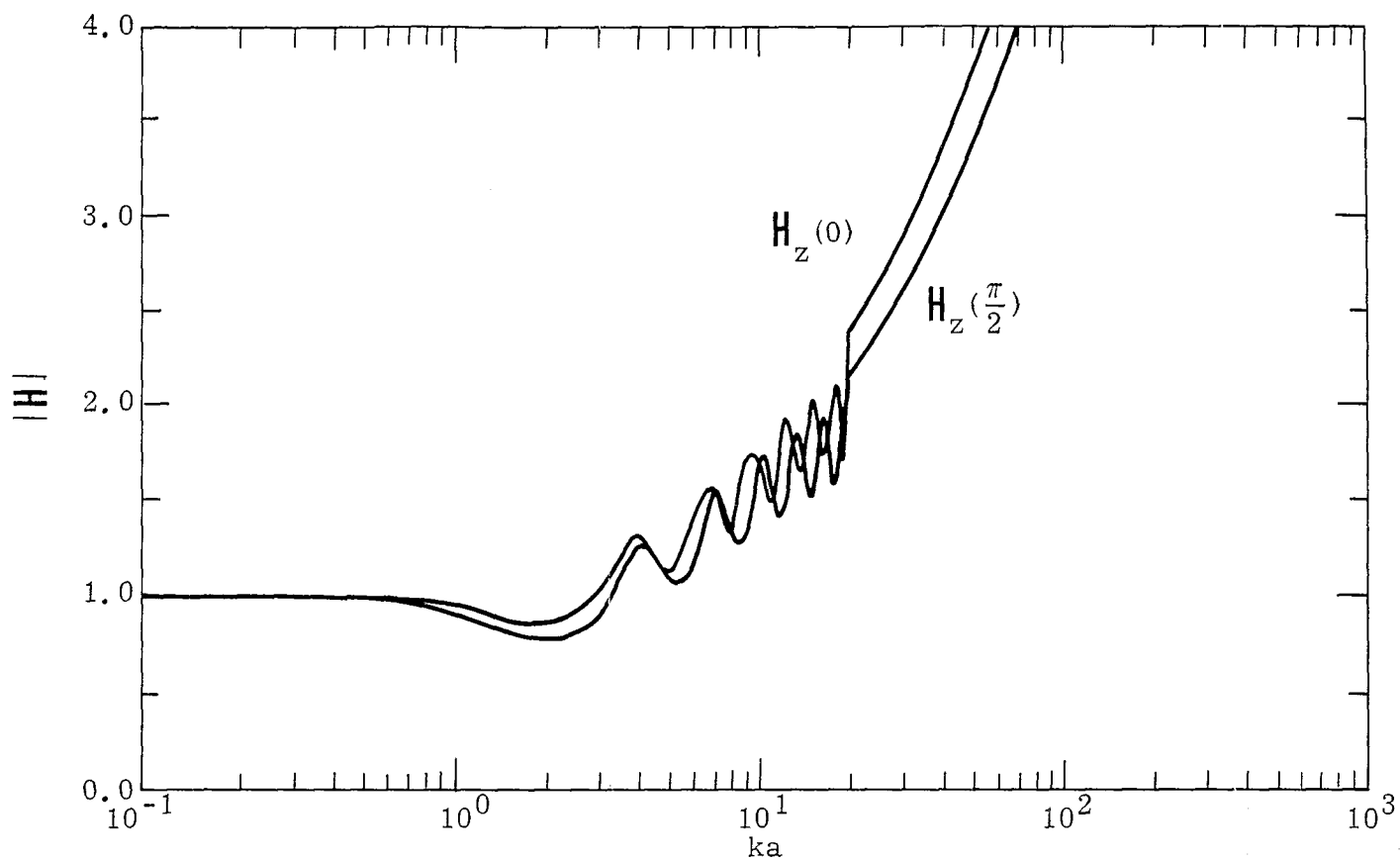
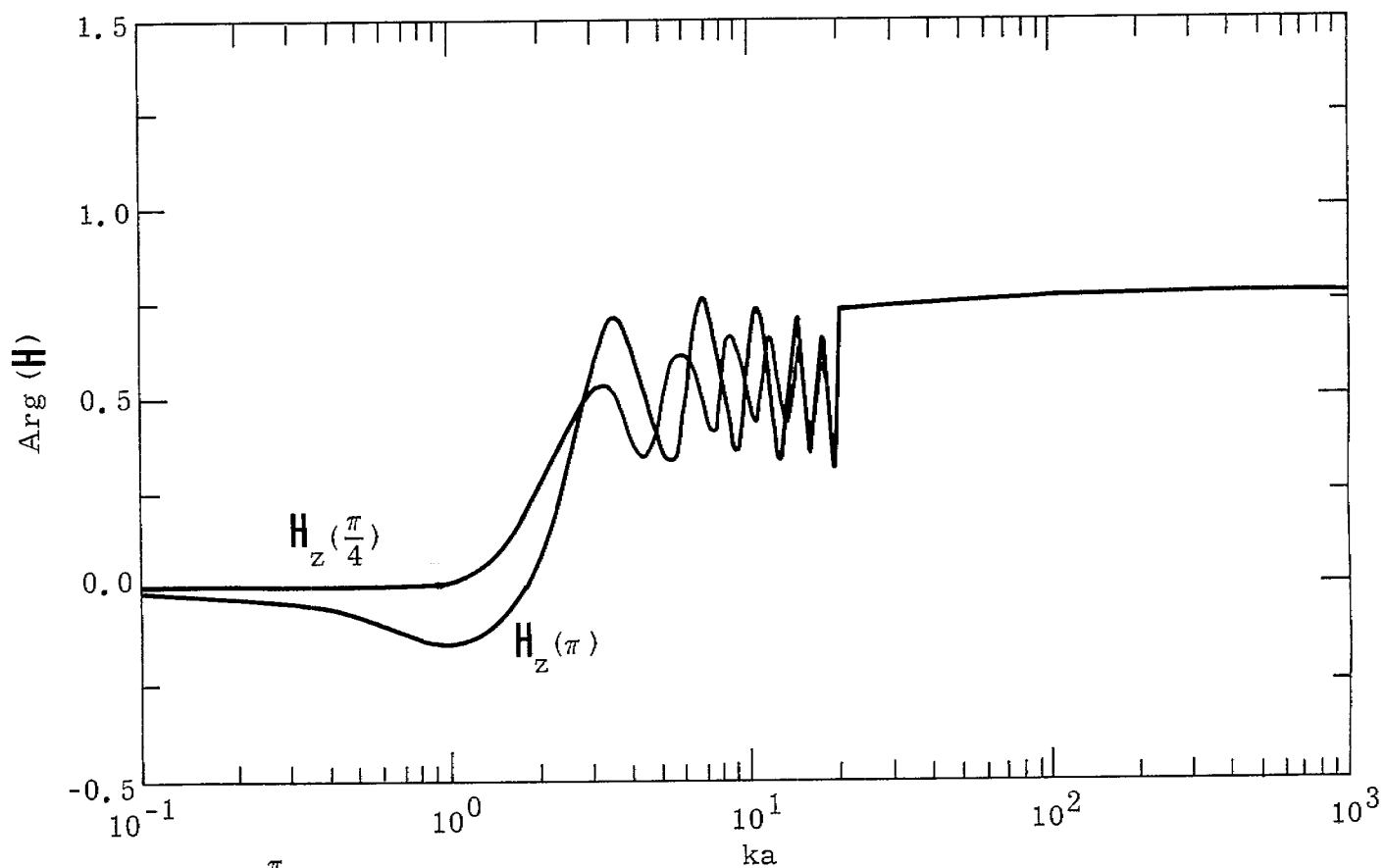
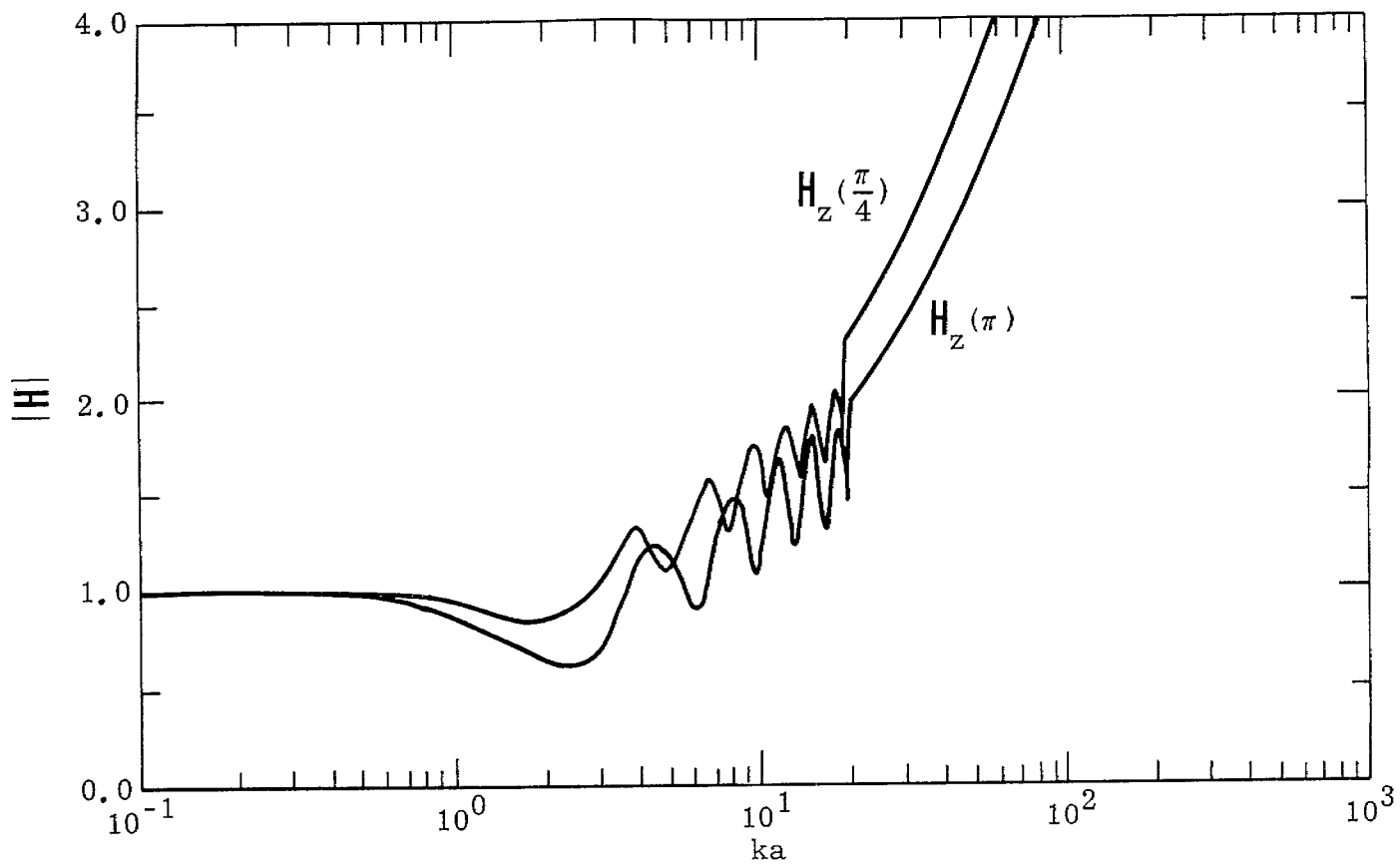


Figure 9-10. Step-function Response for the \underline{E} -field for $b/a = 0.05$ and $\psi = 0.1$ with ϕ as a Parameter



A. $\phi = 0$ and $\frac{\pi}{2}$.

Figure 9-11. H -field for $b/a = 0.05$ and $\psi = 0.1$ with ϕ as a Parameter



B. $\phi = \frac{\pi}{4}$ and π .

Figure 9-11. Continued

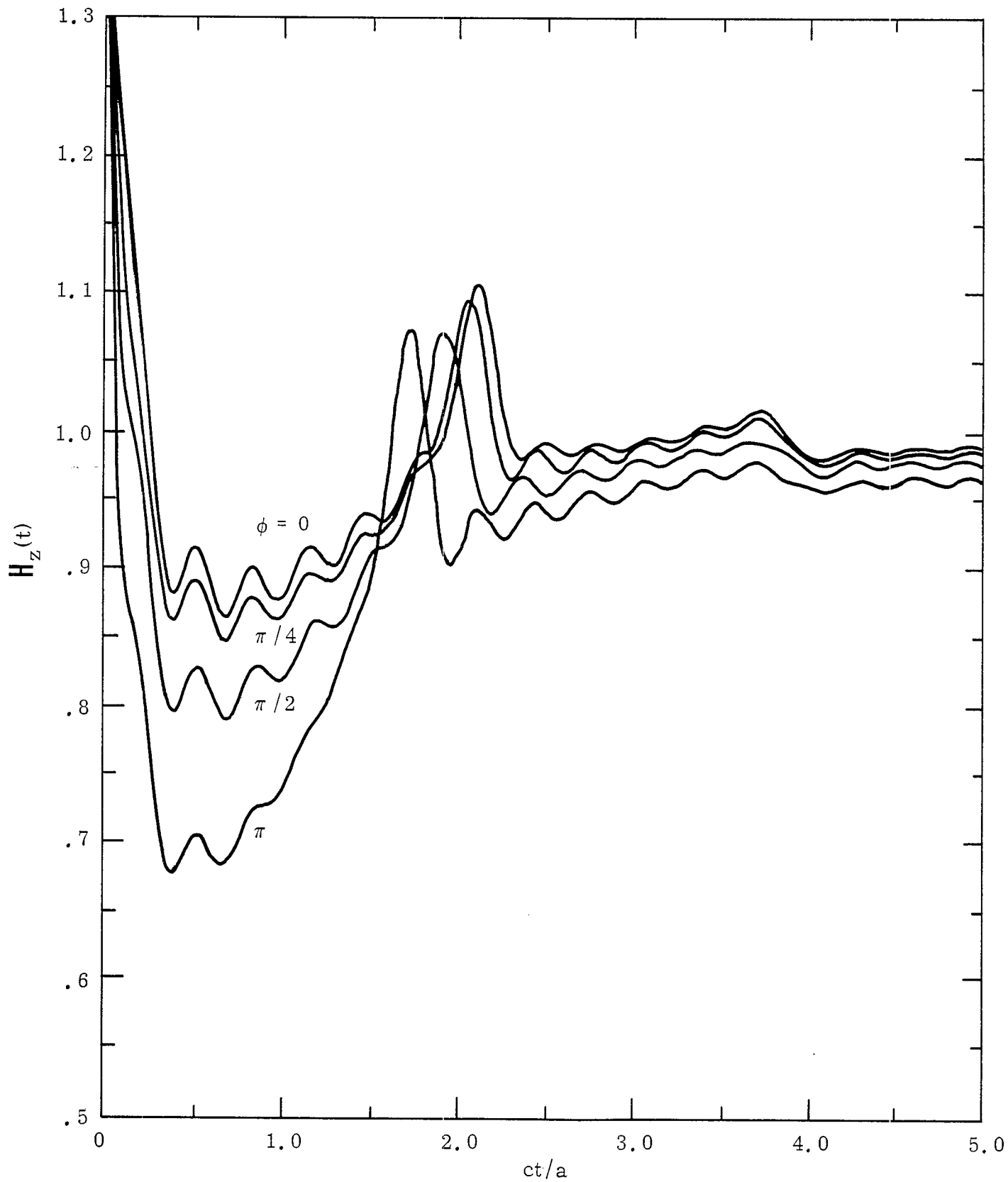
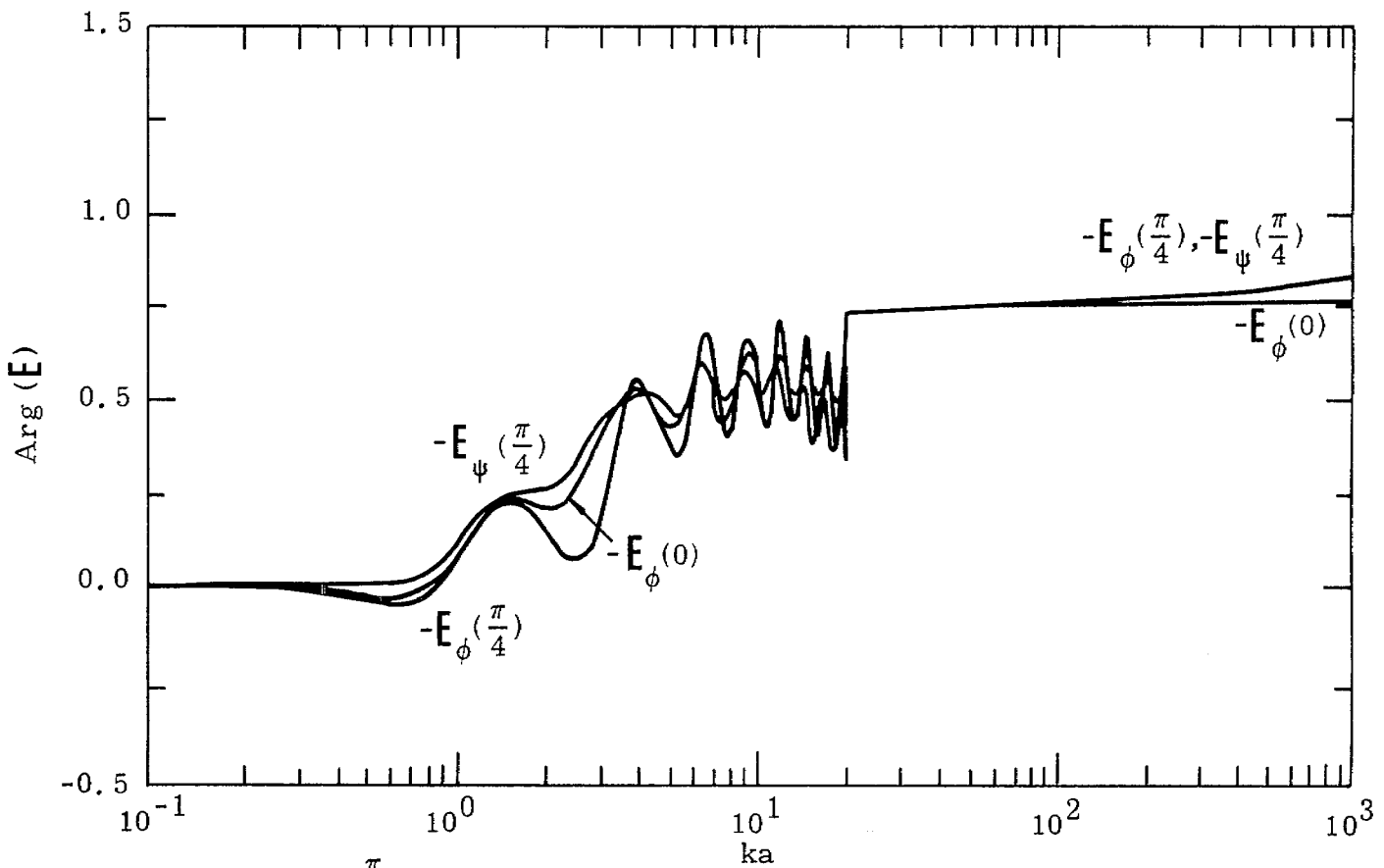
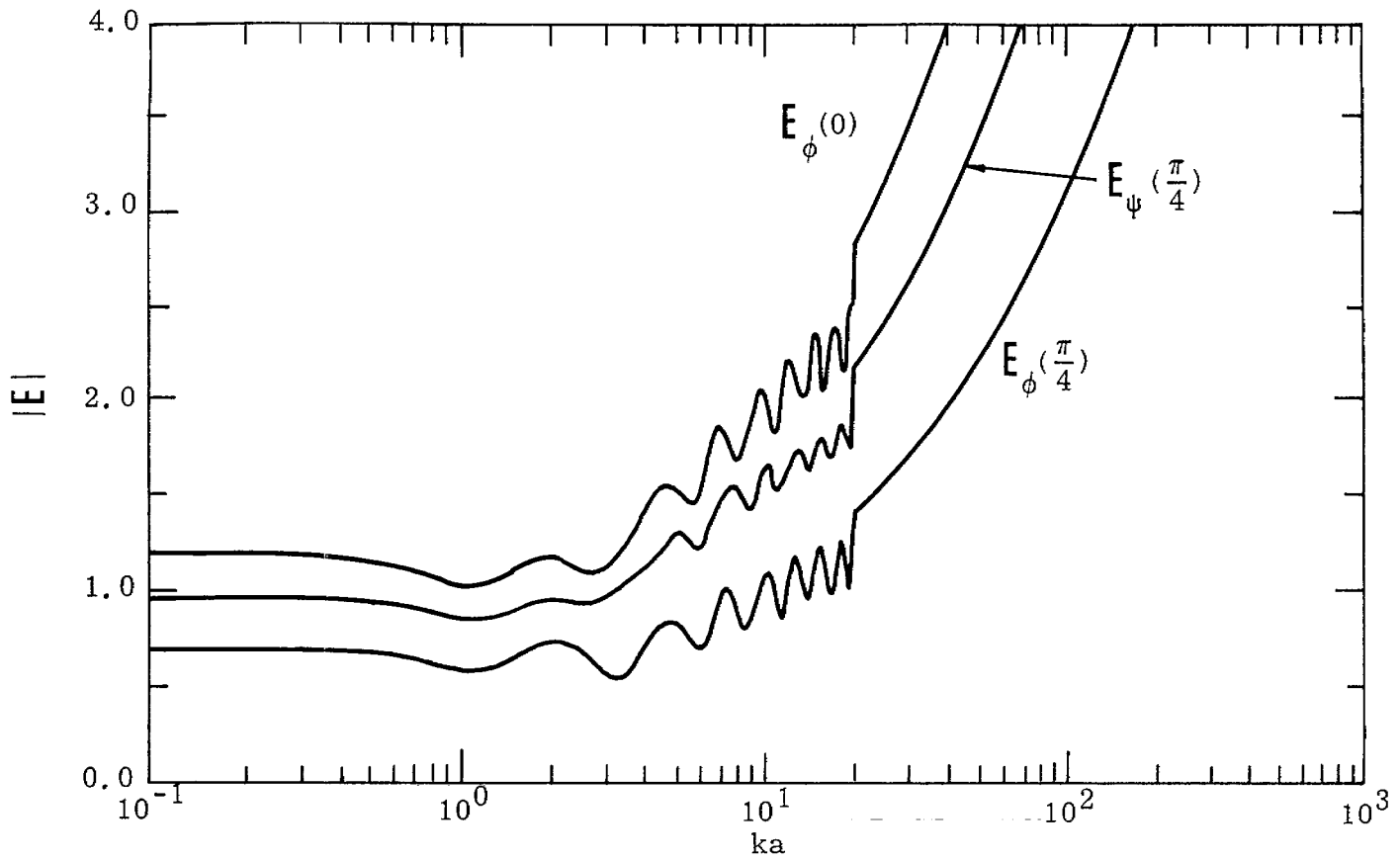
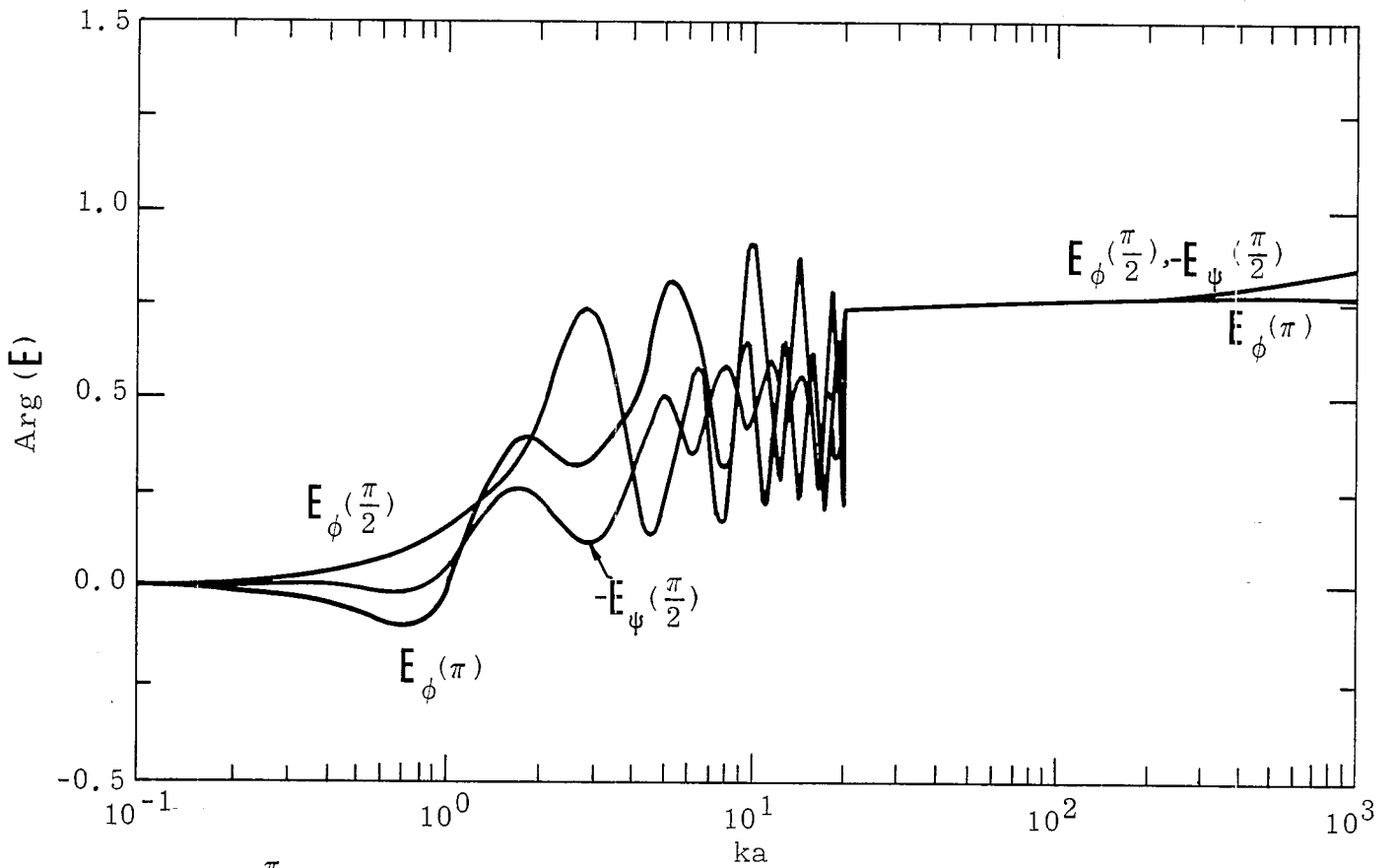
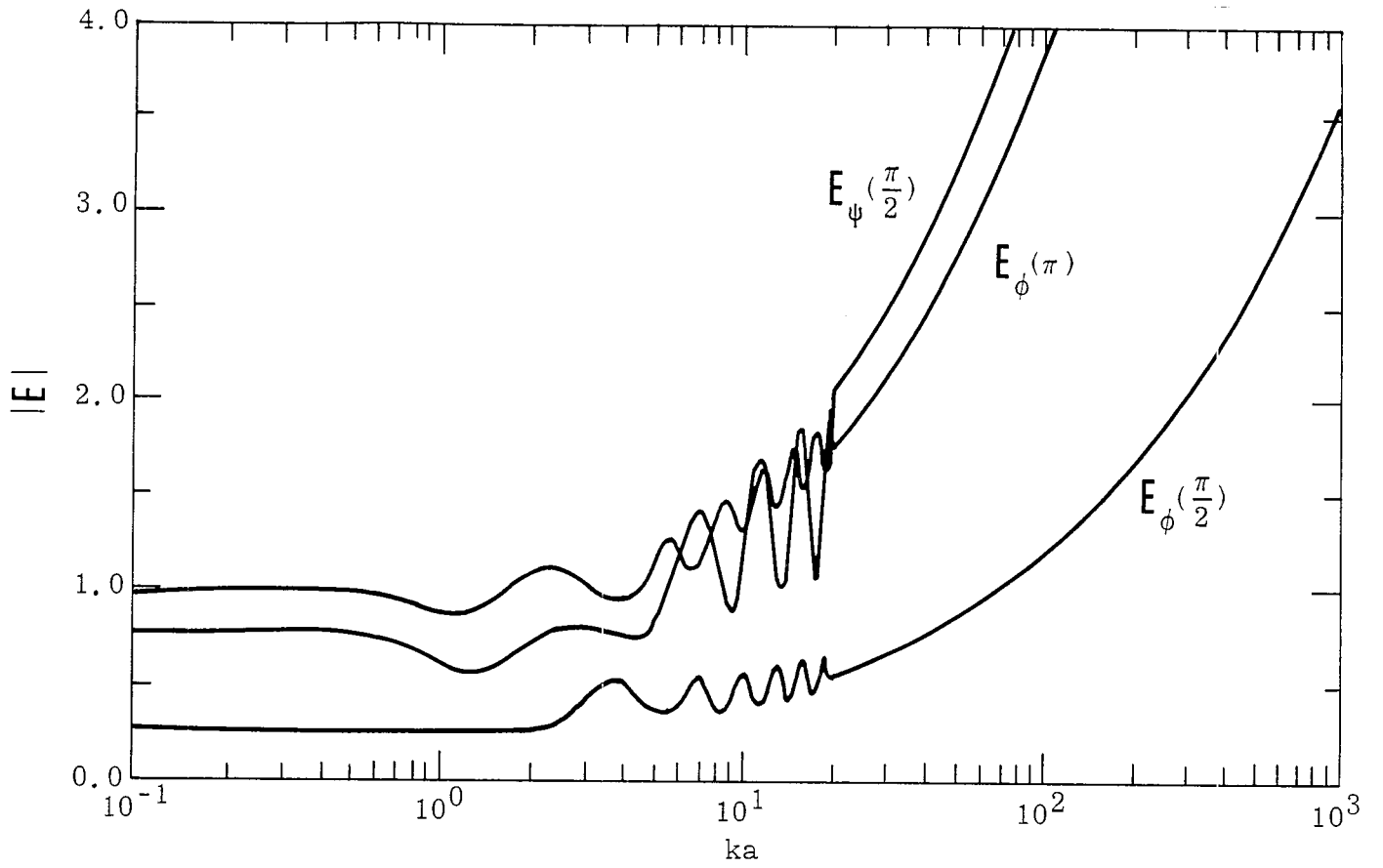


Figure 9-12. Step-function Response for the H_z -field for $b/a = 0.05$ and $\psi = 0.1$ with ϕ as a Parameter



A. $\phi = 0$ and $\frac{\pi}{4}$.

Figure 9-13. E -field for $b/a = 0.05$ and $\psi = 0.25$ with ϕ as a Parameter



B. $\phi = \frac{\pi}{2}$ and π .

Figure 9-13. Continued

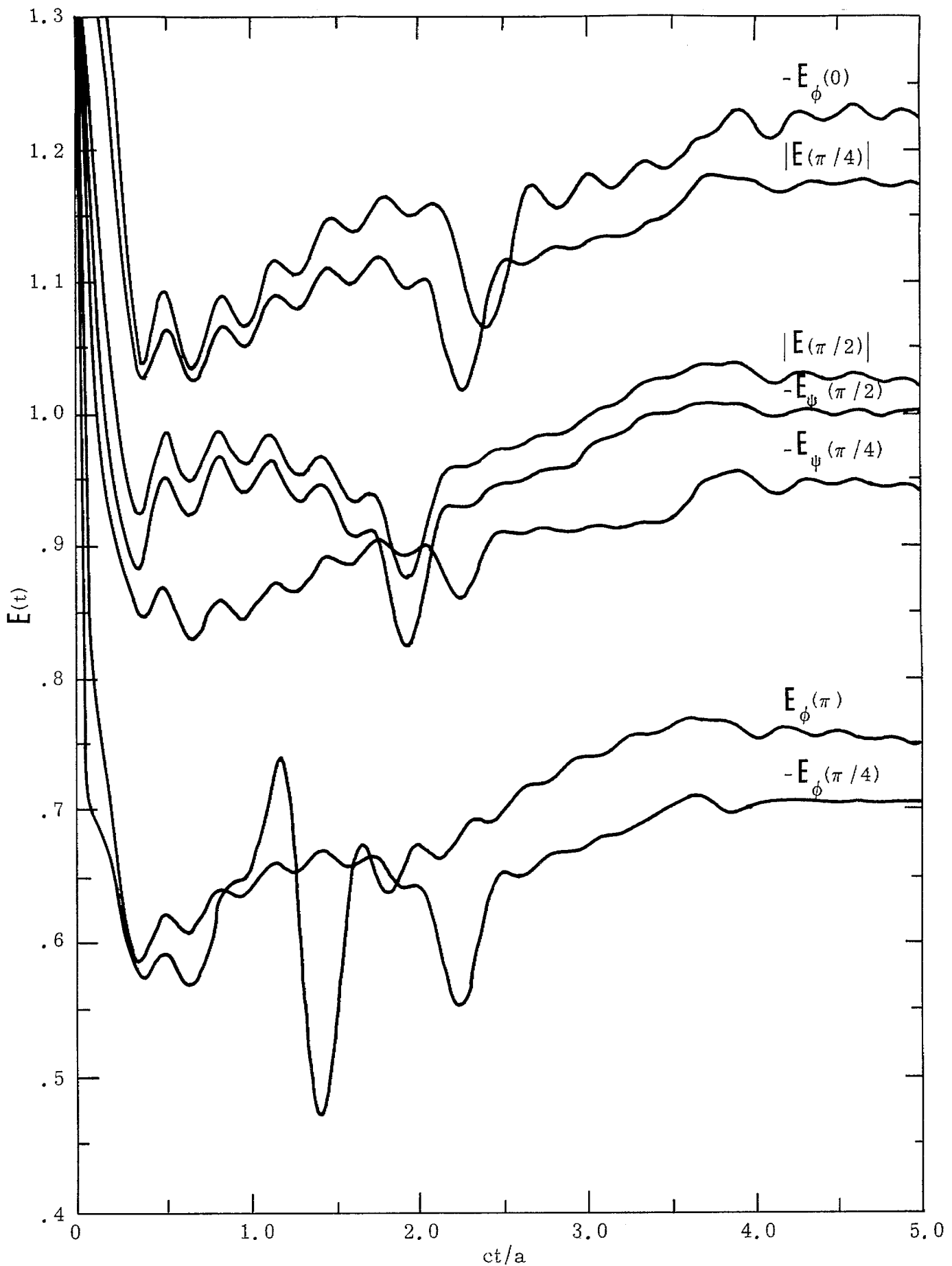
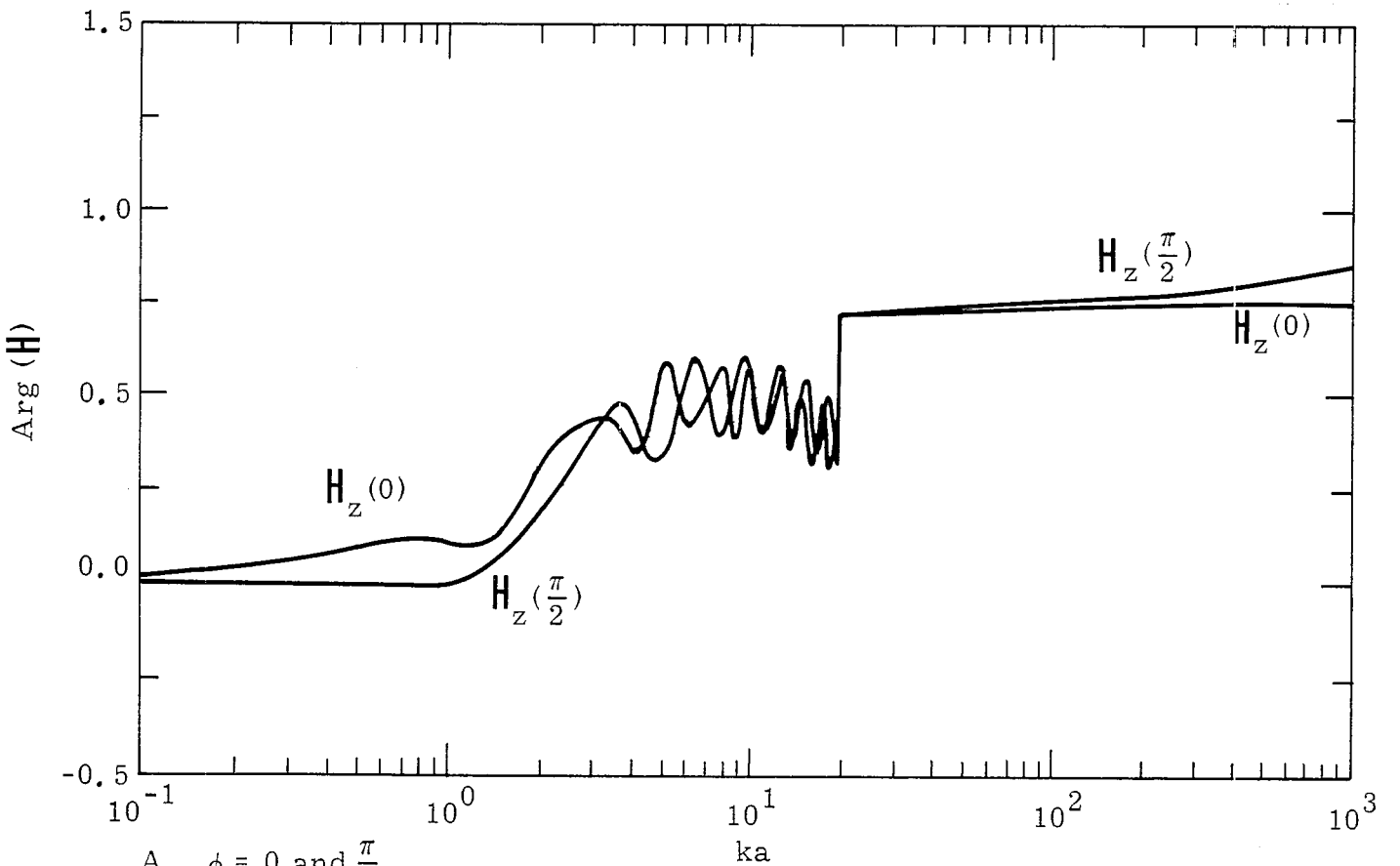
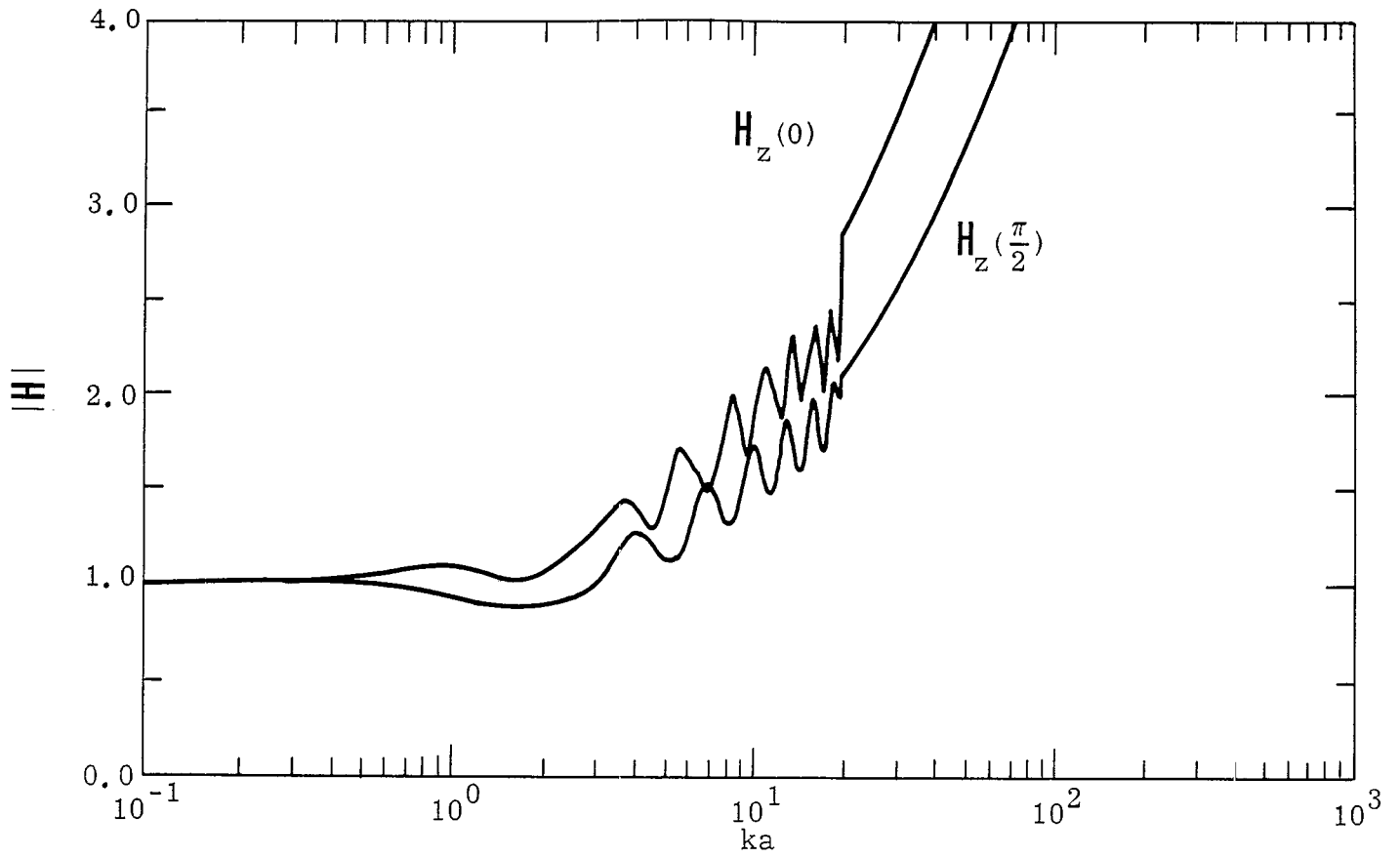
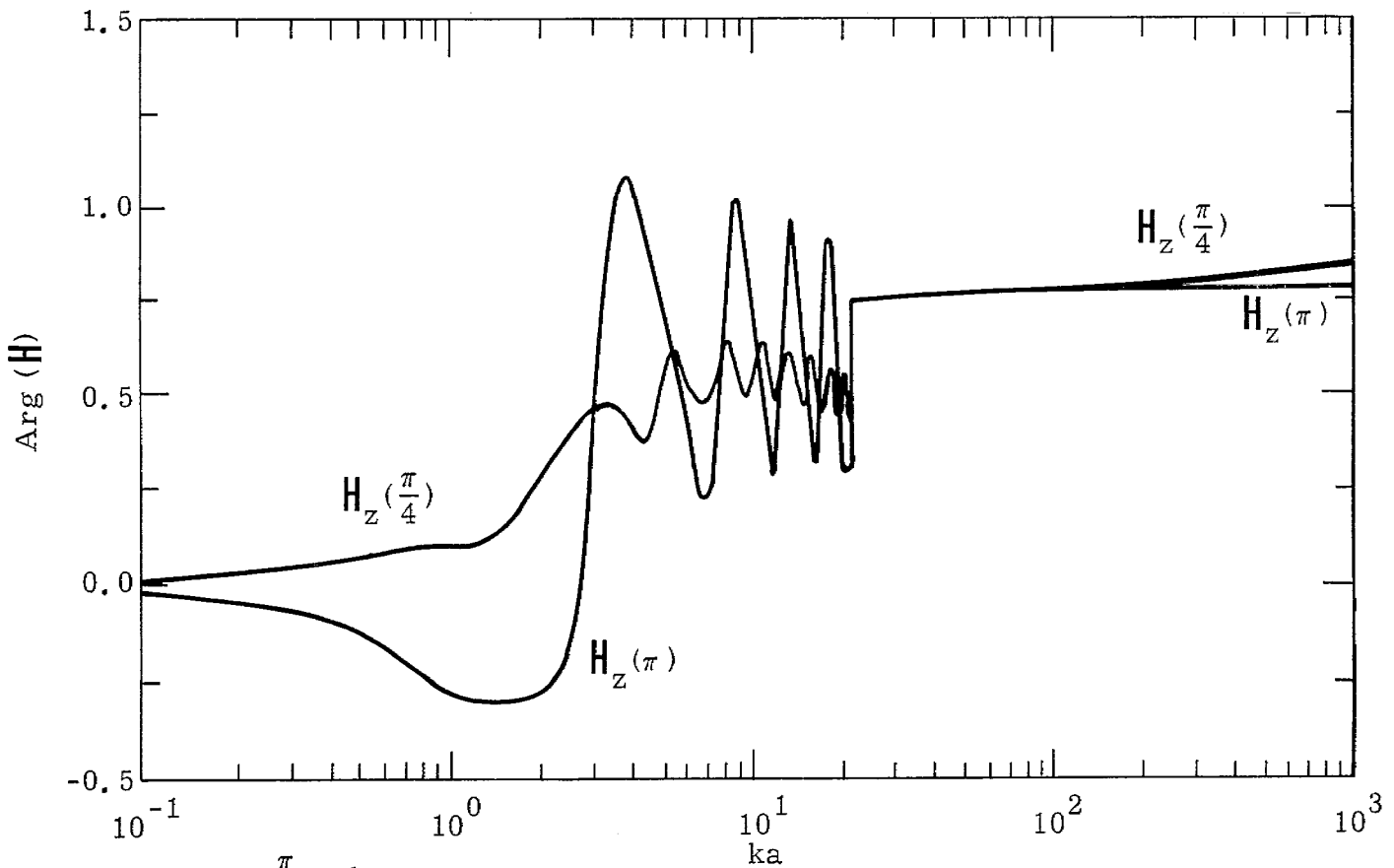
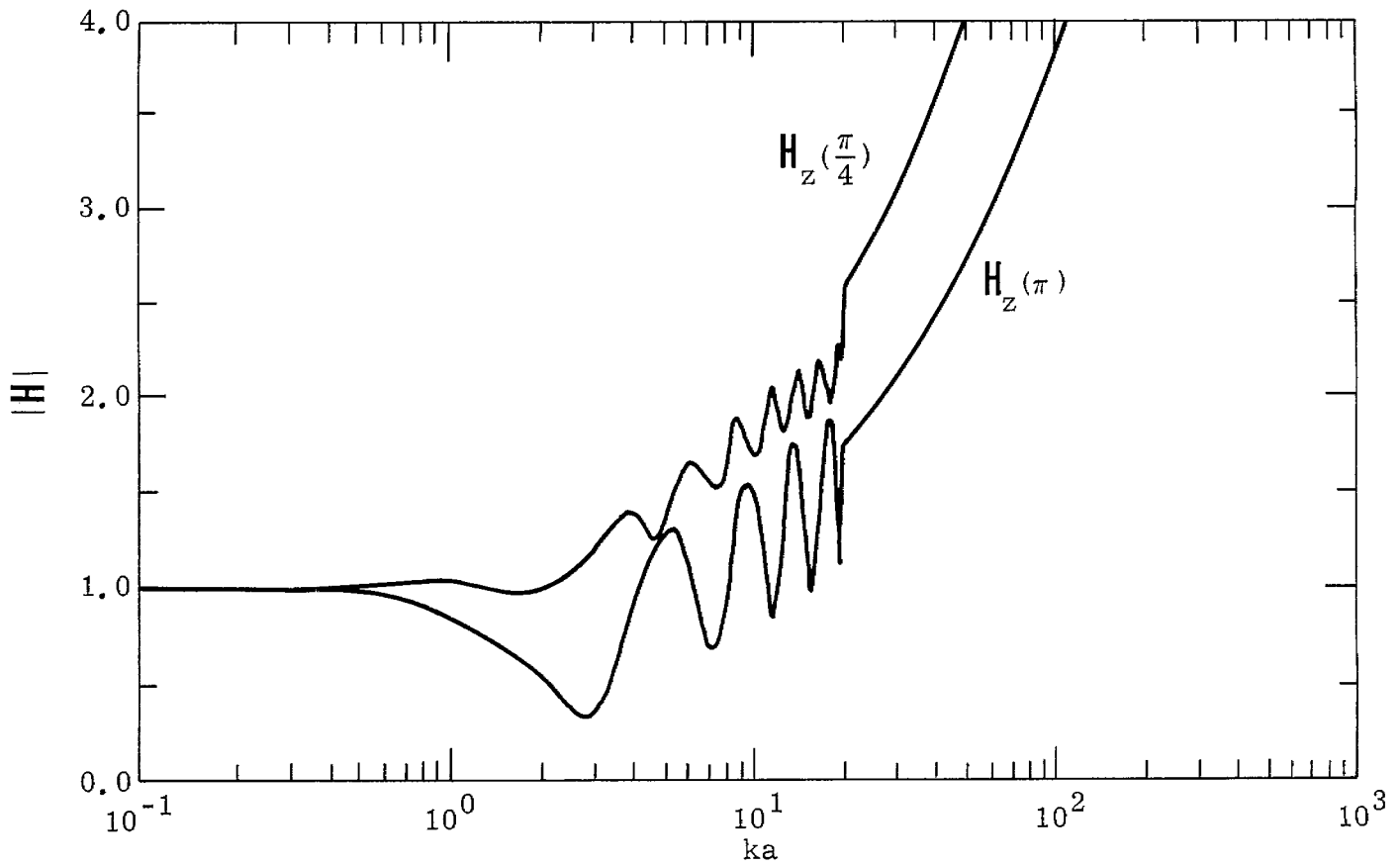


Figure 9-14. Step-function Response for the \mathbf{E} -field for $b/a = 0.05$ and $\psi = 0.25$ with ϕ as a Parameter



A. $\phi = 0$ and $\frac{\pi}{2}$.

Figure 9-15. H -field for $b/a = 0.05$ and $\psi = 0.25$ with ϕ as a Parameter



B. $\phi = \frac{\pi}{4}$ and π .

Figure 9-15. Continued

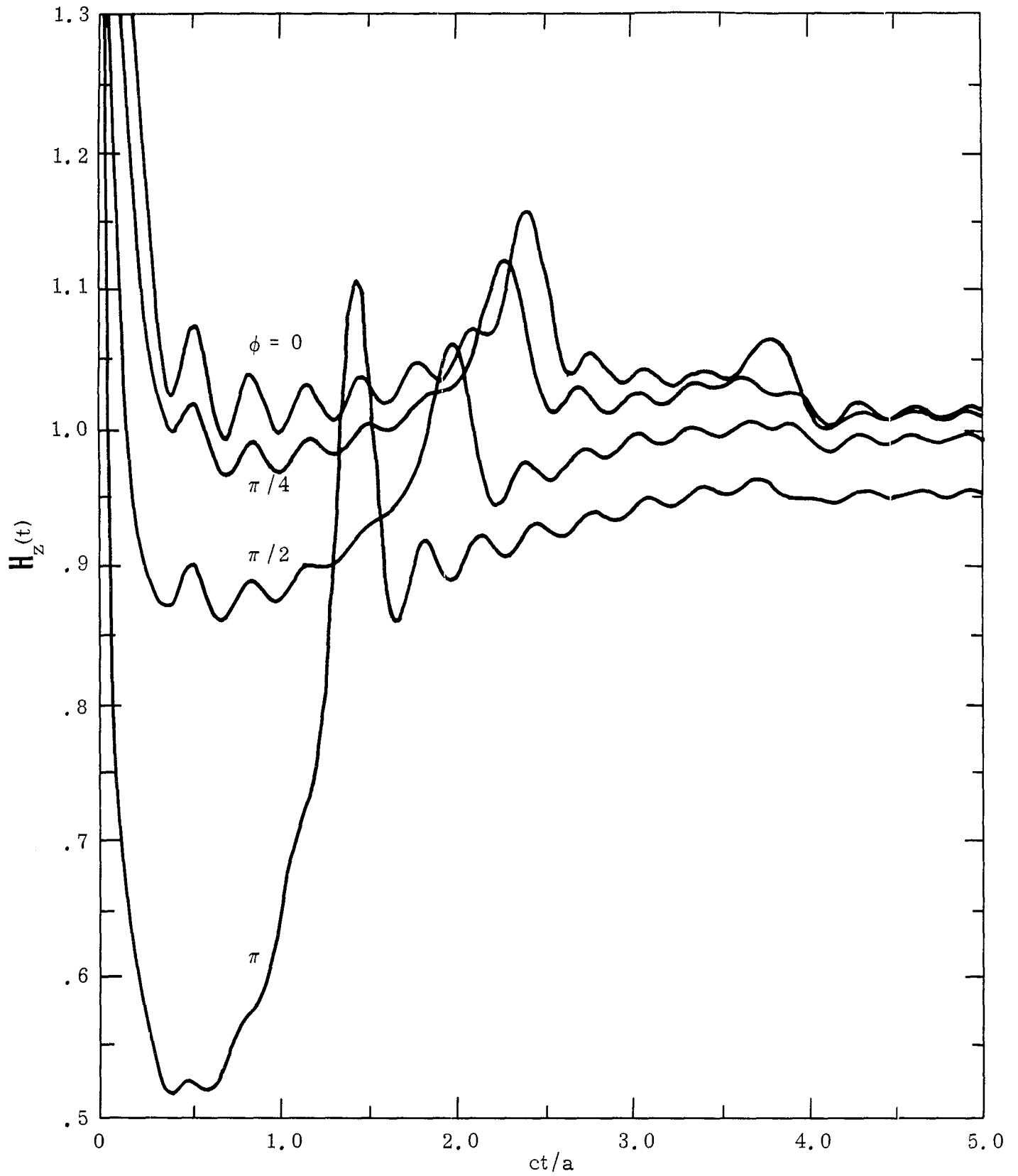
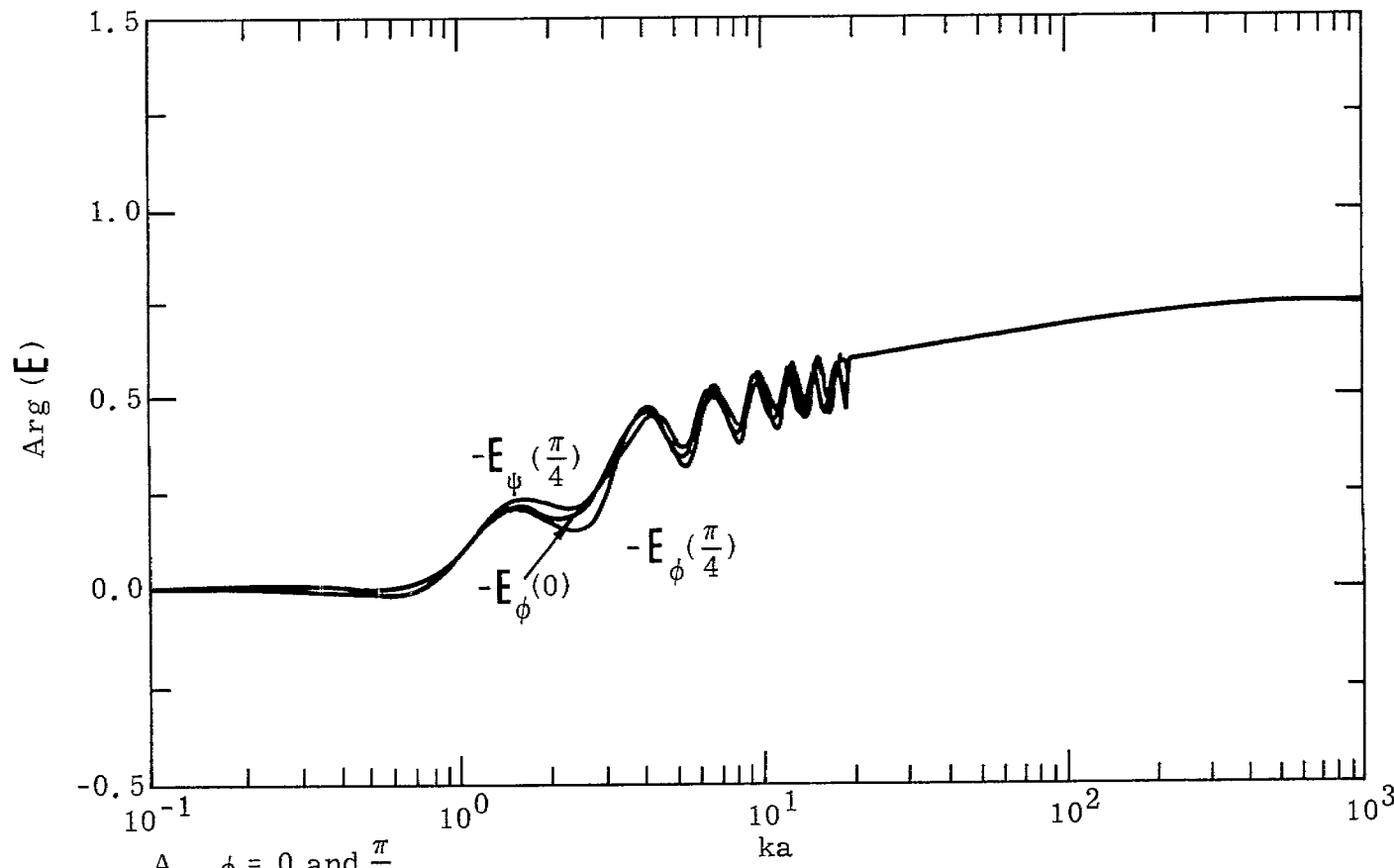
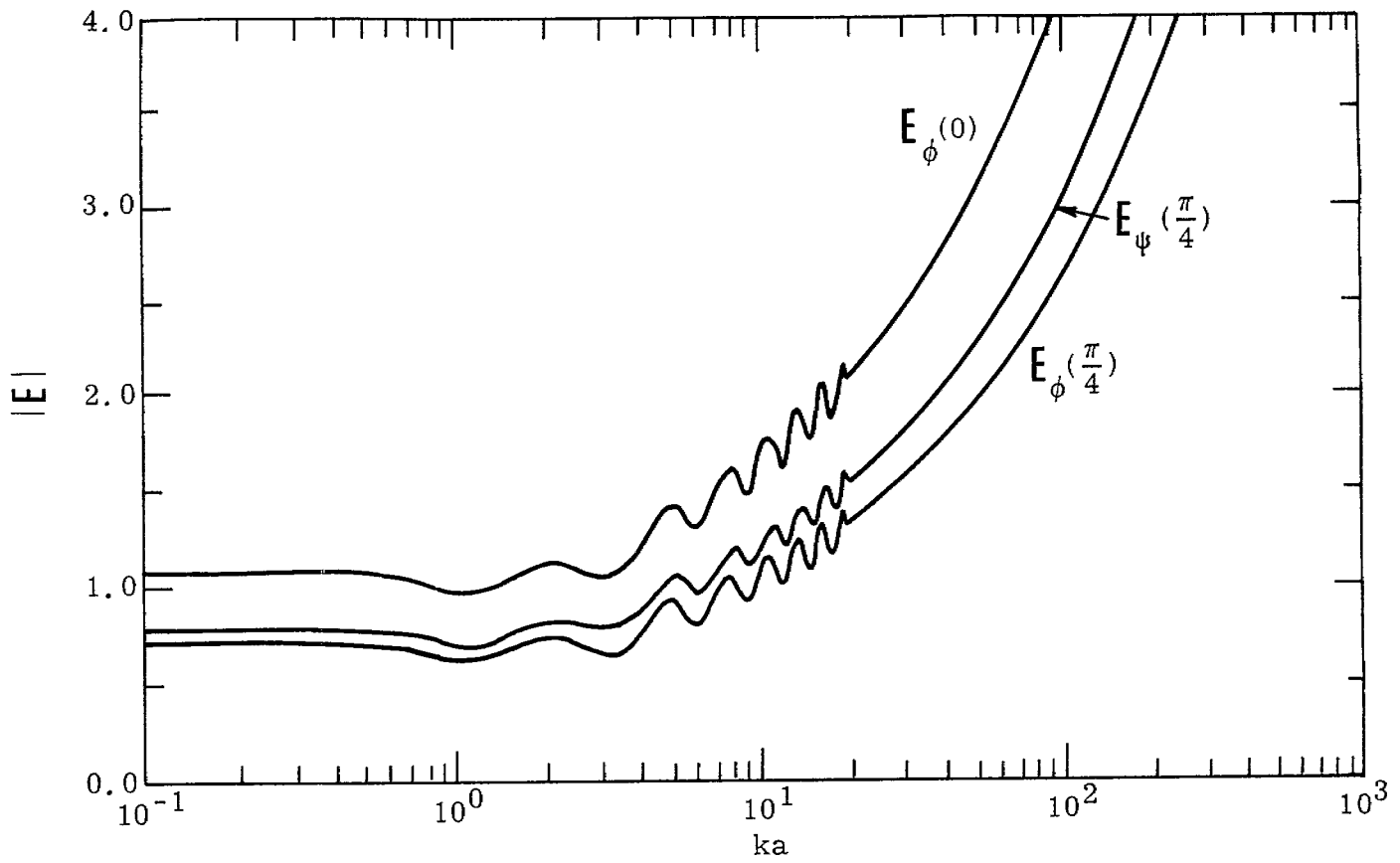
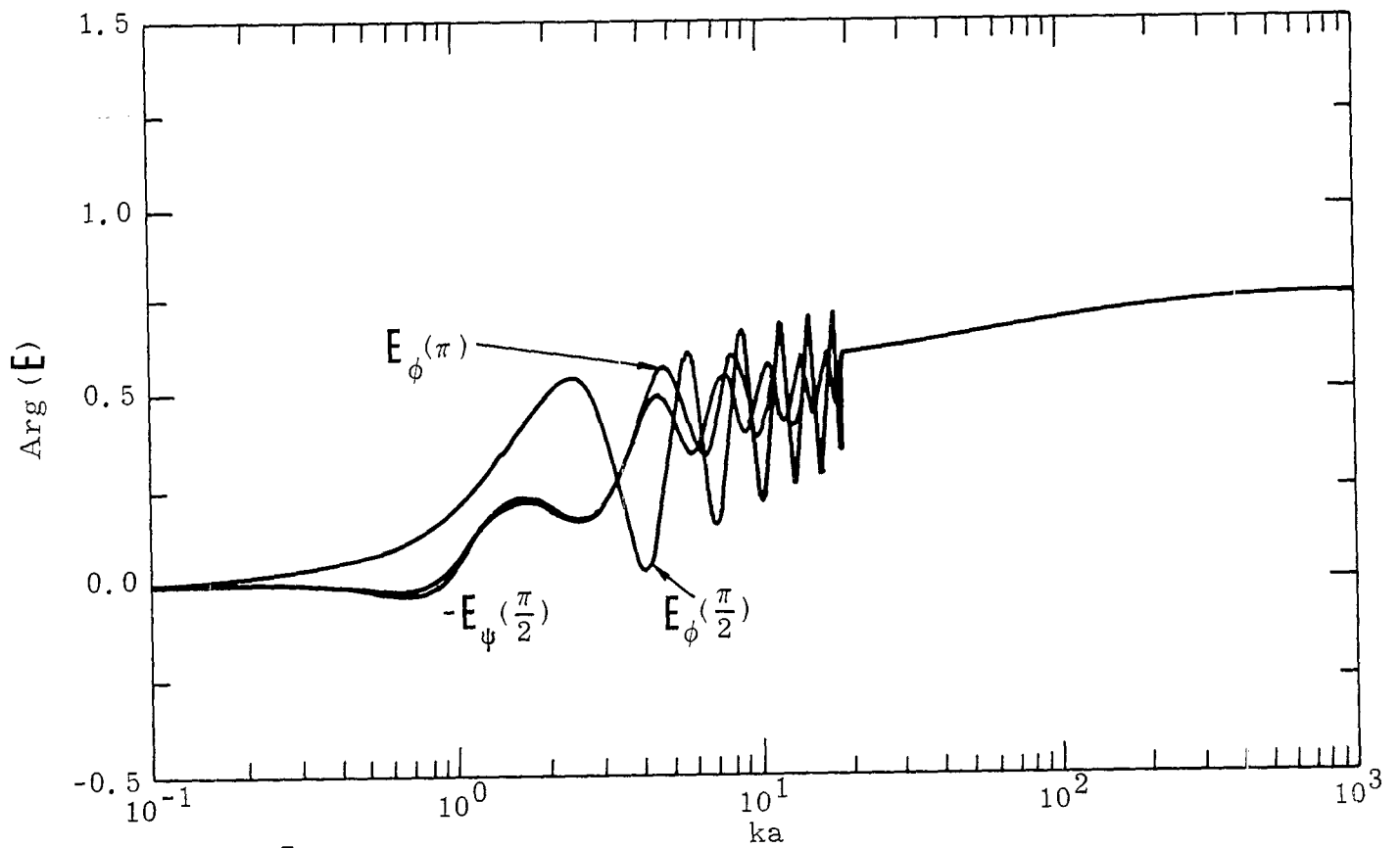
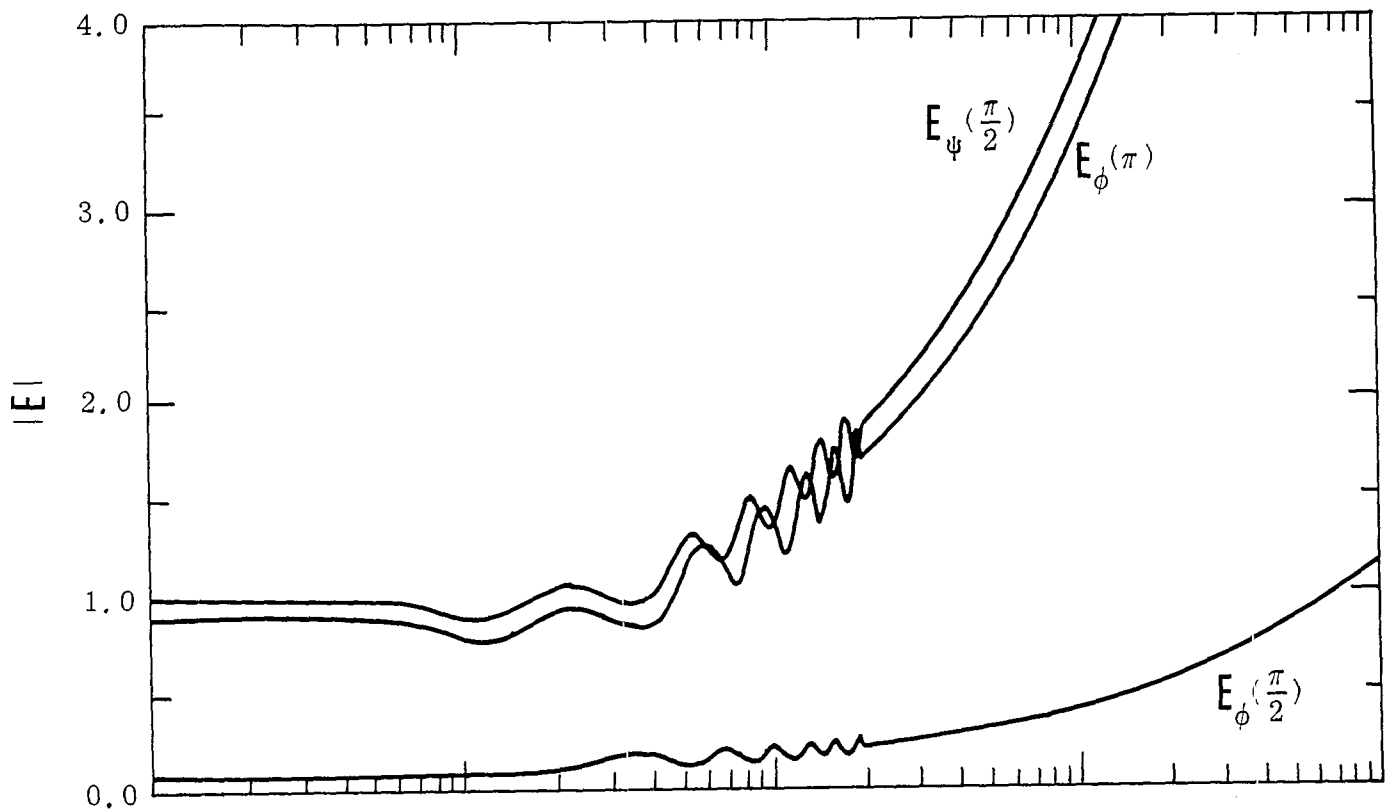


Figure 9-16. Step-function Response for the H_z -field for $b/a = 0.05$ and $\psi = 0.25$ with ϕ as a Parameter



A. $\phi = 0$ and $\frac{\pi}{4}$.

Figure 9-17. E -field for $b/a = 0.01$ and $\psi = 0.1$ with ϕ as a Parameter



B. $\phi = \frac{\pi}{2}$ and π .

Figure 9-17. Continued

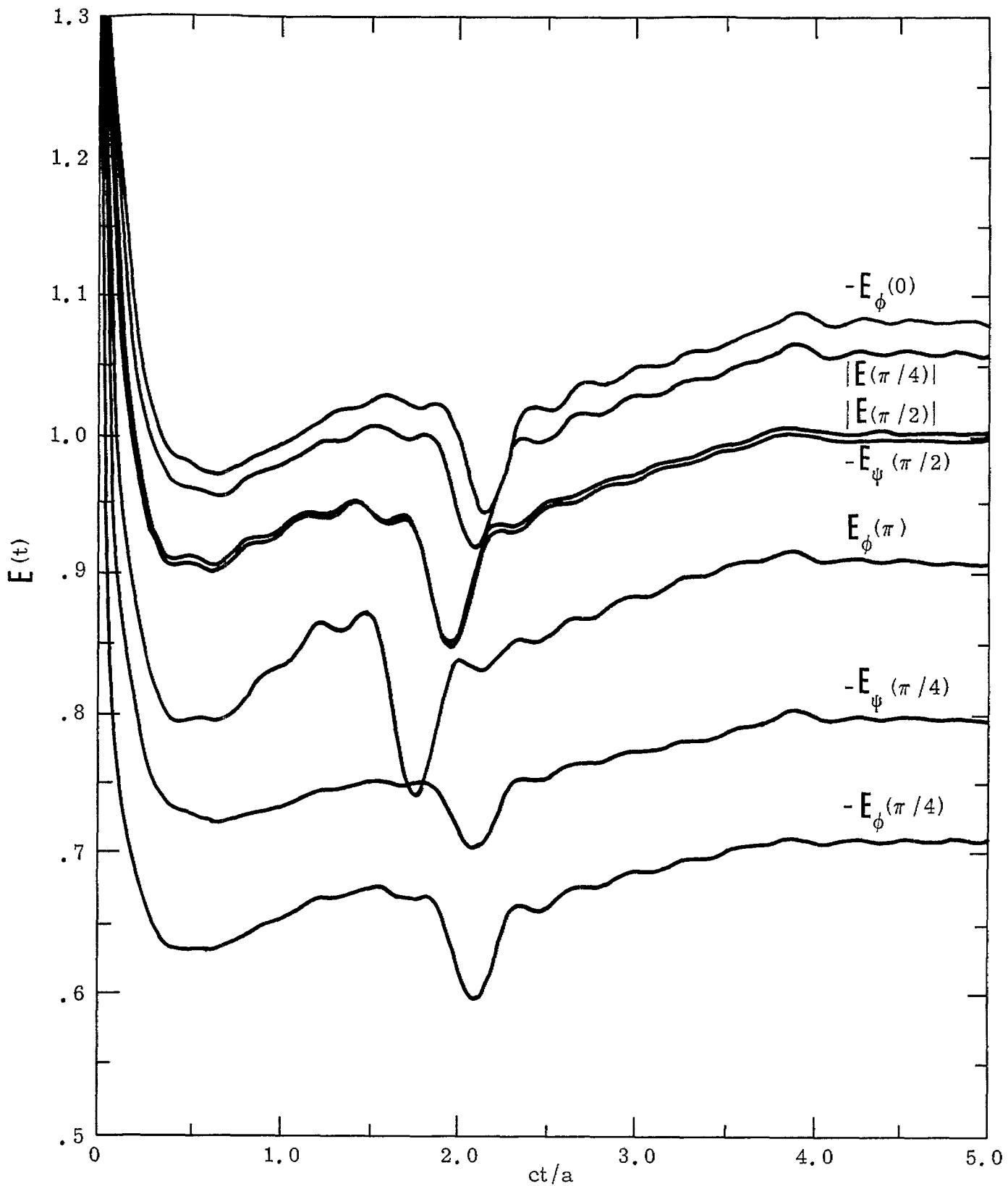
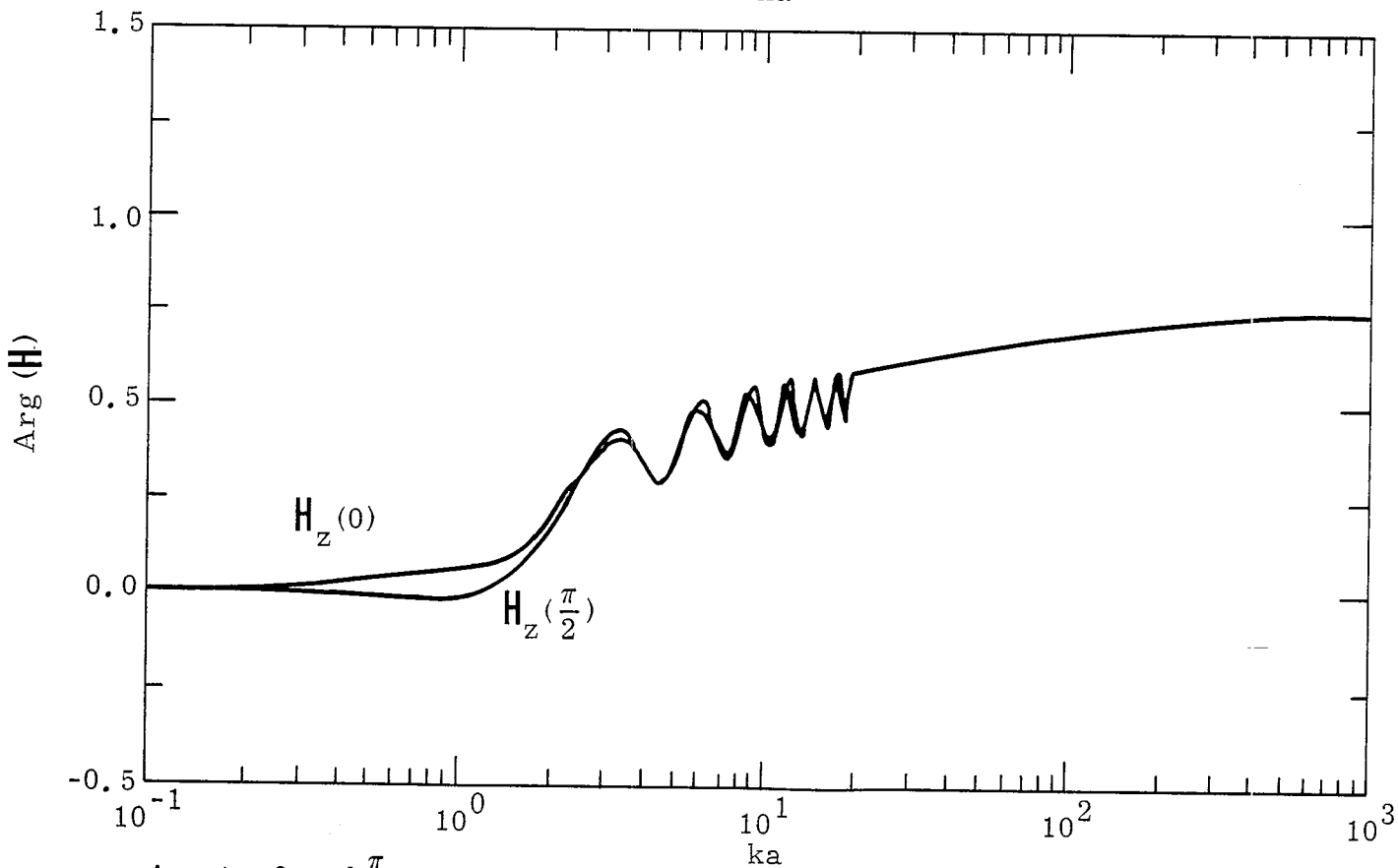
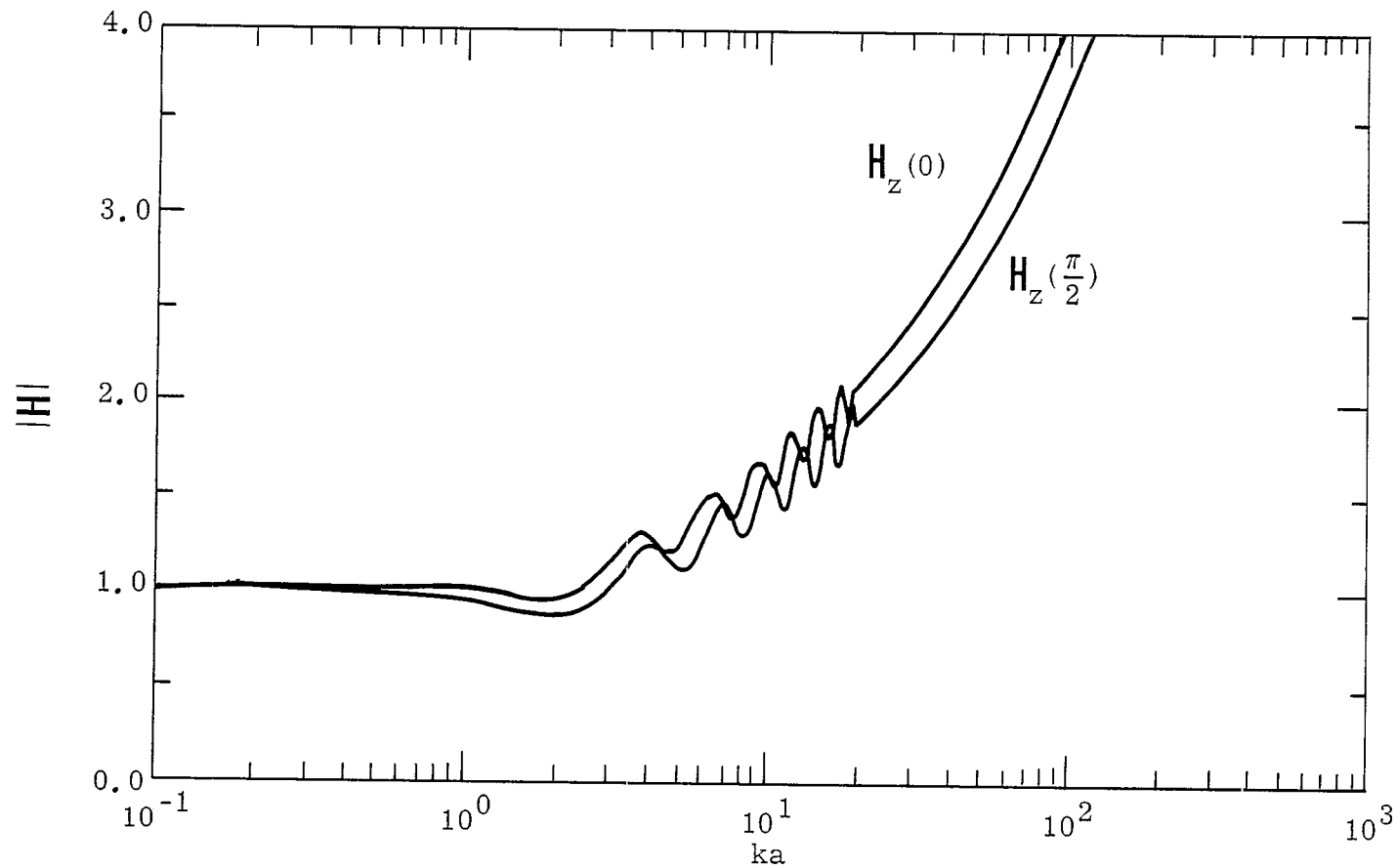
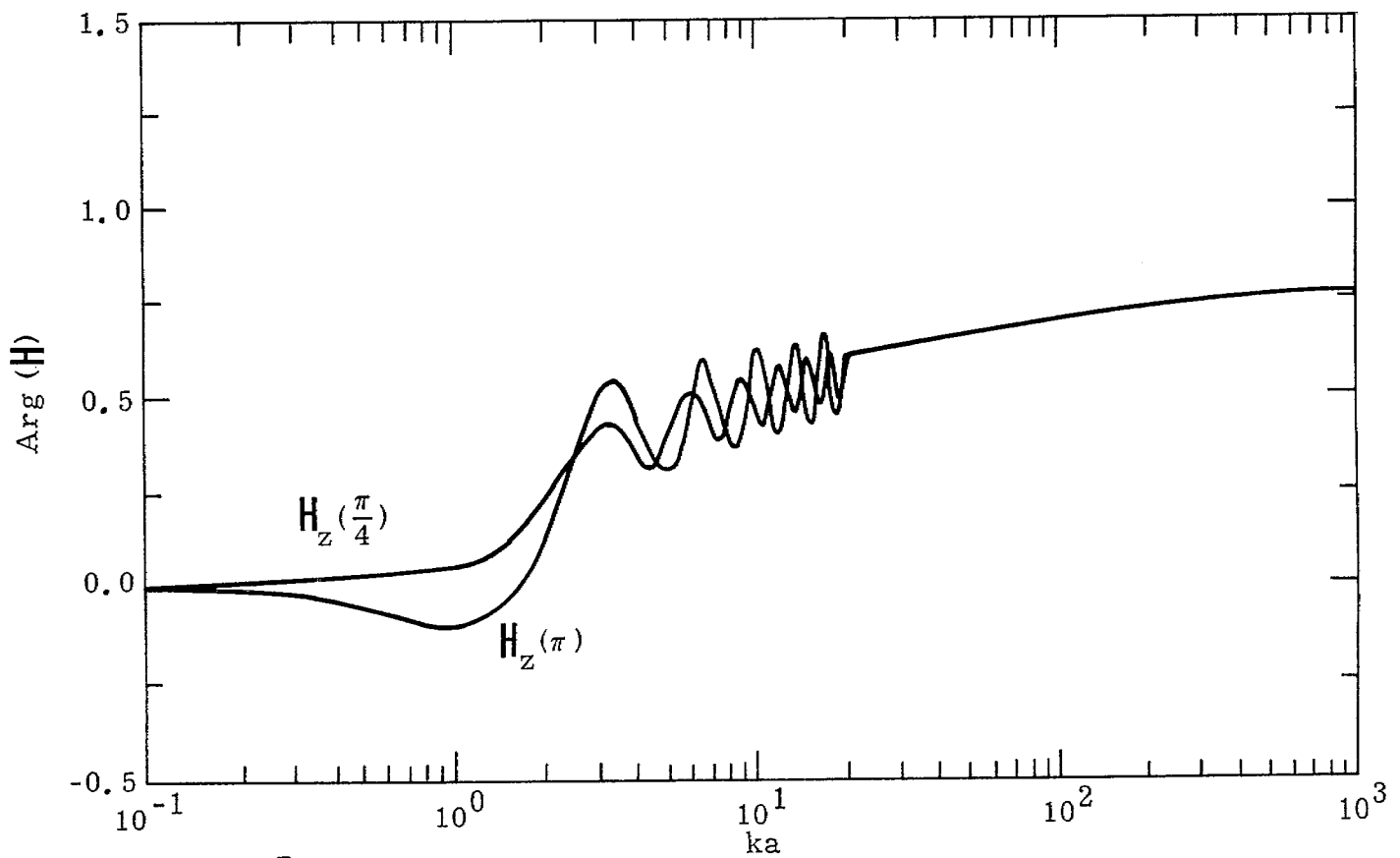
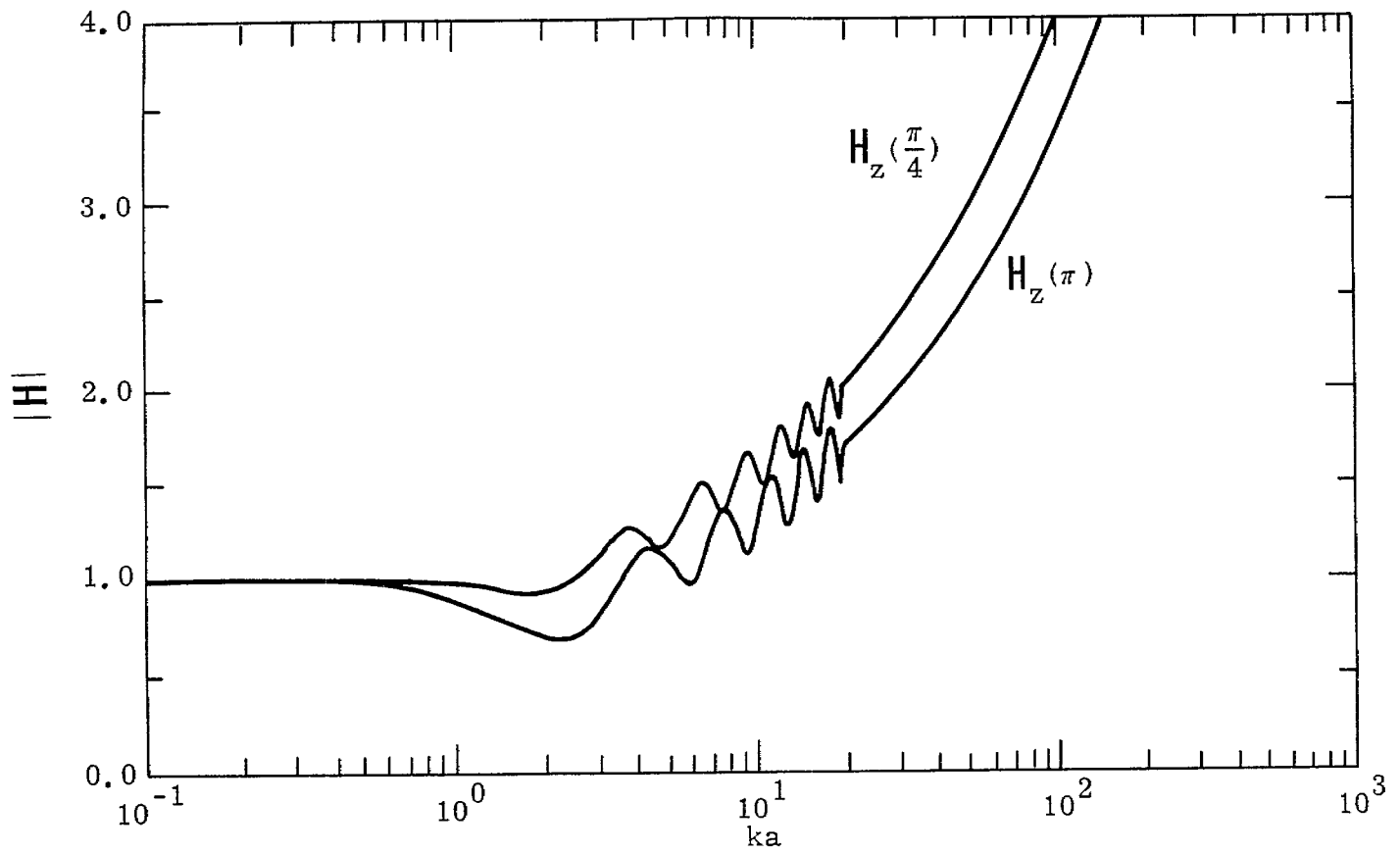


Figure 9-18. Step-function Response for the \mathbf{E} -field for $b/a = 0.01$ and $\psi = 0.1$ with ϕ as a Parameter



A. $\phi = 0$ and $\frac{\pi}{2}$.

Figure 9-19. H -field for $b/a = 0.01$ and $\psi = 0.1$ with ϕ as a Parameter



B. $\phi = \frac{\pi}{4}$ and π .

Figure 9-19. Continued

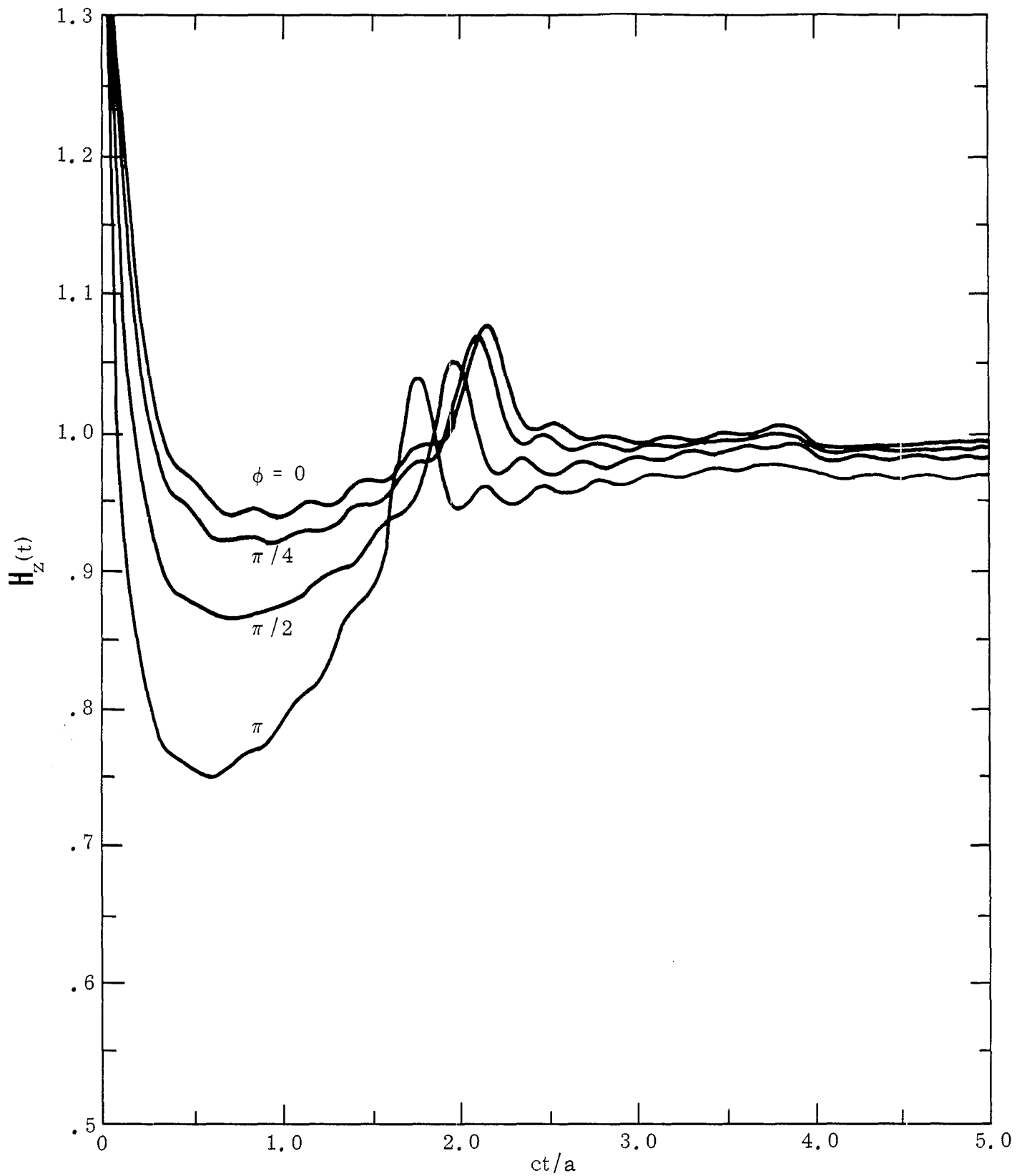
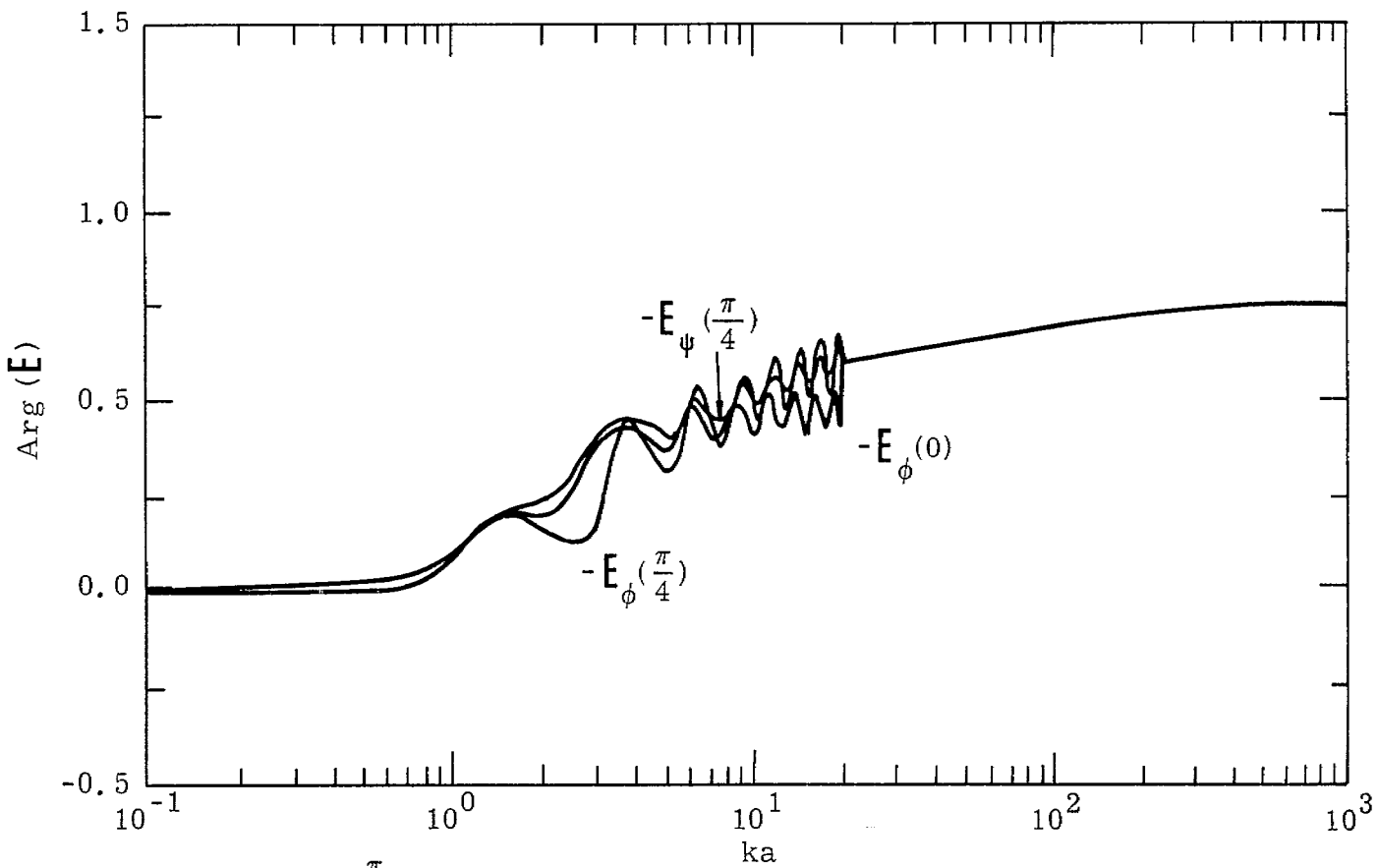
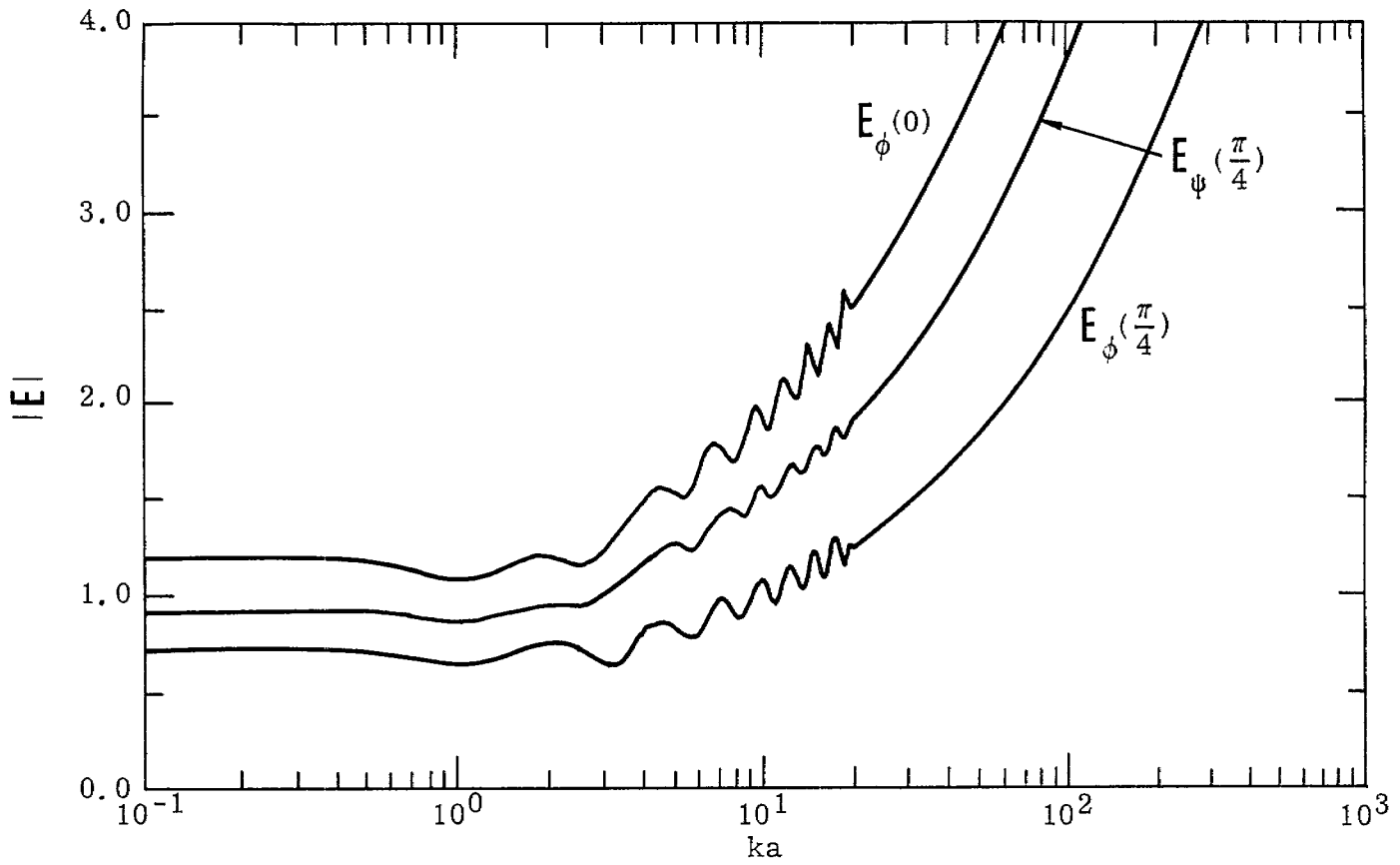
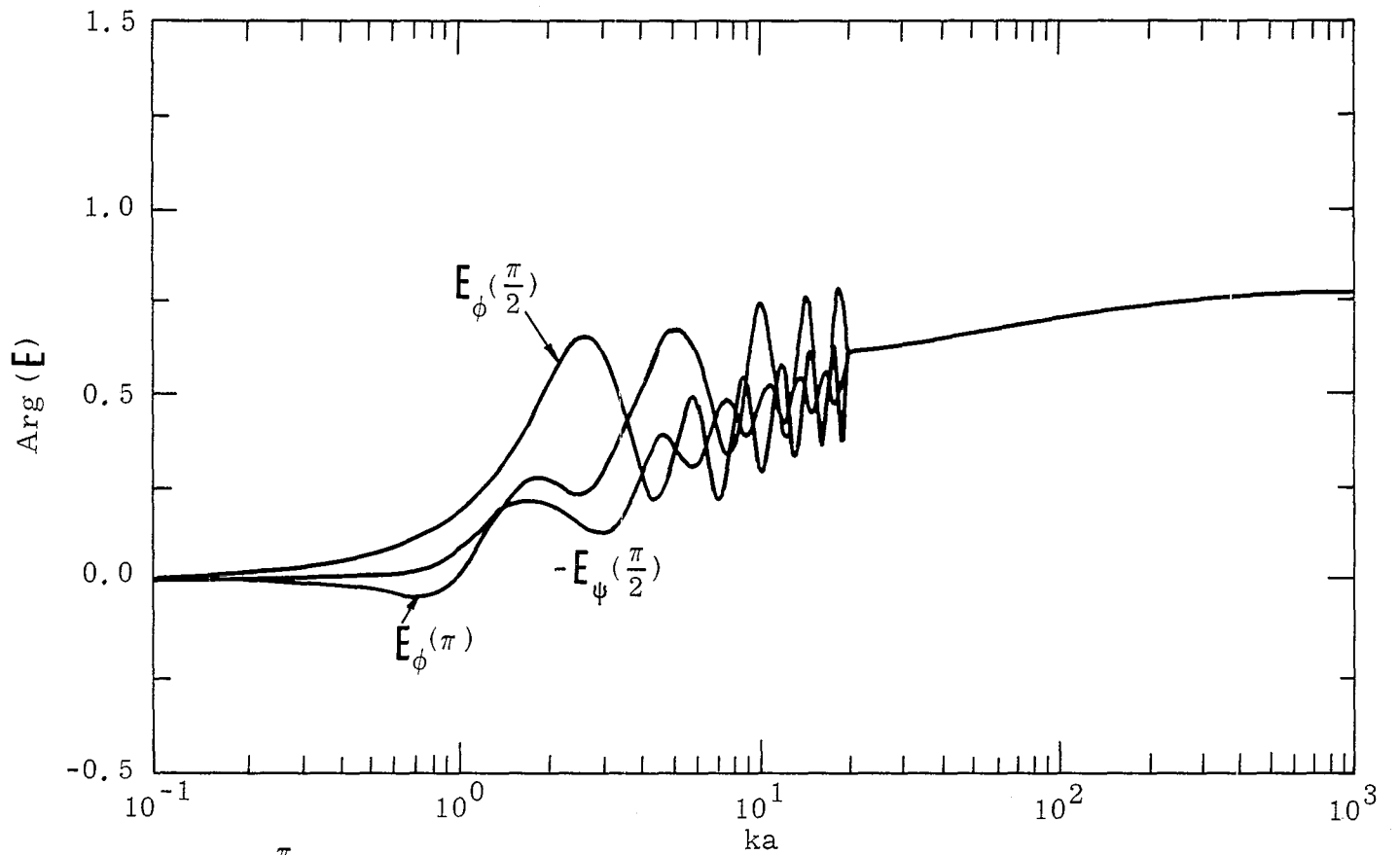
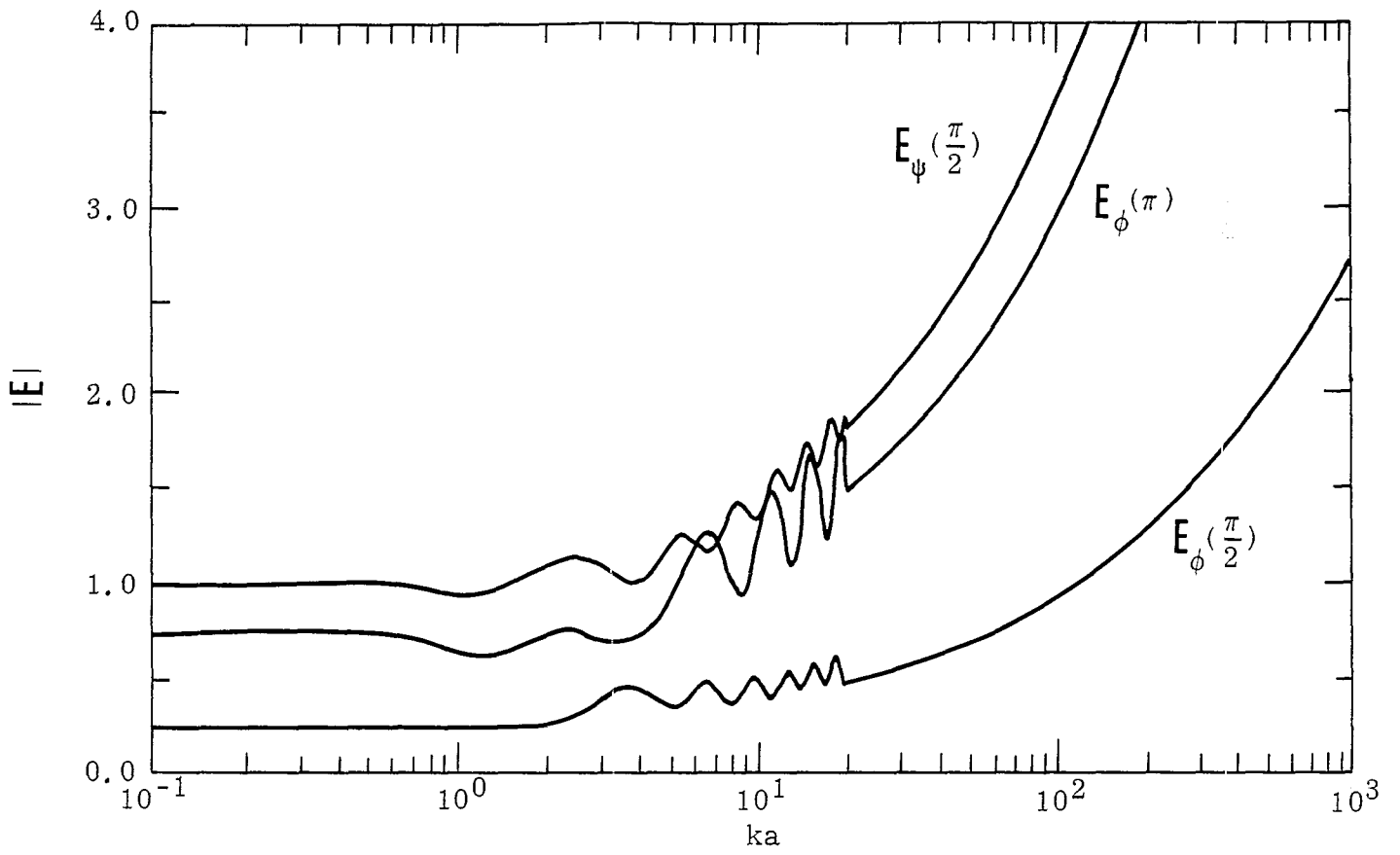


Figure 9-20. Step-function Response for the H -field for $b/a = 0.01$ and $\psi = 0.1$ with ϕ as a Parameter



A. $\phi = 0$ and $\frac{\pi}{4}$.

Figure 9-21. E -field for $b/a = 0.01$ and $\psi = 0.25$ with ϕ as a Parameter



B. $\phi = \frac{\pi}{2}$ and π .

Figure 9-21. Continued

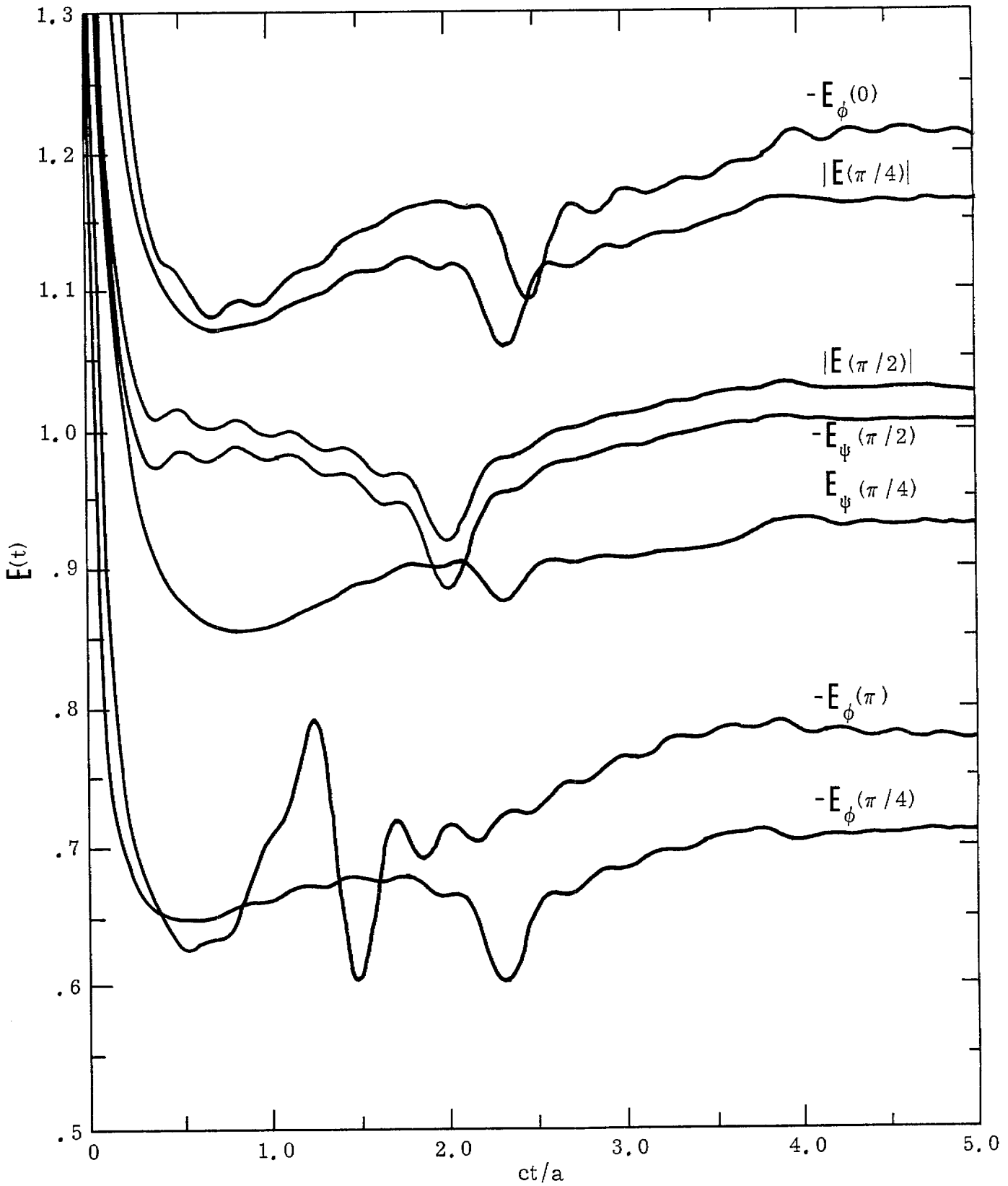
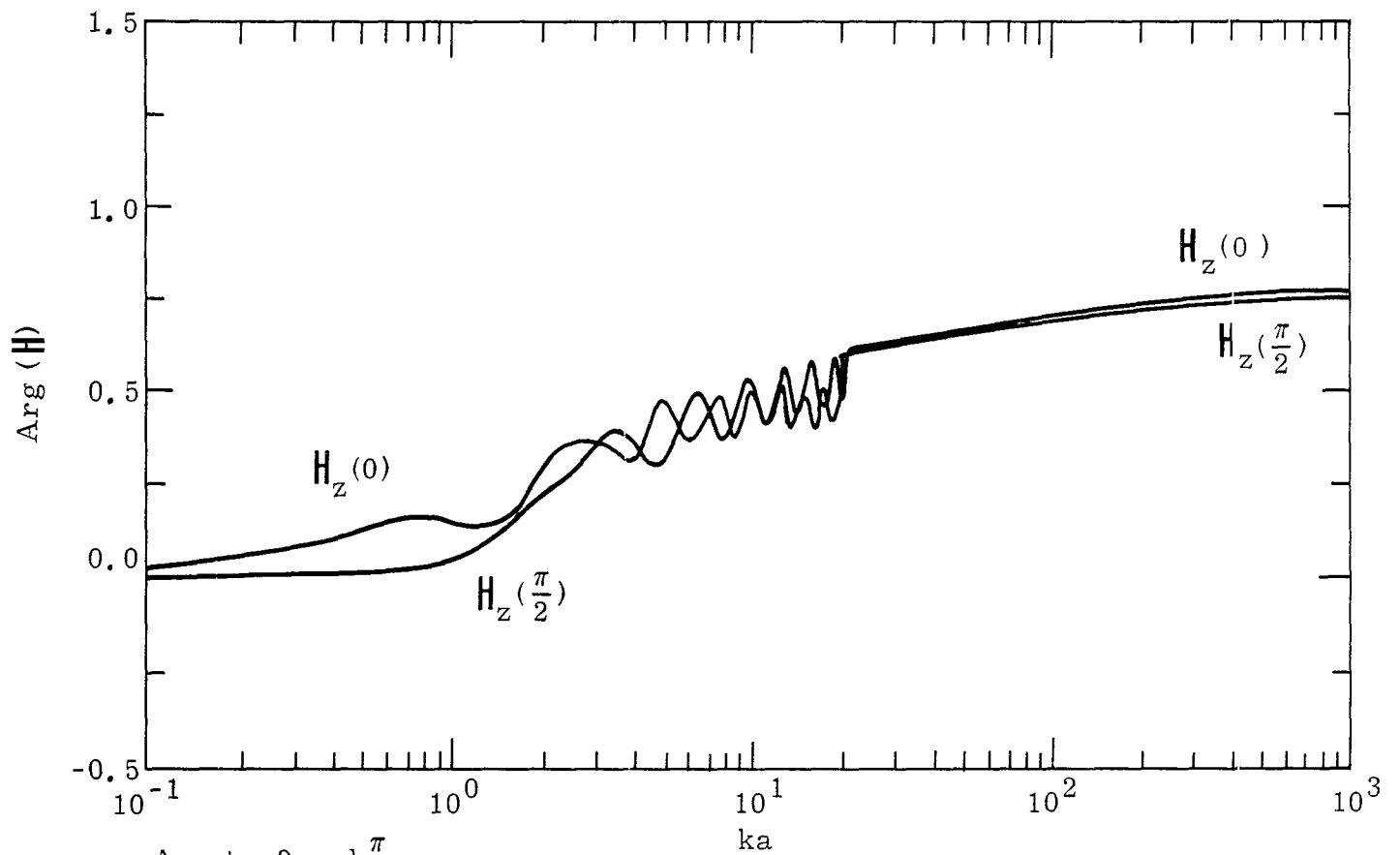
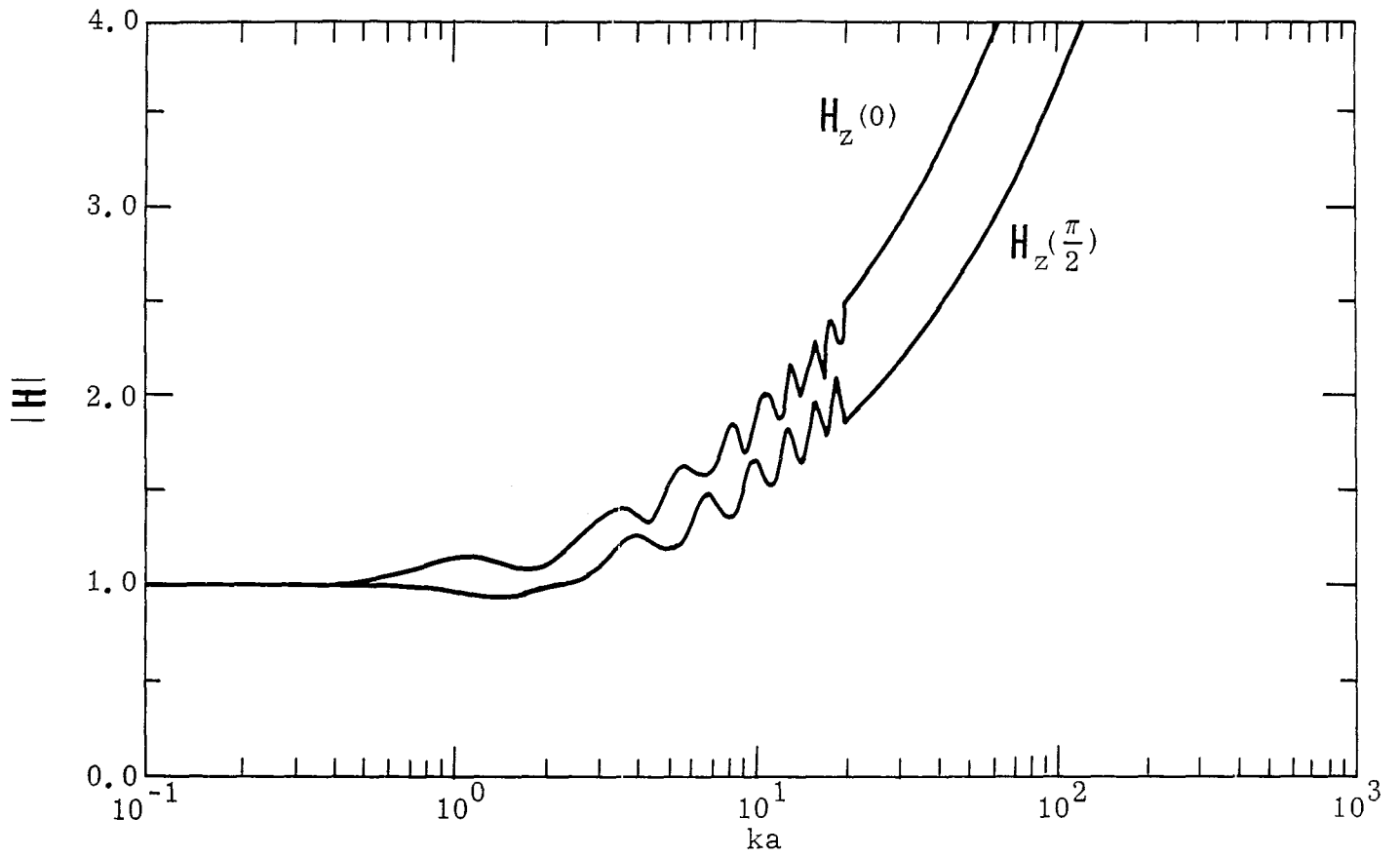


Figure 9-22. Step-function Response for the E -field for $b/a = 0.01$ and $\psi = 0.25$ with ϕ as a Parameter



A. $\phi = 0$ and $\frac{\pi}{2}$.

Figure 9-23. H-field for $b/a = 0.01$ and $\psi = 0.25$ with ϕ as a Parameter

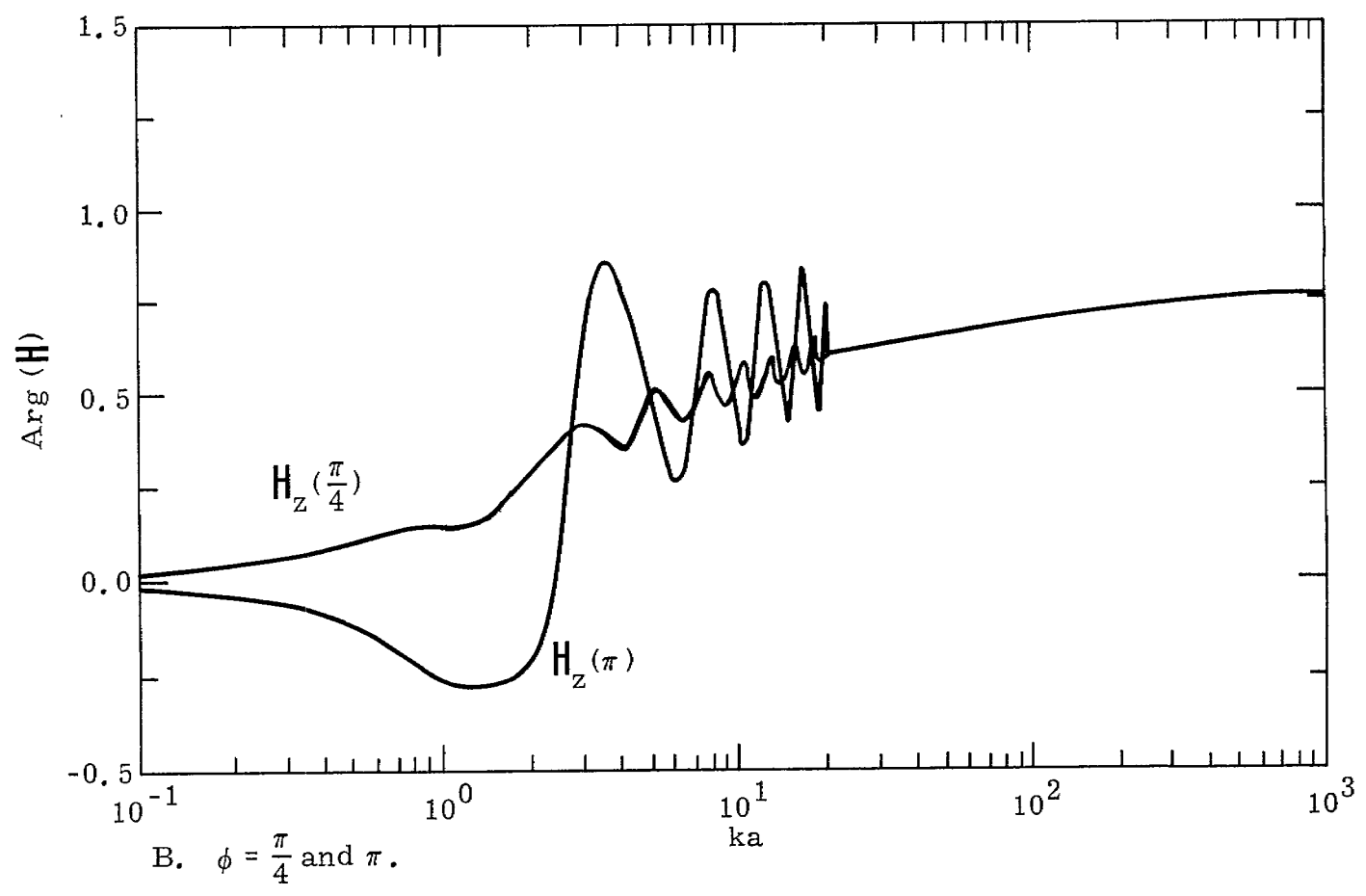
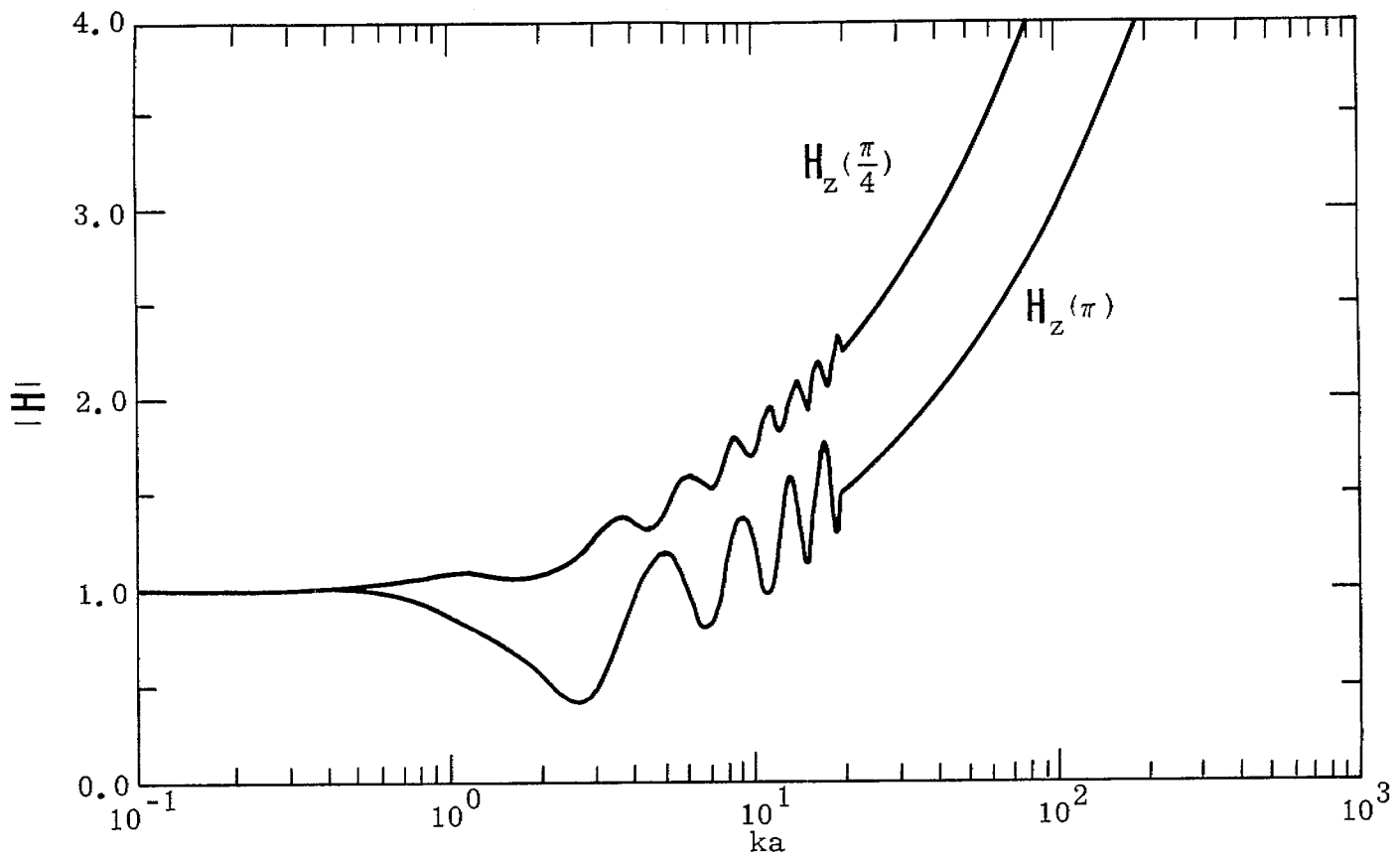


Figure 9-23. Continued

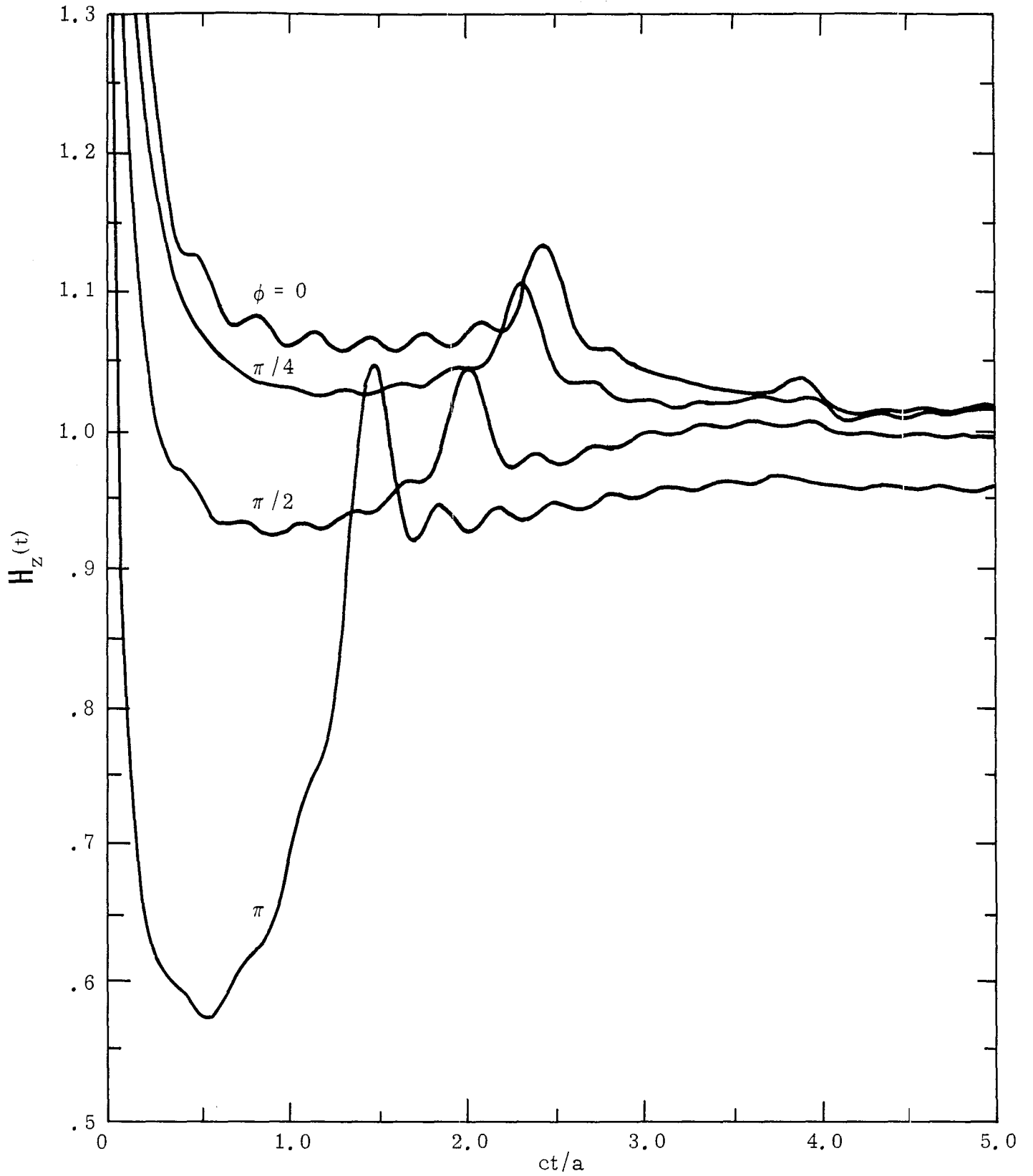
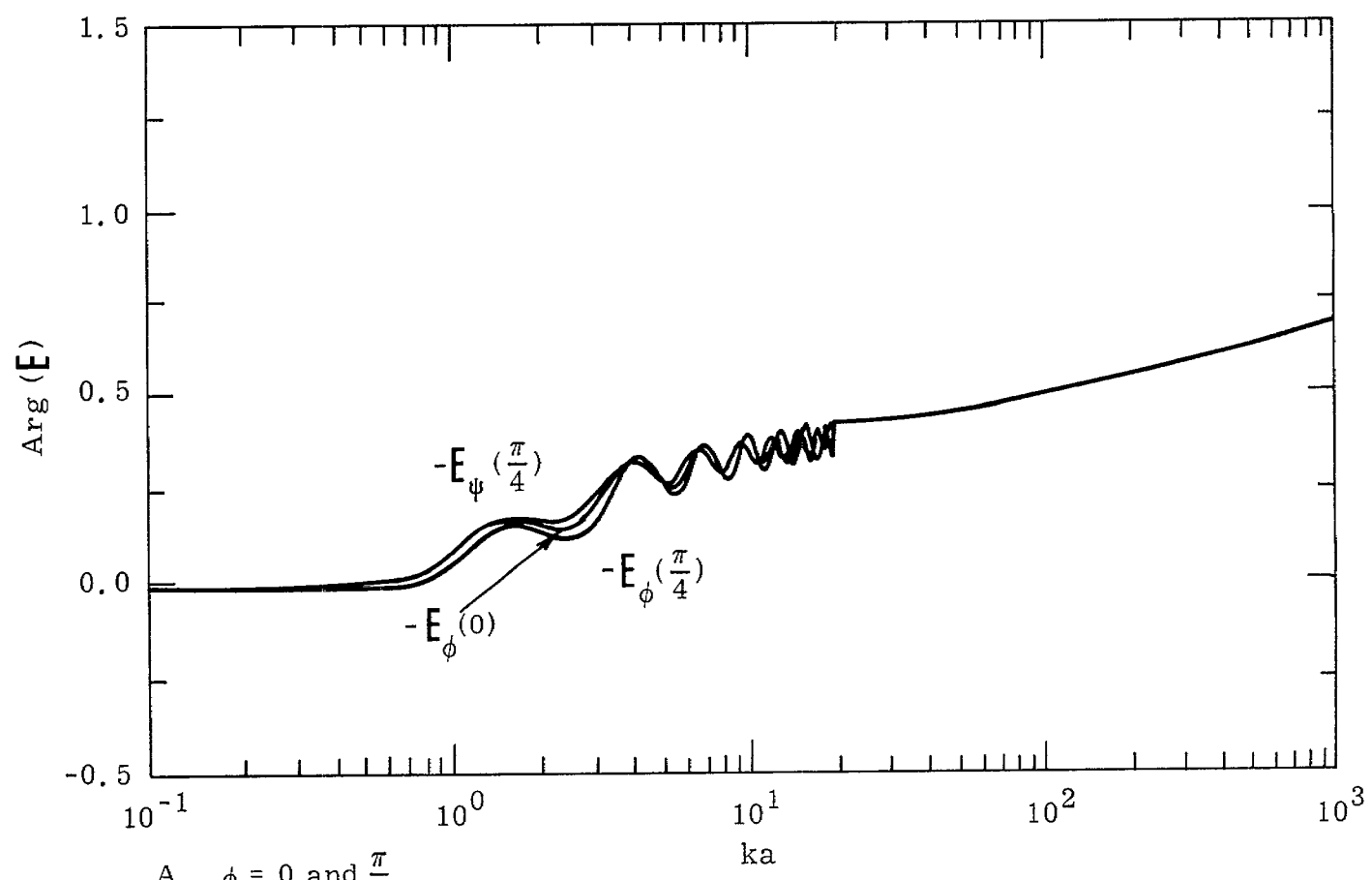
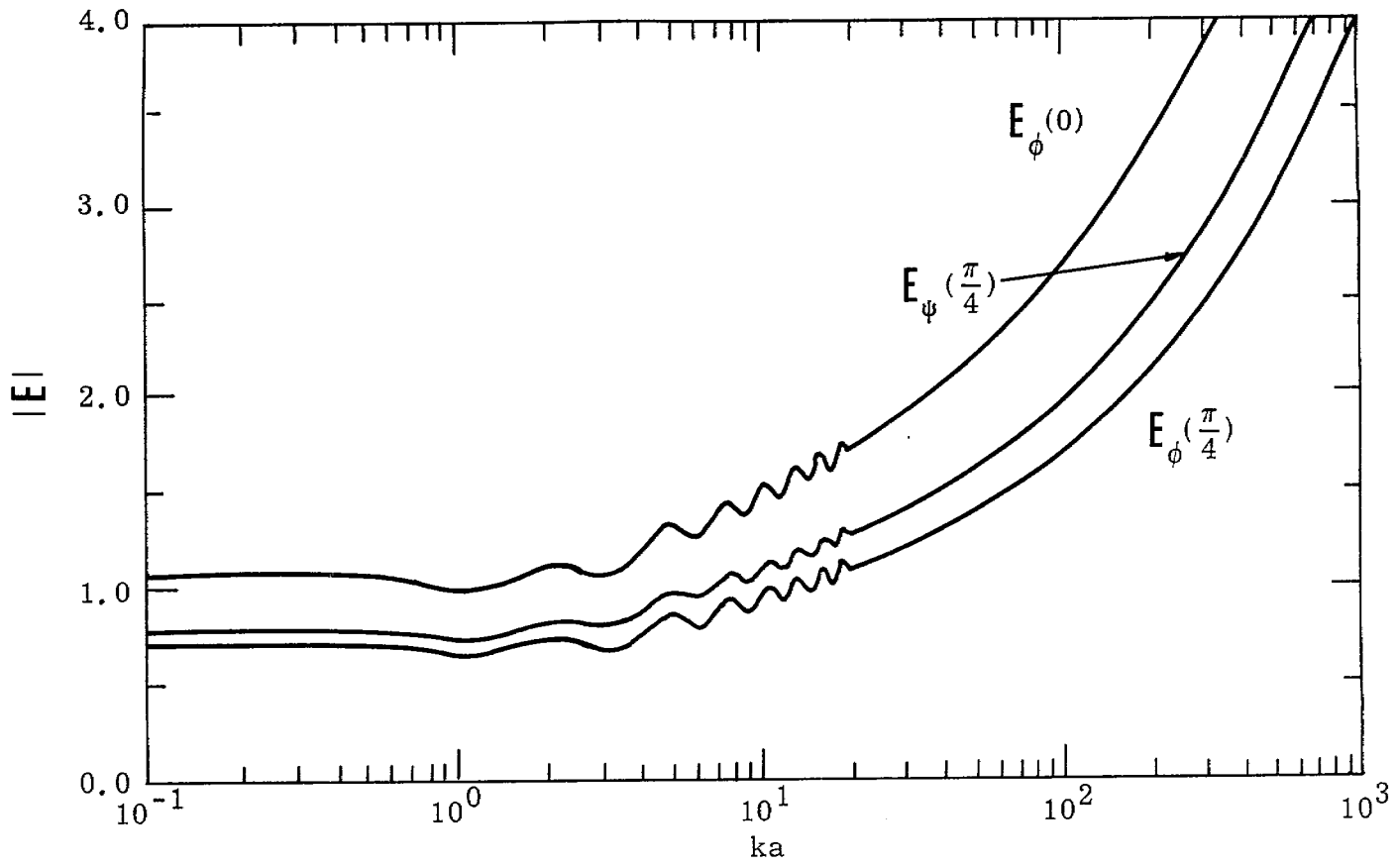
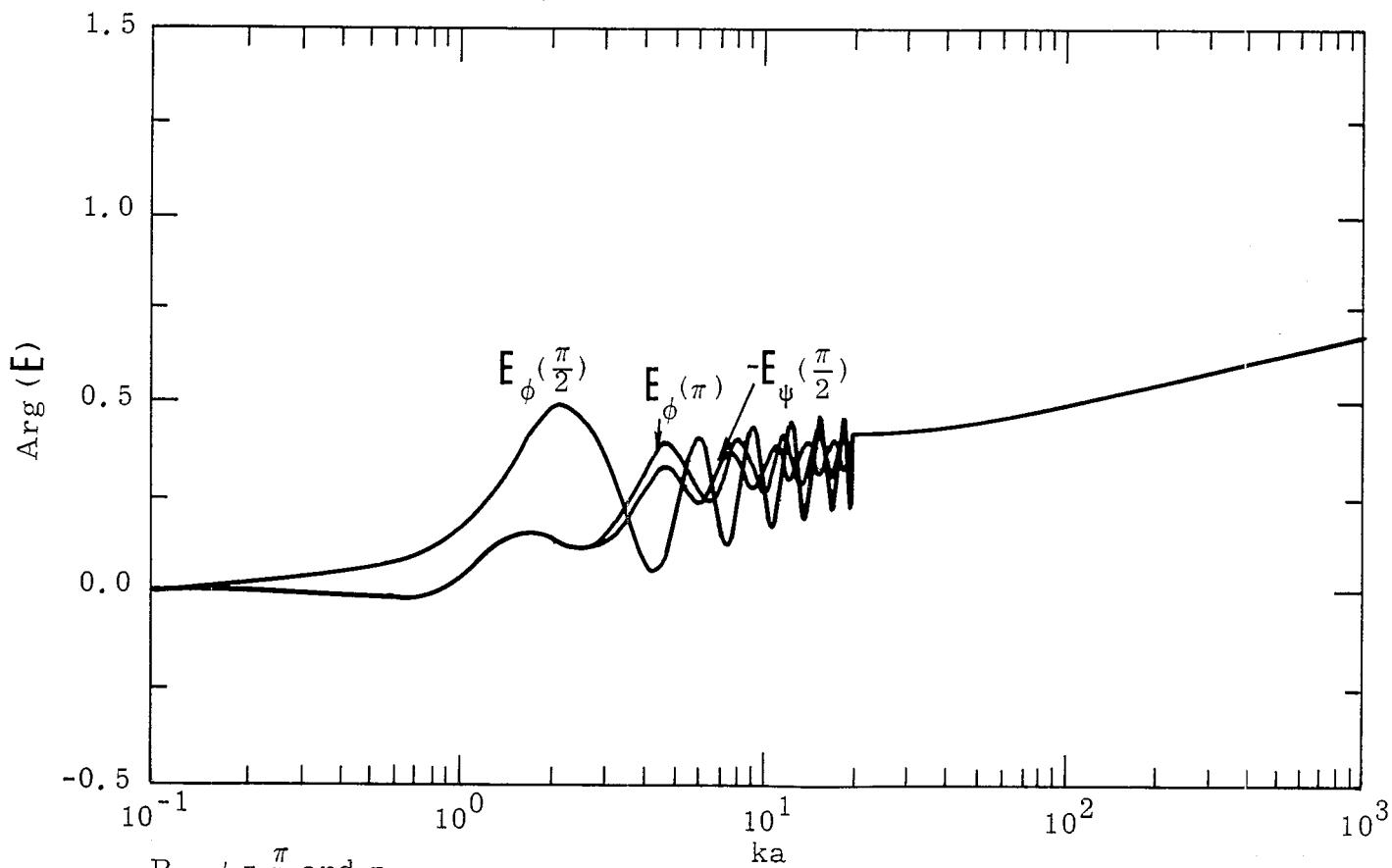
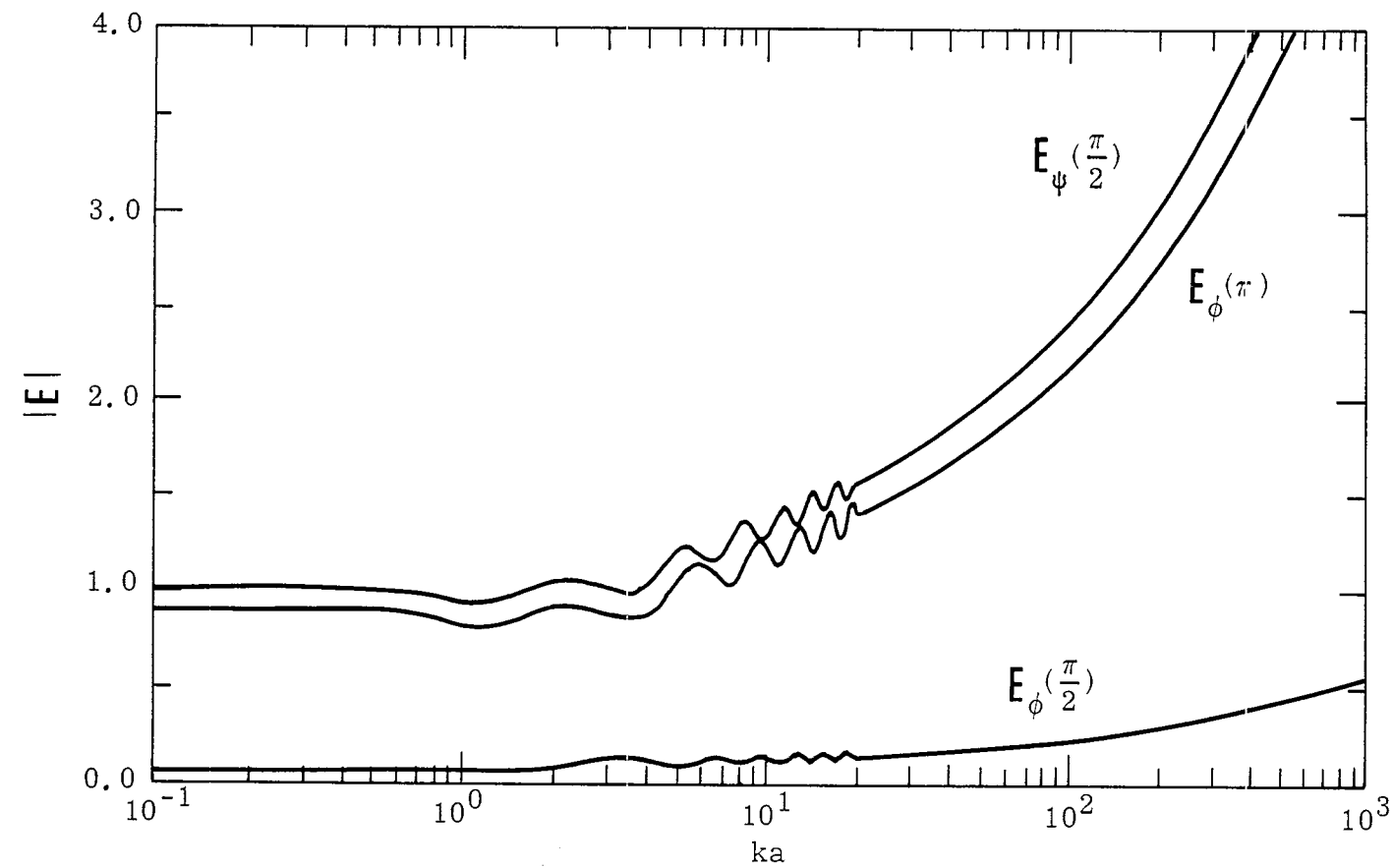


Figure 9-24. Step-function Response for the H_z -field for $b/a = 0.01$ and $\psi = 0.25$ with ϕ as a Parameter



A. $\phi = 0$ and $\frac{\pi}{4}$.

Figure 9-25. E -field for $b/a = 0.001$ and $\psi = 0.1$ with ϕ as a Parameter



B. $\phi = \frac{\pi}{2}$ and π .

Figure 9-25. Continued

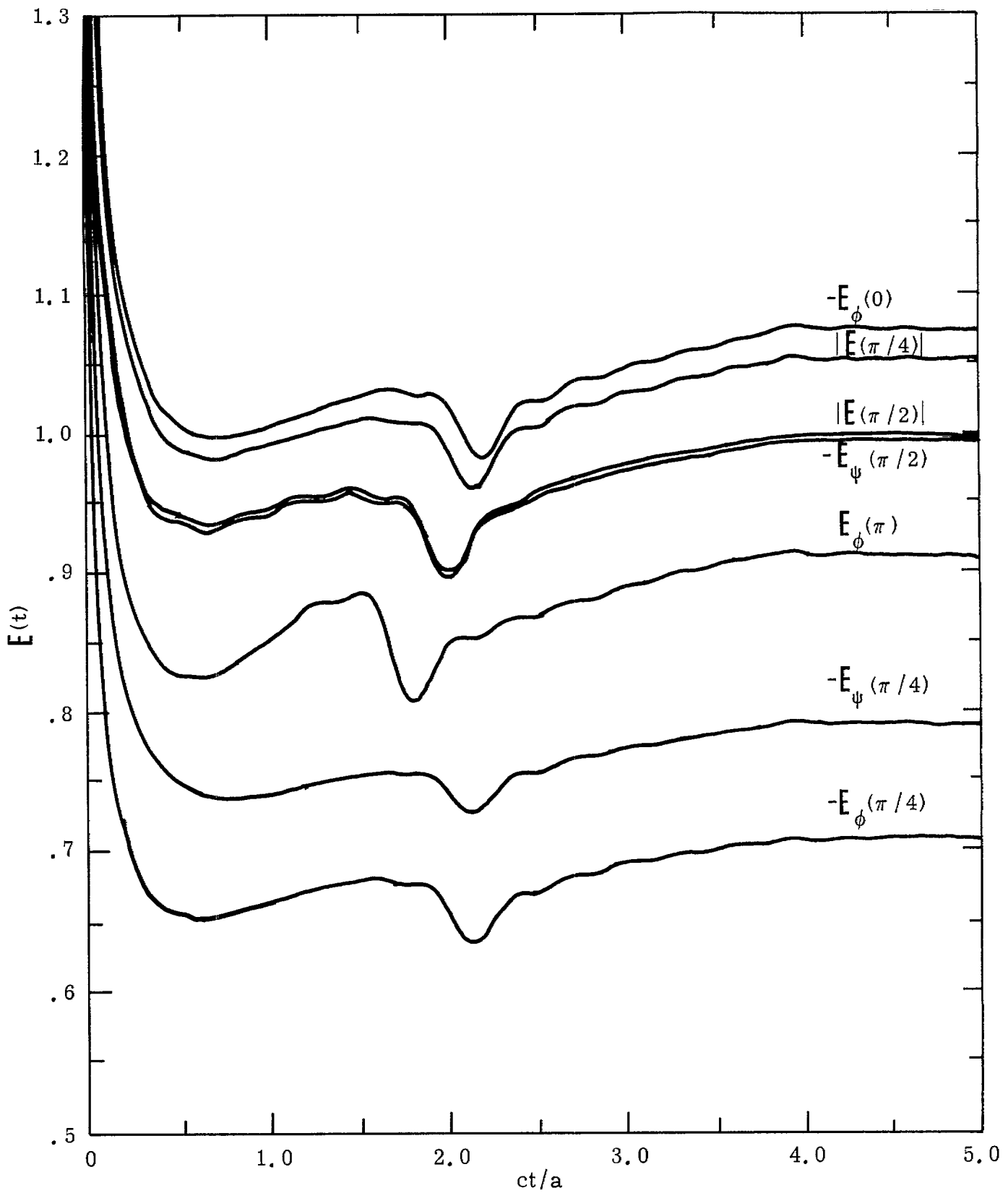


Figure 9-26. Step-function Response for the E -field for $b/a = 0.001$ and $\psi = 0.1$ with ϕ as a Parameter

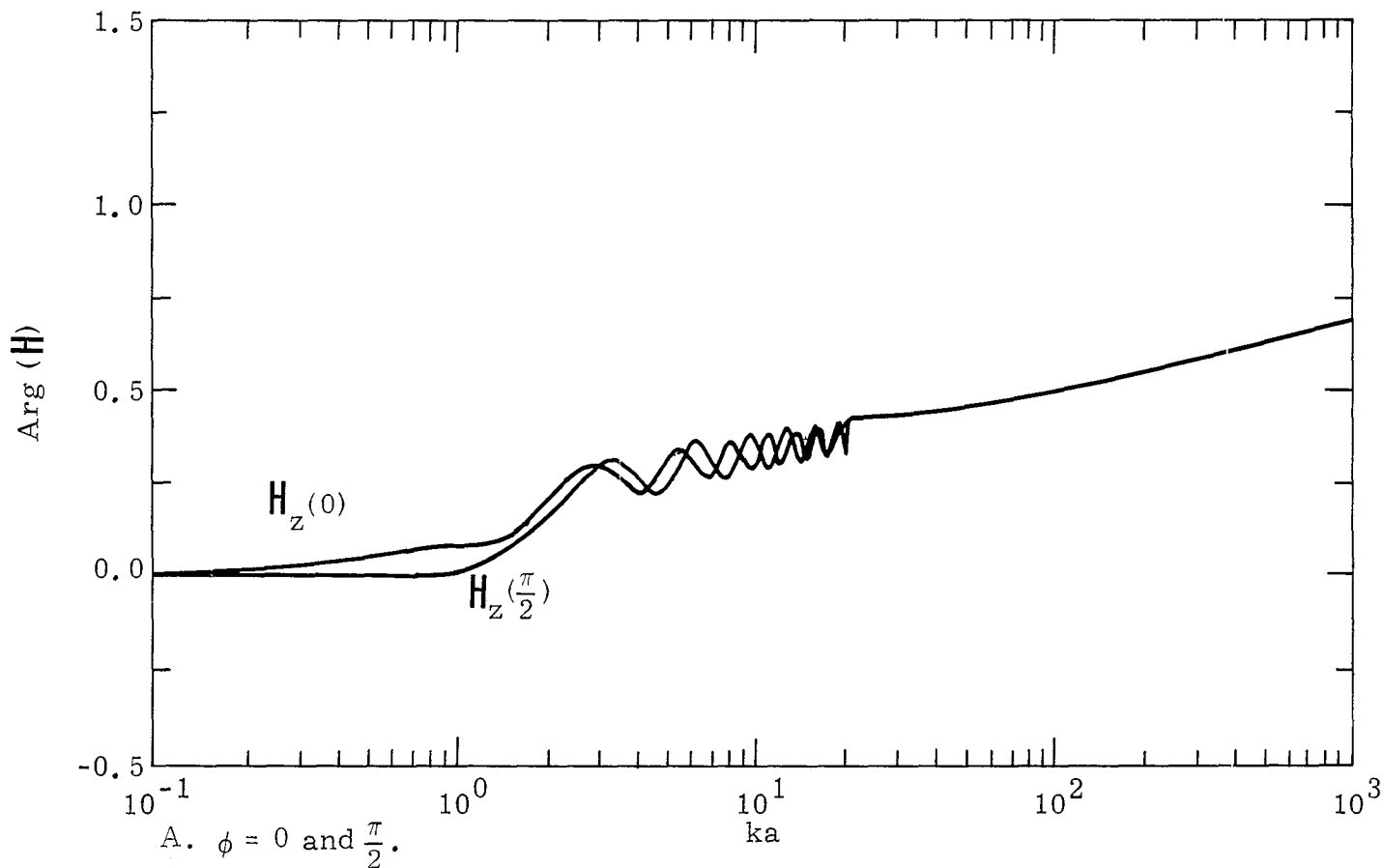
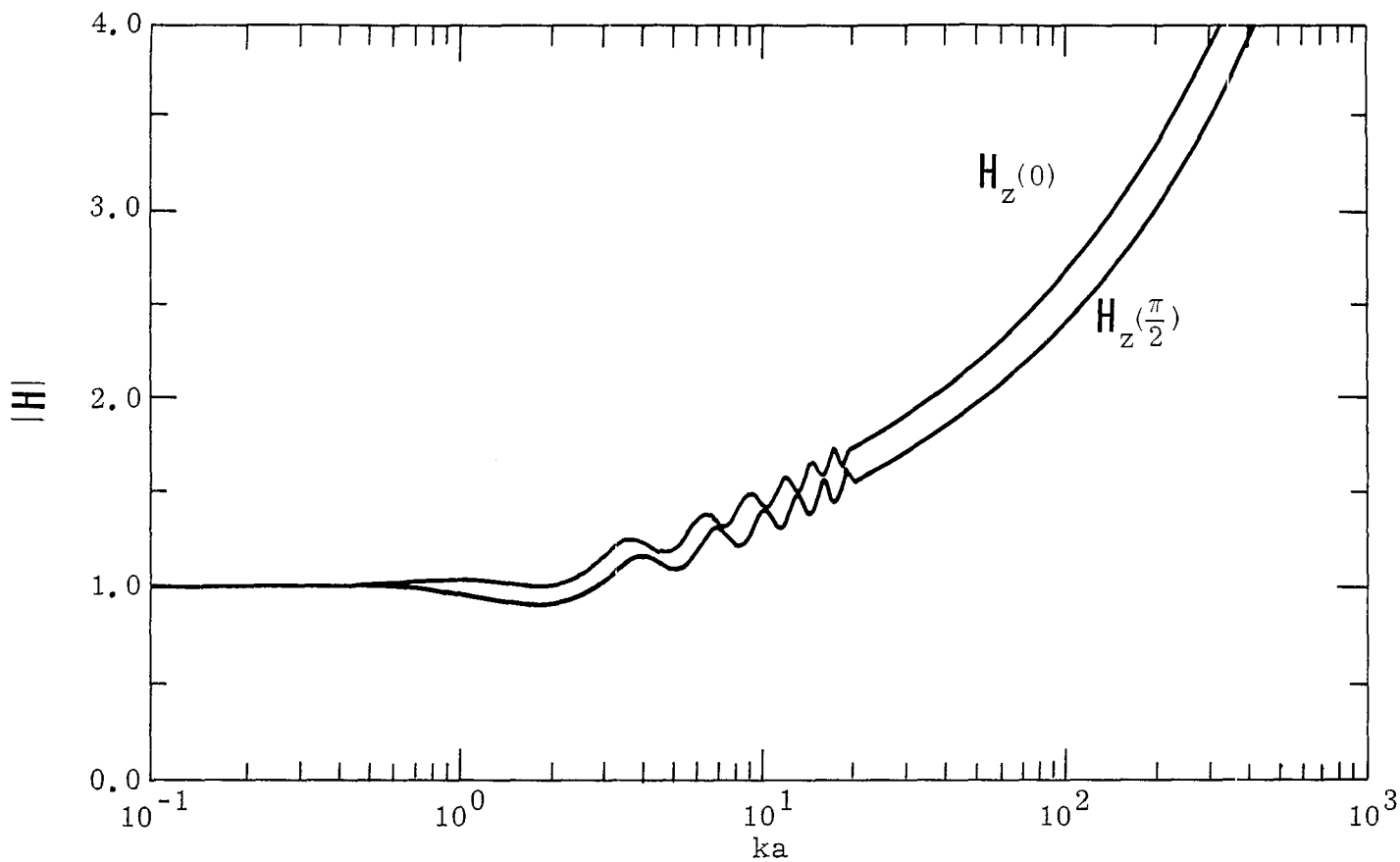
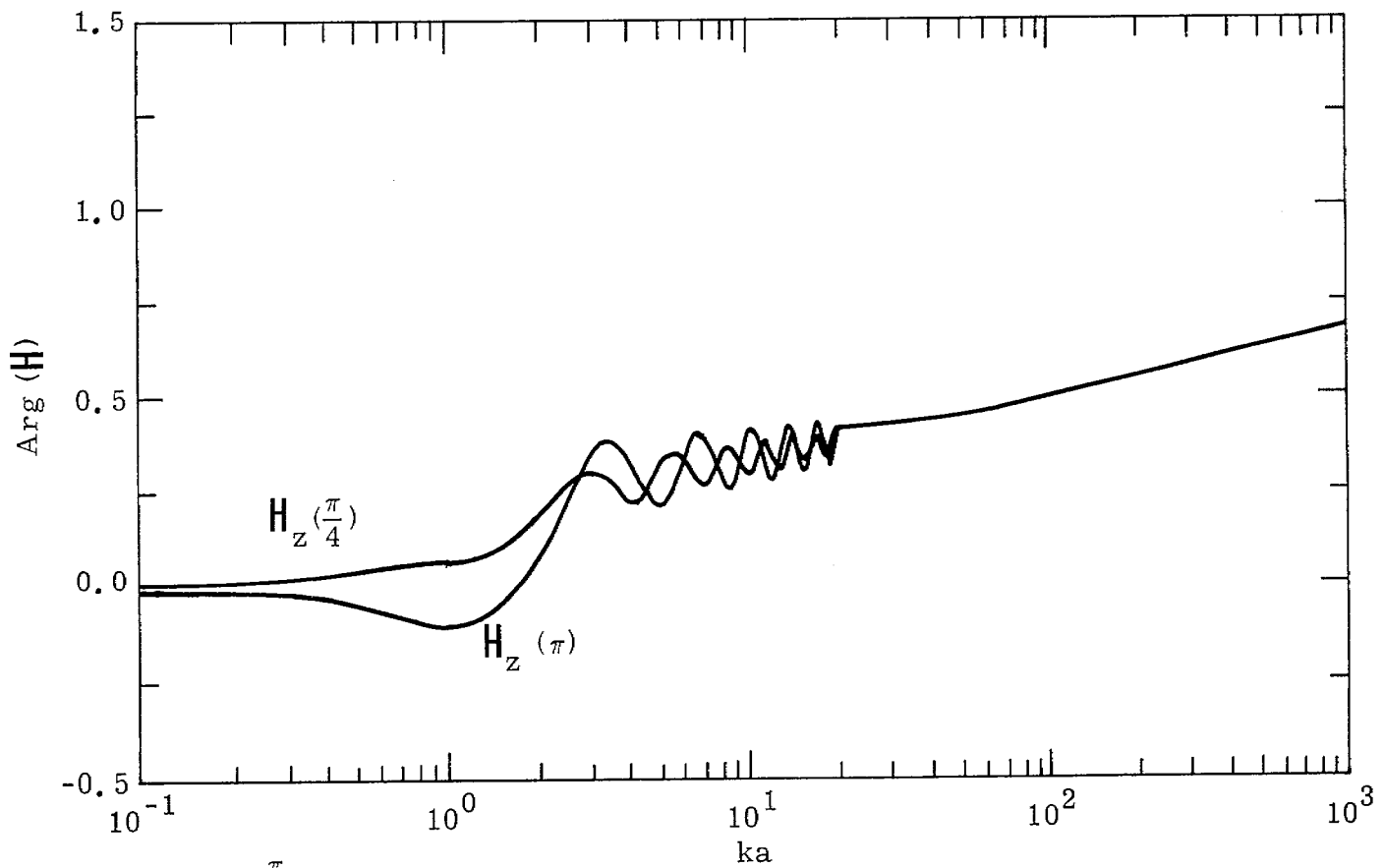
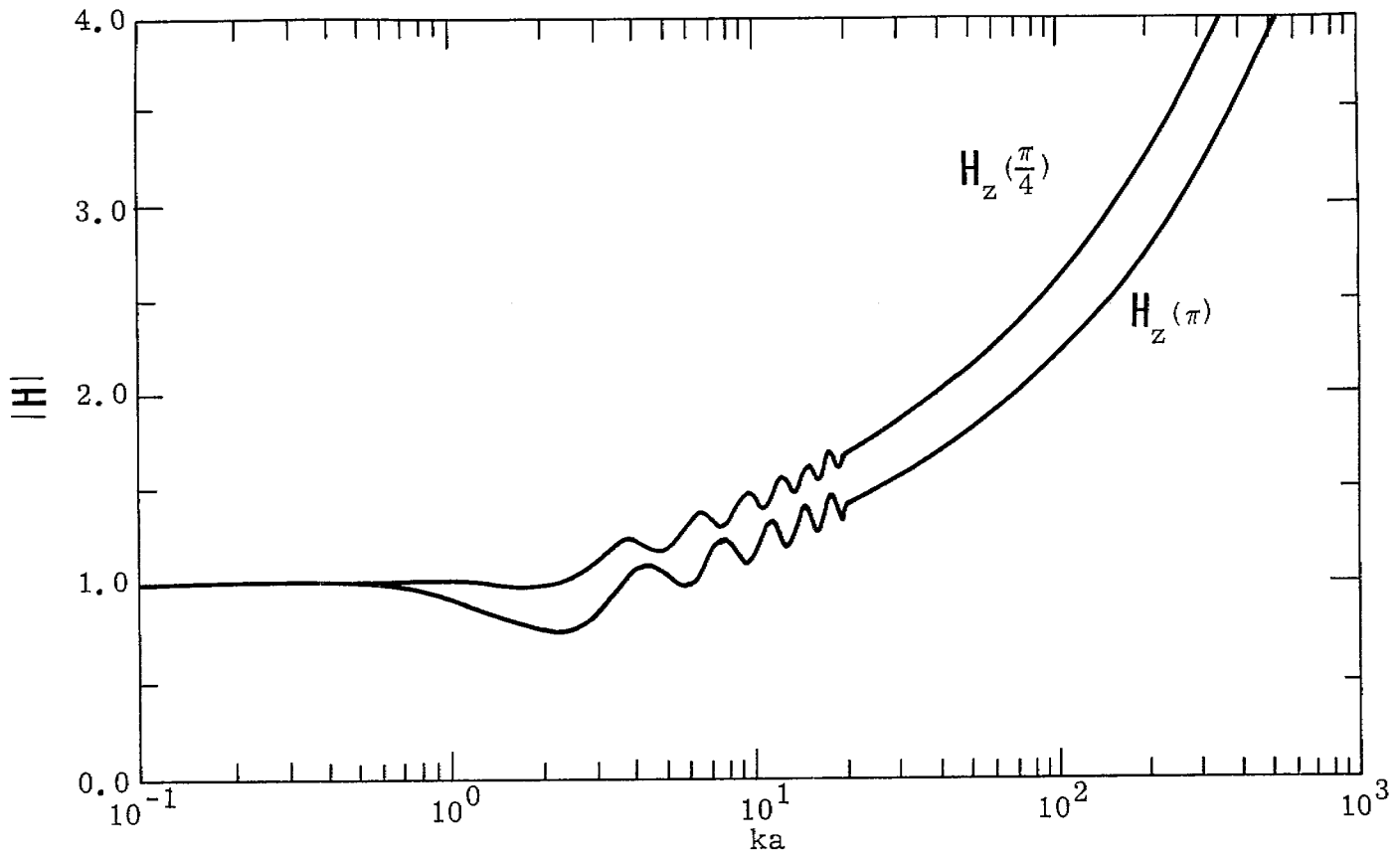


Figure 9-27. H -field for $b/a = 0.001$ and $\psi = 0.1$ with ϕ as a parameter



B. $\phi = \frac{\pi}{4}$ and π .

Figure 9-27. Continued

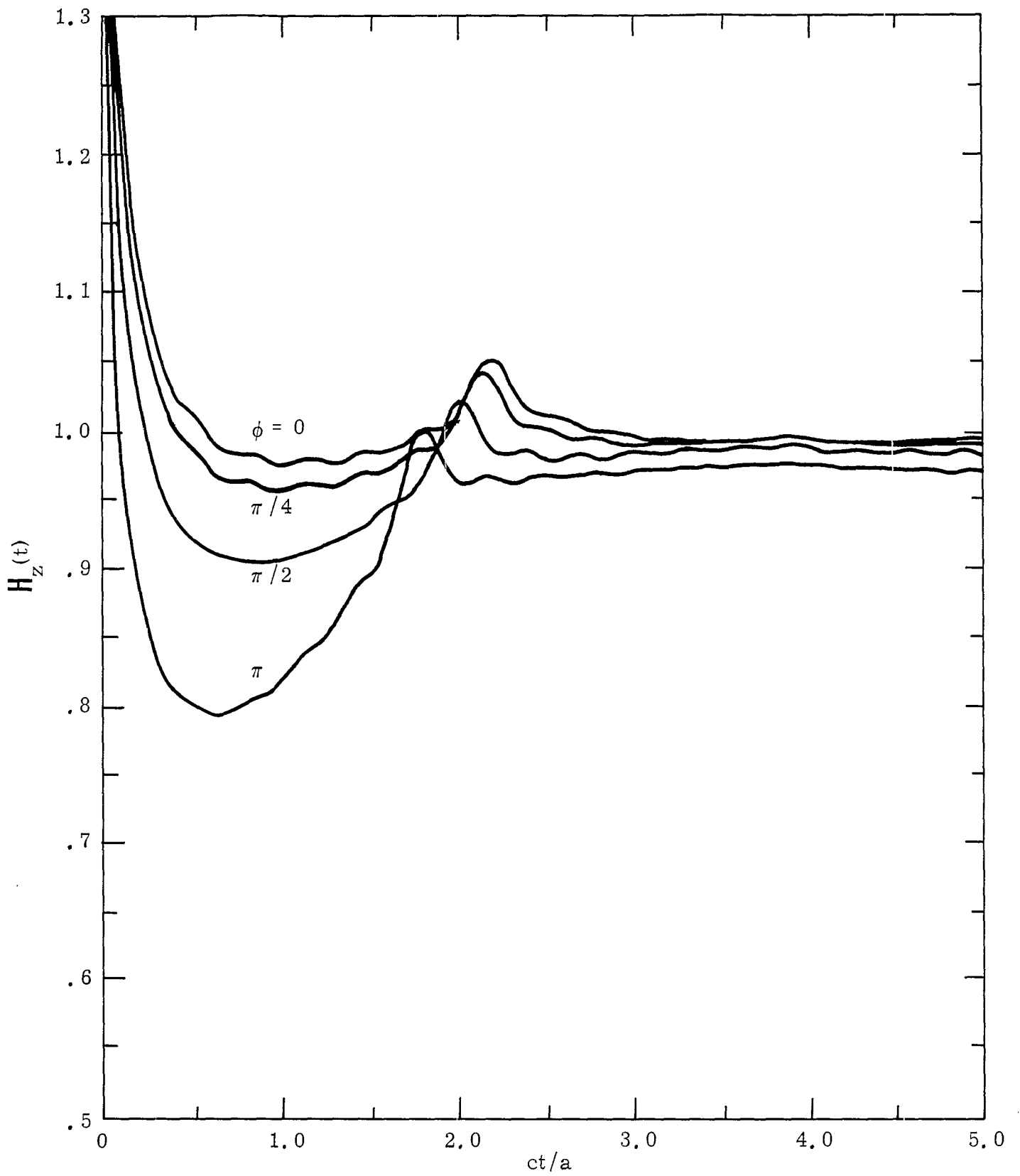
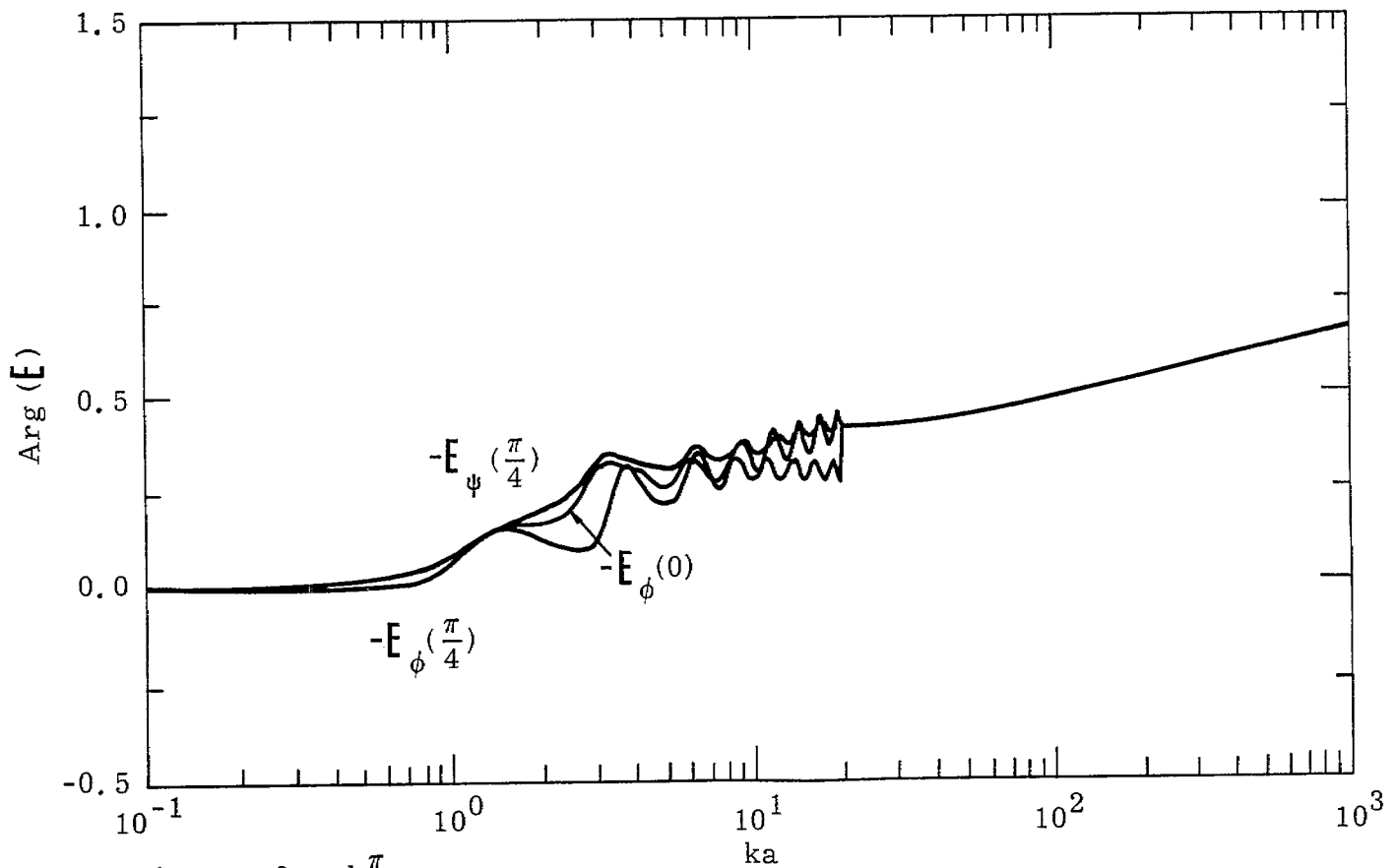
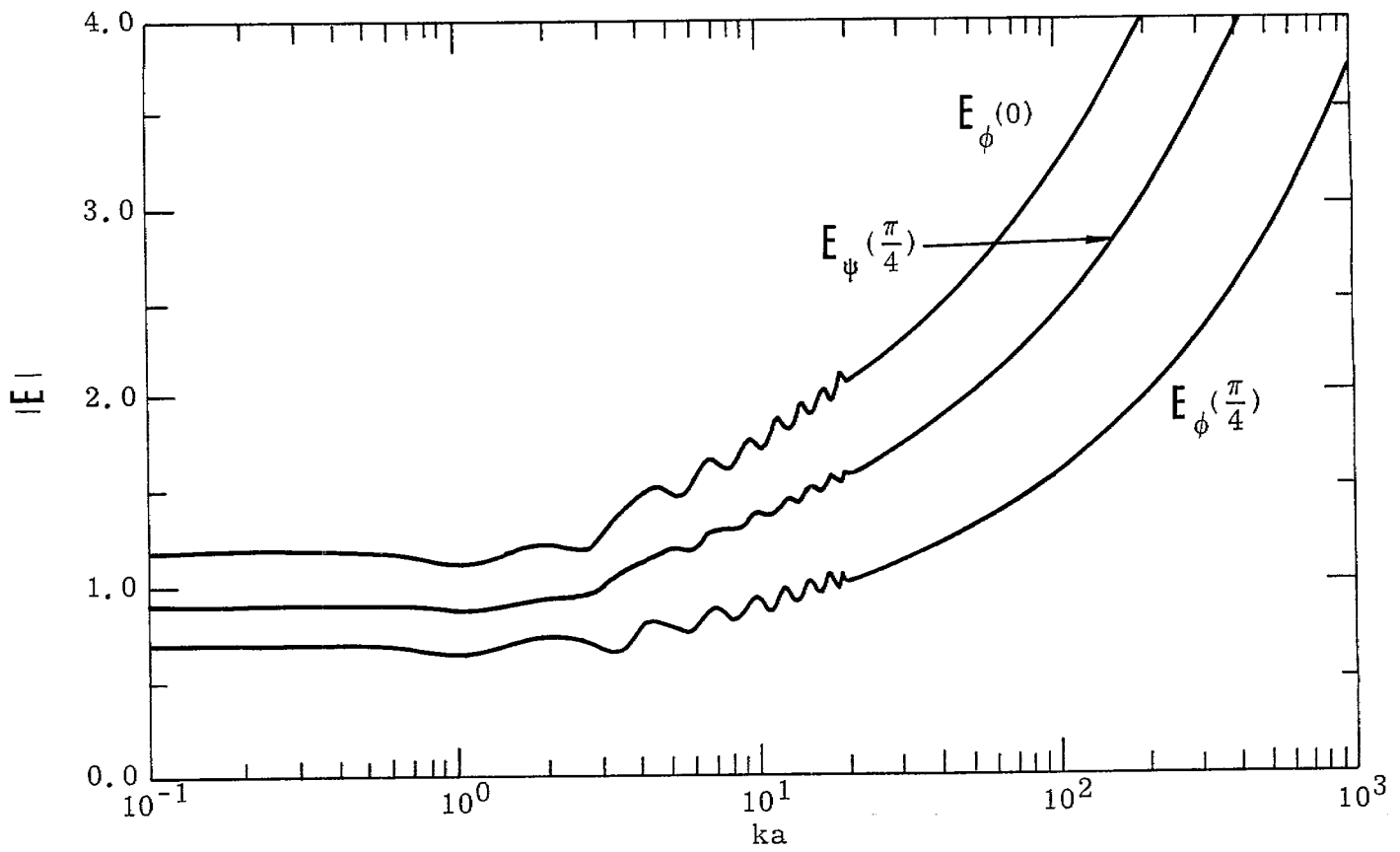
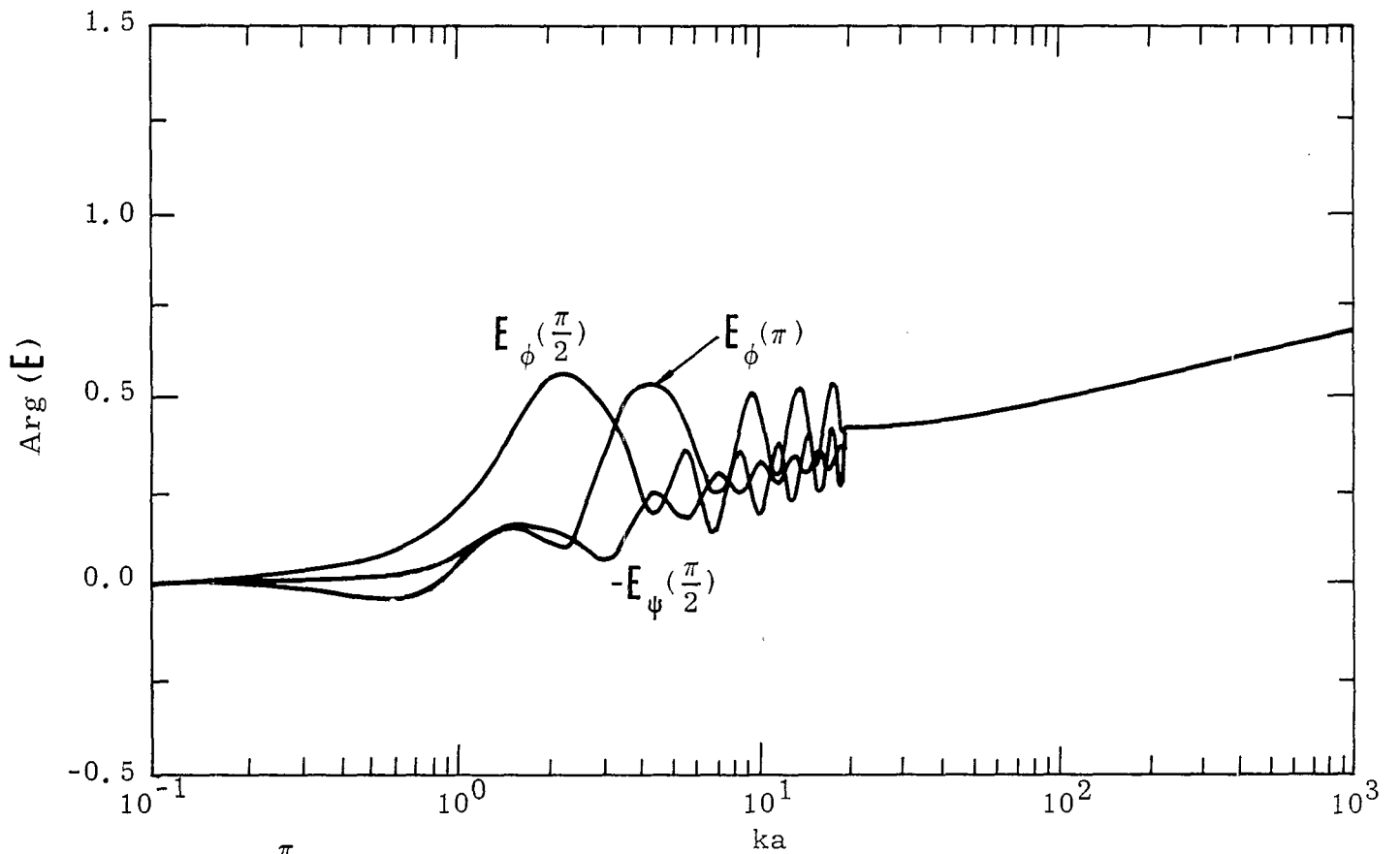
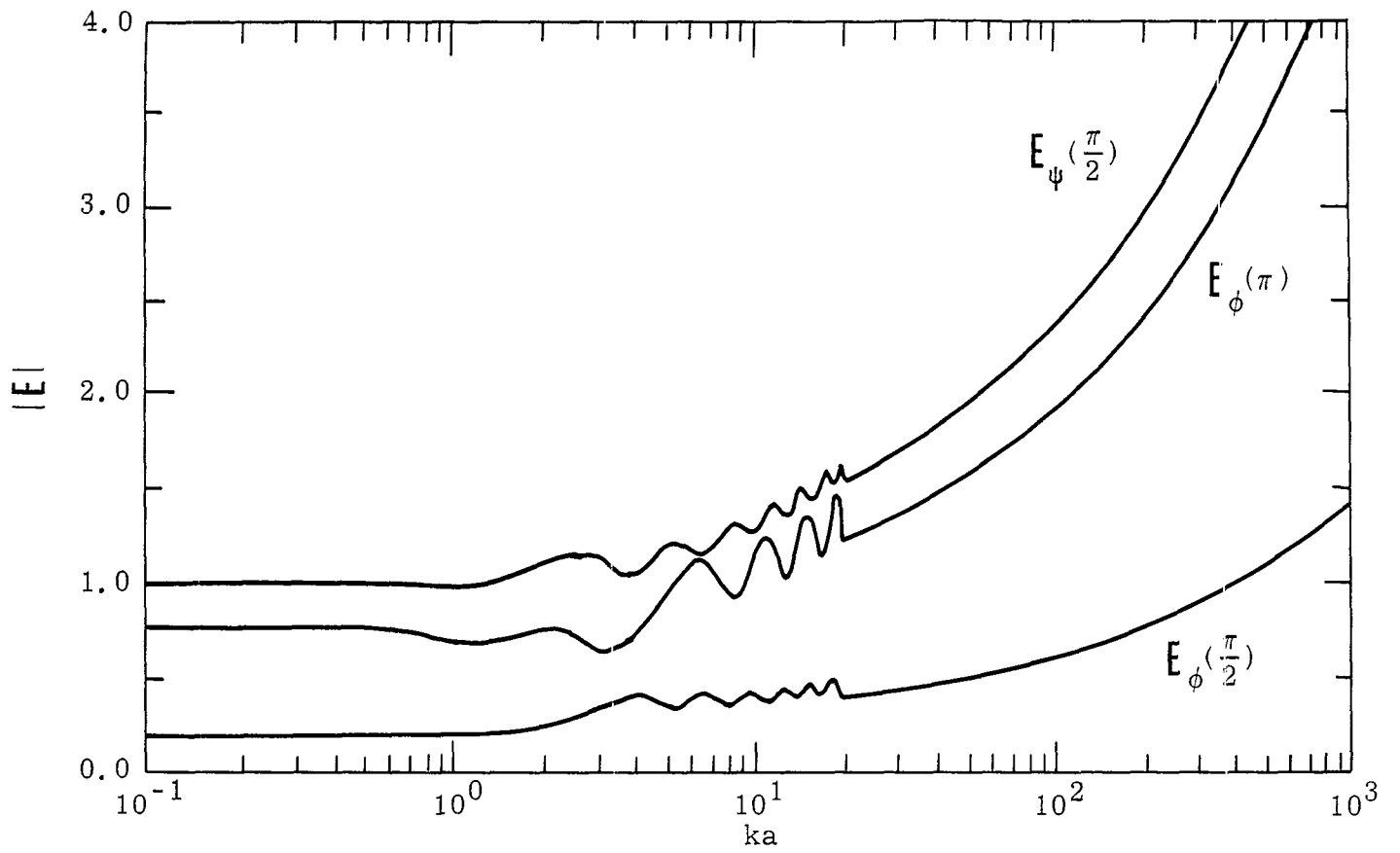


Figure 9-28. Step-function Response for the H -field for $b/a = 0.001$ and $\psi = 0.1$ with ϕ as a Parameter



A. $\phi = 0$ and $\frac{\pi}{4}$.

Figure 9-29. E -field for $b/a = 0.001$ and $\psi = 0.25$ with ϕ as a Parameter



B. $\phi = \frac{\pi}{2}$ and π .

Figure 9-29. Continued

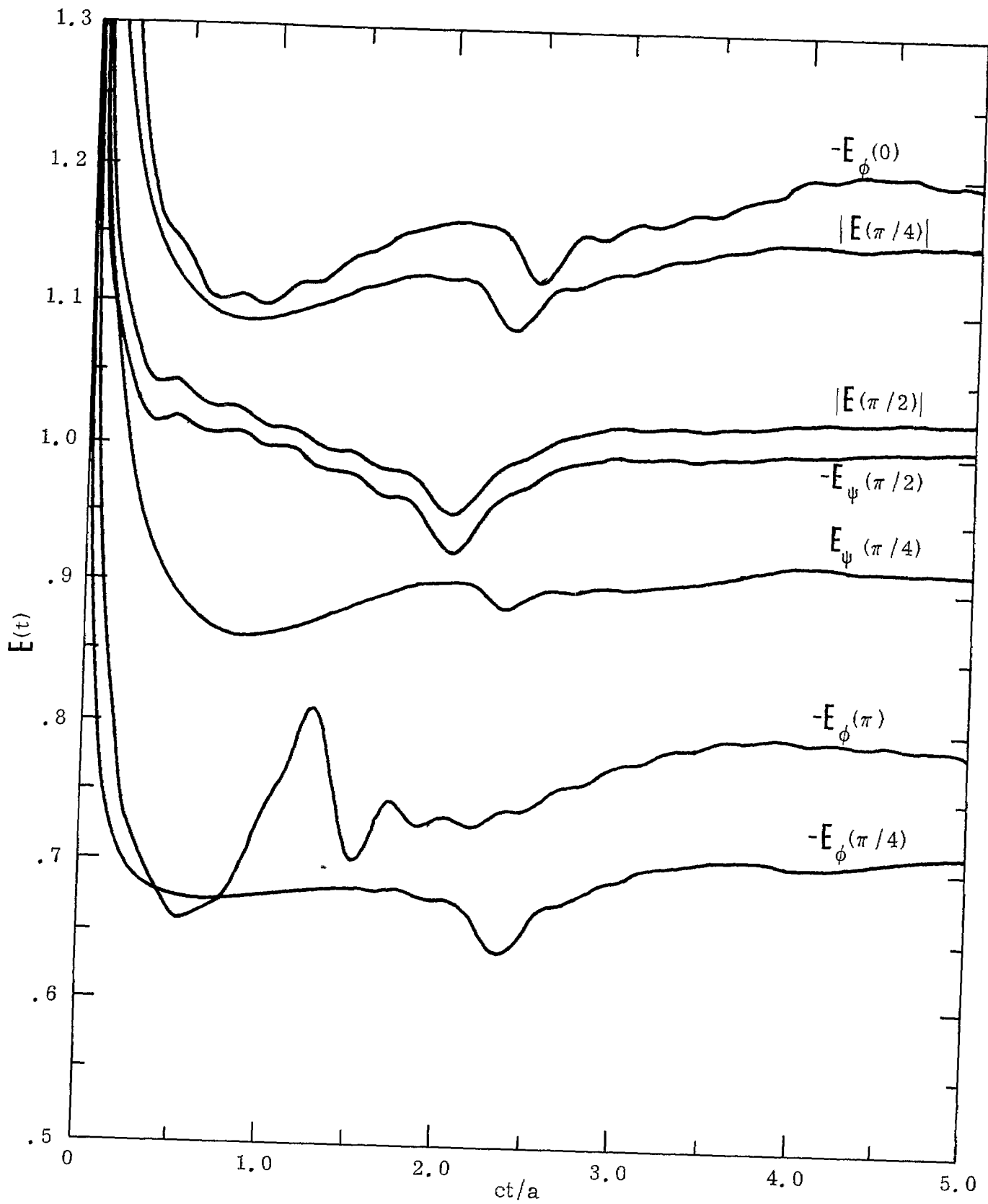


Figure 9-30. Step-function Response for the E -field for $b/a = 0.001$ and $\psi = 0.25$ with ϕ as a Parameter

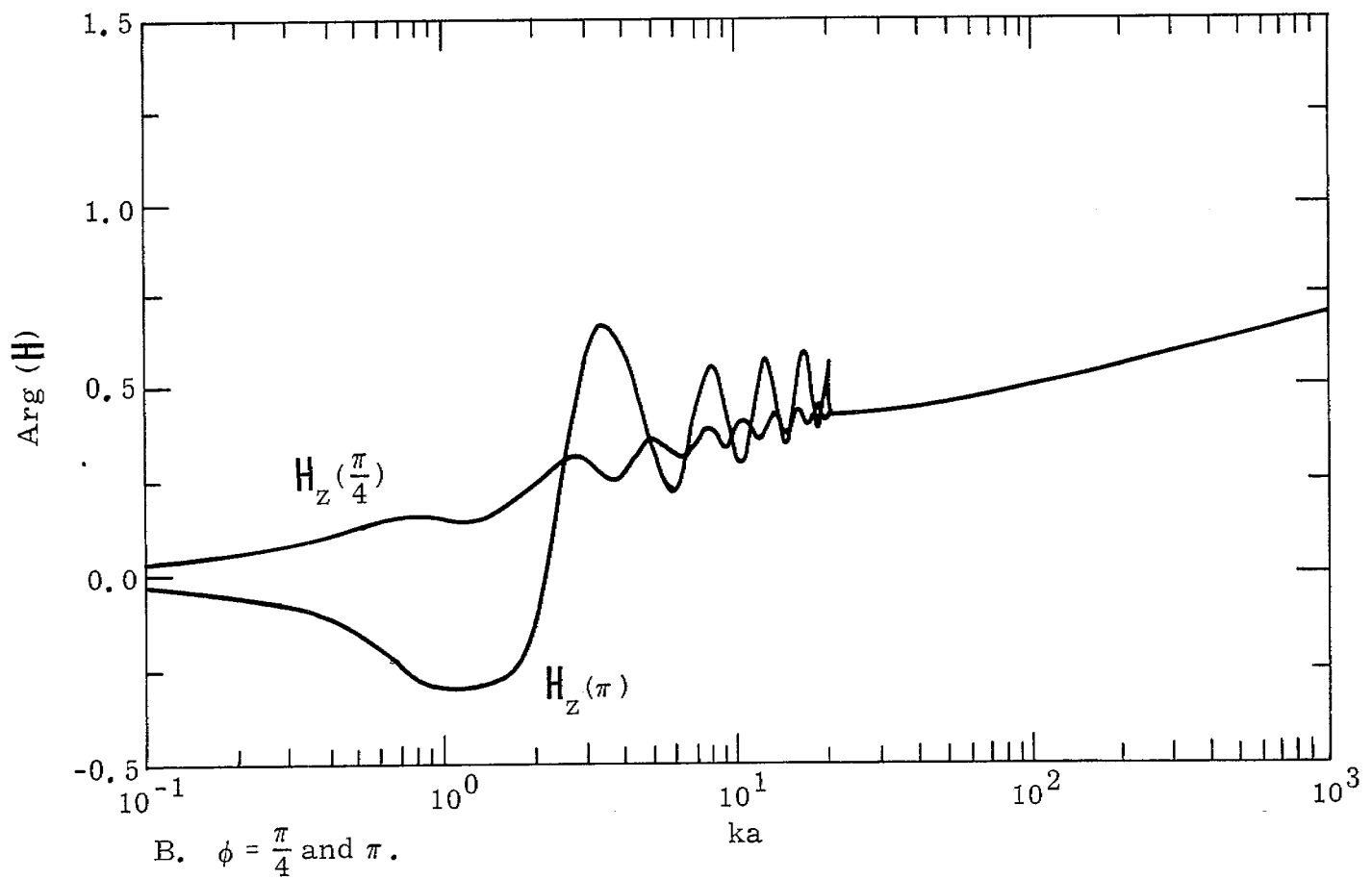
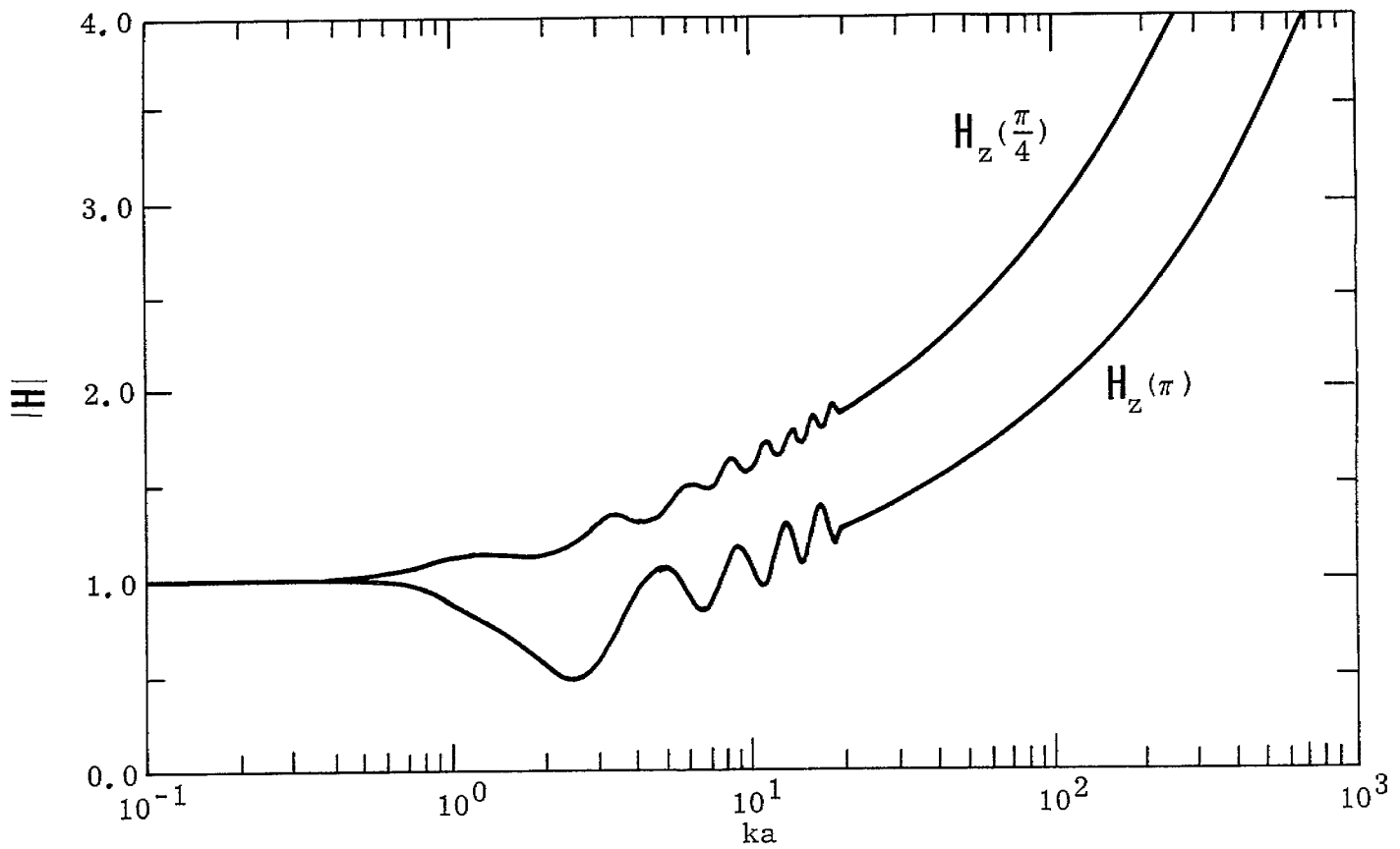


Figure 9-31. Continued

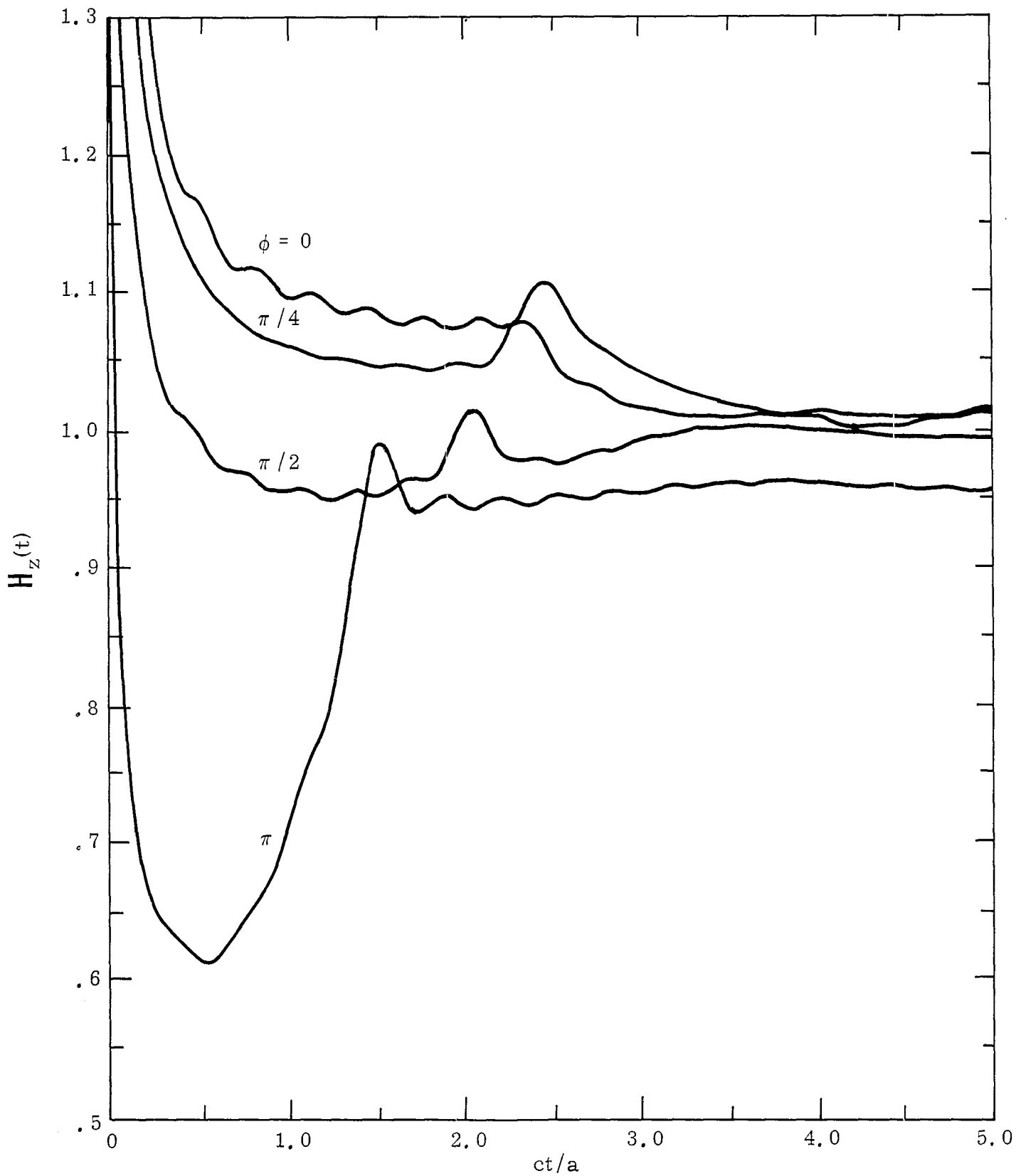


Figure 9-32. Step-function Response for the H_z -field for $b/a = 0.001$ and $\psi = 0.25$ with ϕ as a Parameter

X. Summary

In this note, mode method is introduced to calculate the near field of an antenna. We have derived the electric modes \vec{N}_n and magnetic modes \vec{M}_n for the toroidal antenna. They are a function of the coordinate systems used and are independent of the antenna properties. The amplitude for the higher order modes decreases as the distance from the symmetry point increases. In a toroid, the symmetry point is the center. The Fourier component of the current on the toroid \vec{i}_n is regarded as the excitation factor which is a function of the loading impedance as well as the source and is decreased in amplitude as n increases. As we have found in SSN 160, the zero order mode contributes to the magnetic field and the first order mode contributes to the electric field at the center. Then, the higher order modes become more and more important as we move away from the center. For example, the summation of as little as four modes already well approximates the field at $\psi = 0.05$ for ka up to 50. On the other hand, fourteen modes are necessary in order to adequately represent the field at $\psi = 0.25$. However, as we move further away from the center, particularly when ψ is close to one, then a lot of modes have to be considered [11]. For ψ greater than one, the number of modes needed will decrease as ψ increases because there is another symmetry point at infinity. This is similar to the characteristic modes for the far field introduced in [12, 13]. However, the characteristic modes are chosen to orthogonalize the power patterns and depend not only on the loading impedance but also on the source function. They have to be calculated each time if the load and the source of asymmetric distributions are used.

For these mode structures defined in this paper, one needs only to calculate them once for each type of antenna. The loading impedance and the source function only affect the excitation factors \vec{i}_n , the only

parameters which have to be computed from time to time for various loading conditions. Although i_n could be calculated separately for a uniform load, as shown in this note, it would couple with each other for various n in a non-uniform loaded antenna and the current computation is certainly more involved. The mode expansion technique introduced in this note only simplifies the calculation for the fields, not for the current. One still has to find out the current distribution on the antenna by conventional methods such as experimental measurements or theoretical analysis including the numerical computation.

Although, only a simple example on a circular loop antenna is given in this note, mode theory is also applicable to other types of antennas, and it is very useful and convenient for calculating the field near the symmetry points even in the near zone. Actually, one may consider these mode formulas for symmetry types, such as the toroidal, cylindrical or spherical shapes, etc., of antenna as some kind of special functions and tabulate them in a general engineering handbook. Once the loading impedance and the source function of the antenna are determined, one may calculate the excitation factor for each mode and compute the field immediately.

XI. References

- [1] C. E. Baum and H. Chang, "Fields at the Center of a Full Circular TORUS and a Vertically Oriented TORUS on a Perfectly Conducting Earth", Sensor and Simulation Notes 160, Dec. 1972.
- [2] C. E. Baum, H. Chang and J. P. Martinez, "Analytical Approximations and Numerical Techniques for the Integral of the Anger-Weber Function", Mathematics Note 25, Aug. 1972.
- [3] T. T. Wu, "Theory of the Thin Circular Loop Antenna," Journal of Mathematical Physics, Vol. 3, No. 6, 1962, pp 1301-1304.
- [4] L. D. Licking and D. E. Merewether, "An Analysis of Thin-Wire Circular Loop Antennas of Arbitrary Size", Interaction Notes 53, Aug. 1970.
- [5] M. Abramowitz and I. A. Stegun, Editors, Handbook of Mathematical Functions, AMS 55, National Bureau of Standards, 1964.
- [6] K. Iizuka, "The Circular Loop Antenna Multiloaded with Positive and Negative Resistors", IEEE-Antenna and Propagation, Vol. 13, Jan. 1965, pp 7-20.
- [7] R. F. Harrington, Field Computation by Moment Methods, The Macmillan Company, New York, 1968.
- [8] F. M. Tesche, "On the Singularity Expansion Method as Applied to Electromagnetic Scattering from Thin Wires", Interaction Notes 102, April, 1972.
- [9] R. W. Latham and K. S.H. Lee, "Radiation of an Infinite Cylindrical Antenna with Uniform Resistive Loading", Sensor and Simulation Note 83, April 1969.
- [10] C. H. Papas, "On the Infinitely Long Cylindrical Antenna", Journal of Applied Physics, Vol. 20, May 1949, pp 437-440.
- [11] R. L. Fante, J. J. Otazo, and J. T. Mayhan, "The Near Field of the Loop Antenna," Radio Science, Vol. 4, No. 8, Aug. 1969, pp 697-701.

- [12] R. J. Garbacz and R. H. Turpin, "A Generalized Expansion for Radiated and Scattered Fields", IEEE-Antenna and Propagation, Vol. 19, No. 3, May 1971, pp 348-358.
- [13] R. F. Harrington and J. R. Mautz, "Theory of Characteristic Modes for Conducting Bodies", IEEE-Antenna and Propagation, Vol. 19, No. 5, Sept. 1971, pp 622-628.